

Geohydrological impact of co-disposed coal material into an opencast pit

HJ Botha
21618488

Dissertation submitted in fulfilment of the requirements for the degree *Magister Scientiae* in **Environmental Sciences** (specialising in **Hydrology and Geohydrology**) at the Potchefstroom Campus of the North-West University

Supervisor: Prof I Dennis

May 2016

DECLARATION

I Hendrik Johannes Botha hereby declare that this dissertation is my own work and has not been submitted to any University for degree purposes. All work written by other authors and used in the dissertation are fully acknowledged.

This is submitted for the Magister Scientiae in Environmental Sciences (specialising in Hydrology and Geohydrology) at the Potchefstroom Campus of the North-West University.

Hendrik Johannes Botha



Signature

Student No.: 21618488

ABSTRACT

Investigations have shown that receiving water bodies, which mainly include rivers, streams and the more complicated geohydrological system, are part of the primary end receivers of harmful contaminants from identified coal mining waste bodies. Some of these potential dangers include acid drainage (AD) and saline drainage (SD), which have dire effects on the surroundings. In the compilation of this dissertation the characteristics of the Northern KwaZulu Natal (KZN) coal fields and waste disposal methods are explored.

A logical approach to dealing with some of the problems and risks associated with conventional disposal methods of coal wastes at a coal mine are considered and assessed. Various disposal methods implemented at a typical coal mine are assessed and simple co-disposal technique, whereby the various waste product are mixed before and after deposition are explored.

The geological attributes of the KZN coal fields and the geochemical research results indicates that on its own, coal discard has great potential to produce long term SD and that coal tailings have a lower SD potential. Co-disposed results are promising and the buffering against long term chemical changes are noted. The end result is a waste product which is less reactive to the environment as well as easier to manage when it comes to mine closure.

Geochemical laboratory testing results as well as long term monitoring data of the study area were integrated into a groundwater numerical model to illustrate the potential of co-disposed techniques versus that of conventional disposal methods. By exploring this alternative waste disposal method, gave more clarity on aspects relating to sustainable coal mine closure. Furthermore, the information gained from thus study sets the foundation for further research to accurately define and understand the co-disposal principle, as well as the better understand the environmental and management risks associated with it.

Keywords

Co-disposal, geochemistry of co-disposed coal, buffer against acid drainage, KZN coalfields acid potential

ACKNOWLEDGEMENTS

I would like to thank the following for their contributions and help with this project:

- My heavenly Father for giving me the necessary insight, perseverance and guidance throughout this project;
- My darling wife Lisa Botha for her love, encouragement and support;
- My mother (Alida Botha) and father (Niel Botha) for their encouragement, love and financial support;
- Pieter Labuschagne for helping with the initiation of this project as well as providing guidance with the numerical modelling process;
- Dr. Rainier Dennis for allowing me to use the NWU Potchefstroom Campus geophysical equipment;
- Prof. Ingrid Dennis for reviewing and commenting on the masters dissertation document;
- GCS (Pty) Ltd for the usage of their software and supplying me with project related data and financing; and
- Tendele Coal Mining (Pty) Ltd for allowing me to undertake this study and to publish the results and findings in order to contribute in the work towards a more sustainable environment in all industries.

SUMMARY OF KEY TERMS

Advection - The process by which solutes are transported by the bulk motion of the flowing groundwater.

An unconfined, water table or phreatic aquifer - Different terms used for the same aquifer type, which is bounded from below by an impermeable layer. The upper boundary is the water table, which is in contact with the atmosphere so that the system is open.

Aquifer - A body of rock, consolidated or unconsolidated, that is sufficiently permeable to conduct groundwater and to yield significant quantities of water to wells and springs.

Compartment - In a slope-aquifer system, an area formed by an undulation of the water table generally conforming to an undulation in the overlying topography. The crests of the water-table undulations represent natural groundwater divides that, under natural conditions, restrict the movement of groundwater to the boundaries of the compartment.

Cone of Depression - A depression in the potentiometric surface of a body of groundwater that has the shape of an inverted cone and develops around a well/mine shaft/open pit mine from which water is being withdrawn.

Confined aquifer - A formation in which the groundwater is isolated from the atmosphere at the point of discharge by impermeable geologic formations; confined groundwater is generally subject to pressure greater than atmospheric pressure.

Discharge Area - An area in which there is an upward component of hydraulic head in an aquifer. Groundwater flows toward land surface in a discharge area and escapes as a spring, seep, base flow to streams, or by evaporation and transpiration.

Dispersion - The measure of spreading and mixing of chemical constituents in groundwater caused by diffusion and mixing due to microscopic variations in velocities within and between pores.

Drawdown - The decline of the water table or potentiometric surface as a result of withdrawals from wells or excavations.

Effective porosity - The percentage of the bulk volume of a rock or soil that is occupied by interstices that are connected.

Equipotential line - A line in a two-dimensional groundwater flow field on which the total hydraulic head is the same at all points.

Fault - A fracture or fracture zone along which there has been displacement of the sides relative to one another parallel to the fracture.

Fracture - A crack, joint, fault or other break in rocks caused by mechanical failure.

Groundwater table - The surface between the zone of saturation and the zone of aeration; the surface of an unconfined aquifer.

Heterogeneous - Indication of a non-uniformity in a structure.

Hydraulic conductivity (K) - The volume of water that will move through a porous medium in unit time under a unit hydraulic gradient through a unit area measured perpendicular to the area [L/T]. Hydraulic conductivity is a function of permeability and the fluid's density and viscosity.

Hydraulic gradient - The rate of change in the total head per unit distance of flow in a given direction.

Hydraulic Head - Generally, the altitude of the free surface of a body of water above a given datum.

Hydrodynamic dispersion - Comprises of processes namely mechanical dispersion and molecular diffusion.

Interflow - The lateral movement of water in the unsaturated zone during and immediately after precipitation. Interflow occurs when the zone above a low permeability horizon becomes saturated and lateral flow is initiated parallel to the barrier.

Joint - A fracture in rock along which there has been no visible movement.

Mechanical dispersion - The process whereby the initially close group of pollutants are spread in a longitudinal as well as a transverse direction because of velocity distributions.

Metamorphic Rock - A rock formed at depth in the earth's crust from pre-existing rocks by mineralogical, chemical and structural changes caused by high temperature, pressure and other factors. Examples include slate, schist and gneiss.

Observation borehole - A borehole drilled in a selected location for the purpose of observing parameters such as water levels.

Perched Water Table - The upper surface of a body of unconfined groundwater separated from the main body of groundwater by unsaturated material.

Permeability - Related to hydraulic conductivity, but is independent of the fluid density and viscosity and has the dimensions L^2 . Hydraulic conductivity is therefore used in all the calculations.

pH - A measure of the acidity or alkalinity of a solution, numerically equal to 7 for neutral solutions, increasing with increasing alkalinity and decreasing with increasing acidity.

Piezometric head (ϕ) - The sum of the elevation and pressure head. An unconfined aquifer has a water table and a confined aquifer has a piezometric surface, which represents a pressure head. The piezometric head is also referred to as the hydraulic head.

Porosity - The ratio of the aggregate volume of interstices in a rock or soil to its total volume. It is usually stated as a percentage.

Potentiometric Surface - An imaginary surface representing the total head of groundwater and defined by the level to which water rises in tightly cased wells. The water table is a particular potentiometric surface.

Pumping tests - Conducted to determine aquifer or borehole characteristics.

Recharge - The addition of water to the zone of saturation; also, the amount of water added.

Sandstone - A sedimentary rock composed of abundant rounded or angular fragments of sand set in a fine-grained matrix (silt or clay) and more or less firmly united by a cementing material.

Sedimentary Rock - A layered rock resulting from the consolidation of sediment deposited by some geologic agent such as water, wind, or ice. Typical sedimentary rocks include sandstone, limestone and shale.

Shale - A fine-grained sedimentary rock formed by the consolidation of clay, silt or mud. It is characterised by finely laminated structure and is sufficiently indurated so that it will not fall apart on wetting.

Specific storage (S_0) - A saturated confined aquifer is the volume of water that a unit volume of aquifer releases from storage under a unit decline in hydraulic head. In the case of an unconfined (phreatic, water table) aquifer, specific yield is the water that is released or drained from storage per unit decline in the water table.

Static water level - The level of water in a borehole that is not being affected by withdrawal of groundwater.

Storativity - The volume of water an aquifer releases from or takes into storage per unit surface area of the aquifer per unit change in head.

Total dissolved solids (TDS) - A term that expresses the quantity of dissolved material in a sample of water.

Transmissivity (T) - The two-dimensional form of hydraulic conductivity and is defined as the hydraulic conductivity multiplied by the saturated aquifer thickness.

Vadose zone - The zone containing water under pressure less than that of the atmosphere, including soil water, intermediate vadose water, and capillary water. This zone is limited above by the land surface and below by the surface of the zone of saturation, that is, the water table.

Water table - The surface between the vadose zone and the groundwater, that surface of a body of unconfined groundwater at which the pressure is equal to that of the atmosphere.

ABBREVIATIONS AND ACCRONYMS

| | |
|-----------------|--|
| ABA | Acid Base Accounting |
| AD | Acid Drainage |
| AMD | Acid Mine Drainage |
| ANC | Acid Neutralising Capacity |
| AP | Acid Potential |
| ARD | Acid Rock Drainage |
| CDD | Coal Discard Dumps |
| DWA | Department of Water Affairs (now Department of Water and Sanitation) |
| DWAF | Department of Water Affairs and Forestry |
| DWS | Department of Water and Sanitation |
| EC | Electrical Conductivity (mS/m) |
| Fe | Iron (mg/l) |
| H ⁺ | Hydrogen Atom (Proton) |
| ICP | Inductively Coupled Plasma |
| K | Hydraulic Conductivity (m/day) |
| KZN | KwaZulu Natal |
| LOM | Life Of Mine |
| mamsl | Meters above mean sea level |
| mbgl | Meters below ground level |
| MPA | Maximum Potential Acidity |
| NAG | Net Acid Generation |
| NGDB | National Groundwater Database |
| NNP | Net Neutralisation Potential |
| NP | Neutralisation Potential |
| OB | Overburden |
| OH ⁻ | Hydroxide |
| PCD | Pollution Control Dam |
| ROM | Run of Mine |
| S | Storativity |
| SD | Saline drainage |
| SMD | Saline Mine Drainage |
| SO ₄ | Sulphate (mg/l) |
| TDS | Total Dissolved Solids (mg/l) |

| | |
|-----|-------------------------------|
| TSS | Total Suspended Solids (mg/l) |
| XRD | X-ray powder diffraction |

CONTENTS

| | |
|---|------|
| <i>DECLARATION</i> | i |
| <i>ABSTRACT</i> | ii |
| <i>ACKNOWLEDGEMENTS</i> | iii |
| <i>SUMMARY OF KEY TERMS</i> | iv |
| <i>ABBREVIATIONS AND ACCRONYMS</i> | viii |
| 1 Introduction | 1 |
| 1.1 Permeable | 1 |
| 1.2 Problem Statement | 2 |
| 1.3 Scope of work and objectives | 2 |
| 1.4 Dissertation structure | 3 |
| 2 Literature Review | 5 |
| 2.1 Coal | 5 |
| 2.1.1 Classification..... | 5 |
| 2.1.2 Distribution..... | 6 |
| 2.1.3 Chemistry of coal | 7 |
| 2.2 Waste disposal and problems at coal mines | 8 |
| 2.2.1 Discard Dumps | 8 |
| 2.2.2 Tailings ponds..... | 10 |
| 2.2.3 Groundwater and surface water pollution..... | 11 |
| 2.3 Co-Disposal | 13 |
| 2.3.1 Material hydro physical properties..... | 14 |
| 2.4 Groundwater modelling..... | 17 |
| 2.4.1 Model types | 19 |
| 2.4.2 Numerical groundwater modelling..... | 19 |
| 3 Methodology | 22 |
| 3.1 Approach | 22 |
| 3.2 Limitations | 26 |
| 4 Study Area..... | 28 |

| | | |
|-------|---|----|
| 4.1 | Mining Site | 28 |
| 4.1.1 | Site Layout..... | 28 |
| 4.1.2 | Project Boundaries | 28 |
| 4.2 | Mining Operations..... | 30 |
| 4.3 | Geographical Setting | 32 |
| 4.3.1 | Geology | 32 |
| 4.3.2 | Climate, topography and surface water drainage | 34 |
| 4.3.3 | Hydrogeology..... | 40 |
| 4.3.4 | Monitoring Network | 42 |
| 4.3.5 | Groundwater movement | 48 |
| 5 | Discussion and results | 50 |
| 5.1 | Field Work | 50 |
| 5.2 | Geophysics | 51 |
| 5.2.1 | Geophysical equipment used..... | 51 |
| 5.2.2 | Electro Magnetic and Magnetic traverses | 52 |
| 5.2.3 | Electromagnetic and Magnetic interpretation | 55 |
| 5.3 | Drilling and Aquifer Testing | 61 |
| 5.3.1 | Aquifer tests..... | 61 |
| 5.4 | Hydrochemistry | 63 |
| 5.4.1 | Monitoring network hydrochemistry | 63 |
| 5.5 | Geochemistry | 70 |
| 5.5.1 | Sampling Methodology | 70 |
| 5.5.2 | Sample Preparation | 70 |
| 5.5.3 | Mineralogy and total element analysis | 73 |
| 5.5.4 | Acid-Base Accounting and Net-Acid Generation Test | 76 |
| 5.5.5 | ABA and NAG test results..... | 79 |
| 5.5.6 | Static leaching test..... | 83 |
| 5.5.7 | Kinetic Leach Tests..... | 84 |
| 6 | Numerical Modelling | 91 |

| | | |
|-------|---|-----|
| 6.1 | Conceptualisation and model grid | 92 |
| 6.1.1 | Model Grid | 93 |
| 6.1.2 | Boundary conditions | 93 |
| 6.2 | Flow model and Calibration..... | 100 |
| 6.3 | Sensitive Analyses..... | 103 |
| 6.4 | Transport Modelling of disposal options | 107 |
| 6.4.1 | Conventional disposal..... | 109 |
| 6.4.2 | Co-disposal..... | 112 |
| 7 | Conclusion | 115 |
| 7.1 | Concluding remarks on geochemical testing | 115 |
| 7.2 | Concluding remarks on numerical and transport model | 116 |
| 7.3 | Concluding remarks regarding hypothesis | 117 |
| 7.4 | Way forward and further research..... | 117 |
| 8 | References | 118 |

LIST OF FIGURES

| | |
|---|----|
| Figure 1-1: Locality map of Somkhele anthracite mine..... | 4 |
| Figure 2-1: A representative structure of chemical groups in a bituminous coal. Retrieved from (Levine et al., 1982). | 8 |
| Figure 2-2: Discard dump hydrology retrieved from (James, 1997). | 9 |
| Figure 2-3: Typical hydrology of a tailings settling pond..... | 11 |
| Figure 2-4: Representation of co-disposal beach. Retrieved from (Morris and Williams, 2000) | 14 |
| Figure 2-5: Rhombohedral vs cubic packing vs co-disposed (adapted from Morris and Williams, 1997a) | 17 |
| Figure 2-6: Modelling protocol diagram (adapted from Anderson and Woessner, 1992) .. | 20 |
| Figure 4-1: Somkhele mining areas and study area boundaries..... | 29 |
| Figure 4-2: Average yearly rainfall for the study area | 35 |
| Figure 4-3: Study area geology | 37 |
| Figure 4-4: Study Area topography | 38 |
| Figure 4-5: Cross section of opencast pit backfilled with tailings (A-A') | 39 |
| Figure 4-6: Cross section of opencast pit backfilled with discard (B-B')..... | 39 |
| Figure 4-7: General lithology cross section | 41 |
| Figure 4-8: Identified aquifer layers based on hydrogeology characteristics..... | 41 |
| Figure 4-9: Groundwater fluctuations with time for mining Area 2 | 42 |
| Figure 4-10: Hydrocensus map | 47 |
| Figure 4-11: Topographic elevation vs groundwater elevation | 48 |
| Figure 4-12: Study area groundwater levels | 49 |
| Figure 5-1: EM and Magnetometer survey traverses..... | 53 |
| Figure 5-2: EM and Magnetometer traverses with anomalies..... | 54 |
| Figure 5-3: EM and Magnetometer results along Somkhele Pit A profile 1 | 56 |
| Figure 5-4: EM and Magnetometer results along Somkhele Pit A profile 4 | 57 |
| Figure 5-5: EM and Magnetometer results along Somkhele Pit A profile 7. | 58 |
| Figure 5-6: EM and Magnetometer results along Somkhele Pit A profile 7. | 59 |
| Figure 5-7: EM and Magnetometer results along Somkhele Pit E profile 3. | 60 |
| Figure 5-8: EM and Magnetometer results along Somkhele Pit E profile 4. | 61 |
| Figure 5-9: Piper plot: hydrocensus boreholes | 65 |
| Figure 5-10: Piper plot: monitoring boreholes near opencast pits | 66 |
| Figure 5-11: Geochemical sampling locations | 72 |
| Figure 5-12: Potential Acid Generation and Classification of Samples (adapted from Fourie, 2014) | 81 |
| Figure 5-13: Discard material sulphate vs total dissolved solids in leachate produced ... | 86 |

| | | |
|--------------|--|-----|
| Figure 5-14: | Tailings material sulphate vs total dissolved solids in leachate produced ... | 86 |
| Figure 5-15: | Co-Disposed material sulphate vs total dissolved solids in leachate produced | 87 |
| Figure 5-16: | Discard, tailings and co-disposed material leachate alkalinity..... | 87 |
| Figure 5-17: | Discard, tailings and co-disposed material leachate pH..... | 88 |
| Figure 6-1: | Geohydrological conceptual model of study area | 95 |
| Figure 6-2: | Conceptual model cross section A-A' | 96 |
| Figure 6-3: | Conceptual model cross section B-B' | 96 |
| Figure 6-4: | Model grid and boundaries..... | 97 |
| Figure 6-5: | Opencast pit backfilled with tailings..... | 98 |
| Figure 6-6: | Opencast pit backfilled with discard | 99 |
| Figure 6-7: | Calculated vs observed heads calibrated (steady state) | 101 |
| Figure 6-8: | Groundwater flow directions and flow velocity map | 102 |
| Figure 6-9: | Sensitive Analysis: Jacobian (neutral) variations..... | 103 |
| Figure 6-10: | Sensitive Analysis: Calibrated residuals histogram..... | 104 |
| Figure 6-11: | Sensitive Analysis: Hydraulic conductivity sensitivity | 104 |
| Figure 6-12: | Sensitive Analysis: Calculated versus the observed heads | 105 |
| Figure 6-13: | Sensitive Analysis: Uncertainties of the parameters | 106 |
| Figure 6-14: | Simulated groundwater sulphate concentrations for conventionally disposed coal wastes at selected observation points | 110 |
| Figure 6-15: | Simulated sulphate plumes for conventional disposal of tailings and discard into an opencast void | 111 |
| Figure 6-16: | Simulated groundwater sulphate concentrations for co-disposed coal wastes at selected observation points..... | 113 |
| Figure 6-17: | Simulated sulphate plumes for co-disposal of tailings and discard into an opencast void | 114 |

LIST OF TABLES

| | | |
|-------------|--|-----|
| Table 2-1: | Classification of coal based on rank | 5 |
| Table 2-2: | Sources of water pollution in coal mining areas | 12 |
| Table 2-3: | Model approaches | 18 |
| Table 2-4: | General model types used for groundwater modelling | 19 |
| Table 4-1: | Typical phases and impacts of a coal mine | 30 |
| Table 4-2: | Stratigraphy of the study area | 34 |
| Table 4-3: | Rainfall station locations and yearly precipitation averages..... | 35 |
| Table 4-4: | Monitoring boreholes in study area | 43 |
| Table 4-5: | Hydrocensus boreholes and monitoring boreholes in other areas | 44 |
| Table 5-1: | Field Work Summary | 50 |
| Table 5-2: | Geophysical equipment used..... | 51 |
| Table 5-3: | Summary of calculated aquifer parameters (T, K and S values)..... | 62 |
| Table 5-4: | Stacked column time series data for boreholes in study area..... | 67 |
| Table 5-5: | Sample description and lab number | 71 |
| Table 5-6: | XRD results and mineral classification | 75 |
| Table 5-7: | ABA screening methods used (adapted from Prince, 1997; and Fourie, 2014) | 78 |
| Table 5-8: | NAG screening methods used (Edited from Miller., 1997)..... | 79 |
| Table 5-9: | ABA (Acid-base accounting) results..... | 81 |
| Table 5-10: | NAG (Net acidic generation) results | 81 |
| Table 5-11: | ABA average for tailings and discard samples..... | 82 |
| Table 5-12: | Potential for various material to generate acid drainage. | 82 |
| Table 5-13: | Major constituents from peroxide leach testing | 84 |
| Table 5-14: | Major constituents analysed in leachate (Sample AIS 871, Discard) | 88 |
| Table 5-15: | Major constituents analysed in leachate (Sample AIS 878, Tailings Opencast Pit) | 89 |
| Table 5-16: | Major constituents analysed in leachate (Co-Disposed in 1:1 ratio)..... | 90 |
| Table 6-1: | Starting Input Parameters | 94 |
| Table 6-2: | Final parameters for the flow model (after calibration)..... | 107 |
| Table 6-3: | Time steps and constant concentrations (conventional disposal) | 108 |
| Table 6-4: | Time steps and constant concentrations (co-disposal)..... | 109 |
| Table 8-1: | ICP-OES results of the peroxide leach testing..... | 149 |
| Table 8-2: | ICP-OES results (Sample AIS 871, Discard) | 150 |
| Table 8-3: | ICP-OES results (Sample AIS 878, Tailings Opencast Pit)..... | 150 |
| Table 8-4: | ICP-OES (Sample AIS 878 and AIS 871 in 1:1 ratio) | 151 |

LIST OF APPENDICES

| | |
|--|-----|
| Appendix A: Geophysical data | 124 |
| Appendix B: Borehole Logs..... | 136 |
| Appendix C: Pump Test Analysis Results | 141 |
| Appendix D: Hydrochemistry data | 143 |
| Appendix E: ICP-OES Results | 149 |

1 INTRODUCTION

1.1 PERMEABLE

Located 85 km northwest of Richards Bay in KwaZulu-Natal (KZN), Somkhele is South Africa's largest producer of metallurgical grade anthracite. The mine is operated by Petmin's wholly-owned subsidiary Tendele Coal and falls in the KwaLuhlanga River catchment, which is an ephemeral or seasonally flowing tributary of the Umfolozi River. The Prospecting Lease area extends from Hluhluwe in the north to the Umfolozi River in the south and across to the Umfolozi Hluhluwe Game Park to the west, and past the Somkhele village to the east.

Four main coal seams are present and the Main Seam averages 10.8 m in thickness (maximum 17.8 m). The Tendele mine has a series of open pits and a coal processing plant, which are fully operational at a nominal capacity of 1.44 million run of mine (ROM) tonnes per year. Somkhele's coal product is low in phosphorus, sulphur and calcium, which makes it a viable reductant in the titanium and ferrochrome industries in South Africa. Its product is in demand for the pelletising and sintering of iron ore (Botha and Singh, 2012).

Somkhele has a current 20-year life of mine (LOM) at annual production of more than 1.2 million marketable tonnes of anthracite. It produces metallurgical anthracite for export via Richards Bay to iron ore pelletising and sintering markets, mostly in Brazil, and for the South African ferroalloy industry. The third plant at Somkhele was commissioned in February 2013 and has increased the yield and added process flexibility to the mine. It has capacity to produce 480,000 tonnes of energy coal from rewashed discard. Current mining operations cover approximately 10% of the 22,000 hectares on which Petmin has rights (Petmin, 2013).

Coal mining by opencast methods affects the environment of the mining area. During the mining operation, huge amounts of water is discharged on the surface to facilitate the mining process. The discharged water often contains high loads of total dissolved solids (TDS), total suspended solids (TSS), sulphate, iron, calcium, magnesium and heavy metals, which contaminate the surface and groundwater at Somkhele. The study area map is available in Figure 1-1.

1.2 PROBLEM STATEMENT

Modern day coal mines have various negative impacts on the environment, even though they follow mitigation and preventative measures. Some of these potential dangers include acid drainage (AD), saline drainage (SD), sediment runoff, oil and fuel spills, leaching of contaminants (typically from overburden (OB) dumps, pollution control dams (PCDs), coal discard dumps (CDDs), tailings settling ponds and active mining pits), sewage effluent and coal dust transported by wind (Tiwary, 2001; Schüring et. al, 1997; Yilmaz, 2011). Somkhele is an anthracite coal mine which makes use of open-pit procedures to mine the four main coal seams that are present in the area. Somkhele's coal product is low in phosphorus, sulphur and calcium content, however the environmental dangers and risk coupled with coal mining still exists. The mine has recently started to simultaneously backfill tailings and discard material into two different opencast voids. This means that the two waste products are being stored separately and the risk associated with managing two different waste streams are increased.

1.3 SCOPE OF WORK AND OBJECTIVES

The purpose of this study was to propose an alternative waste management scenario at a mine where old waste disposal techniques are still being practiced.

The objective of this study was therefore, to prove the hypothesis: Co-disposal of coal waste into a previously mined opencast void, is a better solution to prevent and buffer against chemical changes in the coal material, than to dispose the waste products separately. The dissertation was tested by:

- Updating the monitoring network within the study area for numerical modelling and hydrochemistry data purposes. A series of boreholes were drilled along the current opencast voids being backfilled with material and geophysical traverses were conducted along the pit boundaries to focus on the in-situ aquifer mechanics.
- Co-disposal and conventional disposal was simulated and geochemically assessed by performing static and kinetic laboratory tests on the coal material.
- The outcome of the geochemical test were assessed and a conservative groundwater numerical model was created to illustrate the potential impact of the above mentioned disposal scenarios.

1.4 DISSERTATION STRUCTURE

The dissertation is structured as follows:

1. Chapter 1: Introduction
 - a. General introduction describing the study area, the problem statement, scope of work and objectives as well as dissertation structure.
2. Chapter 2: Literature Review
 - a. Coal chemistry, deposition and coal types are discussed briefly in order to familiarise the reader with the types of coal, coal waste types, coal waste handling facilities and general problems associated with conventional waste disposal methods.
 - b. Co-disposal techniques are explored and discussed as well as the physical properties of a typical co-disposed coal material is explored.
 - c. Groundwater numerical modelling and existing models are discussed.
 - d. The numerical model process is discussed briefly.
3. Chapter 3: Methodology
 - a. The methodological approach is discussed as well as the sources of data and the project limitations.
4. Chapter 4: Study Area
 - a. The mining site is discussed and the project boundaries are conceptualised.
 - b. Mining operations and risks for opencast mining methods are briefly discussed.
 - c. The geographical setting of the study area within the project boundaries are discussed in terms of stratigraphy, geology, climate, topography, hydrogeology, drainage, groundwater movement and the current monitoring network.
5. Chapter 5: Discussion and results
 - a. The field work component is discussed and the results obtained during the geophysical survey, drilling and aquifer testing, hydrochemistry testing and geochemical testing are presented and discussed.
6. Chapter 6: Numerical modelling
 - a. The numerical flow modelling and transport modelling components for the conventional and co-disposal scenarios are discussed and the results are reported on.
7. Chapter 7: Conclusion
 - a. A brief conclusion is made in terms of “is co-disposal better than conventional disposal”.
 - b. Recommendations and way forward for future research are discussed.

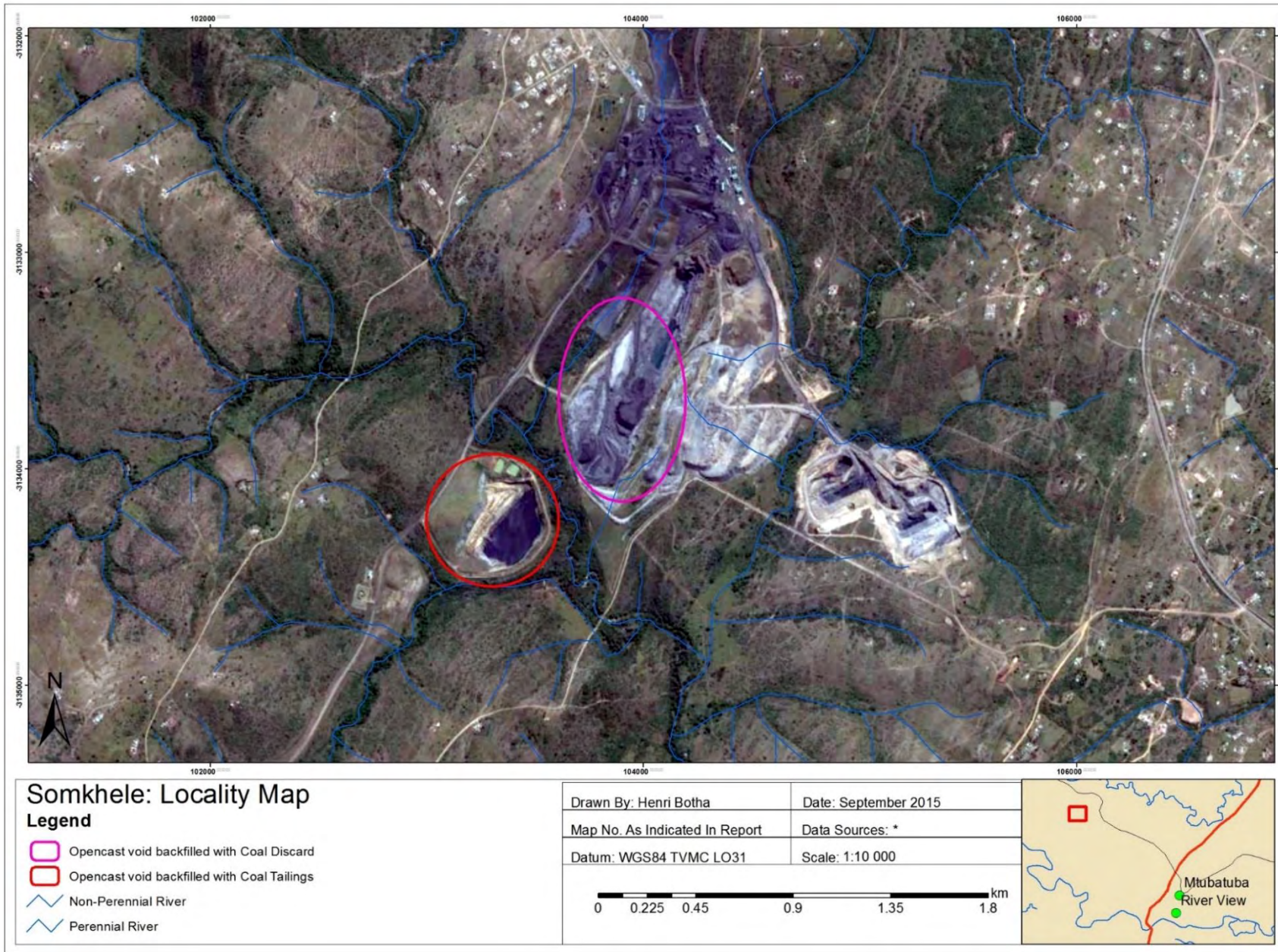


Figure 1-1: Locality map of Somkhele anthracite mine

2 LITERATURE REVIEW

2.1 COAL

2.1.1 Classification

Coals are composed dominantly of combustible organic matter and are the best known kind of carbonaceous sediment. Coal however, contains various amounts of impurities, known as ash, which are largely siliclastic minerals. Coal is defined as a readily combustible rock comprising more than 50% by weight and more than 70% by volume of carbonaceous material, formed from compaction or induration of variously altered plant remains similar to those of peaty deposits. Differences in the kinds of plant materials (type), in degree of metamorphism (rank), and range of impurities (grade), are characteristics of the varieties of coal (Boggs, 2011). The types of coal based on and the degree of coalification or carbonification and metamorphism are listed in Table 2-1.

Table 2-1: Classification of coal based on rank

| Rank | Description | Carbon content |
|----------------------|--|----------------|
| Peat | Unconsolidated, semi carbonized plant remains with high moisture. | Low |
| Lignite (brown coal) | Brown to brownish black with high moisture content. Usually retains the original woody plant fragments. Dominantly Cretaceous or Tertiary in age. | <69 |
| Bituminous coal | Hard, black coal that contains fewer volatiles and less moisture content than Lignite. Has a greater carbon content than Lignite and commonly displays thin layers of alternating bright and dull bands. | 69-86 |
| Subbituminous coal | Properties intermediate between lignite and bituminous coal. | <69 |
| Anthracite | Bright black, shiny rock that breaks with conchoidal fractures. Largely of Carboniferous age. | 86-98% |

| Rank | Description | Carbon content |
|-------------|---|----------------|
| Cannel coal | Non-banded dull, black coals that also breaks with conchoidal fractures, however they have bituminous rank and are much volatile than anthracite. | <69 |
| Bone coal | Very impure coal containing high ash content. | Low |

* Table compiled from (Boggs, 2011)

2.1.2 Distribution

Coals occur in rocks ranging in age from Precambrian to Tertiary, and peat equivalents of coal are present in Quaternary sediments. Coal originate in climates that promote plant growth under depositional conditions that favour preservation of organic matter. Although ancient coals accumulated at all latitudes from the equator to Polar Regions, most were deposited and is found in middle latitudes (Boggs, 2011). As plants and trees died, their remains sank to the bottom of the swampy areas, accumulating layer upon layer and eventually forming a soggy, dense material called peat. The peat being close to the water surface was then subjected to rapid burial because the accumulation rate exceeded the decomposing rate.

Over long periods of time, the makeup of the earth's surface changed, and seas and great rivers caused deposits of sand, clay and other mineral matter to accumulate, burying the peat. Sedimentary rocks (sandstone, mud rock and siltstone) were formed, and the pressure caused by their weight squeezed water from the peat material. Increasingly deeper burial and the heat associated with it, gradually changed the material to coal and anthracite (KET, 2014). The major coal resources in the world are in China, the United States, Russia, Germany, India, Australia, South Africa and Poland (Boggs, 2011).

In South Africa mountain-valley glaciers were widely developed around the Karoo basin. No less than six ice centres surrounded the basin. Along the western margin of the Karoo basin, the Dwyka tillite on the south is conformable on the Cape System, but northward progressively overlaps successively older strata. The primary cause of coal deposition on the eastern side of the continent, KZN and Mpumalanga, is related to the main requisite for both tillite and coal formation in a cool climate with large amounts of precipitation. Heavy rainfall takes place where moisture bearing winds associated with warm ocean currents intersects dry cool polar winds. The heaviest precipitation in intermediate latitudes takes place throughout times immediately preceding glacial maximum events. Because of the earth's rotation the equatorial currents move from east to west, and moisture bearing currents move from the equator towards both the poles along the eastern margins of the continent. Due to these current heavy precipitation is caused causing luxuriant plant growth. The accumulation of vegetation in these marshy basins results in the formation of coal. Ocean-current patterns were thus required for the deposition of coal along eastern margins of continents (Meyerhoff and Teichert, 1971).

2.1.3 Chemistry of coal

According to Levine et al. (1982) coal is structurally very complex and organic material dominates, typically representing 85-95% (wt/wt) of a dry coal. These organic materials occur in various different petrographic types, called "macerals," which reflect the nature of the precursor plant material. Various inorganic materials, particularly aluminosilicates and pyrites (especially in high-sulphur coals), comprise 5-15% of the coal. Relatively small "nuclei" of aromatic and naphthenic rings are coupled to one another by "bridges" of aliphatic chains or heteroatoms. In addition to these covalent bridges, there are a significant number of polar groups such as hydroxyls (OH^-) that can contribute to the integrity of the coal structure by means of electrostatic binding. Oxygen appears in this structure in various chemical forms. Some oxygen's occur as substituents (in the form of carboxyl or phenol groups) attached at the edge of the nuclei. Others are buried as heteroatoms in aromatic or naphthenic rings. Still others occur as bridges between the nuclei as ethers. These types of oxygen functional groups strongly influence coal reactivity, and their relative numbers vary significantly as a function of coal rank. Figure 2-1 indicates the structure of bituminous coal.

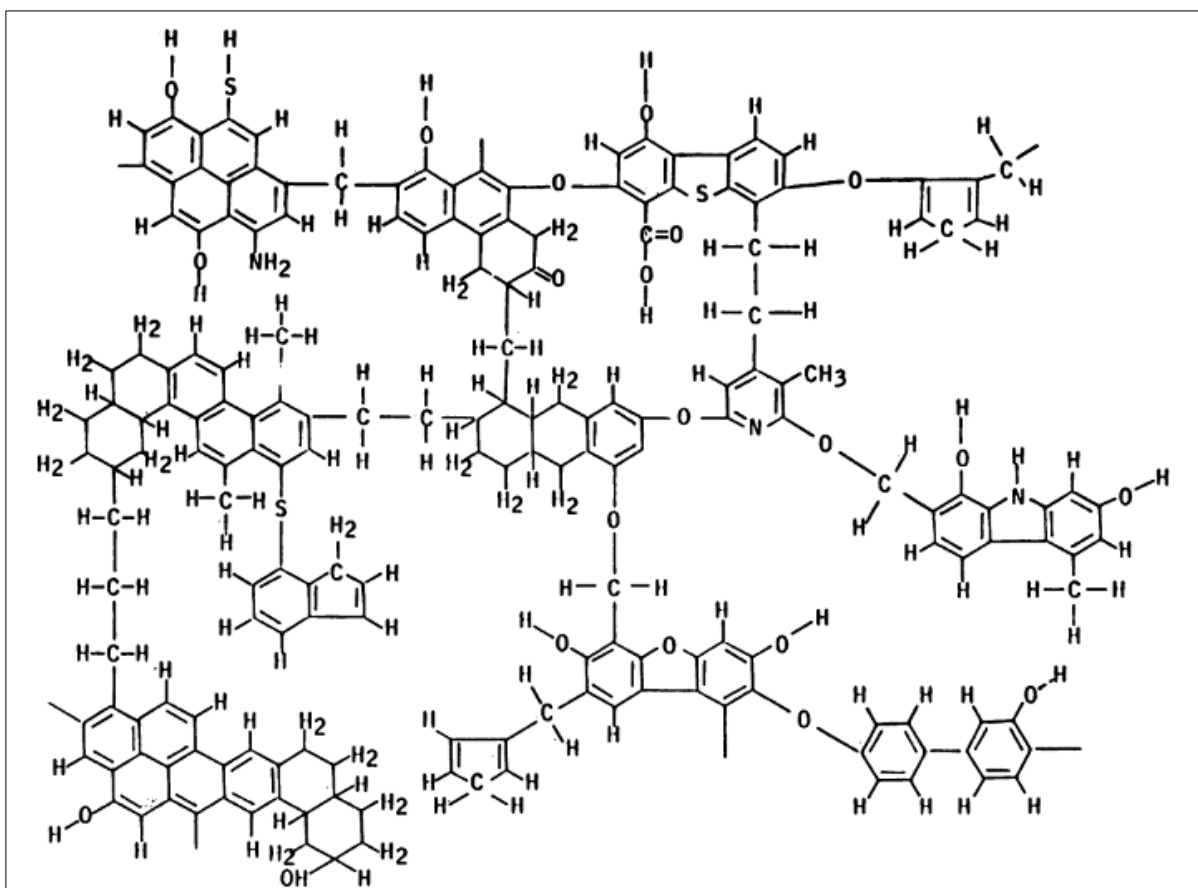


Figure 2-1: A representative structure of chemical groups in a bituminous coal. Retrieved from (Levine et al., 1982).

2.2 WASTE DISPOSAL AND PROBLEMS AT COAL MINES

2.2.1 Discard Dumps

One of the major causes of groundwater contamination is the disposal of waste materials directly onto the land surface. Coal discard is typically transported by excavation trucks, and dumped onto the land surface. The waste may occur as individual mounds or it may be spread out over the land. If the waste material contains soluble products, they will infiltrate the land and may lead to groundwater contamination.

According to Lloyd (2000), the typical raw coal from most South African collieries has about 23-35% ash, 22-24% volatile matter and 44-50% fixed carbon content. He also states that in contrast to this that the discard coal typically has well over 40% ash, 15-25% volatile matter and <35% fixed carbon content, and therefore discard coal can be described as a very poor material.

Land damage is a major impact of an opencast mine which is degraded by excavation, vegetation stripping, dumping of overburden material/waste rock and other accompanying operations. Disposal of solid waste generated by mining activities including overburden/waste rock, sub-grade ore and mineralized reject could result in environmental contamination and cause lowering of the groundwater level and deterioration in surface and groundwater quality. Leachate water and runoff water from overburden/waste rock dumps also contaminate nearby water streams. The principle pathways by which leached contaminants can enter into groundwater are leakage or spills from storage ponds, subsequent leaching to groundwater, storm water run-on/off uncontrolled leaching from heaps and dumps during mining or after closure (Tiwary et al., 2005).

Figure 2-2 illustrates the typical design of a coal discard dump and the hydrological processes associated with it. It can clearly be seen that the main contributing factor for seepage and percolation to the groundwater table is infiltration from rainwater. The infiltrating water enables contaminants to migrate through the discard dump as well as to undergo various oxidation and reduction reactions. The water not infiltrated is removed by evaporation/evapotranspiration and the remainder runs off the dump as surface water runoff. Due to the infiltration, the groundwater seepage inflow and physical size of the dump, a phreatic groundwater surface develops. The presence of water within the voids of a dump seriously affects the dumps stability depending on the quantity or elevation of the phreatic surface (limit of saturation) (IIT, 2015).

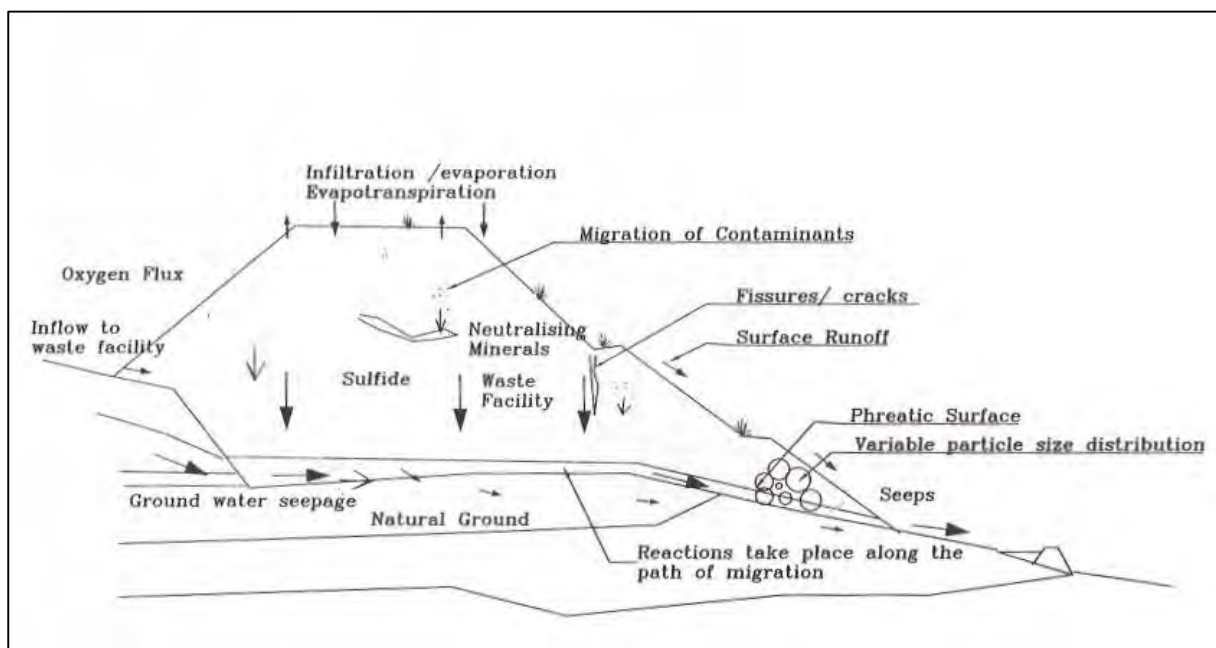


Figure 2-2: Discard dump hydrology retrieved from (James, 1997).

2.2.2 Tailings ponds

Coal tailings is a fluid produced by washing coal with water and chemicals prior to shipping the coal to market. This waste product cannot be recycled, or broken down into usable substances and is a major cause of concern. Storage procedures may not be environmentally sound over a long period of time. According to Fujii et al. (1984), a water based coal tailings has a composition composing of:

- At least one compound selected from the group consisting of a polyether polyol compound prepared by adding 4 to 800 moles, on the average, of ethylene oxide and/or propylene oxide to a compound containing at least one active hydrogen atom in the molecule, a compound prepared by partially or completely esterifying the hydroxyl groups of the compound, a compound obtained by partially or completely phosphating, sulphating or carboxyalkylating the hydroxyl groups of the compound or a salt thereof, a compound prepared by crosslinking the compound with a crosslinking agent, a compound prepared by reacting the compound with an epihalohydrin and an isocyanate-terminated compound prepared by reacting the compound with a polyvalent isocyanate,
- At least one surface active agent selected from the group consisting of a sulfonation product of naphthalene or its salt or an aliphatic aldehyde addition condensate thereof, an aliphatic aldehyde condensate of a sulfonic acid group-containing aminotriazine or a salt thereof and a sulfonation product of creosote oil or its salt or an aliphatic aldehyde addition condensate thereof,
- Water and a coal powder.

Tailings are pumped from the processing plant to settling ponds or dewatered and transported to discard dumps. Settling ponds are sometimes lined with clay to reduce leachate movement into the groundwater. In the absence of liners, trace elements and radionuclides in leachate can move into underlying soil and groundwater and are subject to a variety of chemical, physical and biological factors that govern their mobility and availability in the environment (Van Hook, 1979). Figure 2-3 illustrates a conceptual design of a typical tailings settling pond.

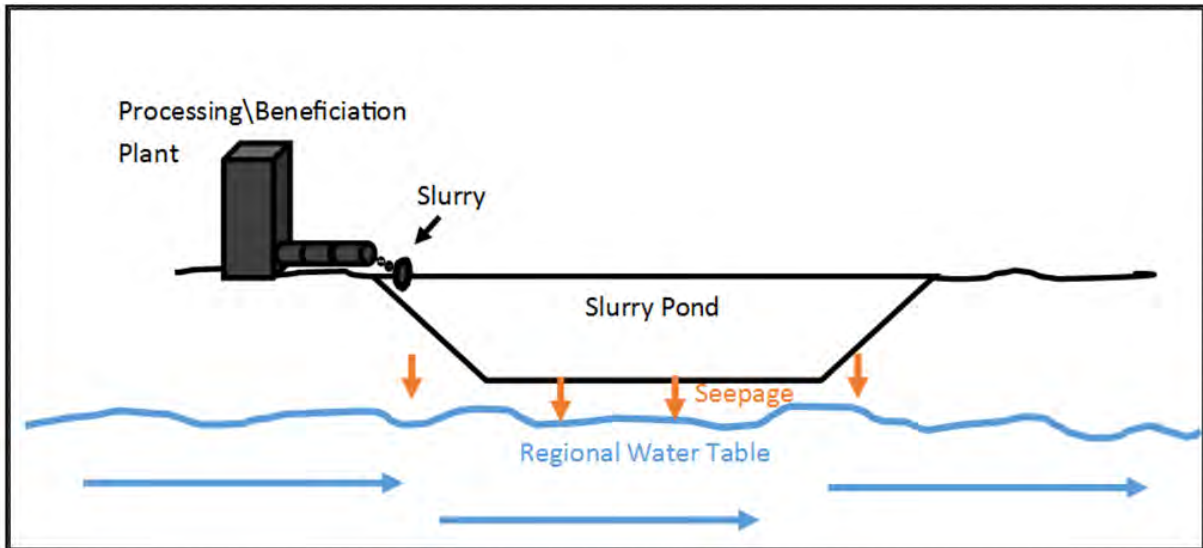
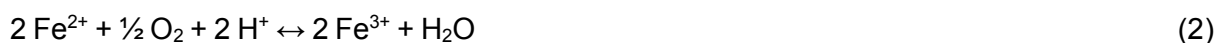
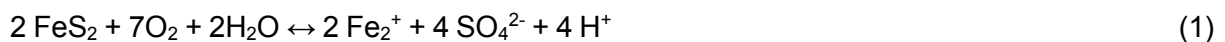


Figure 2-3: Typical hydrology of a tailings settling pond

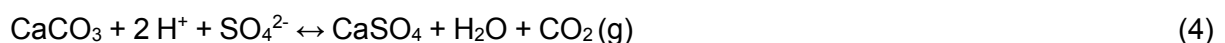
2.2.3 Groundwater and surface water pollution

Coal mining by opencast methods and storage of the waste products produced during the mining phase affects the environment of the area. In the process of mining huge amounts of water is discharged onto the surface, or abstracted from the ground in order to facilitate the mining operation. By doing this the water often is subjected to mixing, mining dust, used during processing and discarded along with waste material. This drastically changes the composition of the water and contaminates clean surface water and groundwater sources, increasing total dissolved solids (TDS), hardness, heavy metals and decreasing the pH. The primary concern for all coal mines is the production of acid from coal waste products.

In a mining environment acid drainage is primarily caused by oxidation of pyrite (FeS_2). The common chemical reactions for the reaction of pyrite with oxygen and water is indicated below (Appelo and Postma, 2007):



And in the presence of carbonate rich rock (SD):



From the reaction in Equation 1 and Equation 2 it can be seen that SO_4^{2-} , Fe^{2+} and H^+ (acid) are the dominant products that form due to pyrite oxidation. These are also the constituents which are monitored in a typical coal mine environment and indicates if AD or SD is taking place. Table 2-2 summarise some sources of groundwater and surface water pollution, typically encountered at coal mines.

Table 2-2: Sources of water pollution in coal mining areas

| Source | Description |
|--|--|
| Drainage from mining sites including AMD and mine water | Mine excavation typically have a water influx, either due to rainfall or to interception of ground water flows. This water is generally an unwanted feature of mining. The water can however, sometimes be used for processing and dust suppression and the rest may have to be pumped out. It can be contaminated by particulate matters, oil, grease, unburnt explosives and other chemicals. If the coal excavated coal seems contain high amount of pyrites the mine water may be acidic and could pollute nearby water stream after being discharged. |
| Leaching of contaminants from overburden, discard dumps and tailings/settling ponds. | In overburden and discard dumps which allows rainfall to drain into them, some toxic metals may be dissolved and leach from the heap into a nearby water course. The problem becomes more complicated when the dump contains pyritic waste. |
| Oil and fuel spills/workshop effluents | In the case of opencast mines, a large number of mining machineries and vehicles are used and every mine has its own workshop area. Workshop effluents contain high amounts of oil and grease which are released during washing of the machineries and vehicles. Sometimes spillage of oil and other toxic reagents occur which ultimately affects the water regime. |
| Sediment runoff | Runoff after a rain event can give rise to serious contamination problems. The disturbed land or active overburden dumps piled up near the mine are usually very susceptible to erosion and silting is thus a wide spread results. A variety of other contaminants may also be transported into water courses by runoff. Sometimes overburden dump material is piled along the bank of a river and thus increases the suspended particulate load into the surface water. |
| Sewage effluent from the site | The water used for domestic and sanitary purpose also becomes a source of contamination if not treated properly before discharge. It may be contaminated with detergents, suspended solids and organic matters. |

*Table compiled from (Tiwarly, 2001).

2.3 Co-Disposal

There are many different approaches to handle and dispose waste material. Among them are co-disposal (mixing of waste products before transport and disposal), co-displacement (fine and coarse waste products are transported separately and mixed prior to disposal) and co-mingling (coarse and fine waste are transported separately and mixed together after deposition). The co-disposal of fine coal tailings and coarse coal wastes by combined pumping through a pipeline followed by subaerial deposition is among the most promising of the coal-mine waste disposal options (Morris and Williams, 1997b; Pullum, 2007; Gowan and Williams, 2010). By co-disposing waste one makes much better use of the available storage on the mine site. This allows one to improve the water return from waste impounds and facilitate their rehabilitation (Morris and Williams, 1997c).

In Australia the technique was pioneered at the Jeebropilly Colliery near Ipswich, south-eastern Queensland, where it operates at as little as 15% of the cost of earlier conventional waste disposal. It is now also practised at Gordonstone and North Goonyella mines in central Queensland and is being considered at other mines in Queensland and New South Wales (Morris and Williams, 1997a).

According to Morris and Williams (2000), co-disposal beaches formed by down-slope deposition comprises a plunge pool at the discharge pipe, a relatively steep primary beach, and a relatively flat secondary beach adjoining a decant pool, refer to Figure 2-4. Secondary beaches comprises mostly fine wastes. Primary beaches comprise mostly coarse reject and have permeabilities much greater than those of the coal tailings. The primary beaches, thus drains very rapidly and are accessible to pedestrian and vehicles even during deposition.

Morris and Williams (2000) also states that the porosities (λ) of coarse coal waste deposits on primary co-disposal beaches formed by down slope deposition are generally comparable to those natural sediments and of the corresponding coarse coal rejects alone.

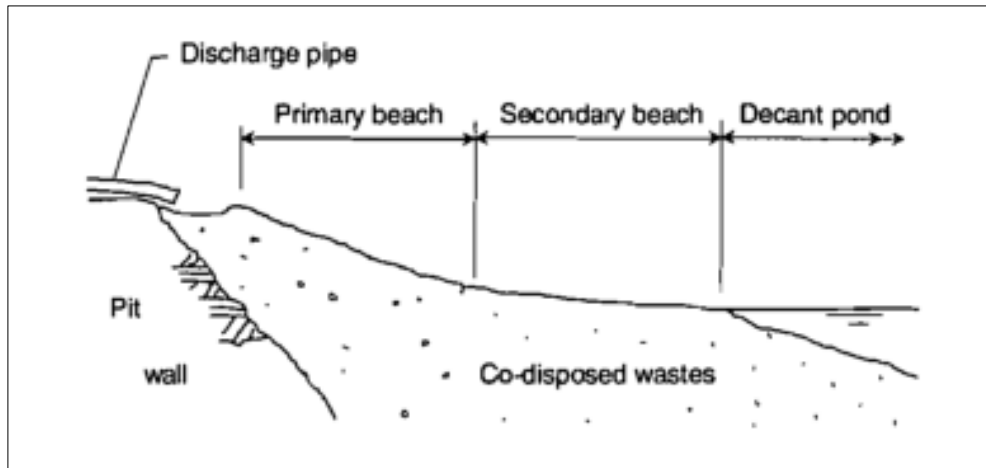


Figure 2-4: Representation of co-disposal beach. Retrieved from (Morris and Williams, 2000)

2.3.1 Material hydro physical properties

To achieve full potential of co-disposal, both the morphology and properties of the waste deposits must be known and understood.

2.3.1.1 Porosity

The arrangement and shape of soil particles help to determine porosity. Porosity is the amount of void space between soil particles (DWA, 2013).

The arrangement or packing of material particles plays a role in porosity. Particles can either be stacked in a pyramid shape sitting on top of two other particles (rhombohedral packing) or directly on top of each other (cubic packing). It is important to remember that the diameter size of the grains and the shape of the particles are not always spherical. Particles exist in many shapes and sizes and these shapes pack in a variety of ways that may increase or decrease porosity. Mixing of grain sizes and shapes (co-disposing) generally lowers porosity for the voids of bigger particles are filled with smaller particles.

According to Fetter (1994) well-sorted sand or gravel has a porosity ranging from 25-50 %, silt material has a porosity ranging from 35-50 % and clay a porosity ranging from 33-60 %. Though, the porosity of the clay material may be high the permeability of the material is very low and are in most cases classified as aquitards or aquicludes. Based on Morris and Williams (1997a) research, coarse wastes (discard) particle size typically range from 0.1-50 mm and fine coal tailings (tailings) wastes are typically <0.1 mm. Therefore, porosity of the coal waste material is very similar to that of natural occurring sand and clay materials.

2.3.1.2 Permeability

Permeability is the measure of ease for a soil or a rock to transmit a fluid (DWA, 2013). The pore space size and the interconnectivity of the spaces determine the permeability of a material. Water can move between granular voids and fractures, and the larger the pore space the more permeable the material. Permeability however, decreases in material which is poorly sorted. The reason for this is due to the smaller particles which fill the openings created by the larger grains (Morris and Williams, 1997c).

According to Fetter (1994) the permeability of well sorted material (discard and larger particle material) ranges from 10^{-2} to 1 m/day and clay to silty sands (tailings material) range from 10^{-9} to 10^{-4} m/day.

2.3.1.3 Specific yield

Water trapped within the pore spaces of material is not always part of the moving groundwater. Similar to surface tension and adhesion properties of water onto glass, water also clings to soil particles. The specific yield is therefore, the volume of water that drains from saturated rock/material due to gravity to the volume of rock (DWA, 2013).

Specific yield is influenced by grain size and the smaller the grain size within the material the lower the specific yield. Therefore, smaller particles have a greater surface area and will retain more water for the water will remain behind clinging to the small particle surfaces. According to Fetter (1994) coarse material has an average specific yield of 22-27% and fine-very fine material has an average specific yield ranging from 2-18 %.

2.3.1.4 Co-disposal concept

Figure 2-5 illustrates the co-disposal concept where tailings and discard (whether in a rhombohedral or cubic packing) is mixed to form a material with different bulk physical properties. Poorly sorted discard material can be classified as a material with a high porosity (n), high permeability (K), high effective porosity (n_e) and a low water retention capacity. Well sorted discard material can be classified as a material with a medium porosity (for most of the voids are filled with smaller grains reducing void space), medium permeability, medium effective porosity and medium water retention capacity (smaller adhesive clay/silt fraction retaining water in the pores). Tailings before compaction/settling tends to be in a flocculated state. The material is much more cohesive (small platy particles) than discard material increasing the water retention capacity of the material. Therefore, the tailings (coal slurry) can be classified as a material with a high porosity, low permeability, low effective porosity and high water retention capacity.

In a co-disposal state the bulk physical attributes of the material is changed. The change is a net result of the particle distribution and hydro physical properties of the different material types which are mixed together to form a co-disposed material. The co-disposed material has a low permeability (for the pores previously filled with air is now filled with silty/clay material), high porosity (the attributes are inherited from the tailings), low effective porosity (interstices that are connected are decreased) and high water retention capacity (adhesive properties of clay/silty is inherited from tailings material).

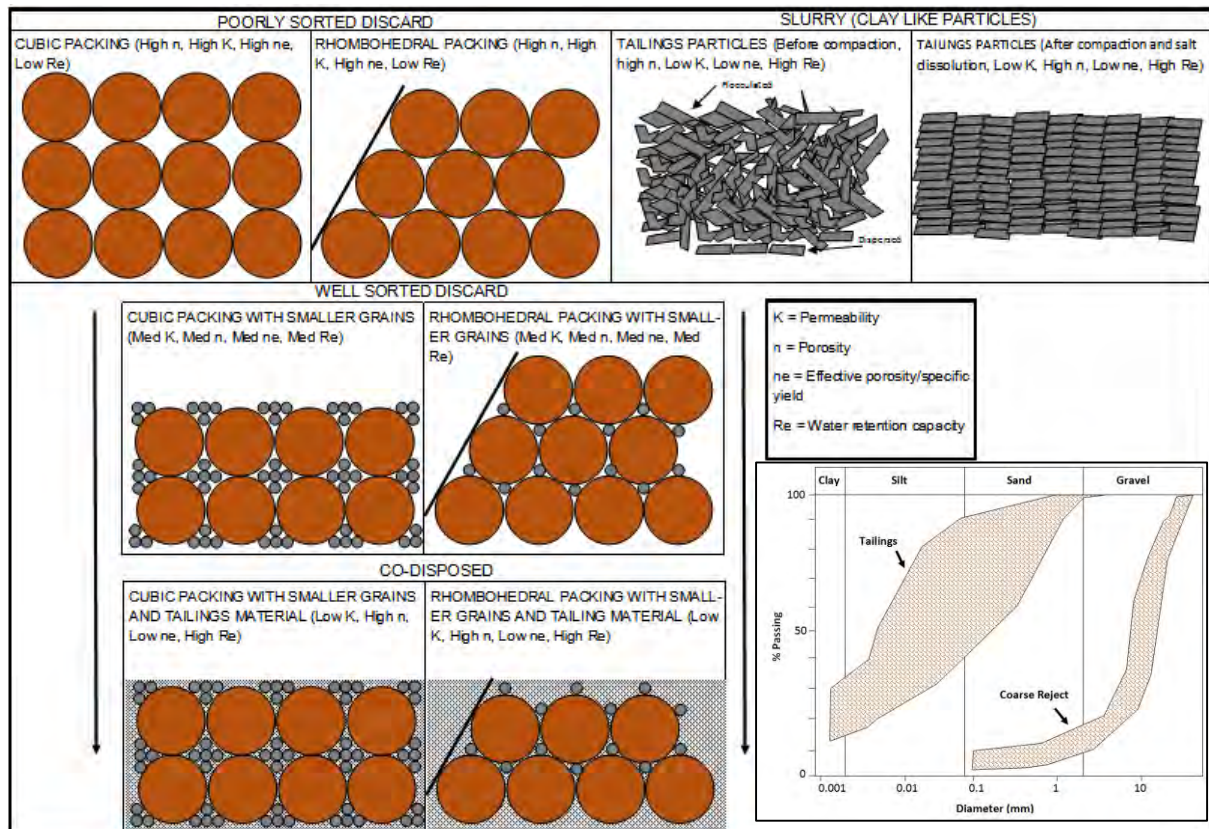


Figure 2-5: Rhombohedral vs cubic packing vs co-disposed (adapted from Morris and Williams, 1997a)

2.4 GROUNDWATER MODELLING

Simulations of a groundwater system refers to the development of a model which is used to mimic the behaviour and the appearance of an actual aquifer system. These models can either be physical, analog or mathematical. Table 2-3 outlines the different modelling approaches.

According to James and Charles (1980); Kresic (2006); Wang and Anderson (1995) numerical models are most appropriate for solving general problems involving aquifers having irregular boundaries, variable pumping and recharge rates, different evapotranspiration rates, heterogeneities as well as numerous surface water-groundwater interaction zones.

Table 2-3: Model approaches

| Model Approach | Description |
|-----------------------------|--|
| Physical Models (sand tank) | Physical models are physically constructed (laboratory sand packs) in order to simulate groundwater aquifer flow characteristics. These models are down scaled to laboratory level however, usually offer intuitive insight into aquifer behaviour. |
| Analog Models | <p>Analog models is subdivided into viscous fluid models and electrical models. These models operate by means of differential equations derived from basics principles of physics. Electrical, fluid flow or the flow of heat through a solid operate on similar physical principles.</p> <p>Viscous fluid models also known as parallel plate models. These models operate on a principle where a fluid more viscous than water is made to flow between two closely spaced parallel plates orientated either horizontally or vertically.</p> <p>Electrical analog models consists out of boards wired with electrical circuits working on the principle that groundwater flow is analogous to the flow of electricity. The analogy is expressed similar to Darcy's law for groundwater flow and Ohm's law for the flow of electricity. Changes in voltage in an electrical analog model are analogous to changes in groundwater head. The biggest drawback of these electrical models have to be developed for every new unique aquifer.</p> |
| Mathematical Models | <p>A mathematical model consists out of a set of differential equations that are known to govern the flow of groundwater in an aquifer system. These models may be deterministic, statistical or a combination of the two. The early stages of developing a mathematical model begins with compiling a conceptual model of the physical behaviour of a system and how the system operates. Once the conceptual model is created the physics are translated into mathematical terms and incorporated into either an analytical or a numerical model.</p> <p>Analytical models make use of simplified equations to obtain solutions. These models are fairly restrictive for many analytical solutions require that the flow medium be isotropic and homogeneous.</p> <p>Numerical models make use of matrix solver equations to numerical approximate a solution to a given groundwater scenario. Numerical models are further divided into two types, namely finite difference and finite element models. Both model types consists out of nodal points which are superimposed over a problem domain however, finite element consists out of triangular and quadrilateral elements while finite difference use block-centred or mesh centred nodes in a grid like spacing.</p> |

*Table adapted from James and Charles (1980); Wang and Anderson (1995).

2.4.1 Model types

Numerical groundwater models can generally be divided into a subset of four groups (Kresic, 2006; SWS, 2011; James and Charles, 1980), namely groundwater flow models, solute transport models, heat transport models and deformation models. This subgroup of model types can further be subdivided into those describing fractured and those describing porous media. These models can all be used to estimate aquifer parameters. In addition, there are models which are able to solve multiphase flow (unsaturated modelling) and multi-fluid flow (two mediums with a different viscosity) problems. Table 2-4 list the four general model types used for groundwater modelling.

Table 2-4: General model types used for groundwater modelling

| Type | General Description |
|-------------------------|---|
| Groundwater flow models | Groundwater flow models solves water supply problems in terms of hydraulic head which is normally derived from a single equation. These models can be used for water supply, regional aquifer analyses, near borehole performance, groundwater/surface water interactions and dewatering operations. |
| Solute transport models | Solute transport models solves concentration equations of a chemical species in tandem to that of the groundwater flow (hydraulic head) equation. These models are normally used to simulate water quality. Furthermore, these models are most often used to model sea water intrusions, landfills, waste injections, radioactive waste storage, holding ponds and any other source of groundwater pollution. |
| Heat transport models | Heat transport models solves problems involving heat in addition to the groundwater flow equation, very similar to the solute transport model, but in terms of heat. These models are most often used to model geothermal, thermal storage, heat pump and thermal pollution. |
| Deformation models | Deformation models combines a groundwater flow model with a set of equations that describe an aquifers deformation processes. |

* Adapted from James and Charles (1980); Kresic, (2006) and SWS (2011).

2.4.2 Numerical groundwater modelling

A geohydrological model is a representation of a system and begins when one formulates a concept of a hydrological system. Most groundwater modelling objectives are aimed at predicting the consequences of a proposed action and can be used in an interpretive manner or to study processes in generic geology setting (Anderson and Woessner, 1992; Spitz and Moreno, 1996). A typical model application protocol diagram is indicated in Figure 2-6 and the processes involved are further explained in this section.

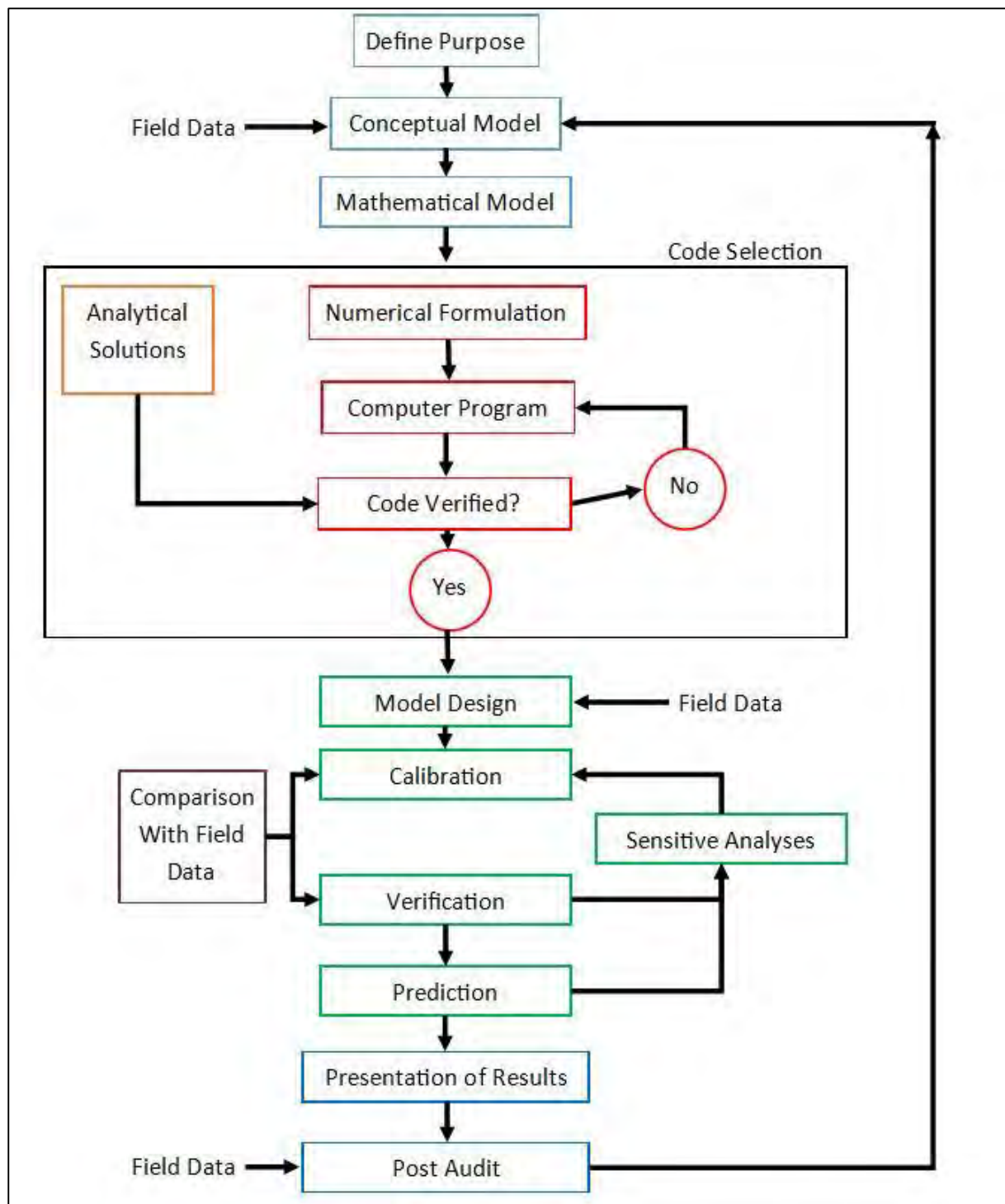


Figure 2-6: Modelling protocol diagram (adapted from Anderson and Woessner, 1992)

The modelling protocol further explained (adapted from Anderson and Woessner, 1992; Rapantova et al., 2007):

1. Purpose: The purpose helps determine what code will be selected and what governing groundwater equation will be solved.

2. Conceptual Model: In this step the model system boundaries and hydrostratigraphic units are identified. Aquifer parameters, hydrologic stresses and field data are assembled as well as information on the water balance. This step usually goes hand in hand with a field site visit.
3. Computer Code: The algorithm which will solve the mathematical model numerically is identified. The generated numerical solution is compared to other analytical and numerical solutions as part of the code verification process.
4. Model Design: In this step the conceptual model is put into a suitable form for modelling. A grid is designed, time steps are selected, boundary and initial conditions are specified, and preliminary aquifer parameters and hydrologic stresses are assigned. Transport model modules are also selected and initial concentrations as well as contaminant types are specified.
5. Calibration: In this step the model is calibrated to produce an output which reproduces field-measured heads and flows. Calibration is done by trial and error adjustment of parameters or by using an automated parameter estimation code (e.g. PEST).
6. Sensitive Analysis: A sensitive analysis is performed in order to establish the effect of uncertainty on the calibrated model. The uncertainty owing to the inability to define the extent spatial distribution of parameters in the problem domain is a common model influencing factor.
7. Model Verification: In this step a second set of field data is produced in order to establish greater confidence in the model by making use of the calibrated parameters and stresses.
8. Prediction: In this step the response of the system to future events is quantified. This is achieved by running the model with the calibrated values for parameters and stresses.
9. Predictive Sensitive Analysis: This is done to quantify the effect of uncertainty in parameter values on the prediction.
10. Presentation: All the modelling protocol steps are summarised and a clear presentation of model design and results is displayed.
11. Audit: Updated field data is input in the model to produce similar but updated output data. In this step the model grid may be refined and hydraulic parameters may be adjusted to update the model.

3 METHODOLOGY

3.1 APPROACH

The potential environmental impact of co-disposed coal wastes versus that of separately disposed coal waste products (conventional methods), was assessed by means of a case study. The main objective was to geochemically assess the different waste disposal scenarios, to develop a conceptual model and to construct a numerical model which mimics and illustrates the potential leachate released into an aquifer system from the disposal method implemented. It was decided to construct a conservative steady-state flow model and transport model to visually illustrate the potential environmental impact from the total and average salt loads of the co-disposed, tailings and discard waste materials. Therefore, the transport model is a worst case model reproducing the results seen on a laboratory level for the geochemical tests performed.

The methodological approach is subdivided into three phases namely, the field work, sampling and data gathering phase; the laboratory testing, data interpretation and conceptualisation phase; and the numerical modelling phase.

1. Phase 1: Field work, sampling and data gathering

- a. Coal discard and tailings material was collected from the opencast pits which are separately being backfilled with the coal waste material. Approximately 25-50 kg of both samples were collected in separate containers and sealed to keep oxygen out. The samples were shipped to a laboratory for geochemical analysis.
- b. A hydrocensus was conducted within a 2 km radius of the opencast pit. The objective was to obtain groundwater and hydrochemistry data for the general area. The Department of Water and Sanitation (DWS) National Groundwater Archive (NGA) database indicated that there are some NGA boreholes present in the area (NGA, 2015). Unfortunately none of these boreholes could be located. However, a few old exploration boreholes were found and groundwater level and chemistry data was obtained.

- c. During the data gathering event geophysics was conducted. The geophysical equipment used was a proton precession magnetometer (Mag) as well as an electro-magnetometer (EM). A series of traverses were walked downstream of both opencast pits backfilled with the coal waste material. The objective was to obtain structural geological (faults, dolerite sills and dykes) information around the opencast pits. These geological structures are known to be preferential flow paths for groundwater migration (Adams et al., 2001) and hence if pollution is to occur it will most likely migrate along these paths.
- d. After the geophysical data was retrieved a series of 5 monitoring boreholes were sited and drilled at the approximate locations of the identified anomalies. The boreholes were all drilled to a depth of 50 mbgl and perforated casing was installed at the identified seepage zones and water strikes. The objective of these monitoring boreholes was to obtain site specific water level data as well to monitor for pollution already taking place as a result of the conventional disposal techniques implemented by the mine.
- e. Approximately 1 month after drilling, a series of constant rate pump tests were conducted. Pump tests were only conducted on three boreholes located downstream of the opencast pit backfilled with coal tailings. The aim of the pump tests was to establish the aquifer parameters in term of hydraulic conductivity (K) and transmissivity (T).
- f. A literature review was conducted to retrieve and interpret hydrological, geohydrological, geological and geochemical information used in this dissertation.

2. Phase 2: Laboratory testing and field data interpretation

- a. Co-disposal was simulated on a laboratory level and the waste products were subjected to a series of geochemical tests. Both tailings and discard material was submitted for x-ray diffraction (XRD) tests to identify the major and accessory minerals comprising the waste. Static tests, which included acid base accounting (ABA), net acid generation (NAG) and peroxide leach tests were conducted. Additionally, kinetic column leach testing was conducted to assess the leachate potential over a period of 25 weeks. The results were screened as described by Lapakko and Lawrence (1993) and Prince (1997). The results were compared in terms of acid potential, neutralisation potential, leachate potential (salt load) and leachate quality.

- b. Groundwater level and hydrochemistry data was collected on a quarterly basis for a year and a half after drilling of the monitoring boreholes. Additionally all existing groundwater level and chemistry data, dating back to 2008 were obtained. The existing and newly obtained hydrochemistry data were integrated into a single chemistry database. All the hydrochemistry and groundwater level data relevant to the study area, is used in the numerical groundwater flow and transport model.
- c. Geophysical data was analysed in Excel. EM and Mag data was processed and were superimposed onto single graphs. Each graph represented the starting point and ending point, as well as the distanced walk with each geophysical instrument. The anomaly peaks were individually analysed with the help of literature (Haigh and Smith, 1975; Dondurur and Pamukcy, 2002).
- d. Pump test data was analysed by using software driven techniques. Excel was used for manual analysis and Schlumberger Aquifer Test automatic solver software was also used. Theis, Cooper-Jacob and Theis Recovery solver equations and techniques as described by Kruseman and De Ridder (2000) was implemented to calculate hydraulic conductivity (K), transmissivity (T) and Storativity (S) parameters for the aquifer. For the Excel analysis only Cooper-Jacob methods were used. S-values were compared to literature S-values for the area (DWAF, 2006). All the S-values were found to be an order from actual values. This is a result of not being able to monitor drawdown in a observation borehole while pumping the test borehole. Storativity is distance depended and therefore, calculated values were substituted with literature values in the groundwater flow model.
- e. Mean annual rainfall (MAP), groundwater recharge and mean annual evapotranspiration (MAE) values were obtained from the Groundwater Resource Assessment II (GRA2) study completed for South Africa in June 2005. Additional data was obtained from the Water Resources of South Africa WR2005 Information System as well as the Department of Water and Sanitation Hydrological Data Web Site. No groundwater recharge methods were applied for all the necessary data is available for the area.
- f. Groundwater-surface water interactions were established by implementing Darcy's equation. Furthermore, the head differences between the boreholes in the study area were determined to establish predominant groundwater flow.

- g. A conceptual model was developed. The model is derived from both the field and literature collected data. Part of the conceptualisation process was to pre-determine the potential receivers of pollution within the vicinity of the opencast pits. The receivers were identified with the aid of the Best Practice Guidelines G4 risk based approach for impact prediction (DWA, 2008). In implementing this approach it was necessary to define both the source and pathway(s) to the identified receivers. The components are classified as follows:
- i. The source in the context of predicting an impact on a water resource at a mining site is defined as any mining process which could potentially be a risk of impact to a water resource on or at a mine. The source term may include, underground mine voids, opencast pits, waste rock dumps, coal discard dumps, tailings disposal facilities, ore and product stockpiles, neighbouring mines and any other potential impact source (DWA, 2008). In the case of the conceptual model for Somkhele, the Sources are the opencast pits into which coal waste is being backfilled. Though the material characteristics (leachate potential) may be different for each waste product, the source remains at the same point of origin.
 - ii. The pathway in context of predicting an impact on a water resource at a mining site is defined as the movement of contaminants through the vadose (unsaturated) zone, through an aquifer, through surface runoff in storm water, through mining voids (underground or opencast) and migration of sulphate minerals or other contaminants as an airborne agent (dust) (DWA, 2008). In the case of the conceptual model for Somkhele the Pathway refers to the aquifer system through which seepage or solutes can migrate.
 - iii. The receiver in the context of predicting an impact on a water resource at a mining site, is defined as all water users (receptors) within the vicinity of the impact source. This includes groundwater users abstracting contaminated groundwater through a borehole for domestic, irrigation or livestock use, aquatic fauna and flora in a receiving watercourse (DWA, 2008). There are no groundwater users within the vicinity of the opencast pits. Therefore, receivers in the study area are the non-perennial streams flowing through the area.

3. Phase 3: Numerical modelling phase

- a. A groundwater flow and mass transport model was created from the conceptual model. The groundwater flow model was ran and calibrated in steady state via trial and error methods (changing one parameter at a time and comparing the output). A sensitive analysis was then performed on the steady state flow model. A conservative transport model was set up to illustrate the potential impact of co-disposed coal waste into both opencast pits in comparison to disposing the waste products separately (as is currently practiced at the mine). The transport model simulation is based on the sulphate trends observed during the kinetic column leach tests. Constant concentrations were estimated and assigned to time steps within the model to mimic the laboratory data obtained from the kinetic leach tests.
- b. The extent of the seepage plumes produced, the geochemical attributes of the material producing the plumes, the seepage quality as well as all the characteristics of co-disposed and separately disposed coal waste products were assessed and the hypothesis was tested. It was discovered that most of the hypotheses was proven by the kinetic geochemical tests performed in the laboratory. Therefore, the numerical model was created to illustrate the potential reduction in the total pollution salt loads to an aquifer system if co-disposal is implemented.

3.2 LIMITATIONS

The project had a few limitations and are recorded as follows:

- Budget did not allow for in-situ geotechnical testing of the waste material. The hydrological and geotechnical properties were therefore, derived from literature and tests conducted on the same or similar material in other studies.
- Budget did not allow for the exploration and geochemical testing of different co-disposal mixing ratios. A single ratio had to be decided on and the dissertation was tested based on the outcome.
- Kinetic leach tests take a long time to be conducted and are expensive. Ideally different co-disposal ratios in different columns which accounts for numerous and intensive testing would have been ideal. However, budget only allowed for three kinetic leach tests to be performed.
- There are some unknowns with regards to:

- Aquifer parameters: Pump test were only performed on three boreholes due to limited time and budget. The pump used was also not strong enough to reduce the head enough in the pumping well to be observed in observation boreholes. This created problems in accurately determining the storativity (S) aquifer parameters. Storativity is distance dependant.
- Geological structures: Due to the thick vegetation cover, fences and somewhat irregular shapes of the opencast pits in the study area, it was very difficult to walk long geophysical traverses. Therefore, corrections in drift for both the EM and the Mag had to be made. This caused some uncertainty with regards to the exact location of supposed sub surface structures.
- Groundwater flow model: Due to the alterations of the topography in the mining area it is anticipated that the natural groundwater flow in the area is disturbed. Phreatic surfaces within the overburden material as well as the closing of natural fractures due to explosive forces could have changed the natural groundwater flow paths. Therefore, the simulated flow and transport movements observed in reality could be different than what is simulated even though the model is calibrated.

4 STUDY AREA

4.1 MINING SITE

4.1.1 Site Layout

The Somkhele mining area consists out of three mining rights areas, and they are referred to as Area 1, Area 2 and Area 8 (Luhlanga), refer to Figure 4-1.

Area 1 is situated to the south, towards the Umfolozi River. The area has four opencast pits namely North Pit 1, North Pit 2, East Pit and South Pit. Limited surface infrastructure is found within Area 1 and only haul-roads, pipelines and return water dams are present.

Area 2 is situated in the northern part of the overall mining area and it is here where most of the surface infrastructure is located. There are three pits within Area 2, and they are called Pit A, Pit B and Pits C, D and E (Pits C, D and E are located directly adjacent to each other and forms a larger pit). Infrastructure within Area 2 includes 4 pollution control dams (PCDs), 4 settling ponds, 3 return water dams, 1 storage dam (the Mnyenge clean water dam), 4 stockpiling areas, 4 conservancy tanks, 1 dust suppression plant, and 3 processing plants.

Area 8 lies contiguous and to the east of Area 2 and is sub divided into the Luhlanga and Kwaqubuka areas.

Active open-pit, truck and shovel mining methods are currently taking place in Area 1 and Area 8. Area 2 has completely been minded out and the opencast pits are being used to backfill coal discard and tailings material.

4.1.2 Project Boundaries

The project boundaries are localised to the opencast pit voids which are being backfilled with tailings and discard material. The study area boundaries are represented in Figure 4-1 and includes both opencast pits which are located in Area 2.

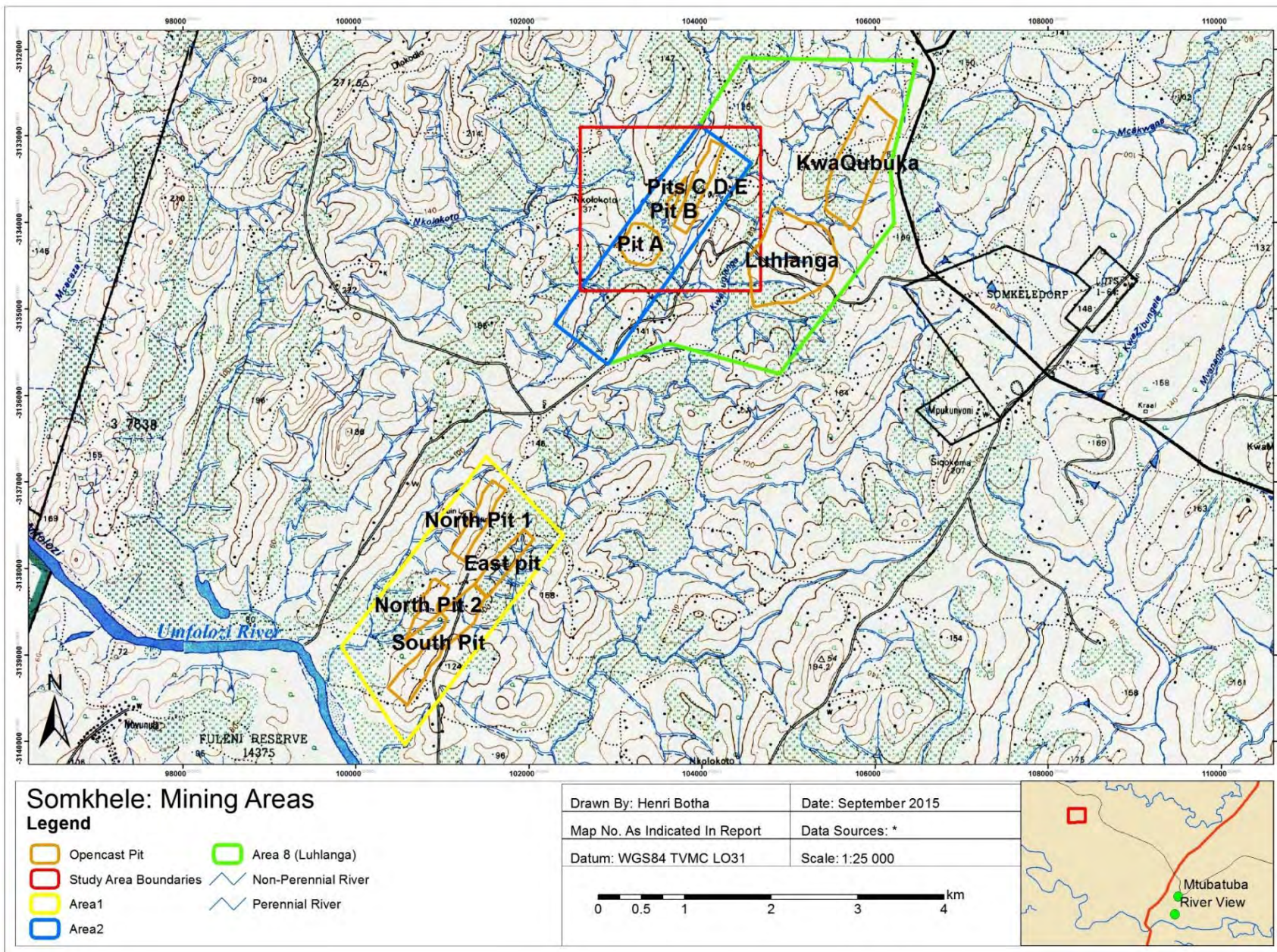


Figure 4-1: Somkhele mining areas and study area boundaries

4.2 MINING OPERATIONS

Somkhele is a typical opencast mine, which involves a type of strip mining procedure in which the ore deposits extend very deep in the ground in a specific dip direction, necessitating the removal of layer upon layer of overburden and ore. Because open-pit mining is employed for ore deposits at a substantial depth underground, it usually involves the creation of a pit that extends below the groundwater table. In this case, groundwater must be pumped out of the pit to allow mining to take place.

The use of heavy machinery is the most common means of removing overburden. Open-pit mining often involves the removal of natively vegetated areas, and is therefore among the most environmentally destructive types of mining (Bastian et al., 2006).

The mining operations can be grouped into several phases, each with its own sets of environmental impacts, and this explains the entire life cycle of a typical coal mine. The phases of mining and their impacts are listed in Table 4-1.

Table 4-1: Typical phases and impacts of a coal mine

| Phase | Procedure | Environmental Impact |
|---------------|--|---|
| Exploration | This phase includes surveys, field studies, and drilling test boreholes and other exploratory excavations. The aim is to obtain information about the location and value of the mineral ore deposit. | The exploratory phase may involve clearing of wide areas of vegetation and soil layers. This may also change natural runoff patterns. |
| Development | The construction of access roads, either to provide heavy equipment and supplies to the mine site or to ship out processed Coal/antracite. | Site preparation and clearing. If a mine site is located in a remote, substantial environmental impacts, especially if access roads cut through ecologically sensitive areas or are near previously isolated communities. |
| Active mining | The active mining consists of two phases: the extraction (excavation) and beneficiation of a metal from the earth. | Formation of overburden rock dumps, dewatering and dust generation all contribute to groundwater and surface water pollution. Furthermore, dewatering has the potential to lower the aquifer water levels within some extent outside the active dewatering zone. Water users within the zone of influence can potentially have declining borehole yields. |

| Phase | Procedure | Environmental Impact |
|---------------------------------------|---|---|
| Disposal of overburden and waste rock | The overburden must be moved or excavated to allow access to the coal seams. The quantity of overburden generated by mining is enormous. | High-volume wastes, sometimes containing significant levels of toxic substances. These are usually deposited on-site, either in piles on the surface or as backfill in open pits. The wastes have the potential pollute the groundwater and surface water within the disposal areas. |
| Ore extraction | Extraction of the mineral ore is made using specialized heavy equipment and machinery, such as loaders, haulers, and dump trucks, which transport the ore to processing facilities using haul roads. | This activity creates a unique set of environmental impacts, such as emissions of fugitive dust from haul roads. Furthermore, pit expansion by using explosives could potentially change preferential flow paths within the surrounding. The shock waves produced from the explosives are large enough to close and open cracks in the surrounding rock. This can have an impact on groundwater and pollution movement. |
| Beneficiation | Grinding (or milling) of the anthracite into smaller particles as well as washing of coal. Coal beneficiation largely depends on gravity difference of coal and ash particles after passing through sizing. | Particulate matters and gaseous pollutants are generated causing a serious air pollution problem in the area. Besides, coal washeries release very large amount of solid and liquid waste which could potentially cause serious groundwater and surface water pollution. |
| Discard and tailings | Ore which has been processed is known tailings or discard. Discard are is the larger quantity of rock which was discarded, as the word suggests, during processing. Tailings is the smaller particles which was mixed with water after and during processing. | Discard is hauled to discard dumps and left to be exposed to the elements (rain, oxygen, sunlight). Tailings is pumped to a settling pond and can often be toxic due to the presence of un-extracted sulfide minerals. Leaching and runoff from the discard dumps as well as tailings ponds have the potential to pollute groundwater and surface water. |

| Phase | Procedure | Environmental Impact |
|------------------------------|---|--|
| Site reclamation and closure | When active mining ceases, mine facilities and the site are reclaimed and closed. | Mines are notorious for their immense impact on the environment often makes impacts only during the closure phase of the mine. Long term acid leaching, mass wasting as well as dust migration can persist for decades and even centuries. The impact on the groundwater and surface water in a mining region can be significant if no rehabilitation or mitigation measures are implemented. Issues relating to mine water decanting can further significantly impact water quality in the mining area. |

* Table compiled from Anon (2014)

4.3 GEOGRAPHICAL SETTING

The following sections discusses geology, geohydrology and the environmental attributes of the study area.

4.3.1 Geology

The Somkhele Anthracite Mine is situated within the Emakwezeni Formation of the Karoo Supergroup, refer to Table 4-2. The Karoo Supergroup comprises the Dwyka, Eccca, Baufort and Stormberg Groups. The Eccca Group comprises the Pietermaritzburg, Vryheid and Volksrust Formations, of which the Vryheid and Volksrust Formations hosts most of South Africa's coal deposits. The Vryheid Formation comprises both coarsening-upward deltaic cycles and fining-upward fluvial cycles, with the latter occurring largely in the middle part of the formation. The regressive Vryheid Formation is sandwiched between the mudrocks of the Pietermaritzburg and Volksrust Formations and is the most widespread lithology in the Hluhluwe-iMfolozi Park where it is downthrown against the older Natal- and Dwyka Group rocks (Johnson et al. 1996).

This formation has been subdivided into the lower sandstones, coal zone and upper sandstone and comprises medium- to coarse-grained sandstone, grey micaceous shale and coal. These sediments were deposited in meandering to braided stream environments and host the seams of the Natal Coalfield in the Natal Midlands. Around Somkhele however, these coal seams occur as occasional, thin and continuous bands and beds less than a meter in thickness. The Volksrust Formation overlies the Vryheid Formation and consists of a monotonous, occasionally bluish mudstone and shale. The Volksrust Formation immediately underlies the Emakwezini Formation of the Bafort Group that hosts the coal in the Somkhele Coalfield (Botha and Singh, 2012; Schluter, 2008).

The Emakwezini Formation comprises mainly of grey, greenish-grey and brown mudstones with interbedded coal seams, medium to coarse grained sandstones and may contain plant fossils and lenses of limestone. The mining of coal within this succession is complicated by the steeply dipping strata and the block faulting which disrupts the continuity of the coal zone. The Emakwezini Formation is conformably overlain by the late Triassic Molteno Formation, which comprises alternating medium to coarse-grained sandstone with secondary quartz overgrowths and thin grey mudrocks. It is then conformably overlain by the Elliot Formation, which predominantly consists of red and purple mudstone, medium-grained sandstone with calcareous concretions, shale and siltstone. The Late Triassic–Early Jurassic Clarens Formation consists of yellowish grey, pale orange or pink, very fine-grained aeolian sandstone that represents the final phase of Karoo basin sedimentation (Botha and Singh, 2012).

The sills and dykes that intrude the Emakwezini Formation and locally affect the coal quality preserve the intricate magma feeder systems to the Drakensberg Volcanic Groups. Later normal faulting associated with rifting on a geocline introduced the moderate easterly dip to the strata and created a succession of fault bounded blocks in which the coal bearing strata is repeated. The repetitions create multiple exploration and open pit mining opportunities.

Table 4-2: Stratigraphy of the study area

| | Group | Formation | Rock Type | Thickness |
|------------------|-----------------|----------------------------|--|-----------|
| Karoo Supergroup | Stormberg Group | Drakensberg Volcanics | Lava (Amygdaloidal) | + 2000m |
| | | Clarens Formation | Aeolian Sandstone | < 40m |
| | | Elliot Formation | Mudstone | ±250m |
| | | Molteno Formation | Sandstone | ±100m |
| | Baufort Group | Emakwezini Formation | Sandstone, Siltstone, Mudstone, Coal | 500-600m |
| | Ecca Group | Volksrust Formation | Shale | ±140m |
| | | Fryheid Formation | Sandstone, Carbonaceous Shale, Coal, Gritstone | ±500m |
| | | Pietermaritzburg Formation | Shale and Sandstone | ±200m |
| | Dwyka Group | Dwyka Formation | Glacial Tillite | ±1000m |

* Table compiled from various sources.

4.3.2 Climate, topography and surface water drainage

Somkhele falls within a sub-tropical climate within Water Management Area 6 “Usuthu to Mhlathuze” and is located in Quaternary Catchment area W23A. The catchment has a mean annual precipitation (MAP) of 750-840 mm/annum and a mean annual evapotranspiration (MAE) of 1400 mm/annum (WR2005, 2005; DWAF, 2006). However, the precipitation is much lower in the study area than on a catchment scale.

Figure 4-2 illustrates the mean annual precipitation recorded at three rain stations close to the study area (the only rain stations available and some distance from the study area) and Table 4-3 lists the yearly rainfall data derived from monthly data. It can be seen that the yearly precipitation has decreased since the year 2006. From the data obtained it is anticipated that the MAP for the study area is in the order of 30-50 mm/annum. A value in this range was applied to the steady-state groundwater flow model.

Table 4-3: Rainfall station locations and yearly precipitation averages

| Station ID | | Coordinates | | Place | |
|------------|------------------|------------------|------------------|-------------------------------|--------------------|
| W3E001 | | Lat: -28.2004 | Lon: 32.41649 | St Lucia @ Charter's Creek | |
| W3E002 | | Lat: -27.9694 | Lon: 32.38439 | St Lucia @ Listers Point Park | |
| W3E003 | | Lat: -28.1171 | Lon: 32.18315 | Farm 3/7638 @ Hluhluwe Dam | |
| Year | W3E001 (mm/y) | W3E002 (mm/y) | W3E003 (mm/y) | Average (mm/y) | Harmonic (mm/y) |
| 2000 | 104.4 | 104.8 | 105.3 | 104.8 | 104.8 |
| 2001 | 54.0 | 47.4 | 65.3 | 55.6 | 54.8 |
| 2002 | 39.7 | 29.6 | 35.2 | 34.8 | 34.4 |
| 2003 | 63.8 | 30.5 | 32.8 | 42.3 | 39.0 |
| 2004 | 79.5 | 46.6 | 71.8 | 65.9 | 63.3 |
| 2005 | 74.5 | 68.0 | 48.3 | 63.6 | 62.0 |
| 2006 | 88.7 | 56.6 | 77.4 | 74.2 | 72.3 |
| 2007 | 68.5 | 56.9 | 44.0 | 56.4 | 55.1 |
| 2008 | 58.0 | 43.9 | 38.2 | 46.7 | 45.6 |
| 2009 | 58.8 | 63.9 | 51.1 | 57.9 | 57.5 |
| 2010 | 65.5 | 40.0 | 60.8 | 55.4 | 53.5 |
| 2011 | 72.0 | 51.4 | 57.1 | 60.2 | 59.3 |
| 2012 | 51.0 | 75.8 | 60.7 | 62.5 | 61.3 |
| 2013 | 45.5 | 50.2 | 51.5 | 49.1 | 48.9 |
| 2014 | 26.9 | 47.1 | 23.3 | 32.5 | 30.3 |

* Data retrieved from DWS (2015).

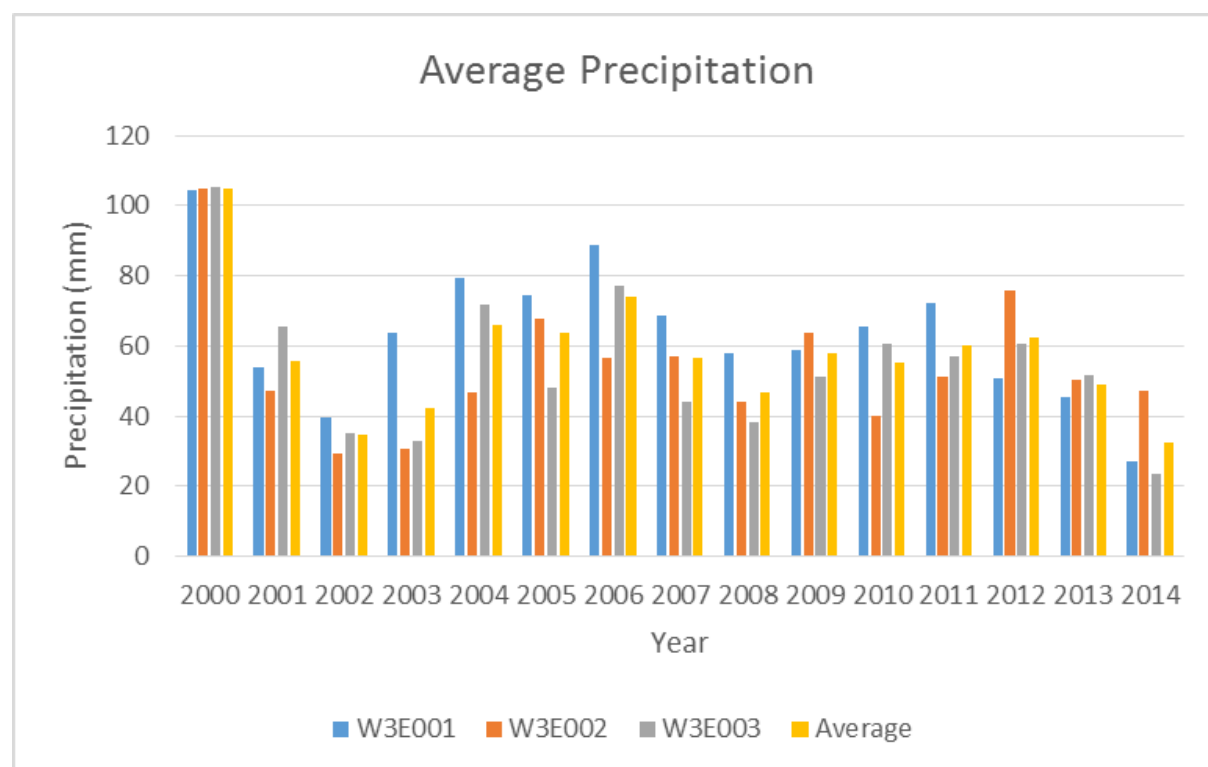


Figure 4-2: Average yearly rainfall for the study area

Figure 4-4 indicates the typical topography of the area. The area is generally hilly and continuously undulating. Somkhele anthracite mine lies in a part of Zululand that where it is relatively flat with low rolling hills and complex assemblages of moderately steep- to steep-sided valleys interspersed between higher lying ridges and koppies. The hills have typical elevations between 30 m and 260 m above mean sea level (mamsl). There are a number of non-perennial streams draining from east to west towards the Umfolozi River. There are no identified wetlands within the study area.

Due to the mining activity, the general topography in the area has changed. Rock dumps, overburden dumps, berms and steep slopes characterise the opencast pit areas. Figure 4-5 and Figure 4-6 indicates cross sections for both opencast pits in Area 2. Both pits have an average depth of approximately 45 to 50 meters below ground level (mbgl).

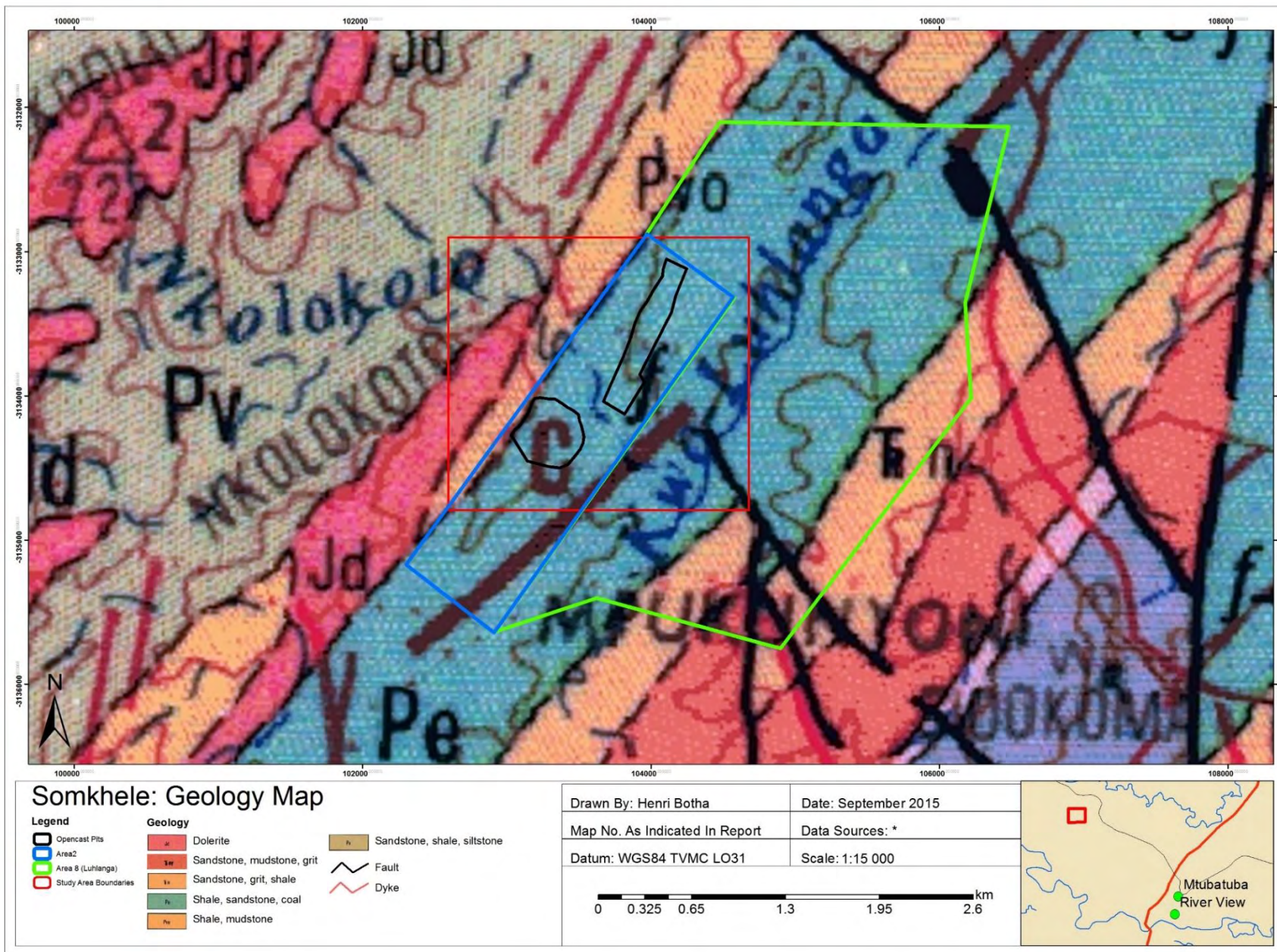


Figure 4-3: Study area geology

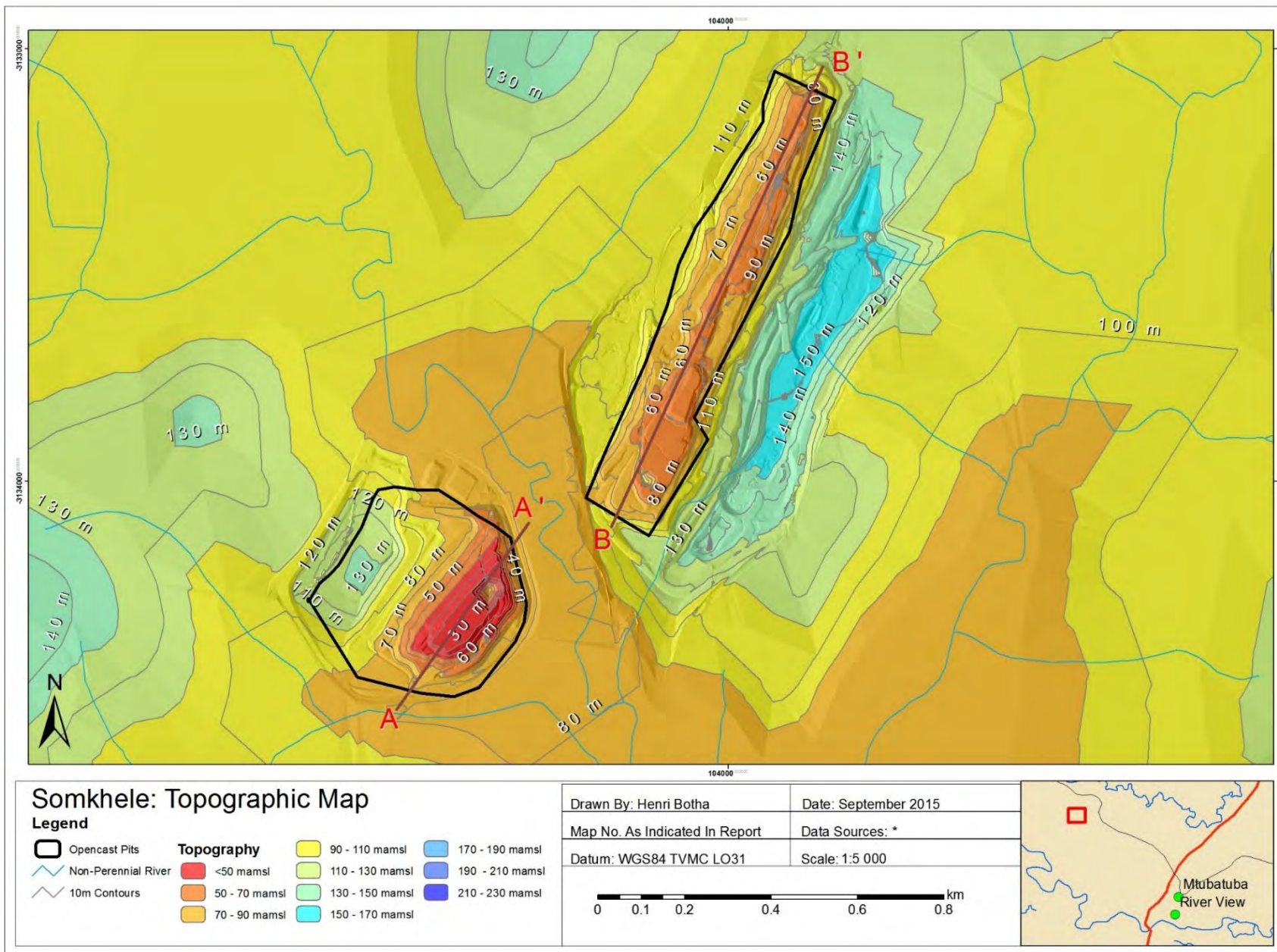


Figure 4-4: Study Area topography

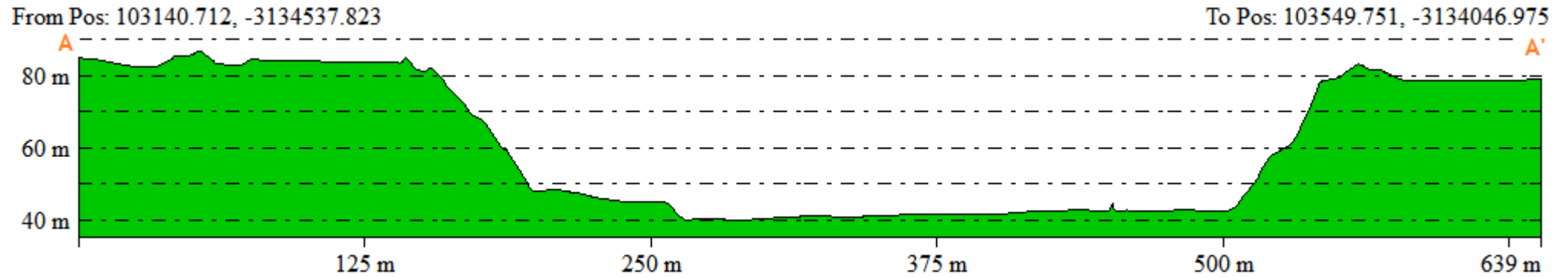


Figure 4-5: Cross section of opencast pit backfilled with tailings (A-A')

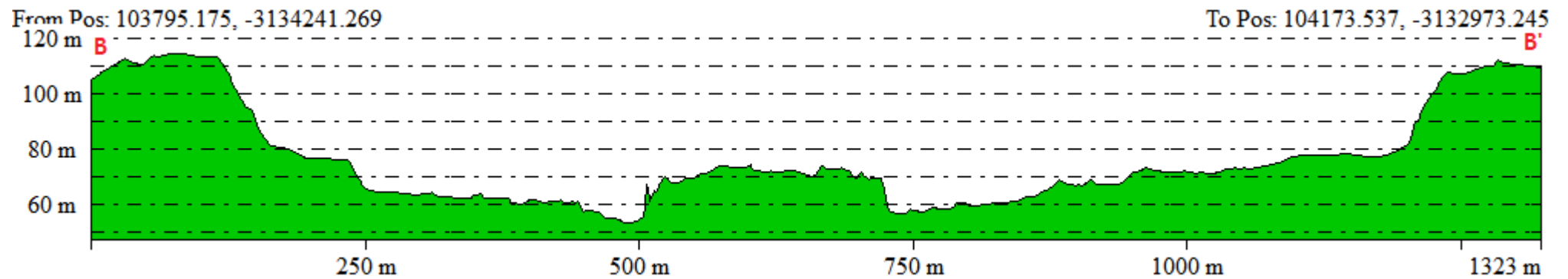


Figure 4-6: Cross section of opencast pit backfilled with discard (B-B')

4.3.3 Hydrogeology

The Somkele Anthracite Mine is situated within the Emakwezeni Formation of the Beaufort Group (Karoo Supergroup). The area has been structurally deformed, with the main structures consisting of block type normal faulting. As a result of the faulting, tilting of strata took place with the direction of dip in a south-easterly direction (average strike of strata is 30°). The general angle of dip of strata in the area of the mine is 22°. Associated with these block faults and related structures, are various dolerite sills and dykes of different ages. These aquifers have no to low potential in terms of development due to these factors, and are of minor regional importance. Therefore, the aquifer can be classified as a Minor Aquifer System according to the Parsons Classification method (Parsons, 1995).

Recorded water strikes (intersection of aquifers) vary between 12 to 102 mbgl for the Karoo aquifers. Shallow groundwater occurrence (<10 mbgl) is associated with younger (post-Karoo age) unconsolidated alluvial sediments, close to major streams. The average depth of weathering in the Karoo age rocks is ±11 m, with recorded weathering up to 25 m deep. Most water strikes were encountered below the weathered zone. It can be assumed that weathered aquifers are of minor importance (from an aquifer supply point of view), especially in the higher ridges. Perched weathered aquifers are likely to form during wet periods and shallow wells have been reported in the lower lying areas, close to streams.

The groundwater within the deeper fractured rock aquifer occurs within discrete zones due to secondary processes such as fracturing, faulting and contact metamorphism along intrusive rock contacts. These aquifers, with the exception of regional faults, normally have a limited extent and interconnectivity. Borehole blow yields from fractured aquifers according to the boreholes drilled in this area are highly variable, ranging from dry to 2.5 l/s.

Figure 4-7 illustrates a cross section of the lithology located along the opencast pits backfilled with discard and tailings material. It can be seen that sandstone, siltstone and dolerite are the predominant rock types in the area.

Figure 4-8 illustrates a cross section of the anticipated aquifer conditions along the opencast pits backfilled with discard and tailings material. The aquifers were classified according to depth, rock type and the underlying and overlying rock types. Rock types wedged between two aquitards or impermeable layers (shale) were classified as confined. Weathered rock and rock located above these impermeable layers were classified as unconfined. Rocks which can promote secondary fracturing (dolerite) were classified as fractured aquifers.

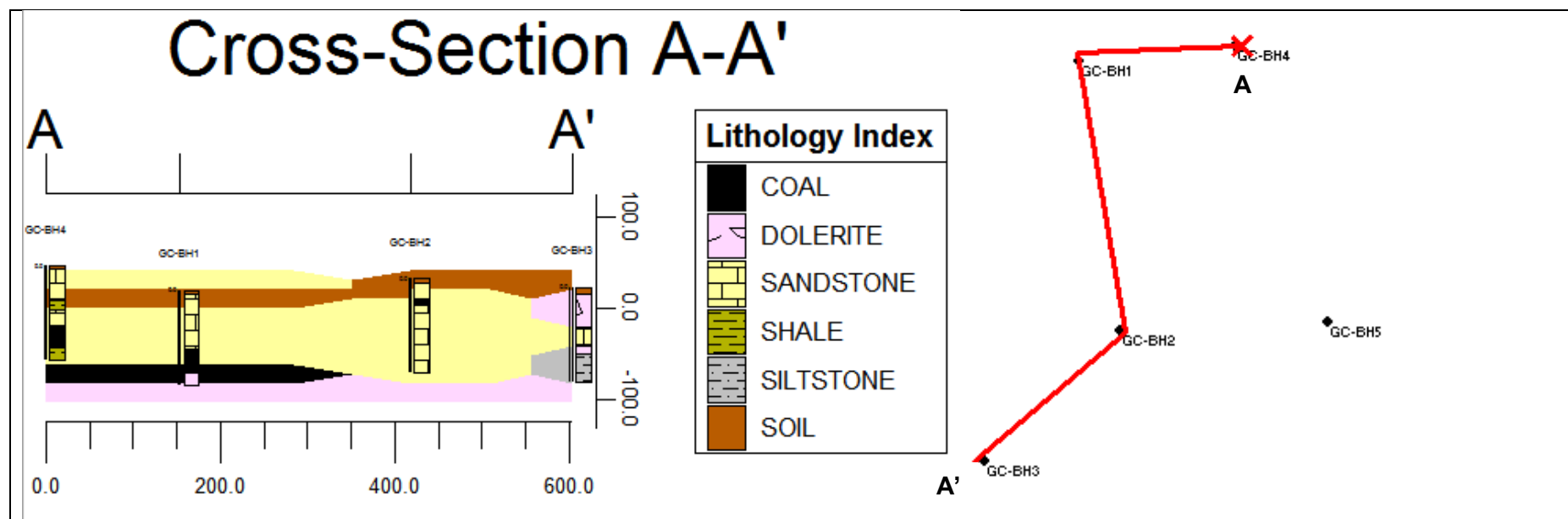


Figure 4-7: General lithology cross section

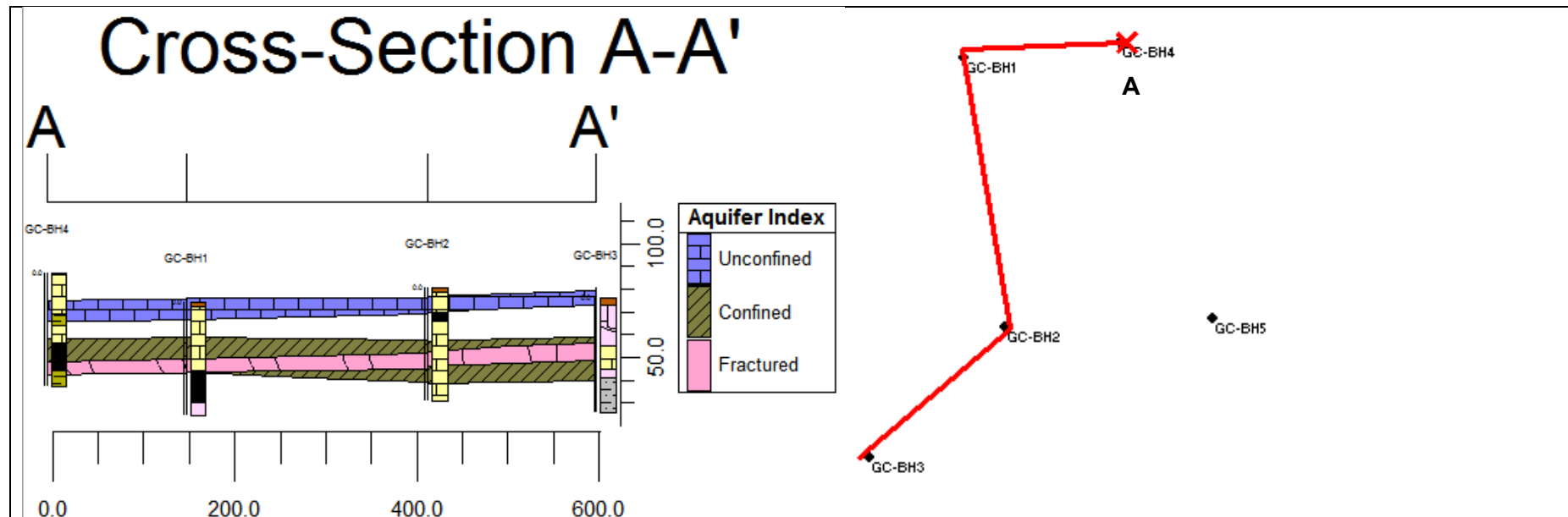


Figure 4-8: Identified aquifer layers based on hydrogeology characteristics

4.3.4 Monitoring Network

Somkhele has a fully operational groundwater and surface water monitoring network. GCS (Pty) Ltd was assigned to do quarterly monitoring for the mine, dating back to 2008. All the data has been made available for this study and was used in the numerical modelling process.

The groundwater fluctuations with time is illustrated by Figure 4-9. Groundwater levels have remained fairly stable since mining started in 2008. The only borehole which has shown a strange fluctuations is SWX1 which is drilled on the boundary of the opencast backfilled with tailings material. The decrease in groundwater levels must have been caused by a dewatering event before the pit was filled with tailings material.

The monitoring boreholes which fall in the study area are shown in Figure 4-10 and are tabulated in Table 4-4.

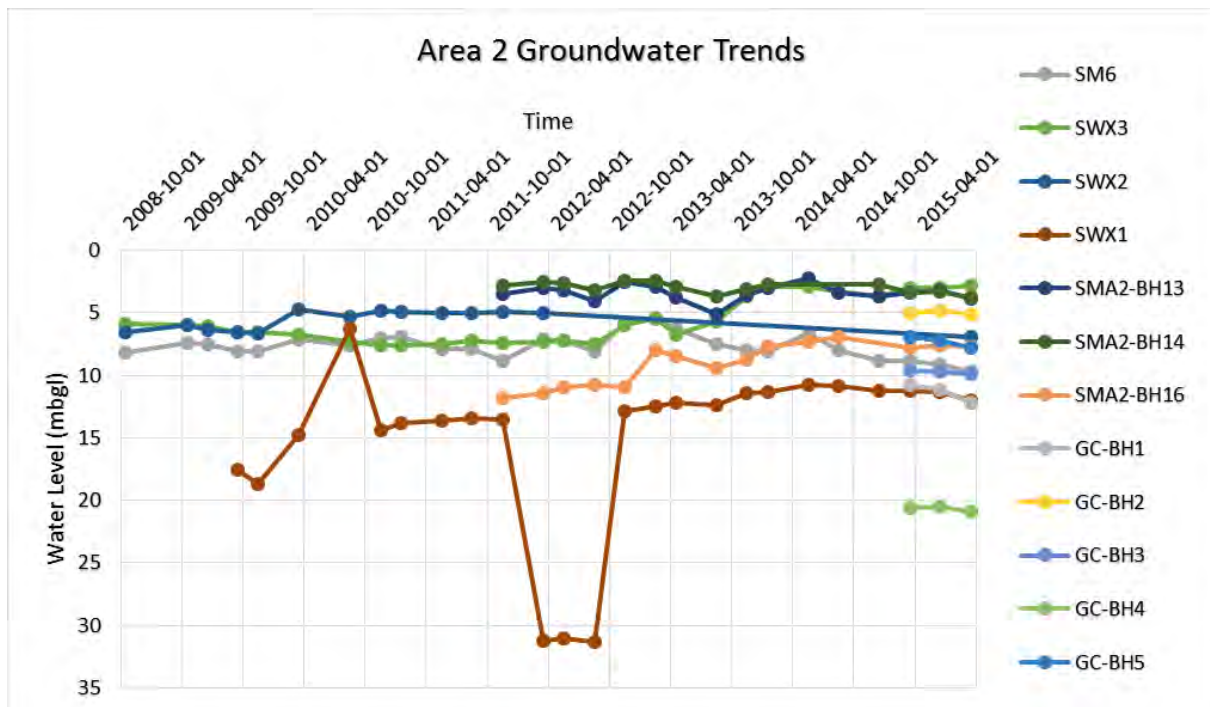


Figure 4-9: Groundwater fluctuations with time for mining Area 2

Table 4-4: Monitoring boreholes in study area

| Borehole Name | Latitude (dd) | Longitude (dd) | Description | Latest Groundwater Level June 2015 (mamsl) |
|----------------------|----------------------|-----------------------|--|---|
| SM6 | -28.3248 | 32.048844 | Percussion borehole, southwest of mine (extension of Area 2 coal seam area). | 87.31 |
| SMA2-BH13 | -28.3132 | 32.05678 | North of Pit A, within Area 2. | 86.18 |
| SMA2-BH14 | -28.3157 | 32.05629 | Directly north of Pit A and Nkolokotho stream. | 81.26 |
| SMA2-BH16 | -28.321 | 32.055667 | Directly west of Pit B-E, south of Nkolokotho Stream. | 71.29 |
| GC-BH1 | -28.3176 | 32.055668 | Directly northeast of Pit A, down gradient of pit bench. | 62.37 |
| GC-BH2 | -28.3199 | 32.05608 | Directly East of Pit A. | 75.41 |
| GC-BH3 | -28.3210 | 32.05481 | Directly South of Pit A. | 65.98 |
| GC-BH4 | -28.3175 | 32.05714 | Directly south of Pit B-E. | 66.30 |
| GC-BH5 | -28.3198 | 32.05804 | Directly South of Pit B-E, ± 200m southeast of GC-BH4. | 75.68 |
| SWX1 | -28.3099 | 32.05750 | Directly east of Pit A along the access road. | 69.04 |
| SWX2 | -28.3165 | 32.05395 | Borehole located directly northeast of Pit A. 50m from the PCD. | 78.04 |
| SWX3 | -28.3192 | 32.05587 | Northern most monitoring point within Area 8. | 105.2 |

Table 4-5: Hydrocensus boreholes and monitoring boreholes in other areas

| Borehole Name | Latitude (dd) | Longitude (dd) | Description | Latest Groundwater Level June 2015 (mamsl) |
|----------------------|----------------------|-----------------------|--|---|
| SBH2 | -28.3657 | 32.0223 | Borehole located in mining Area 1. Drilled to the southwest, between the Umfolozi River and the South Pit. | 50.93 |
| SBH3 | -28.3577 | 32.0250 | Borehole located in mining Area 1, Drilled to the northwest of North Pit 1. | 47.4 |
| SBH4 | -28.3434 | 32.0374 | Borehole located in mining Area 1. Borehole was drilled southeast and between North Pit 1 and East Pit. | 110.7 |
| SBH6 | -28.3726 | 32.0254 | Borehole located in mining Area 1. Borehole was drilled to the south of South Pit. | 40.72 |
| SBH7 | -28.3541 | 32.0267 | Borehole located in mining Area 1, Drilled to the northwest of North Pit 1 next to drilling quarters. | 54.69 |
| SBH8 | -28.3663 | 32.0358 | Borehole located in mining Area 1. Borehole is drilled southeast of South and East Pits. | 79.47 |
| SBH9 | -28.3515 | 32.0447 | Borehole located in mining Area 1. Borehole is drilled northeast of North Pit 1. | 123.65 |
| SM4 | -28.3282 | 32.0491 | Hydrocensus borehole discovered to the south of SM6. | 97.86 |

| Borehole Name | Latitude (dd) | Longitude (dd) | Description | Latest Groundwater Level June 2015 (mamsl) |
|---------------|---------------|----------------|--|--|
| SM7 | -28.3119 | 32.0672 | Monitoring borehole located in Area 2. Borehole is drilled next near the workshops. | 95.7 |
| SMA2-BH11 | -28.3083 | 32.0665 | Monitoring borehole located in Area 2. Borehole is drilled east of Pit B-E. | 109.92 |
| SMA2-BH12 | -28.3055 | 32.0600 | Monitoring borehole drilled in mining Area 2. Borehole is drilled next to processing plants and PCD. | 115.04 |
| KQP14 | -28.3165 | 32.0760 | Hydrocensus borehole located in mining Area 8. | 98.02 |
| KQP21 | -28.3109 | 32.0774 | Hydrocensus borehole located upstream of KQP14. | 114.2 |
| KQP89 | -28.3255 | 32.0621 | Hydrocensus borehole found in Area 8. | 70.42 |
| KQP124 | -28.3253 | 32.0667 | Hydrocensus borehole found in Area 8. Borehole located downstream of pit Luhlanga. | 68.88 |
| KQP69 | -28.3167 | 32.0687 | Hydrocensus borehole found in Area 8. Borehole located upstream of pit Luhlanga. | 76.37 |
| SPX10 | -28.3155 | 32.0771 | Monitoring borehole located in Area 8. Borehole is drilled upstream to the north of pit Luhlanga. | 91.61 |

| Borehole Name | Latitude (dd) | Longitude (dd) | Description | Latest Groundwater Level June 2015 (mamsl) |
|---------------|---------------|----------------|--|--|
| KQP74 | -28.3220 | 32.0659 | Hydrocensus borehole found in Area 8. Borehole located downstream of pit Luhlanga. | 63.78 |
| KQP113 | -28.3210 | 32.0645 | Hydrocensus borehole found in Area 8. Borehole located downstream of pit Luhlanga. | 70.44 |
| KQP86 | -28.3232 | 32.0656 | Hydrocensus borehole found in Area 8. Borehole located downstream of pit Luhlanga. | 68.53 |
| KQP59 | -28.3224 | 32.0638 | Hydrocensus borehole found in Area 8. Borehole located downstream of pit Luhlanga. | 70.65 |
| GCS06 | -28.3236 | 32.0638 | Hydrocensus borehole found in Area 8. Borehole located downstream of pit Luhlanga. | 74.8 |
| KQP76 | -28.3247 | 32.0639 | Hydrocensus borehole found in Area 8. Borehole located downstream of pit Luhlanga. | 75.17 |
| KQP51 | -28.3252 | 32.0647 | Hydrocensus borehole found in Area 8. Borehole located downstream of pit Luhlanga. | 70.54 |
| KQP126 | -28.3255 | 32.0635 | Hydrocensus borehole found in Area 8. Borehole located downstream of pit Luhlanga. | 65.61 |

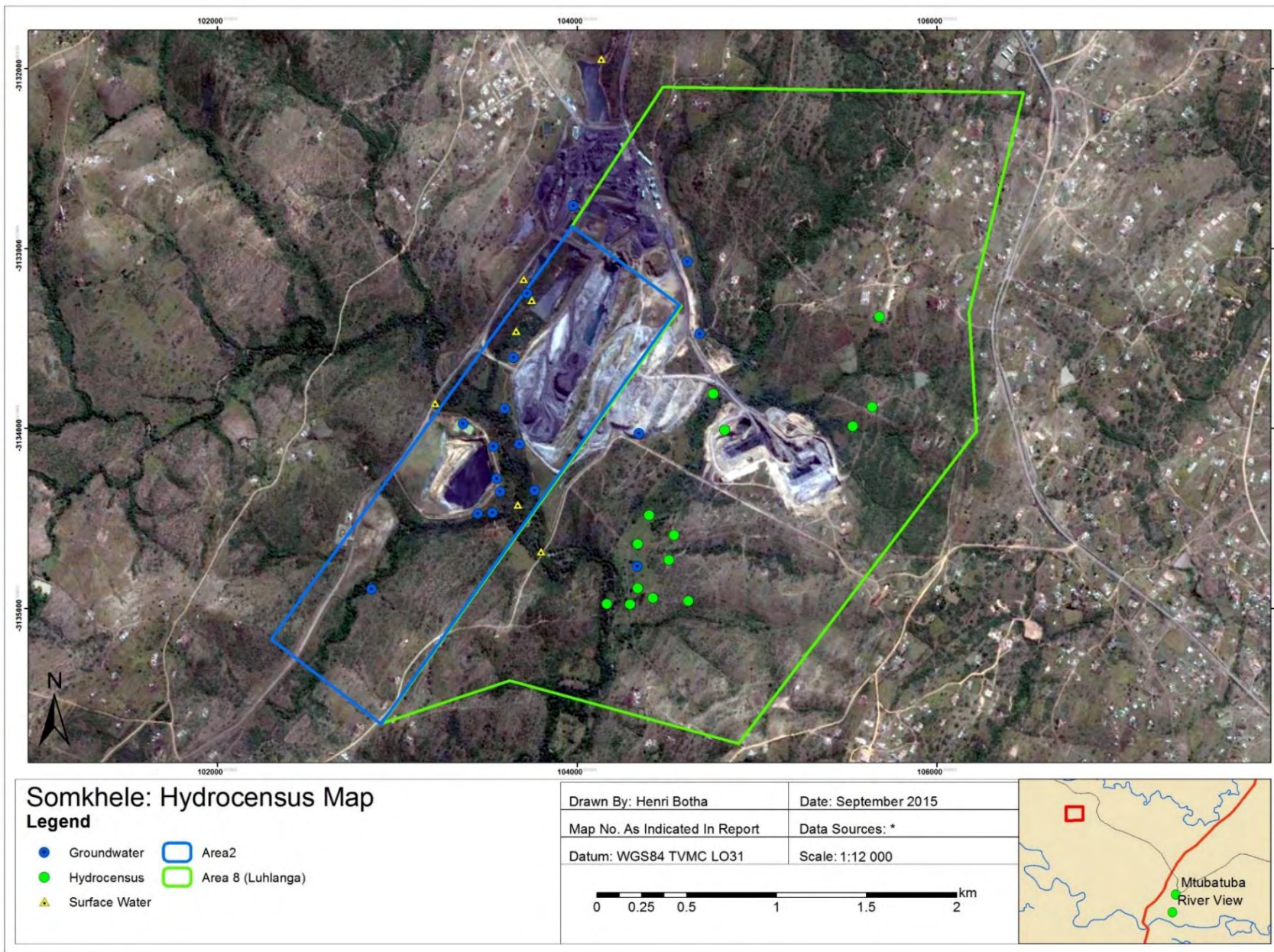


Figure 4-10: Hydrocensus map

4.3.5 Groundwater movement

Groundwater levels were obtained by means of using a field dip meter. The collar elevation of each borehole and the groundwater elevation was plotted to against each other to assess the groundwater distribution. Figure 4-11 indicates the topographic vs groundwater elevation trend. The trend was plotted with monitoring network and hydrocensus groundwater level data. The trend indicates a somewhat strong linear relationship ($R^2 = 87.4\%$) between groundwater elevations and topographic elevations. Therefore, it can be concluded that the groundwater levels mimics the topography in the area and flows from high topographic to low topographic elevations. Based on the observed relationship a groundwater contour map (Bayesian interpolation), refer to Figure 4-12, was created to indicate the groundwater elevations.

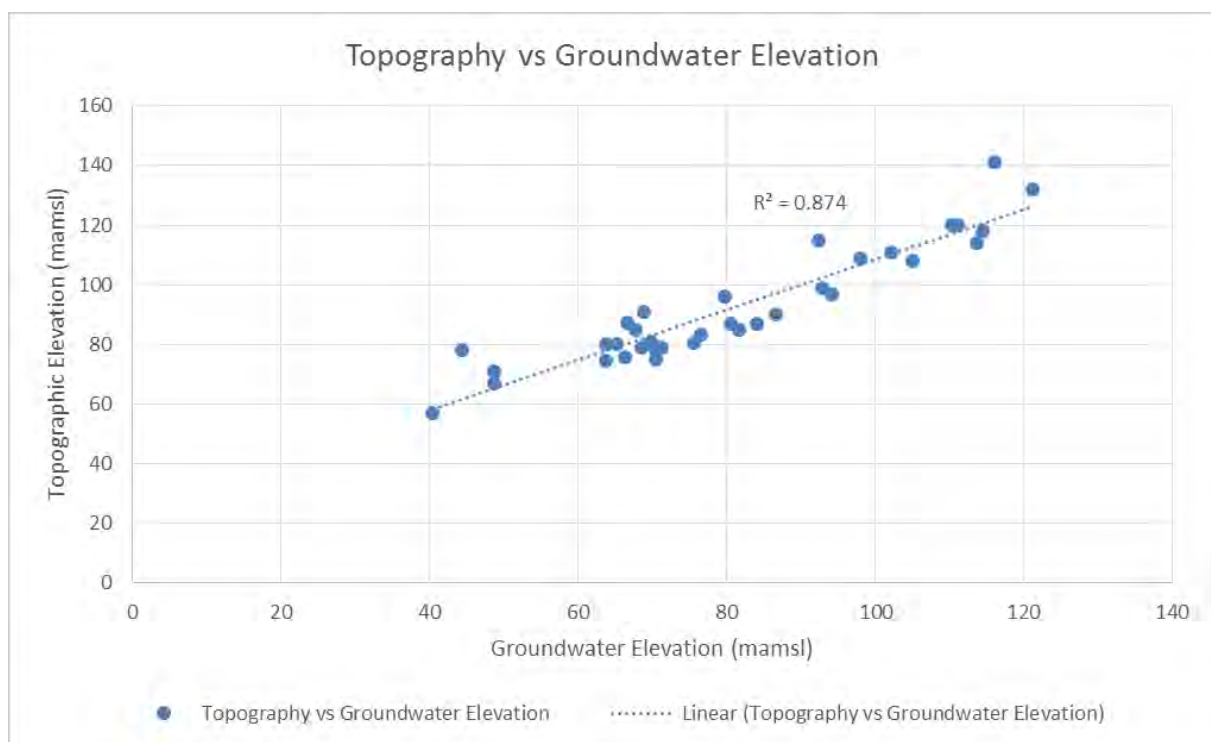


Figure 4-11: Topographic elevation vs groundwater elevation

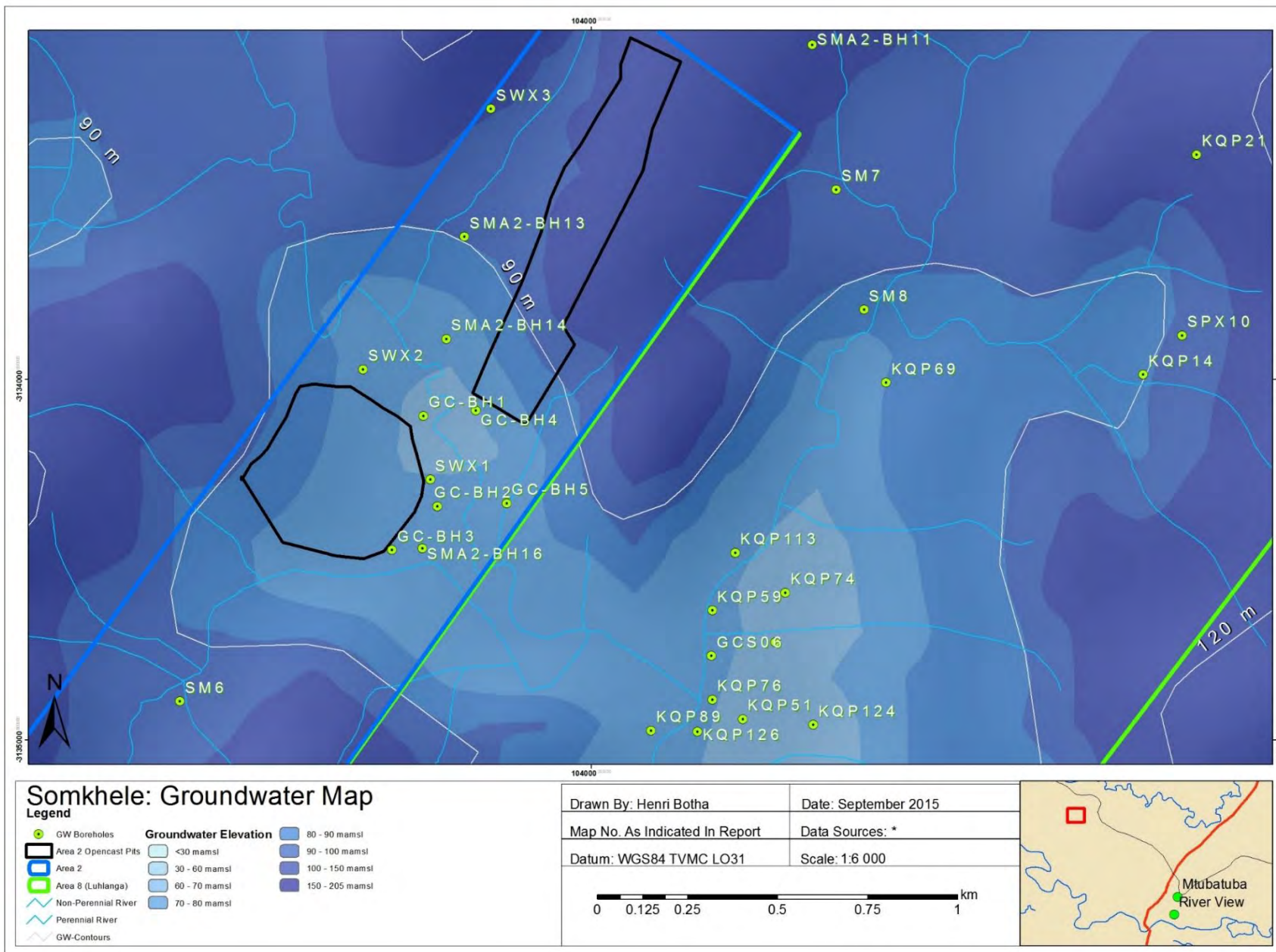


Figure 4-12: Study area groundwater levels

5 DISCUSSION AND RESULTS

5.1 FIELD WORK

Field work was carried out from June 2014 to February 2015. Table 5-1 lists the various field components that were completed in chronological order.

Table 5-1: Field Work Summary

| Item | Description | Aims and objectives |
|--------------------|---|--|
| Geophysical Survey | <ul style="list-style-type: none"> A proton precession magnetometer (G5) and an electro-magnetic (EM-34) was used in the study area to map subsurface bodies around the opencast pits. | <ul style="list-style-type: none"> Identify preferential flow paths in the form of dykes or sills intersecting the opencast pits. Identify depths of the anomalies in order to drill intersecting groundwater monitoring boreholes. Map the extent of the dykes in the area. |
| Drilling | <ul style="list-style-type: none"> Drilling was conducted by Kwa-Natal drilling. Boreholes were drilled by rotary percussion drills. Drilling supervision was undertaken and the boreholes were logged, headworks were installed and the boreholes were added to the Somkhele mine monitoring network. | <ul style="list-style-type: none"> Intersect the geological structures identified in order to compile a stratigraphic log of the geology around the opencast pits. Obtain hydrological parameters by performing aquifer tests on the drilled boreholes. Monitor the groundwater chemistry, obtained water level data, compile a chemistry database. |
| Sampling | <ul style="list-style-type: none"> Geochemical sampling: Sampled fresh discard; Sampled tailings from the opencast pit as well as the processing plants; Water samples were taken for analysis from all the monitoring boreholes within the study area. Groundwater levels were measured with a dip meter. | <ul style="list-style-type: none"> Analysis of all samples gathered with respect to XRD, ABA, NAG, Leach testing, EC, pH and ICP. The aim was to quantify and identify the hydrochemistry status of the site. Chemistry data obtained was used to calibrate the numerical groundwater model and to test the thesis as discussed in the problem statement. |
| Aquifer Tests | <ul style="list-style-type: none"> Aquifer tests were conducted on three of the newly drilled boreholes (GC-BH1, GC-BH2 and GC-BH3) along the southeaster boundaries of pit A. | <ul style="list-style-type: none"> Obtain hydraulic conductivity (K), storativity (S) (using borehole radius for pump was not strong enough to cause drawdown in large area) and transmissivity (T) parameters for the use in the numerical groundwater model. |



5.2 GEOPHYSICS

5.2.1 Geophysical equipment used

The geophysical equipment used to conduct the geophysical survey are listed in Table 5-2 and are briefly discussed.

Table 5-2: Geophysical equipment used

| Type | Electro Magnetometer (EM34-3) | Proton Precession Magnetometer (Mag) |
|------------------------------|---|---|
| Operating Principle | Electromagnetic (EM) methods make use of the response of the ground to the propagation of the electromagnetic fields which are composed of alternating electric intensity and magnetic forces. | The presence of magnetic minerals in rocks cause deviations in the earth's magnetic field. The proton precession magnetometer measures the remnant magnetic field strength of these rocks. |
| Instrument Working Principle | <p>The EM34-3 can be divided into 3 components: 1) two coils known as the transmitter and the receiver coil, 2) the power supply and data processing units attached to each coil and 3) a cable which connects the two coils and data processing units. The cable lengths vary from 10 meters, 20 meters and 40 meters.</p> <p>The instrument operates by using electromagnetic induction. A time-varying (alternating) current is passed through the transmitter coil and is then switched off. During the brief period the time-varying current is active a time varying magnetic field is created (primary field). The time-varying magnetic field causes a time-varying magnetic flux through objects (subsurface bodies) in the vicinity of the transmitter coil. The time-varying magnetic flux through an object gives rise to a time-varying electromagnetic force (emf) within the affected objects. If the objects are conductive, secondary time-varying currents are induced by the emf. The receiver coil interprets the secondary induced emf caused by the conductive subsurface bodies.</p> <p>The secondary magnetic field at the receiver circuit is much smaller than the primary field. This causes a phase lag between the primary and the secondary magnetic fields. BY comparing the magnitudes of the in-phase and out-of-phase components of the recorded signal, the data processing units estimates the conductivities of subsurface conductors.</p> | <p>The proton precession magnetometer consists out of two components: 1) a sensor and 2) the power supply and data processing unit.</p> <p>The sensor is filled with a proton-rich fluid kerosene, encased in a wire coil. The protons act as various small magnets and under normal circumstances the spin axes are randomly aligned. A polarizing current of the order of an amp is passed through the coil, creating a strong magnetic field, along which the moments of the protons in the hydrogen atoms will trend to become aligned. When the current is switched off, the protons realign to the direction of the Earth's field, and together will induce an oscillating voltage in the coil at a frequency proportional to the field strength, emitting an electromagnetic wave as they do so. The sensor measures the difference in induced and native magnetic field strengths and this is measured in Nano Testla (nT).</p> |

| Type | Electro Magnetometer (EM34-3) | Proton Precession Magnetometer (Mag) |
|---------|--|--|
| | The 3 inter-coil spacing's give variable depths of exploration down to 60 meters. In the vertical dipole (horizontal coplanar) mode the EM is very sensitive to vertical geological anomalies. In the horizontal dipole (vertical coplanar) mode the EM is very sensitive to horizontal geological anomalies. This is widely used for groundwater exploration in fractured, faulted and weathered bedrock zones. | |
| Picture |  |  |

* Table compiled from Dennis (2013a); Dennis (2013b); Grantham et al. (1987); Anon (2013); Xia et al. (2001) and Anon (2015).

5.2.2 Electro Magnetic and Magnetic traverses

The EM and Magnetic surveys comprised of a series of lines that were walked along the downstream opencast pit boundaries. Some of the EM and Magnetic lines walked were very short due to the difficult terrain and restricted access areas. Figure 5-1 indicates the orientation as well as the spatial distribution of the EM and Magnetic lines walked. Figure 5-2 indicates the lines with anomalies. Traverses with definite fluctuating conductivities (anomalies) are discussed in this section. All traverse data is available in Appendix A.

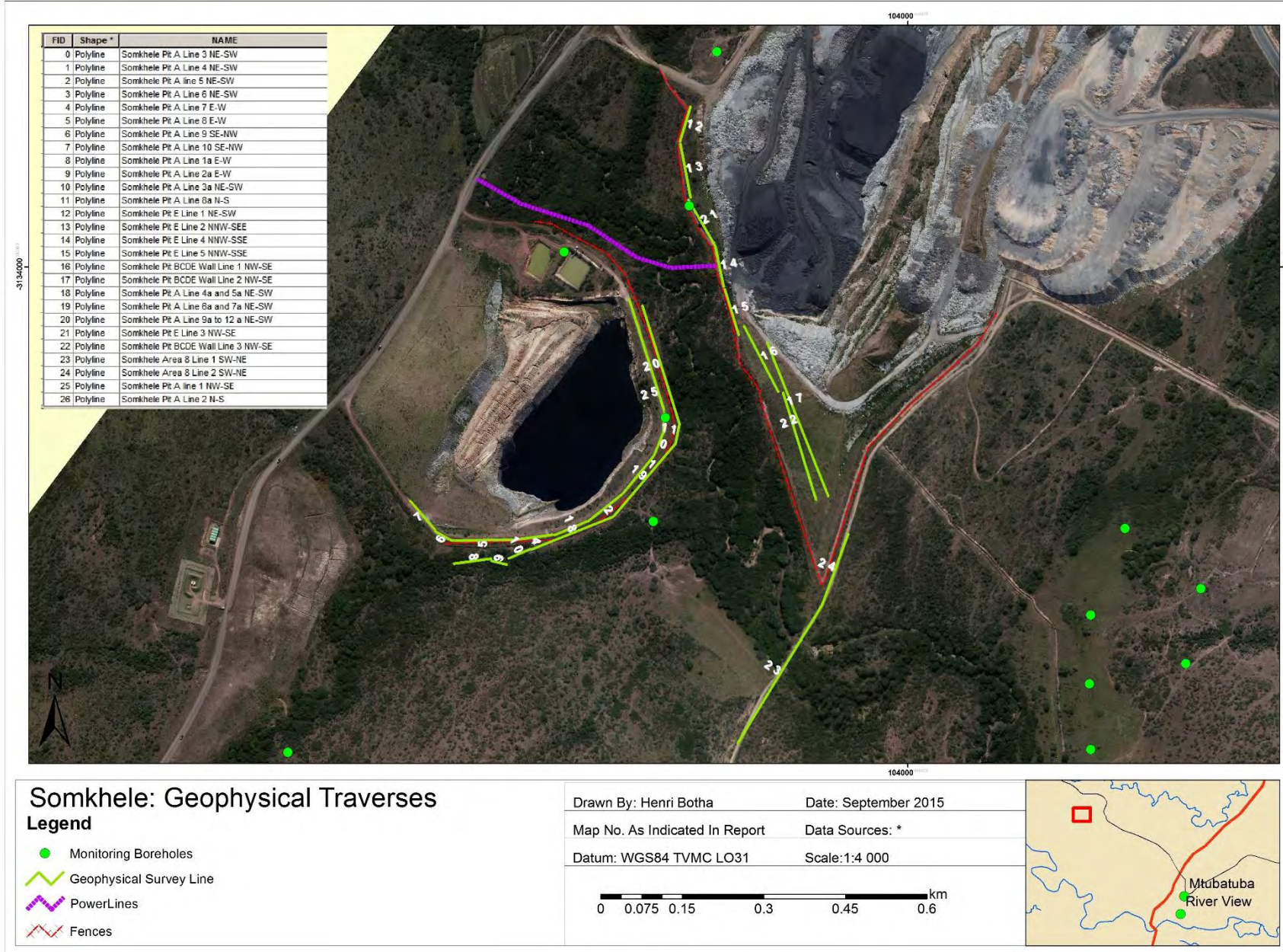


Figure 5-1: EM and Magnetometer survey traverses

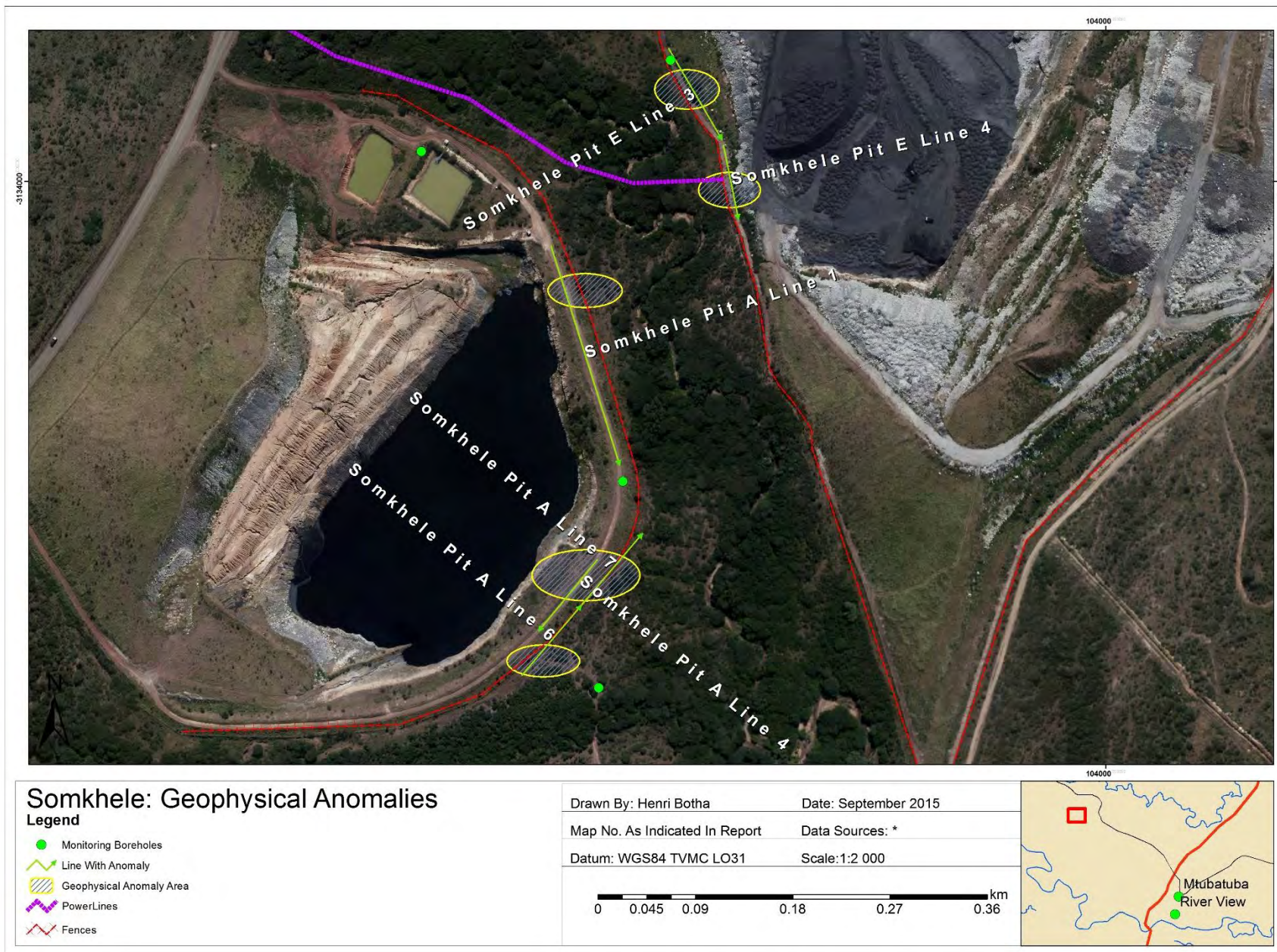


Figure 5-2: EM and Magnetometer traverses with anomalies

5.2.3 Electromagnetic and Magnetic interpretation

The electromagnetic and magnetic interpretations were subdivided into two subsections with regards to the two disposal techniques currently implemented at the mine. Therefore, the lines relevant to the opencast pit backfilled with coal tailings and the lines relevant to the opencast pit backfilled with discard are discussed separately.

The base magnetic reading for the survey area was 28 800 nT. There were fluctuations caused by fences and power lines as well as existing boreholes in the area. These interference sources caused erratic increases and decreases in the total magnetic field strength observed when walking close to; or approaching the structures. The magnetic and electromagnetic data was smoothed and the moving average was used to make the graphs.

5.2.3.1 Opencast backfilled with tailings

The EM-34-3 and Magnetic profile data along the northeast of the opencast pit (Pit A line 1) is shown in Figure 5-3. Electrical conductivity for this profile ranges approximately from 26 mS/m to 56 mS/m for the vertical dipole configuration and approximately 22 mS/m to 42 mS/m for the horizontal dipole configuration. Approximately between $x=20$ m and 80 m, the horizontal dipoles are higher than the corresponding vertical dipoles, although not significantly different, suggesting almost near similar conductance at shallow and a bit deeper depths. Therefore, this surveyed area may be characterised by deep weathering, based on the EM data obtained. A notable conductivity peak on the vertical dipole configuration is however, witnessed at $\approx x=50$ m which could be associated with a possible water-bearing fissure. The 1:250 000 geological map for the area does not indicate any geological structures in this area. The borehole (GC-BH1) drilled in the vicinity of the anomaly indicated weathered dolerite at a depth of approximately 44 mbgl. This could be the water bearing structure identified during the magnetic and electromagnetic survey.

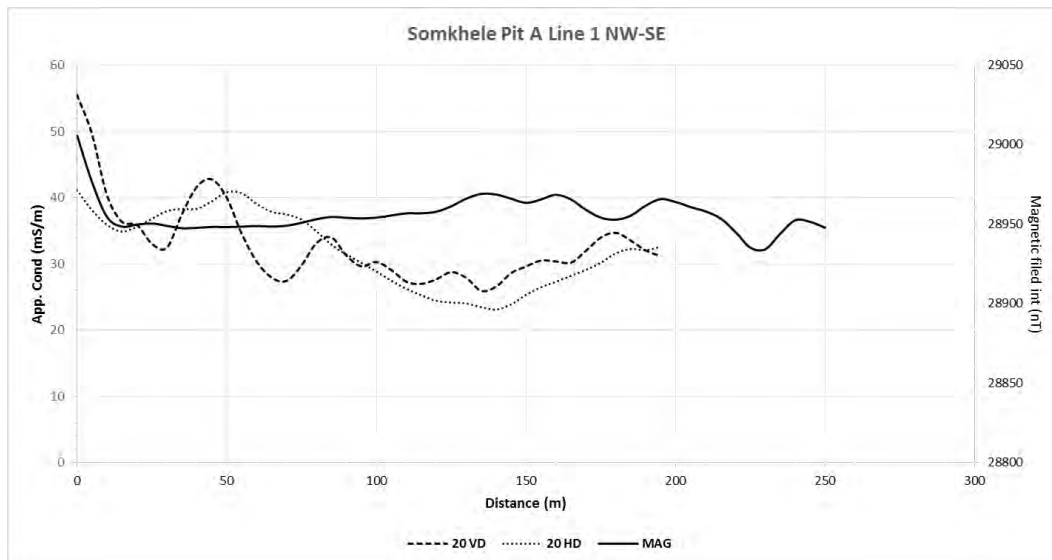


Figure 5-3: EM and Magnetometer results along Somkhele Pit A profile 1

The EM-34-3 profile data along the southeast of the opencast pit (Pit A line 4) is shown in Figure 5-4 where electrical conductivity ranges from ≈ 18 mS/m to ≈ 48 mS/m for the vertical dipole configuration and ≈ 42 mS/m to ≈ 64 mS/m for the horizontal dipole configuration. The horizontal dipoles are therefore higher than the corresponding vertical dipoles everywhere suggesting decreasing conductance with depth. It is anticipated that this may be due to shallow regolith (overburden development), however the geological map for the area does not indicate this. Large variations in apparent conductivity were witnessed, ≈ 64 mS/m for the horizontal dipole and ≈ 18 mS/m for the vertical dipole between $\approx x=5$ m and $\approx x=32.5$ m indicative of a weathering situation. The 1:250 000 geological map for the area does not indicate any geological structures in this area. A monitoring borehole could not be drilled at the exact point of this anomaly to verify the results obtained. A borehole was therefore sites downstream of this point (borehole GC-BH2). The geology predominantly consists out of weathered sandstone, siltstone with a coal seam at approximately 12 mbgl. The electromagnetic anomaly detected could therefore be noise or the interception borehole missed the geological structure identified during the survey.

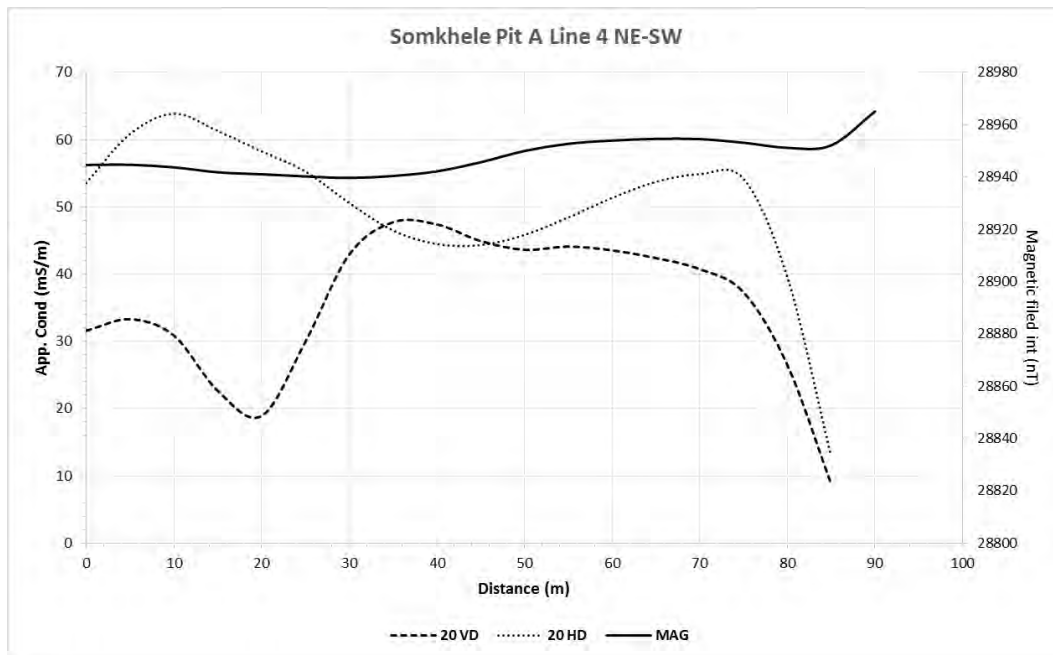


Figure 5-4: EM and Magnetometer results along Somkhele Pit A profile 4

The EM-34-3 and Magnetic profile data along the Somkhele Pit A line 6 is shown in Figure 5-5. Electrical conductivity ranges approximately between 8 mS/m and 39 mS/m for the vertical dipole configuration and approximately 12 mS/m to 49 mS/m for the horizontal dipole configuration. Unlike in the survey profiles in Figure 5-8 and Figure 5-6, the horizontal dipoles are higher than the corresponding vertical dipoles everywhere, suggesting decreasing conductance with depth. This could be due to shallow bedrock, however the geological map does not indicate shallow bedrock outcrops in the area. The mag indicates a lower magnetic peak at approximately 40 m. The reading suggest that there may be a subsurface structure at this point with a remnant magnetism an order lower than the other rock in the area. This could be a zone of weathering however, an aerial magnetic map could not be retrieved for the area to verify this phenomena. Drilling at the approximate (borehole GC-BH3) point of the detected anomaly indicated weathered dolerite at depths of 4, 18 and 32 mbgl. This intercepted structure explains the magnetic peaks observed during the survey.

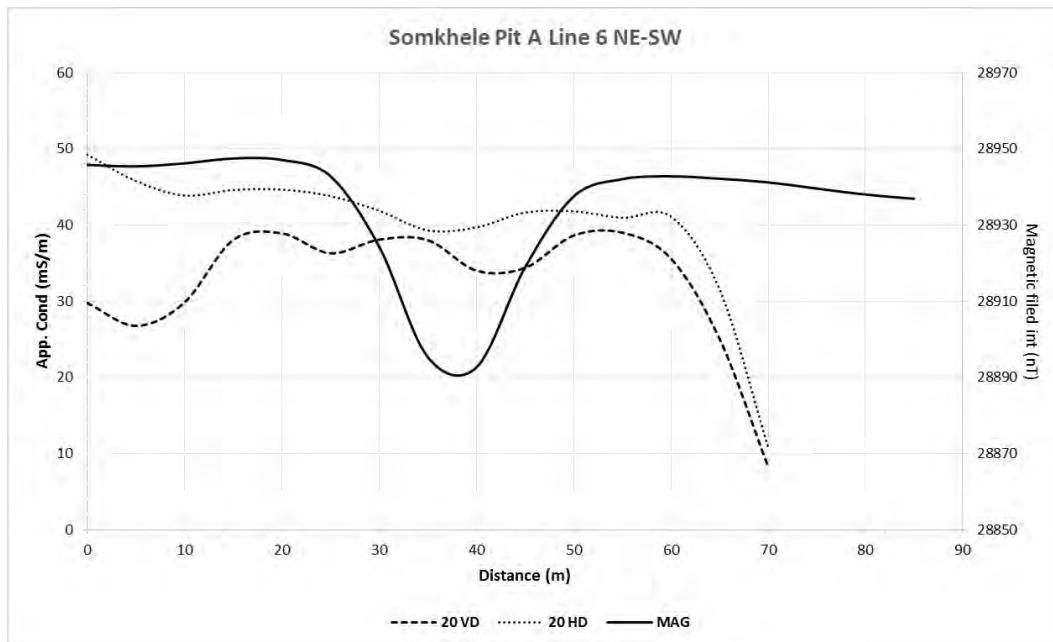


Figure 5-5: EM and Magnetometer results along Somkhele Pit A profile 7.

The EM-34-3 and Magnetic profile data along the north eastern boundary of the opencast pit (Pit A line 7) is shown in Figure 5-6. Electrical conductivity ranges from ≈ 31 mS/m to ≈ 42 mS/m for the vertical dipole configuration and ≈ 23 mS/m to ≈ 44 mS/m for the horizontal dipole configuration. The horizontal dipoles are higher than the corresponding vertical dipoles from $\approx x=0$ m to $\approx x=30$ m from which the vertical dipole becomes higher suggesting shallow weathering from $\approx x=0$ m to $\approx x=30$ m and deep weathering from $\approx x=30$ m onwards to the end of the survey line. The Magnetic data does not indicate an anomaly. The geological map for the area does not indicate any subsurface (sills, dykes or faults) in this area. The borehole drilled in the vicinity of this anomaly (GC-BH2) indicates that weathered sandstone occurs at a depth of approximately 3 mbgl. This explains the higher vertical dipole reading in this area, indicative of shallow weathering.

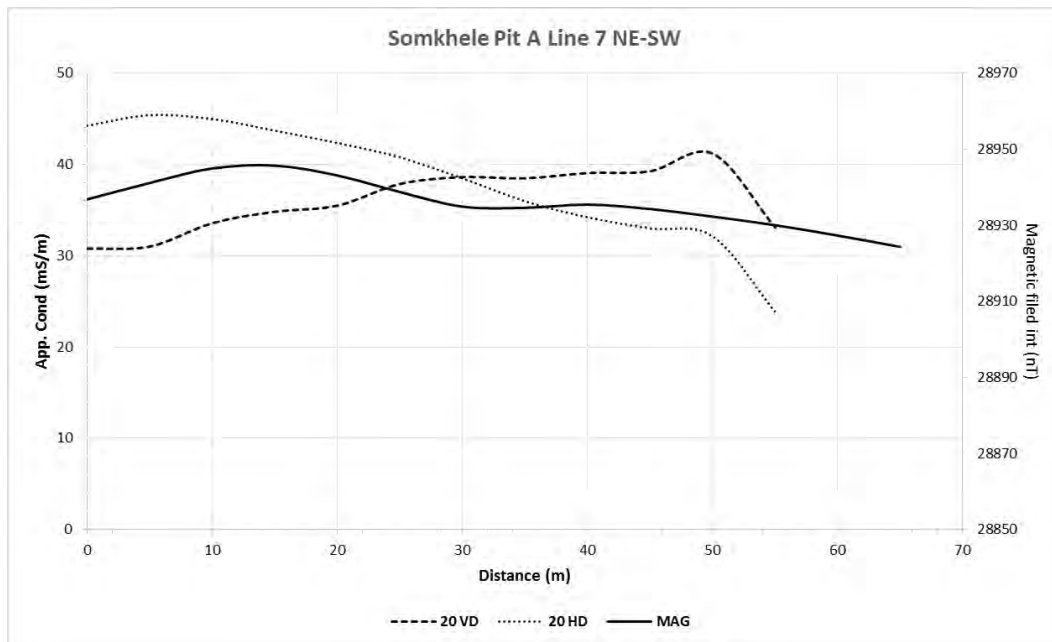


Figure 5-6: EM and Magnetometer results along Somkhele Pit A profile 7.

5.2.3.2 Opencast backfilled with discard

The EM-34-3 and Magnetic profile data along the south eastern boundary of the opencast pit (Pit E line 3) is shown in Figure 5-7 which indicates electrical conductivity ranging from ≈ 30 mS/m to ≈ 70 mS/m for the vertical dipole configuration and ≈ 24 mS/m to ≈ 40 mS/m for the horizontal dipole configuration. Therefore, the vertical dipoles are higher than the corresponding horizontal dipoles everywhere, suggesting increasing conductance with depth and therefore deep weathering. No significant variations in apparent conductivities were witnessed to suggest existence of any structures in the vicinity of the survey line. The Magnetic graph indicates a magnetic peak at $\approx x=10$ m which suggests a possible near vertical structure (possibly a dyke); however, EM data does not correlate to this structure which may suggest that the mag peak observed might have been due to magnetic noise other than the said structure. A number of readings were taken at this point, however the readings stayed consistently elevated. The geology map does not indicate a definite geological structure (fault or dyke) in the area however, there is an old monitoring borehole located in the vicinity of the anomaly. An interception borehole was not drilled at this point.

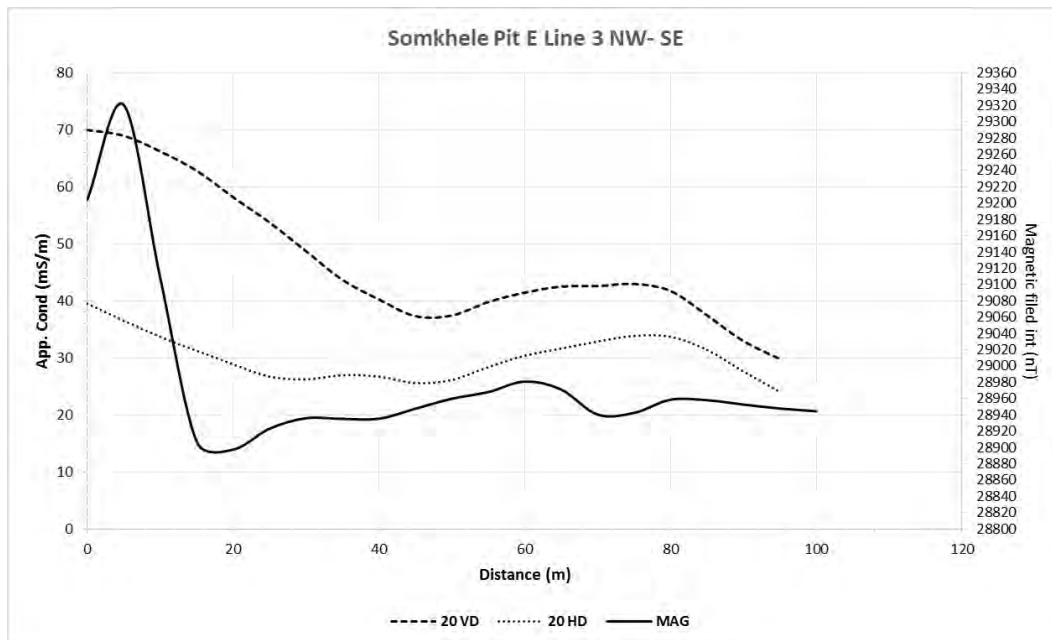


Figure 5-7: EM and Magnetometer results along Somkhele Pit E profile 3.

The EM-34-3 and Magnetic profile data along the south western boundary of the opencast pit (Pit E line 4) is shown in Figure 5-8. Electrical conductivity ranges from ≈ 38 mS/m to ≈ 64 mS/m for the vertical dipole configuration and ≈ 10 mS/m to ≈ 20 mS/m for the horizontal dipole configuration. As with Somkhele Pit E line 3 in Figure 5-7 above, the vertical dipoles are higher than the corresponding horizontal dipoles everywhere, suggesting increasing conductance with depth and therefore deep weathering. No significant variations in apparent conductivity are witnessed which suggests an absence of structures in the vicinity of the survey line. The mag graph indicates a magnetic peak at $\approx x=16$ m which suggests a possible near vertical structure (possibly a dyke); however, EM data does not correlate to this structure which may suggest the that the mag peak observed might have been due to magnetic noise other than the said structure. A number of readings were taken at this point, however the readings stayed consistently elevated. There are some power lines in the vicinity of the anomaly which could explain the magnetic interference observed. A monitoring borehole (GC-BH4) was drilled upstream of this point to verify if the anomaly observed is indeed magnetic interference. The borehole was sited some distance away from this point due to accessibility issues as well as the fact that the drilling rig may not operate within 15-25 m from any power lines (as per the mines regulations). The borehole drilled indicated that the area predominantly consists out of sandstone, shale and coal. Due to the distance between the anomaly observed and the actual drilling position, it is not possible to confirm if the peak observed is magnetic noise or a subsurface structure.

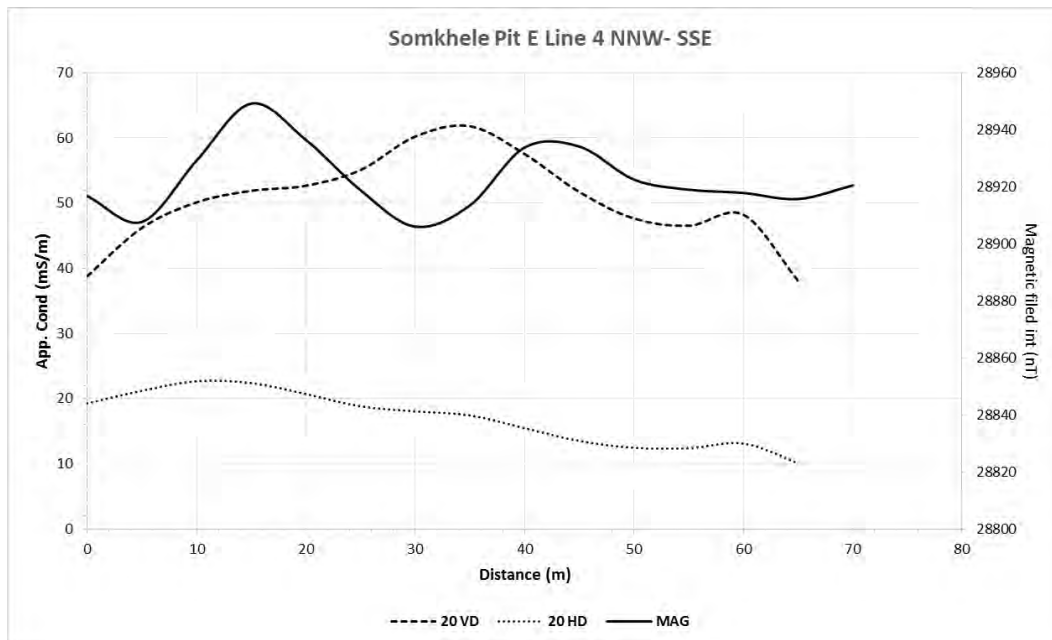


Figure 5-8: EM and Magnetometer results along Somkhele Pit E profile 4.

5.3 DRILLING AND AQUIFER TESTING

Five (5) boreholes, namely GC-BH1, GC-BH2, GC-BH3, GC-BH4 and GC-BH5 were drilled along the south-eastern and south-western boundaries of the opencast pits within the designated study area boundaries. These boreholes were drilled to a depth of 50 m on the approximate points where anomalies were identified during the geophysical survey.

Borehole chippings from the drilled boreholes indicated similar geology within the general area, which predominantly consisted out of siltstone, shale and weathered dolerite. The borehole logs are available in Appendix B.

5.3.1 Aquifer tests

Schlumberger AquiferTest Pro 2015 as well as Excel software was used to calculate the aquifer parameters. AquiferTest Pro is software that was designed for graphical analysis and reporting of pumping test and slug test data. The software suite offers the necessary tools to calculate an aquifer's hydraulic properties such as, storativity, hydraulic conductivity and transmissivity. AquiferTest Pro is adaptable enough to consider confined aquifers, leaky aquifers, unconfined aquifers and fractured rock aquifer conditions (SWS, 2014). Theis, Cooper-Jacob and Theis Recovery solver equations were applied to the pump test data and the transmissivity (T), hydraulic conductivity (K) and storativity (S) values were calculated.

Due to the pump test type and the low flow abstraction rate of the pump, the effective radius of the borehole had to be used to calculate the storativity (S) values. Therefore, the values could be an order or more from the actual storativity values. Ideally a step test with a strong pump should be used to calculate S values. The drawdown in the pumping well as well as an observation borehole in the area is then measured. The radius is substituted into the Cooper-Jacob equation to accurately determine storativity values. Due to the uncertainty in the S values obtained from the aquifer tests, literature S values obtained from the Groundwater Resource Assessment II (GRA2) were used in the numerical model.

The Excel pump test analyses were done using the Cooper-Jacob method as described by Kruseman and De Ridder (2000). The calculated results from both the AquiferTest and Excel analyses were compared and average values were derived. Table 5-3 lists the calculated transmissivity (T), hydraulic conductivity (K) and storativity (S) values for the pump tested boreholes. The data used for the calculations as well as the actual interpretation outputs are attached in Appendix C.

Table 5-3: Summary of calculated aquifer parameters (T, K and S values)

| Borehole ID | Analysis Method | Transmissivity (T) [m ² /d] | Hydraulic Conductivity (K) [m/d] | Storage coefficient (S) |
|-------------|----------------------------------|--|----------------------------------|-------------------------|
| GC-BH1 | Theis | 1.62E-01 | 3.24E-03 | 2.63E-04 |
| | Cooper Jacob | 1.71E-01 | 3.43E-03 | 2.10E-04 |
| | Theis Recovery | 1.67E-01 | 3.34E-03 | |
| | Excel Cooper Jacob Hand Analysis | 1.98E-01 | 3.95E-03 | 2.27E-02 |
| | Average | 1.74E-01 | 3.49E-03 | 7.72E-03 |
| GC-BH2 | Theis | 1.14E-01 | 2.29E-03 | 1.16E-03 |
| | Cooper Jacob | 1.55E-01 | 3.10E-03 | 5.87E-04 |
| | Theis Recovery | 1.90E-01 | 3.79E-03 | |
| | Excel Cooper Jacob Hand Analysis | 7.91E-02 | 1.58E-03 | 3.09E-02 |
| | Average | 1.35E-01 | 2.69E-03 | 1.09E-02 |
| | Theis | 2.15E-01 | 4.30E-03 | 2.68E-04 |
| GC-BH3 | Cooper Jacob | 2.28E-01 | 4.56E-03 | 2.15E-04 |
| | Theis Recovery | 2.91E-01 | 5.82E-03 | |
| | Excel Cooper Jacob Hand Analysis | 2.64E-01 | 5.27E-03 | 1.97E-02 |

| Borehole ID | Analysis Method | Transmissivity (T) [m ² /d] | Hydraulic Conductivity (K) [m/d] | Storage coefficient (S) |
|------------------|-----------------|--|----------------------------------|-------------------------|
| | Average | 2.49E-01 | 4.99E-03 | 6.72E-03 |
| Average For Area | | 1.99E-01 | 1.86E-01 | 3.72E-03 |

5.4 HYDROCHEMISTRY

5.4.1 Monitoring network hydrochemistry

Monitoring data was supplied by GCS (Pty) Ltd who has been conducting quarterly monitoring since 2008. The hydrochemistry data is important for it was used to calibrate the transport model as well as describes the groundwater quality in the mining area. All chemistry data used to produce plots in this section is added in Appendix D.

From the review of the baseline chemistry conditions of the mining area it was discovered that calcium (Ca), sodium (Na), chloride (Cl), magnesium (Mg) and manganese (Mn) concentrations have been elevated since monitoring started in 2008. Therefore, the impact on the environment cannot be assessed by using the above mentioned elements for they are present in fairly great and inconsistent concentrations. According to the International Network for Acid Prevention (INAP, 2014) pH, sulphate (SO₄), iron (Fe) and aluminium (Al) are commonly associated with pollution at coal mines. Therefore, these constituents were primarily used for the interpretation of the geochemistry and hydrochemistry data. Hydrochemistry data for sampled hydrocensus boreholes is represented by Figure 5-9 and hydrochemistry data for the boreholes located in the study area is represented by Figure 5-10.

The following summarises the hydrochemistry data obtained:

- The groundwater quality within the study area is primarily saline (plots within the saline apex corner, refer to Figure 5-9) with naturally elevated Ca, Mg, Na and Cl concentrations. Some points plot very close to the Cl apex, which indicates that Cl is the dominant ion in the groundwater ;
- All groundwater boreholes and surface water monitoring points surveyed exhibit neutral to alkaline pH conditions (refer to Appendix D);

- Proximity boreholes of the opencast pit backfilled with tailings material (GC-BH1, GC-BH2, CG-BH3, SWX1 and SMA2-BH16) indicates saline conditions. These boreholes are located to the southeast of the pit and all of them, with the exception of SWX1 and SMA2-BH16, show relatively low SO_4 concentrations (in the order of 1-80 mg/l). SWX1 and GC-BH2 have elevated sulphate concentrations (in the order of 200-800 mg/l). SWX1 was drilled on the pit hanging wall and GC-BH2 was drilled at the approximate location of the discovered geophysical anomaly. The geology penetrated at GC-BH2 predominantly consist out of interbedded sandstones. It is anticipated that these interbedded sandstone layers could be promoting pollution through the aquifer. SM6 (upstream borehole of the opencast pit backfilled with slurry) is the only borehole within the study area which does not indicate saline water conditions.
- Proximity boreholes of the opencast pit backfilled with discard material (GC-BH4, GC-BH4 and SMA2-BH14) indicates saline conditions. These boreholes are located along the south western boundary of the pit. All these boreholes exhibit neutral pH conditions however, the SO_4 concentrations at these points are elevated (in the order of 80-1200 mg/l).
- All pH conditions are near neutral however, SO_4 concentrations are very high. This indicates SD (Saline Drainage) is taking place rather than AD (Acid Drainage) (INAP, 2014).
- Table 5-4 lists stacked column time series data for the monitoring boreholes located in proximity of the backfilled pits. It can be seen that the concentrations for all major ions fluctuate with time. Ca, Na, Cl and Mg concentrations tend to fluctuate less than SO_4 and HCO_3 concentrations. It is anticipated that these elements are caused by natural rock-water interaction (chemical weathering) in the area. SO_4 concentrations are inconsistent and it is anticipated that SO_4 is primarily caused by pollution from the coal waste material backfilled into the opencast pits.

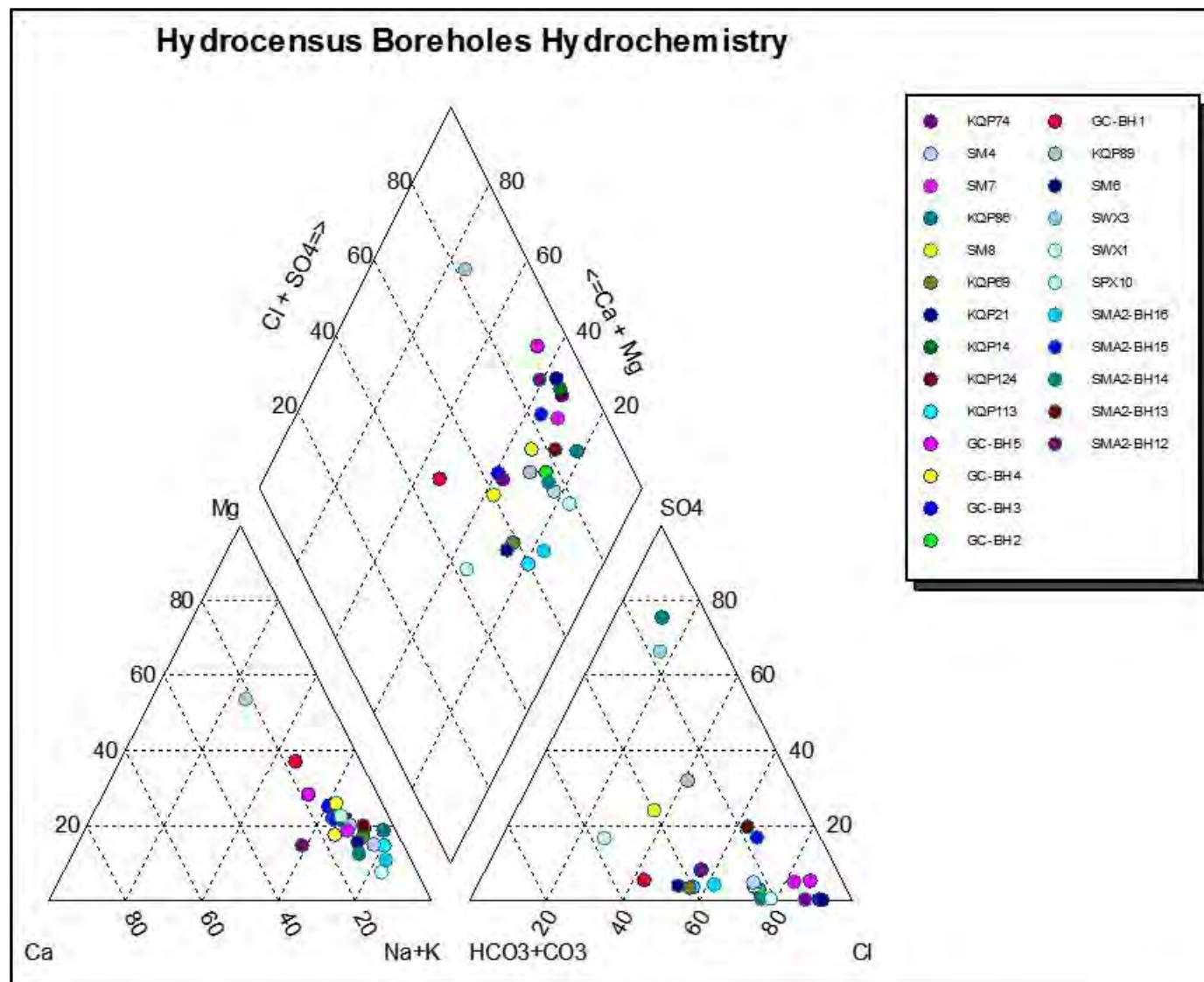


Figure 5-9: Piper plot: hydrocensus boreholes

Opencast Pit Proximity Boreholes Hydrochemistry 2015

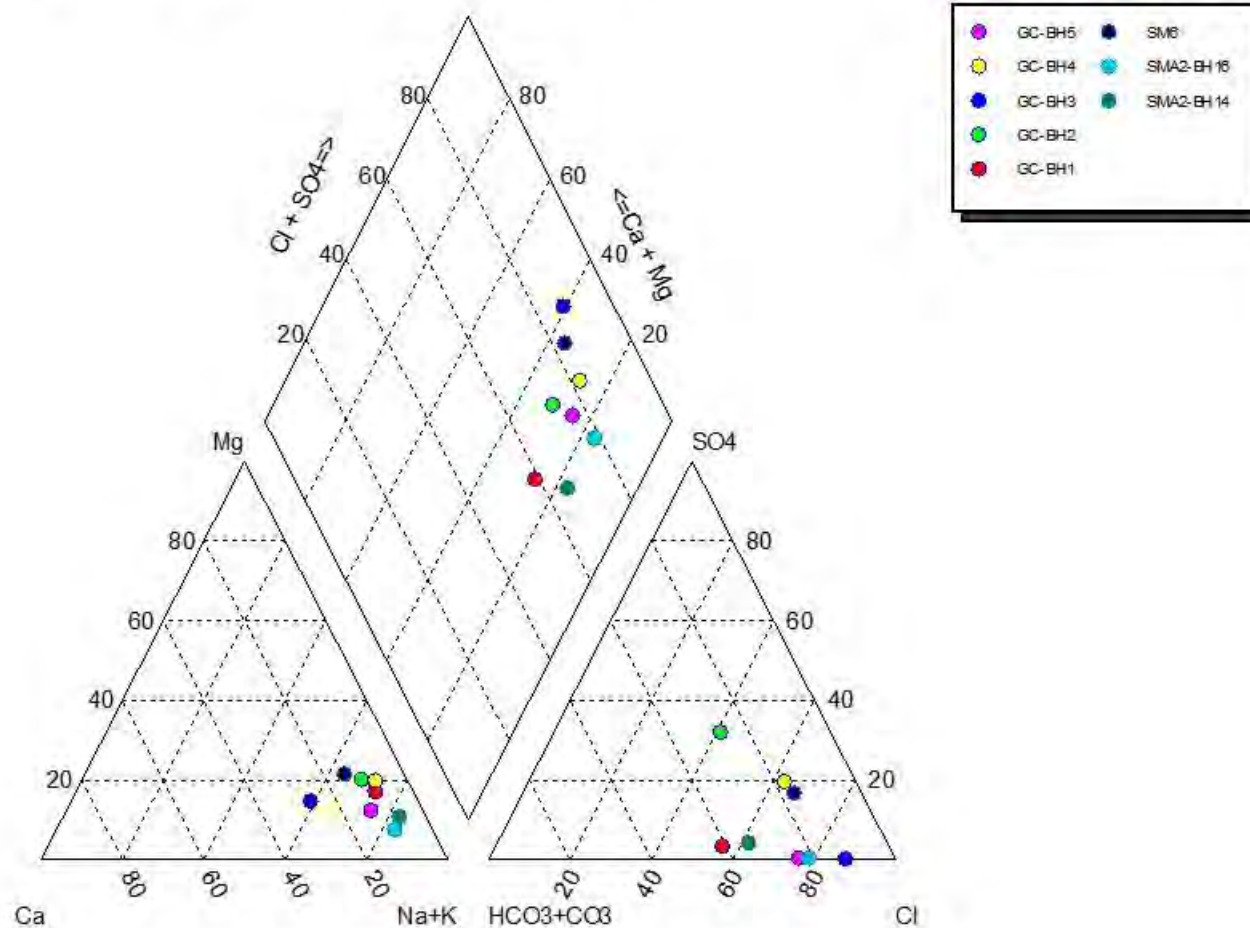
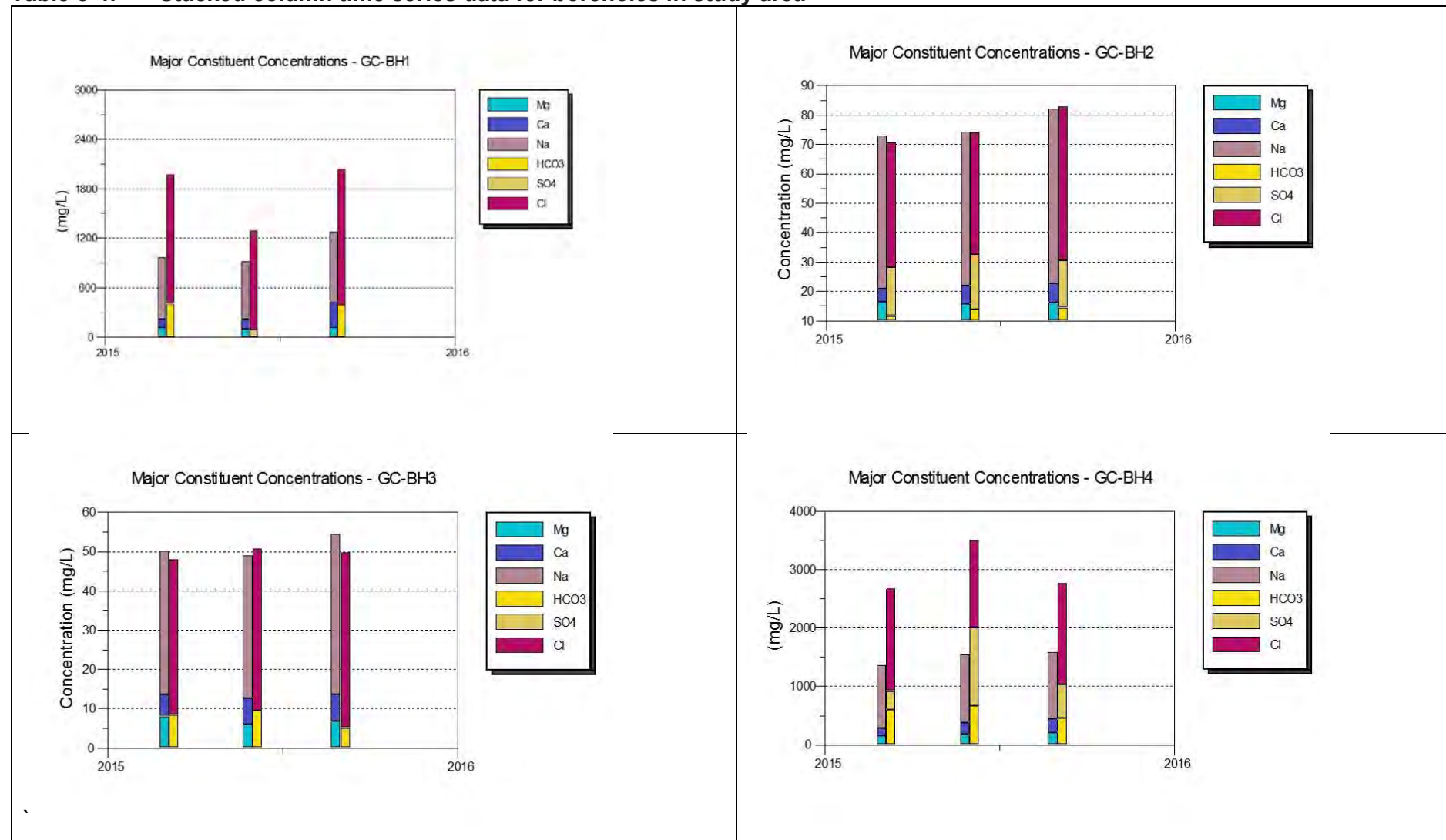
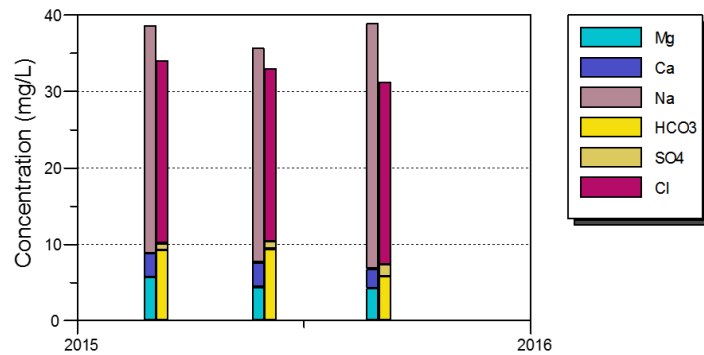


Figure 5-10: Piper plot: monitoring boreholes near opencast pits

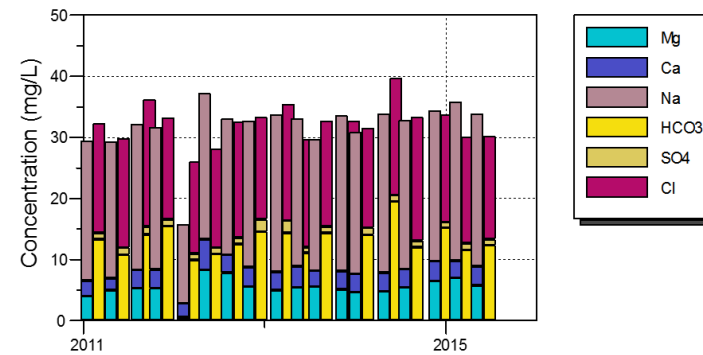
Table 5-4: Stacked column time series data for boreholes in study area



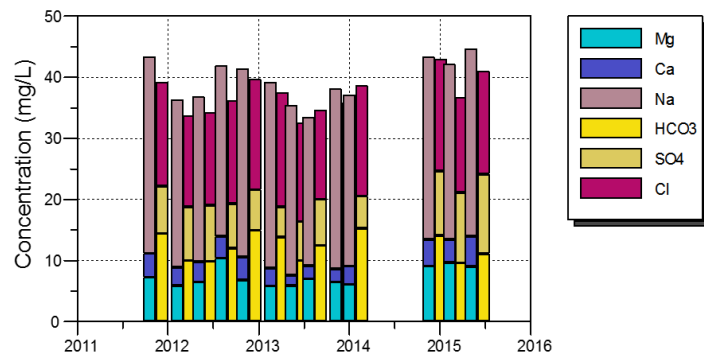
Major Constituent Concentrations - GC-BH5



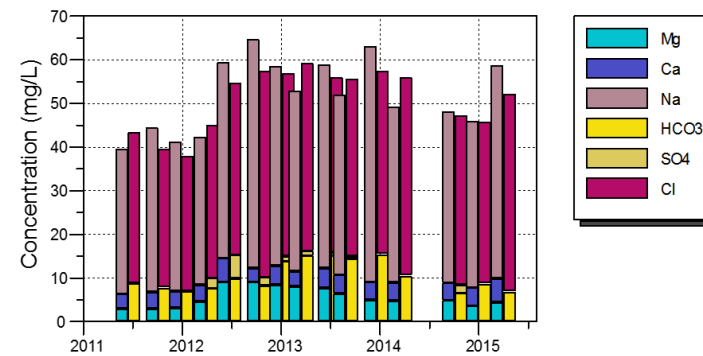
Major Constituent Concentrations - SM6

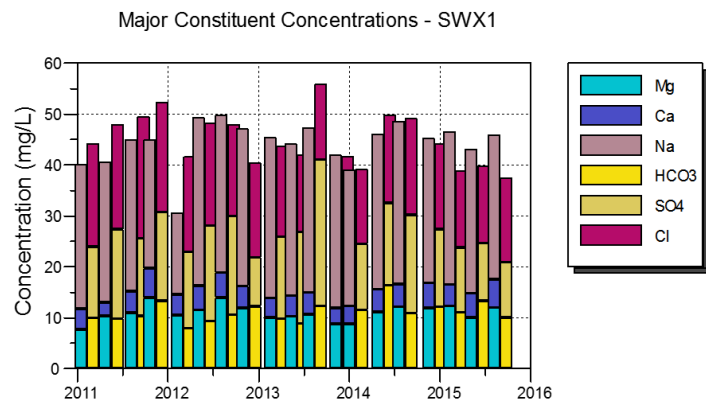


Major Constituent Concentrations - SMA2-BH14



Major Constituent Concentrations - SMA2-BH16





5.5 GEOCHEMISTRY

5.5.1 Sampling Methodology

All samples collected were submitted to Metron Laboratory (Pty) Ltd, Vanderbijlpark for geochemical testing. The description of the samples taken are given in Table 5-5 and the location of sampling are indicated in Figure 5-11.

The samples were collected as follows:

- a. Tailings:
 - a. Samples taken at directly from the plants were collected in 25 litre containers. The tailings material was pumped directly from processing. The containers were sealed with tape to keep oxygen from reacting with the tailings material.
 - b. The tailing sample collected directly from the opencast pit was collected at a depth of approximately 0.5 meters. Approximately 25 kg of the sample was collected with a shovel and placed immediately into industrial strength plastic bags. The bags were immediately sealed after the collection of the sample.
- b. Discard:
 - a. Discard samples were collected in areas where fresh deposition took place after discharge from the plants. Samples were collected approximately 0.5 meters underneath the top most part of the dumped discard piles. The samples were still relatively moist when they were collected. Approximately 50 kg (25kg at AIS871 and 25kg at AIS872) were collected and placed into industrial strength plastic bags. The bags were immediately sealed after collection.

5.5.2 Sample Preparation

Samples were prepped for X-Ray Diffraction (XRD), Acid-Base Accounting (ABA), Net Acid Generation (NAG), Peroxide leach and Kinetic leach testing (humidity columns) as follows:

- Discard material was crushed to 10-15 mm fragments. Required amounts were used for the tests performed.
- Tailings material obtained from the opencast pit was used as collected. Required amounts were used for the test performed.
- Co-Disposed was simulated by synthesising a 1:1 ratio (500g tailings: 500g discard) of the other two sample materials. Required amounts were prepared as discussed above for the tests performed.

Table 5-5: Sample description and lab number

| Lab No. | * | Rock Type | Description | Physical Characteristics | Sample Location |
|---------|---|------------|-------------------------------|--|--|
| AIS871 | | Discard 1 | Discard into pit BCDE sample1 | Dry, Dark black, Hard rock with small pieces of coal, Fragmented blocks, Coal discard. | Lat/Lon: 28° 18' 21.3177" S, 32° 03' 40.3586" E |
| AIS872 | | Discard 2 | Discard into pit BCDE sample2 | Dry, Dark black, Hard rock with small pieces of coal, Fragmented blocks, Coal discard. | Lat/Lon: 28° 18' 51.7114" S, 32° 03' 34.2715" E |
| AIS876 | | Tailings 1 | Plant 1 tailings solid | Wet, Black, Mixture of water and tailings, No structure, Tailings. | Lat/Lon: 28° 18' 17.3593" S, 32° 03' 47.6464" E |
| AIS877 | | Tailings 2 | Plant 2 tailings solid | Wet, Black, Mixture of water and tailings, No structure, Tailings. | Lat/Lon: 28° 18' 14.6162" S, 32° 03' 33.3732" E |
| AIS878 | | Tailings 3 | Opencast pit tailings solid | Wet, Black, Mixture of water and tailings, No structure, Tailings. | Lat/Lon: 28° 19' 13.9629" S, 32° 03' 14.7683" E |

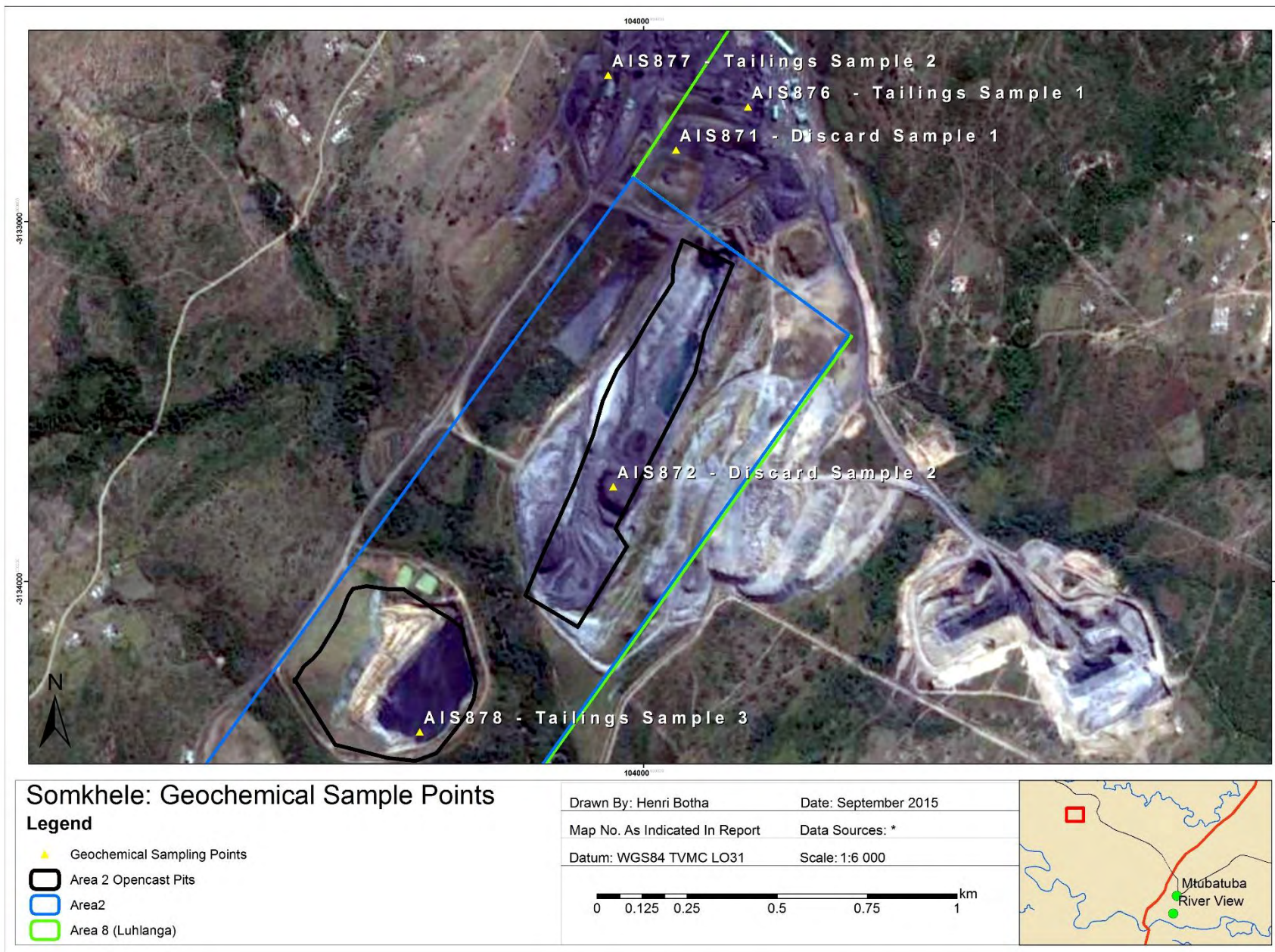


Figure 5-11: Geochemical sampling locations

5.5.3 Mineralogy and total element analysis

5.5.3.1 X-Ray Diffraction (XRD)

The mineralogical composition of the solid rock samples were determined by means of X-Ray Diffraction (XRD). The XRD results and a simplified classification of the identified minerals are listed in Table 5-6. The results are summarised as follows:

- Calcite is present in all 4 samples and dolomite is present in 3 samples, as accessory minerals. Calcite and dolomite is important minerals in the neutralization of acidity produced by pyrite oxidation in acid drainage (AD). More often dolomite is the result of secondary diagenetic processes transforming magnesium calcite into dolomite;
- Graphite is present as a major mineral in all samples;
- Illite was detected as a minor mineral in 3 samples. Common surface environments are not favourable for the formation of the mineral Illite. Illitization becomes a major chemical reaction in sedimentary rocks at high temperatures and is usually a direct alteration of kaolinite and feldspar into discrete Illite;
- Kaolinite was detected as a minor mineral in all samples. Kaolinite is generally precipitated by authigenic processes during coal formation;
- Magnetite is present in all samples as an accessory mineral. Magnetite is found in most igneous and metamorphic rocks as an accessory mineral. It is also known to be an additive in the beneficiation process;
- Muscovite was detected as a minor mineral all samples. If the muscovite is glauconitic, it is evident of marine transgressions. Glauconite characteristically forms small rounded pellets in clastic sediments deposited under marine conditions where the presence of the glauconite also colours the sediments green;
- Pyrite is present in all samples as an accessory mineral. Pyrite is generally elevated in coal with respect to clastic rocks due to formation under reducing conditions and can form during or very shortly after peat accumulation (authigenic) or as veins later in the coal's burial history (epigenetic);
- Quartz is present as a major mineral in all the samples. The quartz grains generally have a detrital origin and originate from the felsic mother rock; and
- Siderite is present in 3 sample as an accessory mineral. Siderite may contribute to the Mn in the mine water as Mn often replaces some of the Fe in the siderite (Apello and Postma, 2007).

From the XRD results obtained it is likely that if natural rock-water interaction occurs (chemical weathering) with the coal waste materials, that Fe, Ca, Mg and S will be the major elements present in the leachate. Therefore, the weathering of the identified minerals will be reflected in the water quality observed at the monitoring boreholes drilled downstream of the opencast pits. Furthermore, it is anticipated that as time progresses and geochemical exchange reactions take place that other forms of the primary weathering products will be seen in the water (S as SO_4 and Fe^{2+} as Fe^{3+} or FeOH). The end chemical compound or constituent can have an effect on the water pH, hardness, alkalinity and salinity.

Table 5-6: XRD results and mineral classification

| XRD - Results (Relative Percentages) | | | | | Mineral Classification | | | | |
|--------------------------------------|-----------|-----------|----------|----------|---|--------------|---|--------------------------|---------------------------------|
| | Discard 1 | Discard 2 | Slurry 1 | Slurry 2 | Mineral | Species ID # | Formula | Mineral type/group | Sub-group |
| Sample ID | AIS871 | AIS872 | AIS876 | AIS877 | Calcite | | CaCO ₃ | Anhydrous Carbonates | Calcite group |
| Description/Rock Type | | | | | Dolomite | | CaMg(CO ₃) ₂ | Anhydrous Carbonates | Dolomite group |
| Calcite | 1.78 | 1.33 | 2.55 | 1.24 | Graphite | | C (Hexagonal interconnected) | Native element mineral | Carbon Polymorph |
| Dolomite | 0.74 | 0.37 | - | 0.35 | Illite | | K(Li,Al) ₂ AlSi ₃ O ₁₀ (OH) ₂ | Phyllosilicate 1:1 layer | Phyllosilicates (Mica) |
| Graphite | 55.48 | 46.30 | 73.99 | 63.82 | Kaolinite | | Al ₂ Si ₂ O ₅ (OH) ₄ | Phyllosilicate 1:1 layer | Phyllosilicate |
| Illite | 8.33 | 10.94 | - | 6.49 | Magnetite | | Fe ₂ O ₃ | Oxide Minerals - Spinal | Spinel group (Iron subgroup) |
| Kaolinite | 5.38 | 5.61 | 4.64 | 4.58 | Muscovite | | KAl ₂ (AlSi ₃ O ₁₀)(OH,F) ₂ | Phyllosilicate 2:1 layer | Mica Group (Muscovite subgroup) |
| Magnetite | 0.79 | 1.13 | 1.00 | 1.22 | Pyrite | | FeS ₂ | Sulfide mineral | Pyrite group |
| Muscovite | 4.81 | 6.40 | 4.78 | 4.90 | Quartz | | SiO ₂ | Tectosilicate | Tectosilicate |
| Pyrite | 1.22 | 0.73 | 0.80 | 0.90 | Siderite | | FeCO ₃ | Anhydrous Carbonate | Calcite group |
| Quartz | 21.09 | 26.70 | 12.25 | 16.33 | # Mineral Type: Red = Fe/Al/Ti-Oxides and hydroxides, Green = Carbonates and Chlorides, Orange = Sulphides and Sulphates, Blue = Phyllosilicates, Black = Ino- and Tectosilicates | | | | |
| Siderite | 0.39 | 0.50 | - | 0.18 | | | | | |

*Native elements identified with the help of (Klein and Dutrow, 2007)

5.5.4 Acid-Base Accounting and Net-Acid Generation Test

5.5.4.1 ABA terminology and screening methods

Acid-base Accounting (ABA) is a static test where the net potential of the rock to produce acidic drainage is determined. The percentage sulfur (%S), the Acid Potential (AP), the Neutralization Potential (NP) and the Net Neutralization Potential (NNP) of the rock material are determined in this test, as an important first order assessment of the potential leachate that could be expected from the rock material. The ABA screening criteria as described by Prince (1997) are listed in Table 5-7. The components of an ABA analysis are further explained below:

- If pyrite is the only sulphide in the rock the AP (Acid Potential) is determined by multiplying the %S with a factor of 31.25. The unit of AP is kg CaCO₃/t rock and indicates the theoretical amount of calcite neutralized by the acid produced;
- The NP is determined by treating a sample with a known excess of standardized hydrochloric or sulfuric acid (the sample and acid are heated to insure a completed reaction). The paste is then back-titrated with standardized sodium hydroxide in order to determine the amount of unconsumed acid. NP is also expressed as kg CaCO₃/t rock as to represent the amount of calcite theoretically available to neutralize the acidic drainage; and
- NNP is determined by subtracting AP from NP (EPA, 1994).

In order for the material to be classified in terms of their acid drainage (AD) potential, the ABA results could be screened in terms of its NNP, %S and NP:AP ratio as follows:

- A rock with NNP < 0 kg CaCO₃/t will theoretically have a net potential for acidic drainage. A rock with NNP > 0 kg CaCO₃/t rock will have a net potential for the neutralization of acidic drainage. Because of the uncertainty related to the exposure of the carbonate minerals or the pyrite for reaction, the interpretation of whether a rock will actually be net acid generating or neutralizing is more complex. Research has shown that a range from -20 kg CaCO₃/t to 20 kg CaCO₃/t exists that is defined as a “grey” area in determining the net acid generation or neutralization potential of a rock. Material with a NNP above this range is classified as *Rock Type IV - No Potential for Acid Generation*, and material with a NNP below this range as *Rock Type I - Likely Acid Generating*; and

- Soregaroli and Lawrence (1998) further states that samples with less than 0.3% sulphide sulphur are regarded as having insufficient oxidisable sulphides to sustain long term acid generation. Material with a %S below 0.3% is therefore classified as *Rock Type IV - No Potential for Acid Generation*, and material with a %S of above 0.3%, as *Rock Type I - Likely Acid Generating*.

Table 5-7: ABA screening methods used (adapted from Prince, 1997; and Fourie, 2014)

| ABA: NPR Screening Criteria | | | ABA: %S Screening Criteria | | | ABA: NNP Screening Criteria | | |
|---|-------------|---|--|--------|--|---|-------------|---|
| Potential Acid Generation | NP:AP (NPR) | Comments | Potential Acid Generation | % S | Comments | Potential Acid Generation | NP:AP (NPR) | Comments |
| Rock Type I: Likely Acid Generating. | < 1 | Likely AMD generating. | Rock Type IV: No Potential for Long Term Acid Generation | < 0.3% | Sample may produce AMD bit will be short term. | Rock Type IV: No potential Acid Generation. | > 20 | No AMD potential |
| Rock Type II: Possibly Acid Generating. | 1-2 | Possibly AMD generating if NP is insufficiently reactive or is depleted at a faster rate than sulphides. | | | | Rock Type I: Likely Acid Generation. | < -20 | Likely AMD potential |
| Rock Type III: Low Potential for Acid Generation. | 2-4 | Not potentially AMD generating unless significant preferential exposure of sulphides along fracture planes, or extremely reactive sulphides in combination with insufficient reactive NP. | Rock Type I: Likely long Term Acid Generation | > 0.3% | Potential for long term AMD. | Uncertain | 20 to -20 | Sample may become acidic or remain neutral. Use with conjunction of the other criteria's to resolve this uncertainty. |
| Rock Type IV: No Potential for Acid Generation. | > 4 | No further AMD testing required unless materials are to be used as a source of alkalinity. | | | | | | |

5.5.4.2 NAG terminology and screening methods

In the Net-Acid Generating (NAG) test hydrogen peroxide (H_2O_2) is used to oxidize sulphide minerals in order to predict the acid generation potential of the sample.

The NAG test provides a direct assessment of the potential for a material to produce acid after a period of exposure (to a strong oxidant) and weathering. The test can be used to refine the results of the ABA predictions.

In general, the static NAG test involves the addition of 25 ml of 30% H_2O_2 to 0.25 g of sample in a 250 ml wide mouth conical flask, or equivalent. The sample is covered with a watch glass, and placed in a fumehood or well-ventilated area. Once "boiling" or effervescing ceases, the solution is allowed to cool to room temperature and the final pH (NAG pH) is determined. A quantitative estimation of the amount of net acidity remaining (the NAG capacity) in the sample is determined by titrating it with NaOH to pH 4.5 (and/or pH 7.0) to obtain the NAG Value (Lapakko and Lawrence, 1993).

Table 5-8: NAG screening methods used (Edited from Miller., 1997)

| Rock Type | NAG pH | NAG Value (H_2SO_4 kg/t) | NNP (CaCO_3 kg/t) |
|--|----------|---|-----------------------------|
| Rock Type Ia. High Capacity Acid Forming. | < 4 | > 10 | Negative |
| Rock Type Ib. Lower Capacity Acid Forming. | < 4 | ≤ 10 | - |
| Uncertain, possibly Ib. | < 4 | > 10 | Positive |
| Uncertain. | ≥ 4 | 0 | Negative |
| Rock Type IV. Non-acid Forming. | ≥ 4 | 0 | Positive |

5.5.5 ABA and NAG test results

The test results from the ABA and NAG test are presented as follows:

- The classification and acid potential of the samples in terms of %S and NP/AP is depicted by Figure 5-12. The averages for both tailings and discard was used to determine the approximate %S and NP/AP ratio for a co-disposed sample.
- The ABA and NAG results are presented in Table 5-9 and Table 5-10, respectively. The screening classification ranges from Rock Type I to IV (possible AD to No AD).
- Average ABA results for the discard, tailings and combined discard and tailings are listed in Table 5-11.

- Table 5-12 indicates the potential AMD risk for the material types.

From the ABA and NAG test results the following observation are made:

- The NP/AP indicates the potential for the rock to generate acid drainage, whereas the %S indicated whether this drainage will be over the long term. In Figure 5-12 the red lines assess the acid potential and the blue lines the long term acid generation potential.
- The total S% was used to determine the Acid Potential (AP) of the rock. This might be an overestimation in some cases as only sulphides produces acid upon oxidation.
- Based on the ABA results all the samples have a low neutralization potential (average 27.68 CaCO₃ kg/t) and high acid potential values (average 41.64 CaCO₃ kg/t).
- All samples, with the exception of one tailings (tailings 1) sample, have a %S higher than 1%. Based on the %S and NP/AP ratio all the samples are likely to have the potential to generate acidic drainage. However, tailings collected from plant 1 (tailings 1) indicates a lower possibility to generate acid, and has a larger neutralisation potential (NP). The tailings is combined in the opencast pit when disposed. Therefore, based on the averages obtained, it is anticipated that acid generation is likely. Refer to Figure 5-12 and for the classification of the discard and tailings.
- The NAG test results in Table 5-10 confirmed that the samples have a high potential for acidification. The discard samples were classified as either high/low capacity acid forming. The tailings samples were classified as non-acid forming and high capacity acid forming.
- Overall, it can be concluded that all the samples have a significant potential to generate acid mine drainage. All the samples have a %S higher than 1% indicating that the rock samples may have the potential for long-term acid-generation. However, tailings samples have a larger acid neutralisation potential.

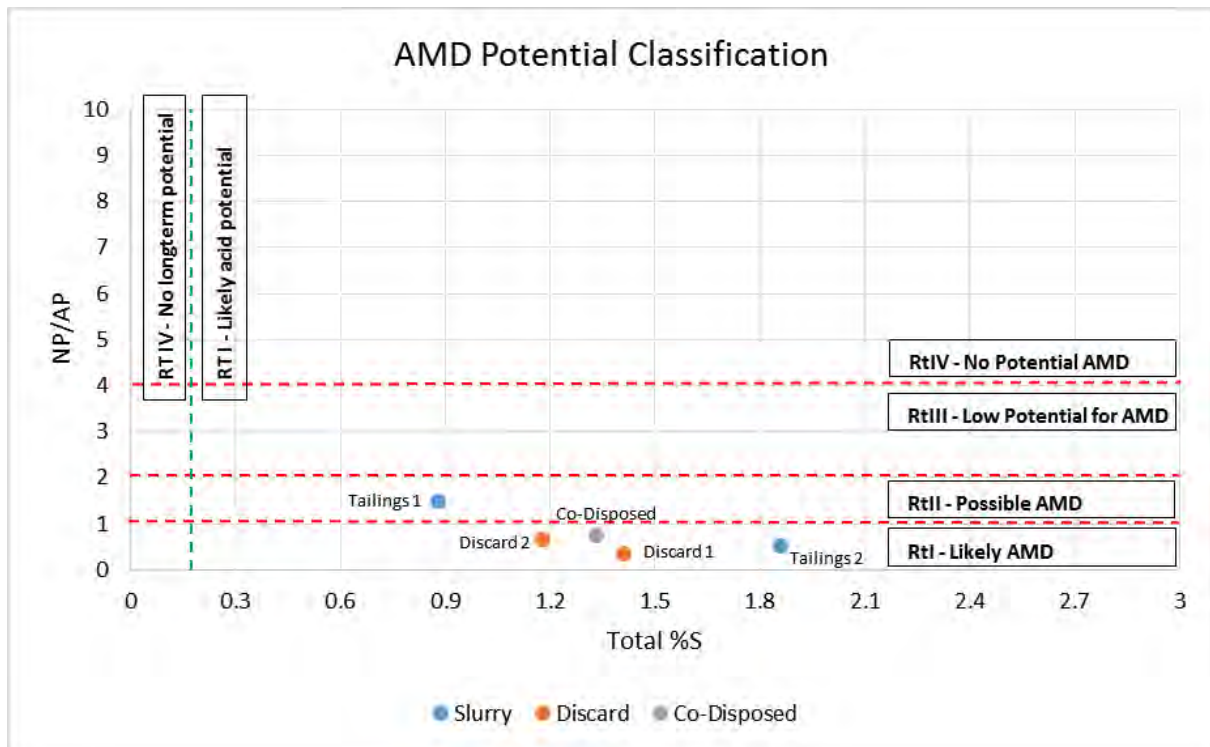


Figure 5-12: Potential Acid Generation and Classification of Samples (adapted from Fourie, 2014)

Table 5-9: ABA (Acid-base accounting) results

| ID | Paste pH | Total %S | AP CaCO ₃ kg/t | NP CaCO ₃ kg/t | NNP CaCO ₃ kg/t | NP/AP | Rock Type NNP | Rock Type %S | Rock Type NP/AP |
|------------|----------|----------|---------------------------|---------------------------|----------------------------|-------|---------------|--------------|-----------------|
| Discard 1 | 6.41 | 1.41 | 44.06 | 15.09 | -28.97 | 0.34 | I | I | I |
| Discard 2 | 6.31 | 1.18 | 36.88 | 24.70 | -12.17 | 0.67 | Uncertain | I | I |
| Tailings 1 | 7.29 | 0.88 | 27.50 | 40.95 | 13.45 | 1.49 | Uncertain | I | II |
| Tailings 2 | 7.23 | 1.86 | 58.13 | 30.00 | -28.13 | 0.52 | I | I | I |

Table 5-10: NAG (Net acid generation) results

| ID | Description | NAG pH: (H ₂ O ₂) | NAG (kg H ₂ SO ₄ /t) | NNP(CaCO ₃ kg/t) | Rock Type |
|--------|-------------|--|--|-----------------------------|---|
| AIS871 | Discard 1 | 2.82 | 16.61 | -28.97 | Rock Type Ia. High Capacity Acid Forming |
| AIS872 | Discard 2 | 3.05 | 9.96 | -12.17 | Rock Type Ib. Lower Capacity Acid Forming |

| ID | Description | NAG pH: (H ₂ O ₂) | NAG (kg H ₂ SO ₄ /t) | NNP(CaCO ₃ kg/t) | Rock Type |
|--------|-------------|---|---|--------------------------------|--|
| AIS876 | Tailings 1 | 7.04 | 0.00 | 13.45 | Rock Type IV. Non-acid Forming |
| AIS877 | Tailings 2 | 2.70 | 22.37 | -28.13 | Rock Type Ia. High Capacity Acid Forming |

Table 5-11: ABA average for tailings and discard samples

| ID | Sample Count | Total %S | AP CaCO ₃ kg/t | NP CaCO ₃ kg/t | NNP CaCO ₃ kg/t | NP/A P | Rock Type NNP | Rock Type %S | Rock Type NP/AP |
|----------------------|-----------------|-------------|---------------------------------|---------------------------------|----------------------------------|-----------|---------------------|--------------------|-----------------------|
| Discard | 2 | 1.29 | 40.46 | 19.89 | -20.56 | 0.49 | I | I | I |
| Tailings | 2 | 1.33 | 42.81 | 35.47 | -7.34 | 0.82 | I | I | I |
| Discard/ta ilings | 4 | 1.31 | 41.64 | 27.68 | -13.95 | 0.66 | I | I | I |

Table 5-12: Potential for various material to generate acid drainage.

| ID Criteria | Sample Count | %S >0.3 Rock Type (NP/AP) I or II | %S <0.3 Rock Type (NP/AP) III or IV | %S 0.1 - 0.3 Rock Type (NP/AP) I or II | %S 0.1 - 0.3 Rock Type (NP/AP) III or IV | %S >0.1 Rock Type (NP/AP) I or II | %S <0.1 Rock Type (NP/AP) III or IV |
|-------------------------------------|-----------------|--|--|--|---|---|---|
| Discard | 2 | 100 | 0 | 0 | 0 | 0 | 0 |
| Tailings | 2 | 100 | 0 | 0 | 0 | 0 | 0 |
| Discard /Tailings | 4 | 100 | 0 | 0 | 0 | 0 | 0 |
| Potential for acid mine drainage | | Likely/pos sibly acid drainage High salt load. | Low to medium potential for acid drainage Medium salt load. | Low potential for acid drainage Low to medium salt load. | Very low potential for acid drainage Very low to low salt load. | No potential for acidic drainage Very low/no salt load. | No potential for acidic drainage Very low/no salt load. |

5.5.6 Static leaching test

Discard and tailings material was submitted for leach testing. System parameters and anions measured in the leachate are listed in Table 5-13 and the ICP-OES analytical results of the leachate are listed in Appendix E. The following pertain to the static leaching test methods used:

- Leaching tests identify the elements that will leach out of waste but do not reflect the site-specific concentration of these elements in actual seepage as a different water/rock ration and contact time will be present in the field; and
- The material was leached by hydrogen peroxide extraction. A solution/rock ratio of 1:100 was used where 100 g of the sample was agitated with 1000 ml of solution for 24h.

For leaching test results the following observations were made:

- The pH of all samples, except AIS 876 (tailings 1) were very acidic. Tailings from plant 1 indicated neutral pH conditions. Sample AIS 871 (discard 1) and AIS 877 (discard 2) showed elevated EC;
- SO_4 concentrations of all samples except AIS 876 (tailings 1) are elevated and the same is observed for NH_4 ;
- NO_3 is elevated and above SANS 241:2011 limits in sample AIS 876 (tailings 1);
- Ca was the dominant cation in the leachate followed by Mg; and
- From the metals Al, Fe and Mn leached out at elevated concentrations. Ni is elevated in one sample and Co was present above detection limits in discard samples 1, discard sample 2 and tailings sample 2 (AIS 871, AIS 872 and AIS 877).

Table 5-13: Major constituents from peroxide leach testing

| Sample ID | | pH | EC (mS/m) | SO ₄ (mg/l) | TALK (mg/l) | Cl (mg/l) | PO ₄ (mg/l) | NO ₃ (mg/l) | NH ₄ (mg/l) | F (mg/l) |
|----------------|------------------|--------------|-----------|------------------------|-------------|-----------|------------------------|------------------------|------------------------|----------|
| AIS871 | Discard 1 | 2.99 | 104.0 | 463.4 | <5 | 15.2 | 0.94 | 0.47 | 1.14 | 0.34 |
| AIS872 | Discard 2 | 3.72 | 77.9 | 312.8 | <5 | <5 | <0.1 | 1.18 | 2.11 | 0.27 |
| AIS876 | Tailings 1 | 6.63 | 41.8 | 126.9 | <5 | <5 | <0.1 | 16.67 | <0.1 | 3.90 |
| AIS877 | Tailings 2 | 2.80 | 147.3 | 454.0 | <5 | 8.0 | 0.52 | 2.51 | 3.05 | 0.22 |
| SANS 241: 2011 | 0-50% of limit | 6 - 8.4 | <85 | <250 | - | <150 | - | <5.5 | <0.75 | - |
| | 50-100% of limit | 5-6; 8.4-9.7 | 85-170 | 250-500 | - | 150-300 | - | 5.5-11 | 0.75 - 1.5 | - |
| | Above limit | <5 ; >9.7 | >170 | >500 | - | >300 | - | >11 | >1.5 | - |

5.5.7 Kinetic Leach Tests

Kinetic tests are distinguished from static tests in that they attempt to mimic natural oxidation reactions of the field setting (INAP, 2014). Column humidity leach tests were performed on 3 separate samples (discard, tailings and co-disposed mixture) over a period of 6 months (25 weeks). The following pertain to the kinetic leaching test methods used:

- Kinetic column leaching test indicate the chemicals that will leach out from the rock material over time as well as the oxidation rate of the sulphide minerals in the material.
- A rock/water ratio of 1:2 was used where 1 kg of samples was leached with 500 ml deionised water weekly. The leachate was analysed for several parameters. Unfortunately leachate quantity collected on a weekly basis from the column for analyses was not supplied by the laboratory, only the analytical results. Therefore, no mass balance(s) could be conducted for actual raw quantity data was not made available.
- The results for the 25 leaches major constituents are listed in Table 5-14, Table 5-15 and Table 5-16. ICP-OES results are listed in Appendix E.

From the kinetic leaching test results the following observations can be made:

- Discard shows elevated Electrical Conductivity (EC) and SO₄ concentrations. The concentrations decrease linearly with time but not as much as for the other samples (exponential trends).

- pH and alkalinity of all samples increased as time progressed. The ABA indicated high %S (>0.3%) values which means that acid generation is likely. However, acid generation was not observed during the test period and pH remained within the alkaline pH range. This is most likely due to initial buffering from carbonate minerals in the waste material (calcite/dolomite as identified with the XRD analysis). However, according to Bradham and Caruccio (1990) and Lapakko (1993) ABA does not relate well to kinetic tests for it is assumed that parallel acid/alkaline releases takes place and does not reflect different particle sizes (EPA, 1994).
- Ni is present within all samples at significant concentrations. The discard sample shows the most elevated metals which included Al, As, Fe, Mn, Ni and Pb.
- The co-disposed sample indicates that buffering against acid generation is obtained and a decrease in SO₄ generation (due to the limited oxidation of pyrite) is achieved. The chemistry follows an exponential change with regards to pH and SO₄ produced.
- The total dissolved solids (TDS) and sulphate (SO₄²⁻) measured in the leachate for the discard, tailings and co-disposed material are indicated in Figure 5-13, Figure 5-14 and Figure 5-15, respectively. It can be seen that the discard material has a higher salt load when compared to the tailings and co-deposited material which has a low salt load. An exponential decrease in the salt produced is observed after 2 weeks. The co-disposal potential is noted, for a material which has the capacity to produce a high salt load (discard) is buffered by a material with a potential to generate a low salt load (tailings). The net product is a co-disposed material with a low salt load leachate potential.
- Figure 5-16 illustrates the change in alkalinity (measured as CaCO₃) for the tested material. It can be seen that the co-disposal leachate alkalinity is greater than that of discard and tailings material on its own. However, there is no clear linear or exponential relationship observed between time and alkalinity. This suggest that the solubility of the calcite and dolomite minerals may be influenced by external factors which includes saturated state, temperature and oxygen ingress.
- Figure 5-17 illustrates the change in pH over the 25 week test period. It can clearly be seen that the pH remains alkaline throughout the test period for all samples. This is an indication of saline drainage (SD). Therefore, Equation 4 (as discussed in section 2.2.3) is occurring. There is no linear relationship observed for the pH recorded during the test period.

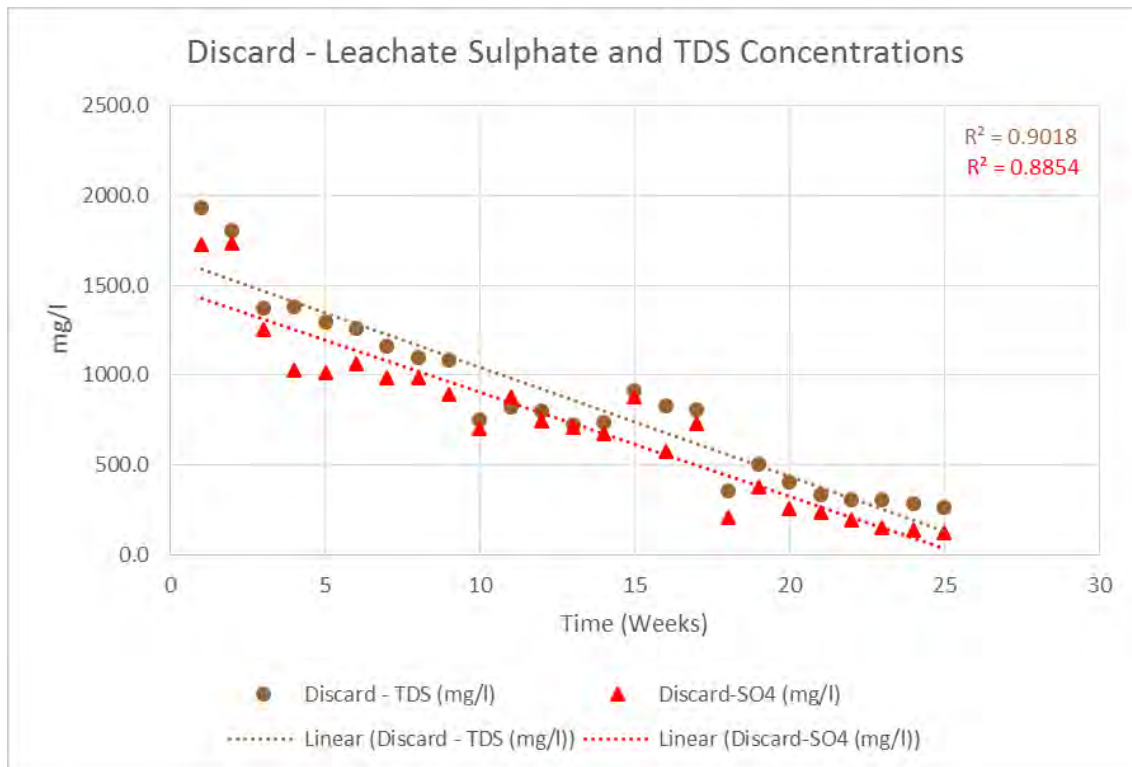


Figure 5-13: Discard material sulphate vs total dissolved solids in leachate produced

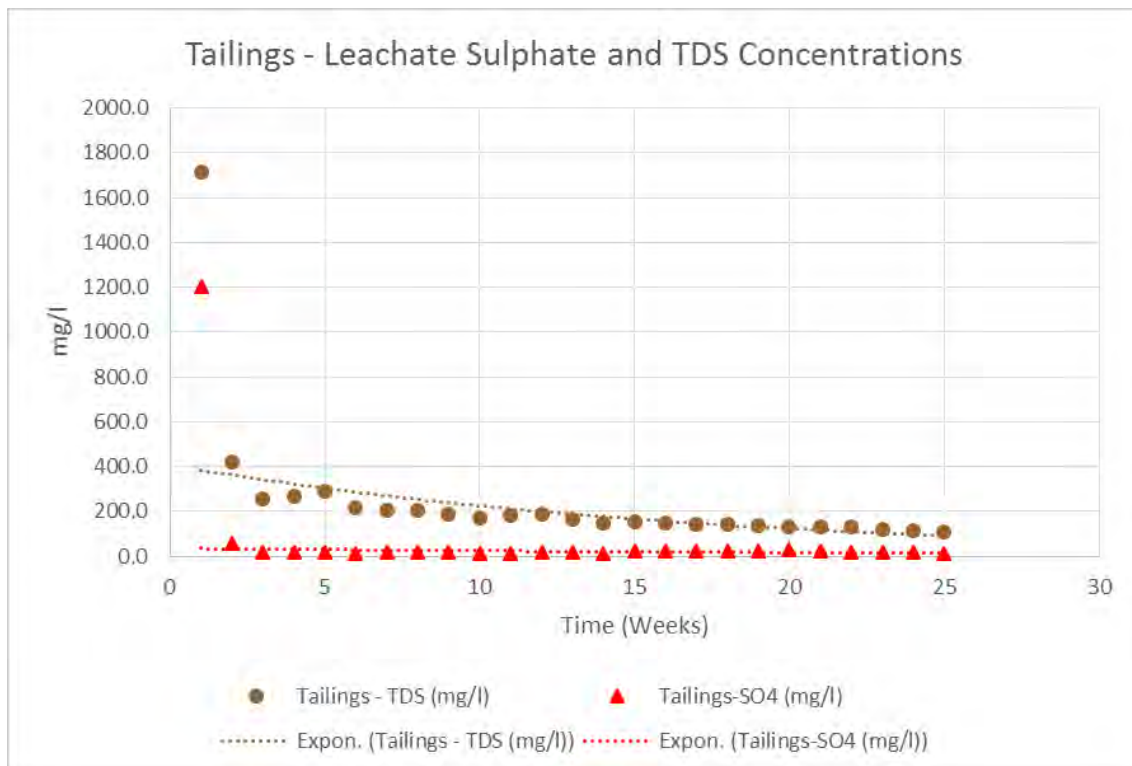


Figure 5-14: Tailings material sulphate vs total dissolved solids in leachate produced

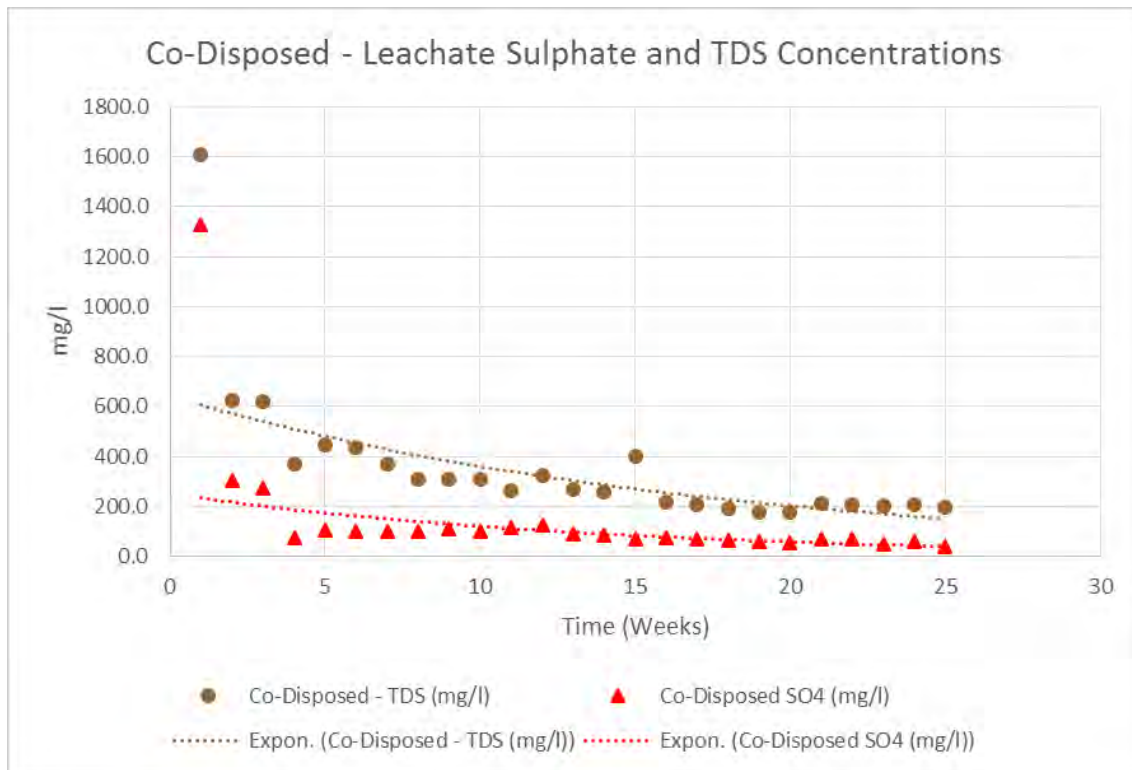


Figure 5-15: Co-Disposed material sulphate vs total dissolved solids in leachate produced

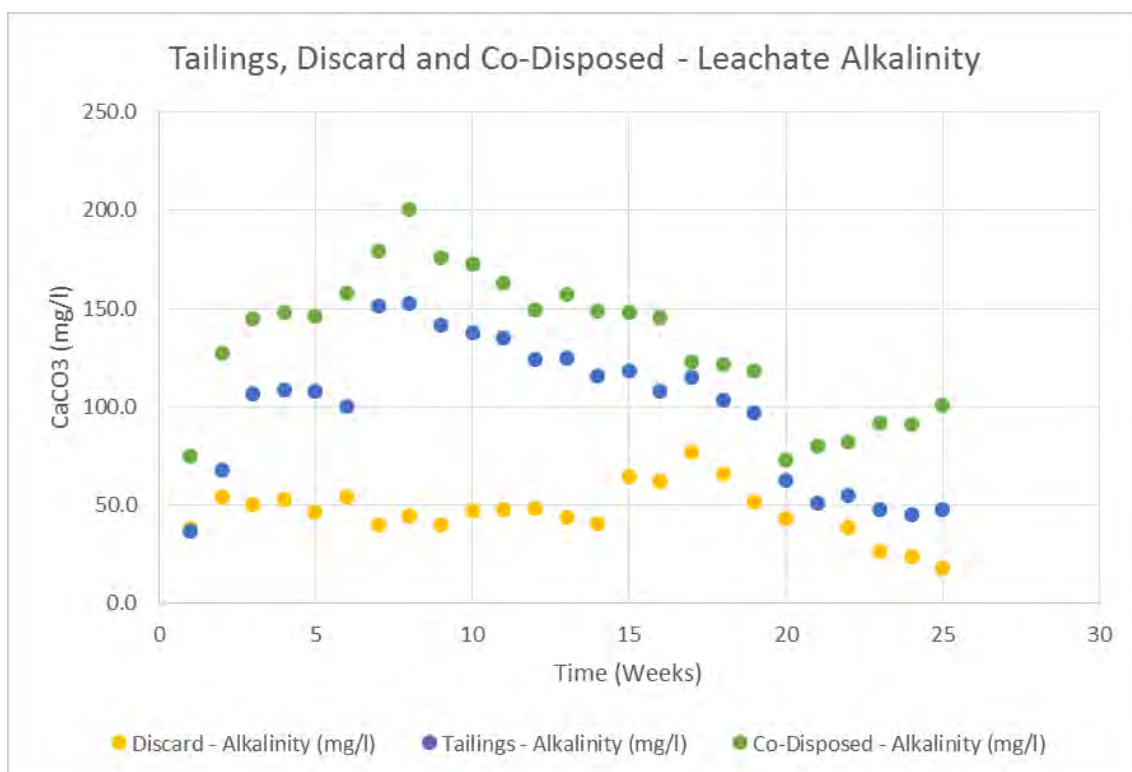


Figure 5-16: Discard, tailings and co-disposed material leachate alkalinity

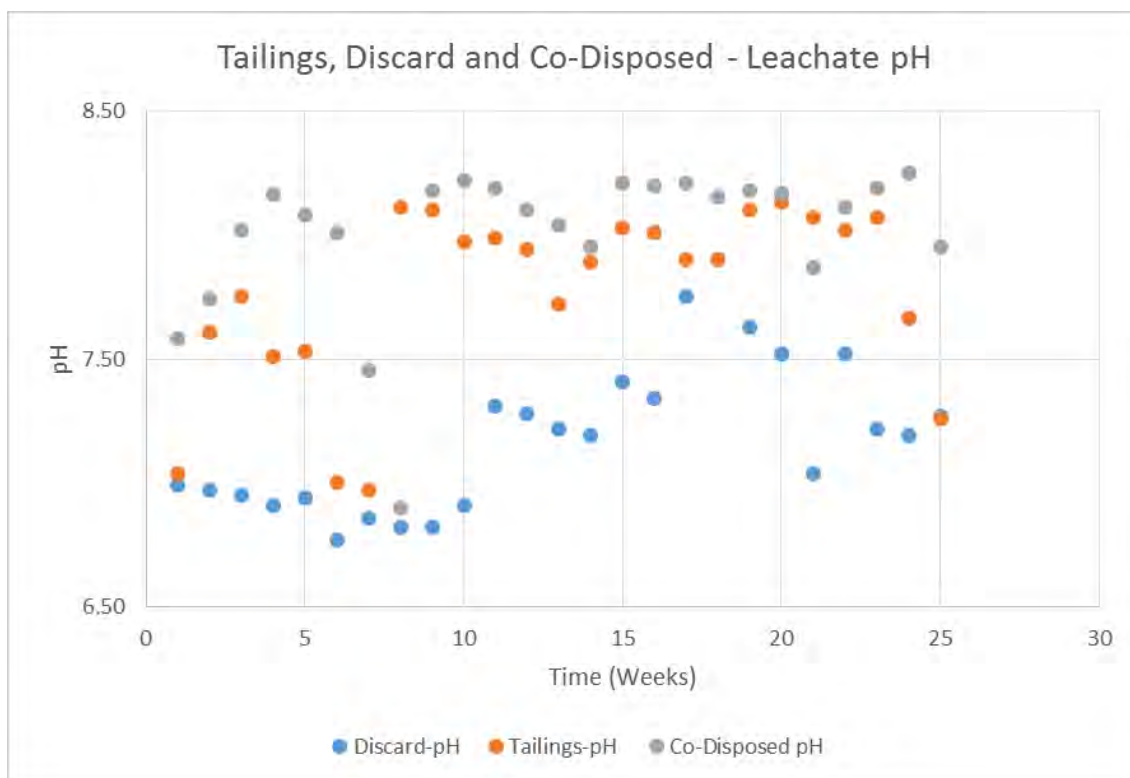


Figure 5-17: Discard, tailings and co-disposed material leachate pH

Table 5-14: Major constituents analysed in leachate (Sample AIS 871, Discard)

| Sample ID | Discard into pit BCDE Sample1 (AIS 871) | | | | | | | |
|-----------|---|-----------|------------------------|-------------------------|-----------|----------------------------|---------------------|----------|
| Leach | pH (Value) | EC (mS/m) | SO ₄ (mg/l) | Total Alkalinity (mg/l) | Cl (mg/l) | PO ₄ as P(mg/l) | Nitrate as N (mg/l) | F (mg/l) |
| 0 | 3.87 | 318 | 1957 | 25.2 | 11.3 | 0.22 | 0.37 | <0.2 |
| 1 | 6.99 | 302 | 1730 | 38.0 | 10.4 | <0.2 | 0.21 | <0.2 |
| 2 | 6.97 | 282 | 1736 | 54.6 | 15.6 | <0.2 | 0.55 | <0.2 |
| 3 | 6.95 | 215 | 1251 | 50.4 | 10.4 | <0.2 | 0.20 | <0.2 |
| 4 | 6.91 | 216 | 1026 | 52.9 | 21.6 | <0.2 | <0.2 | <0.2 |
| 5 | 6.94 | 203 | 1012 | 46.7 | 26.6 | <0.2 | <0.2 | <0.2 |
| 6 | 6.77 | 197 | 1063 | 54.5 | 28.4 | <0.2 | <0.2 | <0.2 |
| 7 | 6.86 | 182 | 988 | 40.0 | 19.1 | <0.2 | <0.2 | <0.2 |
| 8 | 6.82 | 171 | 982 | 44.4 | 11.1 | <0.2 | <0.2 | <0.2 |
| 9 | 6.82 | 169 | 889 | 40.1 | <5 | <0.2 | <0.2 | <0.2 |
| 10 | 6.91 | 117 | 701 | 47.3 | <5 | <0.2 | <0.2 | <0.2 |
| 11 | 7.31 | 129 | 880 | 48.1 | <5 | <0.2 | <0.2 | <0.2 |
| 12 | 7.28 | 125 | 747 | 48.5 | <5 | <0.2 | <0.2 | <0.2 |
| 13 | 7.22 | 113 | 711 | 43.8 | <5 | <0.2 | <0.2 | <0.2 |
| 14 | 7.19 | 115 | 676 | 40.7 | <5 | <0.2 | <0.2 | <0.2 |
| 15 | 7.41 | 143 | 875 | 64.9 | <5 | <0.2 | <0.2 | <0.2 |
| 16 | 7.34 | 130 | 571 | 62.3 | <5 | <0.2 | <0.2 | <0.2 |
| 17 | 7.75 | 126 | 730 | 77.1 | <5 | <0.2 | <0.2 | <0.2 |
| 18 | 7.90 | 55.9 | 206 | 66.1 | <5 | <0.2 | <0.2 | <0.2 |
| 19 | 7.63 | 78.9 | 377 | 51.4 | <5 | <0.2 | <0.2 | 0.22 |
| 20 | 7.52 | 62.9 | 255 | 43.5 | <5 | <0.2 | <0.2 | 0.24 |
| 21 | 7.04 | 51.7 | 235 | 50.7 | <5 | <0.2 | <0.2 | <0.2 |

| Sample ID | | Discard into pit BCDE Sample1 (AIS 871) | | | | | | | |
|---------------|------------------|---|-----------|------------------------|-------------------------|-----------|----------------------------|---------------------|----------|
| Leach | | pH (Value) | EC (mS/m) | SO ₄ (mg/l) | Total Alkalinity (mg/l) | Cl (mg/l) | PO ₄ as P(mg/l) | Nitrate as N (mg/l) | F (mg/l) |
| 22 | | 7.52 | 48.0 | 194 | 38.6 | <5 | <0.2 | <0.2 | <0.2 |
| 23 | | 7.22 | 47.2 | 153 | 26.5 | 6.8 | <0.2 | <0.2 | <0.2 |
| 24 | | 7.19 | 44.5 | 137 | 23.9 | 6.9 | <0.2 | <0.2 | <0.2 |
| 25 | | 7.27 | 41.5 | 122 | 18.0 | 8.3 | <0.2 | <0.2 | <0.2 |
| SANS 241:2011 | 0-50% of limit | 6 - 8.4 | <85 | <250 | - | <150 | - | <5.5 | |
| | 50-100% of limit | 5-6; 8.4-9.7 | 85-170 | 250-500 | - | 150-300 | - | 5.5-11 | |
| | Above limit | <5 ; >9.7 | >170 | >500 | - | >300 | - | >11 | |

Table 5-15: Major constituents analysed in leachate (Sample AIS 878, Tailings Opencast Pit)

| Sample ID | | Tailings NEW batch (AIS 878) | | | | | | | |
|---------------|------------------|------------------------------|-----------|------------------------|-------------------------|-----------|----------------------------|---------------------|----------|
| Leach | | pH (Value) | EC (mS/m) | SO ₄ (mg/l) | Total Alkalinity (mg/l) | Cl (mg/l) | PO ₄ as P(mg/l) | Nitrate as N (mg/l) | F (mg/l) |
| 0 | | | | | | | | | |
| 1 | | - | - | 3591 | 36.5 | 453.5 | <0.2 | 0.84 | - |
| 2 | | 7.04 | 268 | 1203 | 68.1 | 198.8 | <0.2 | <0.2 | 0.82 |
| 3 | | 7.61 | 65.4 | 58.7 | 107 | 71.7 | <0.2 | <0.2 | 0.70 |
| 4 | | 7.75 | 40.1 | 15.9 | 109 | 35.0 | <0.2 | <0.2 | 0.24 |
| 5 | | 7.51 | 42.2 | 15.3 | 108 | 38.3 | <0.2 | <0.2 | <0.2 |
| 6 | | 7.53 | 45.7 | 18.4 | 100 | 42.6 | <0.2 | <0.2 | <0.2 |
| 7 | | 7.00 | 33.5 | 16.3 | 152 | 26.6 | <0.2 | <0.2 | <0.2 |
| 8 | | 6.97 | 31.9 | 16.8 | 153 | 26.9 | <0.2 | <0.2 | <0.2 |
| 9 | | 8.11 | 31.9 | 15.6 | 142 | 22.9 | <0.2 | <0.2 | <0.2 |
| 10 | | 8.10 | 29.3 | 13.3 | 137 | 20.0 | <0.2 | <0.2 | <0.2 |
| 11 | | 7.97 | 26.8 | 14.0 | 135 | 19.5 | <0.2 | <0.2 | <0.2 |
| 12 | | 7.99 | 28.9 | 18.7 | 124 | 19.5 | <0.2 | <0.2 | <0.2 |
| 13 | | 7.94 | 29.5 | 15.3 | 125 | 16.6 | <0.2 | <0.2 | <0.2 |
| 14 | | 7.72 | 25.6 | 11.6 | 116 | 12.1 | <0.2 | <0.2 | <0.2 |
| 15 | | 7.89 | 22.8 | 11.6 | 118 | 12.0 | <0.2 | <0.2 | <0.2 |
| 16 | | 8.03 | 23.8 | 24.8 | 108 | 12.6 | <0.2 | <0.2 | <0.2 |
| 17 | | 8.01 | 23.3 | 24.5 | 115 | 12.0 | <0.2 | <0.2 | <0.2 |
| 18 | | 7.90 | 22.6 | 25.0 | 104 | 11.1 | <0.2 | <0.2 | <0.2 |
| 19 | | 8.10 | 21.5 | 26.6 | 97.1 | 11.1 | <0.2 | <0.2 | <0.2 |
| 20 | | 8.13 | 20.3 | 28.2 | 63.0 | 19.9 | 0.41 | <0.2 | <0.2 |
| 21 | | 8.07 | 20.3 | 26.4 | 50.8 | 37.4 | 0.43 | <0.2 | <0.2 |
| 22 | | 8.02 | 20.5 | 16.5 | 55.2 | 15.8 | <0.2 | <0.2 | <0.2 |
| 23 | | 8.07 | 18.4 | 16.3 | 47.5 | 15.8 | <0.2 | <0.2 | <0.2 |
| 24 | | - | - | 17.1 | 45.0 | 15.6 | <0.2 | <0.2 | <0.2 |
| 25 | | 7.26 | 17.3 | 14.2 | 47.6 | 13.1 | <0.2 | <0.2 | <0.2 |
| SANS 241:2011 | 0-50% of limit | 6 - 8.4 | <85 | <250 | - | <150 | | <5.5 | |
| | 50-100% of limit | 5-6; 8.4-9.7 | 85-170 | 250-500 | - | 150-300 | | 5.5-11 | |
| | Above limit | <5 ; >9.7 | >170 | >500 | - | >300 | | >11 | |

Table 5-16: Major constituents analysed in leachate (Co-Disposed in 1:1 ratio)

| Sample ID | | Discard into pit BCDE sample1 + Tailings NEW batch (AIS871-878) | | | | | | | |
|---------------|------------------|---|-----------|------------------------|-------------------------|-----------|----------------------------|---------------------|----------|
| Leach | | pH (Value) | EC (mS/m) | SO ₄ (mg/l) | Total Alkalinity (mg/l) | Cl (mg/l) | PO ₄ as P(mg/l) | Nitrate as N (mg/l) | F (mg/l) |
| 0 | | 7.37 | 574 | 3934 | 55.1 | 291.3 | <0.2 | <0.2 | 0.59 |
| 1 | | 7.58 | 251 | 1329 | 75.1 | 55.0 | <0.2 | <0.2 | 0.40 |
| 2 | | 7.74 | 97.9 | 305 | 128 | 32.7 | <0.2 | <0.2 | 0.22 |
| 3 | | 8.02 | 96.7 | 273 | 145 | 31.0 | <0.2 | <0.2 | <0.2 |
| 4 | | 8.16 | 57.5 | 71.8 | 148 | <5 | <0.2 | <0.2 | 0.22 |
| 5 | | 8.08 | 69.9 | 107 | 146 | <5 | 0.23 | <0.2 | <0.2 |
| 6 | | 8.01 | 67.9 | 101 | 158 | <5 | <0.2 | <0.2 | <0.2 |
| 7 | | - | - | - | - | - | - | - | - |
| 8 | | 6.90 | 48.1 | 99.2 | 201 | 9.14 | <0.2 | <0.2 | 0.22 |
| 9 | | 8.18 | 48.0 | 109 | 176 | 6.46 | <0.2 | <0.2 | <0.2 |
| 10 | | 8.22 | 48.0 | 98.1 | 172 | 5.87 | <0.2 | <0.2 | <0.2 |
| 11 | | 8.19 | 41.3 | 116 | 163 | 5.40 | <0.2 | <0.2 | <0.2 |
| 12 | | 8.10 | 50.6 | 125 | 149 | 6.84 | <0.2 | <0.2 | <0.2 |
| 13 | | 8.04 | 41.7 | 87.7 | 157 | 6.23 | <0.2 | <0.2 | <0.2 |
| 14 | | 7.95 | 40.0 | 84.4 | 149 | 6.64 | <0.2 | <0.2 | <0.2 |
| 15 | | 8.21 | 42.9 | 70.4 | 148 | 6.14 | <0.2 | <0.2 | <0.2 |
| 16 | | 8.20 | 34.0 | 73.9 | 145 | 6.17 | <0.2 | <0.2 | <0.2 |
| 17 | | 8.21 | 32.5 | 71.4 | 123 | 5.89 | <0.2 | <0.2 | <0.2 |
| 18 | | 8.15 | 30.2 | 64.5 | 121 | <5 | <0.2 | <0.2 | <0.2 |
| 19 | | 8.18 | 27.6 | 60.2 | 118 | <5 | <0.2 | <0.2 | <0.2 |
| 20 | | 8.17 | 27.4 | 54.2 | 73.0 | 16.0 | 0.56 | <0.2 | <0.2 |
| 21 | | 7.87 | 33.2 | 70.0 | 80.2 | 16.6 | <0.2 | <0.2 | <0.2 |
| 22 | | 8.11 | 32.1 | 68.8 | 81.8 | 12.6 | <0.2 | <0.2 | <0.2 |
| 23 | | 8.19 | 31.6 | 46.4 | 91.8 | 14.2 | <0.2 | <0.2 | <0.2 |
| 24 | | 8.25 | 32.2 | 56.7 | 90.9 | 16.2 | <0.2 | <0.2 | <0.2 |
| 25 | | 7.95 | 30.40 | 40.4 | 101 | 13.4 | <0.2 | <0.2 | 0.21 |
| SANS 241:2011 | 0-50% of limit | 6 - 8.4 | <85 | <250 | - | <150 | - | <5.5 | |
| | 50-100% of limit | 5-6; 8.4-9.7 | 85-170 | 250-500 | - | 150-300 | - | 5.5-11 | |
| | Above limit | <5 ; >9.7 | >170 | >500 | - | >300 | - | >11 | |

6 NUMERICAL MODELLING

The numerical model for the project was constructed using Visual Modflow a pre- and post-processing package for the modelling code MODFLOW. MODFLOW is a modular three dimensional groundwater flow model developed by the United States Geological Survey (Harbaugh et al., 2000). MODFLOW uses 3D finite difference discretisation and flow codes to solve the governing equations of groundwater flow. MODFLOW 2005 and WHS solver was applied to solve the flow model. The WHS Solver uses a Bi-Conjugate Gradient Stabilized (Bi-CGSTAB) acceleration routine implemented with Stone incomplete decomposition for preconditioning of the groundwater flow partial differential equations. This solver, as all iterative solvers, approaches the solution of a large set of partial differential equations iteratively through an approximate solution (SWS, 2011). The numerical model is based on the conceptual model developed and from data obtained during the course of this project.

The simulation model used in this modelling study simulates groundwater flow based on a three-dimensional cell-centred grid and may be described by the following partial differential equation:

$$\frac{\partial}{\partial x} \left(K_{xx} \frac{\partial h}{\partial x} \right) + \frac{\partial}{\partial y} \left(K_{yy} \frac{\partial h}{\partial y} \right) + \frac{\partial}{\partial z} \left(K_{zz} \frac{\partial h}{\partial z} \right) \pm W = S_s \frac{\partial h}{\partial t} \quad (5)$$

where:

- K_{xx} , K_{yy} , and K_{zz} are values of hydraulic conductivity along the x, y, and z coordinate axes, which are assumed to be parallel to the major axes of hydraulic conductivity (L/T);
- h is the potentiometric head (L);
- W is a volumetric flux per unit volume representing sources and/or sinks of water, with $W < 0.0$ for flow out of the groundwater system, and $W > 0.0$ for flow in (T^{-1});
- S_s is the specific storage of the porous material (L^{-1}); and
- t is time (T).

Equation (5), when combined with boundary and initial conditions, describes three-dimensional groundwater flow in a heterogeneous and anisotropic medium, provided that the principal axes of hydraulic conductivity are aligned with the coordinate directions (Harbaugh et al. 2000).

6.1 CONCEPTUALISATION AND MODEL GRID

The aquifer that occurs in the area and the spatial relationship between the aquifers, aquifer width, groundwater levels and flow directions, general geology and hydraulic properties are explained by the conceptual model. Figure 6-1 illustrated the developed geohydrological conceptual model. Figure 6-2 and Figure 6-3 illustrates the conceptual aquifer cross sections for the opencast pits backfilled with different waste material. The conceptual model characteristics are summarized as follows:

- Geochemistry for tailings and coal discard material suggests that the discard long term potential is greater than that of the tailings. The discard even in a compacted state has larger effective porosity when compared to that of the finer tailings material. Therefore, the hydraulic properties within the material differ and the groundwater and transport model was created to simulate the geochemistry results obtained.
- The geology outside the pit area (confirmed by drilling the monitoring boreholes) indicates that interbedded sandstone, shale and weathered dolerite characterise the downstream area of the opencast pits. The general geology within the whole study area generally consists out of interbedded siltstone, shale and sandstone (DME, 2005).
- Groundwater occurred as unconfined at shallow depths and changed into confined nature as depth increased. Groundwater levels follow the topographic setting in the area which is an indication of semi-confined to unconfined aquifer conditions. Groundwater levels in lower topographic areas vary from 4 to 12 m bgl and vary from 8 to 25 m bgl in high topographic areas.
- According to literature recharge from rainfall is in the order of 3-6% for the catchment (DWAF, 2006) and was applied to the model. No other calculations were done and only literature recharge values were applied. However, anthropogenic recharge is taking place at the opencast pit backfilled with tailing material due to active pumping. Furthermore, both pits are not covered (backfilled with overburden) and hence it is anticipated that recharge and evaporation is higher in these areas during rainfall events.
- Hydraulic conductivity (K) range between 0.01 and 0.0005 m/day. The hydraulic conductivities may increase significantly along dyke interfaces, horizontal bedding plane interfaces or within horizontal coal layers.
- Geophysical surveys around the pit suggests that there might be a dyke intercepting the opencast pit backfilled with tailings. Boreholes drilled downstream of the opencast pit indicated that there is highly weathered dolerite in the area. In the numerical model the hydraulic conductivity in this supposed area is an order larger than what is observed in other areas due to the dolerite intrusion.

- Hydro chemical characteristics indicates naturally high in Na and Cl concentrations. Therefore, the groundwater can be classified as saline. SO₄ is used as the major constituent to illustrate plume movement from the waste sources.
- The main coal seams all occur below the regional water table.

6.1.1 Model Grid

The groundwater flow model was set up as a three layer, confined/semi-unconfined aquifer. Though the landscape has changes significantly since mining started (rock dumps, berms, overburden stockpiles, voids) changing both the regional groundwater table as well as creating phreatic groundwater surfaces, one is unable to model transport flow from an empty void; or is unable to fill the void with the desire material and associated hydraulic properties after the elevations have been applied to individual top layer cells. Therefore, the aim was to set up a model where the material in the void determines the seepage quantity and quality into the surround aquifer system. Using the pre-mining topography elevations for the top layer and the post-mining topography elevations of the opencast pits for the top of the third layer, made it possible to assign hydraulic properties to the supposed backfilled material.

The first layer extends to a depth of 45-60 meters imitating the opencast pit walls and extends to the approximate total depth of the opencast pits. This was done to assign co-disposal properties to the material within the pit area which interacts with the naturally occurring geology in the area. The second layer is wedged between the other two layers at a thickness of 1.2 meters. This was to help calibrate the transport model for a worst case scenario if a dyke intersects the pit. The third layer represents the impermeable and fractured rock aquifer in depth.

River and stream boundaries were applied to relevant areas and the model mesh size was coarsened to reduce model simulation. Alternatively, the model grid was refined across and along the opencast pit areas to simulate accurate groundwater movement as well as pollution transport. The grid used for the model simulation is indicated in Figure 6-4, Figure 6-5 and Figure 6-6.

6.1.2 Boundary conditions

Boundary conditions express the conditions of known water flux, or known variables, such as the hydraulic head. Different boundary conditions result in different results. Boundary condition options in MODFLOW can be specified either as:

- Specified head or Dirichlet; or
- Specified flux or Neumann; or

- Mixed or Cauchy boundary conditions.

From the conceptual point of view, it was essential to meet two criteria:

- The modelled area should be defined by natural geological and hydrogeological boundary conditions (all hydrogeological structures should be defined within the model domain);
- The mesh size of model grid has to correspond to the nature of the problem being addressed with the model (in this case the transport of contaminants and groundwater flow);
- The borders of the numerical model were chosen at what were considered to be natural flow boundaries. These included higher topographical areas and natural surface drainage paths (streams/rivers). Local hydraulic boundaries were identified for model boundaries:
 - Initial heads were imported as pre-mining groundwater heads;
 - River cells were applied for the streams flowing through the area; and
 - The hydraulic boundaries were selected far enough from the area of investigation to not influence the numerical model behaviour in an artificial manner.

Table 6-1 lists the input parameters for the flow model before calibration.

Table 6-1: Starting Input Parameters

| Parameter | Values used |
|-----------------------------------|---|
| Horizontal hydraulic conductivity | 0.01-0.05 m/d (Cooper-Jacob Analysis) |
| Vertical hydraulic conductivity | 0.01-0.0005 m/d (Cooper-Jacob Analysis) |
| Storage coefficient | 6.4×10^{-3} (Cooper-Jacob Analysis and DWAF, 2006) |
| Specific yield | 0.25 (Morris and Johnson, 1967) |
| Recharge | 40 mm/y |
| Evaporation | 10 mm/y |
| Porosity | 0.25 - 0.35 (Davis, 1969) |
| Top elevation | Corresponds to pre-mining surface topography |
| Bottom elevation of 1st layer | Corresponds to opencast pit depth. |
| Bottom elevation of 2nd layer | Wedge between layer 1 and 2 at a fix width of 1.5m |
| Bottom of 3rd layer | Fixed at an elevation of 0 mamsl |

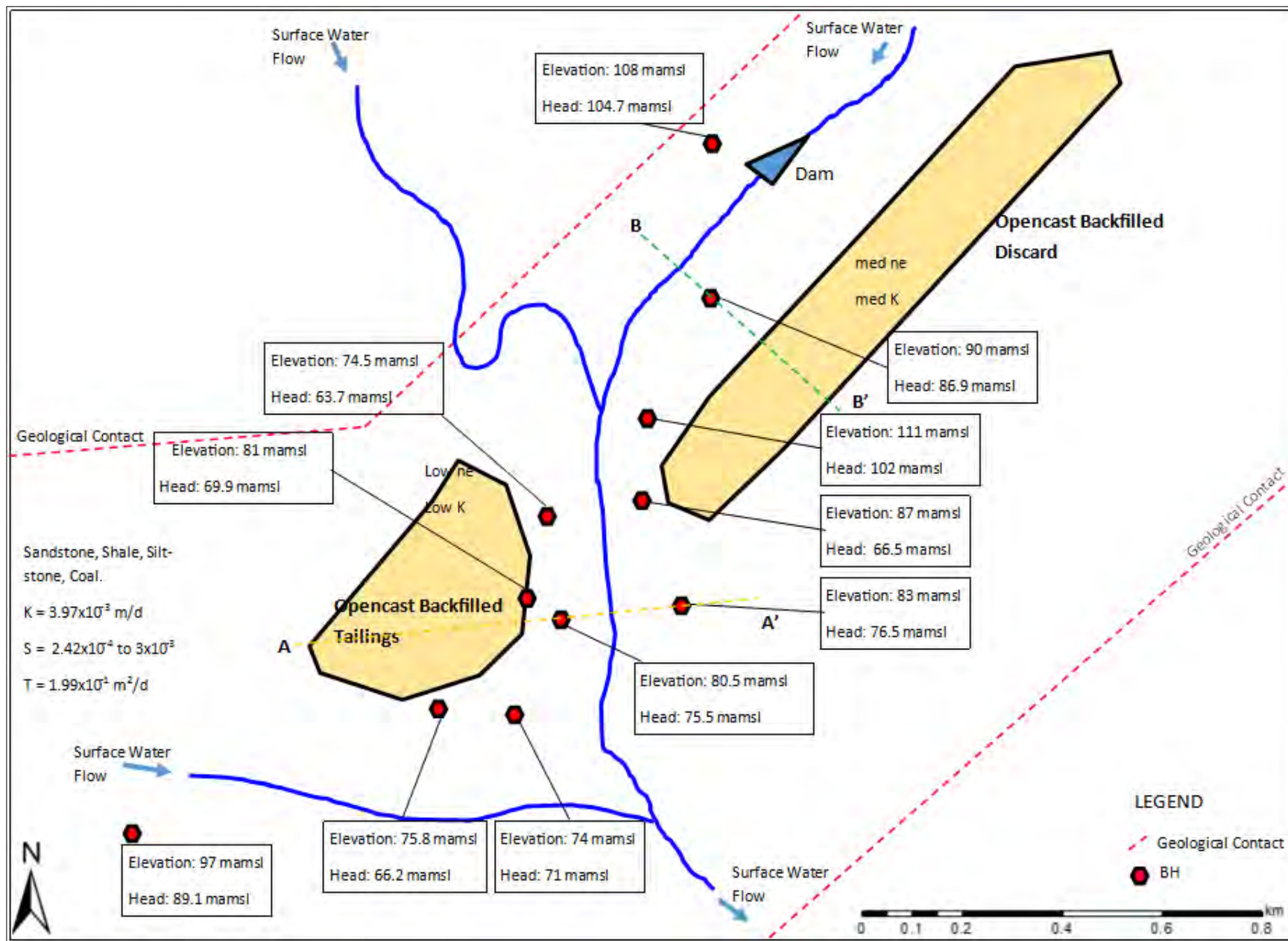


Figure 6-1: Geohydrological conceptual model of study area

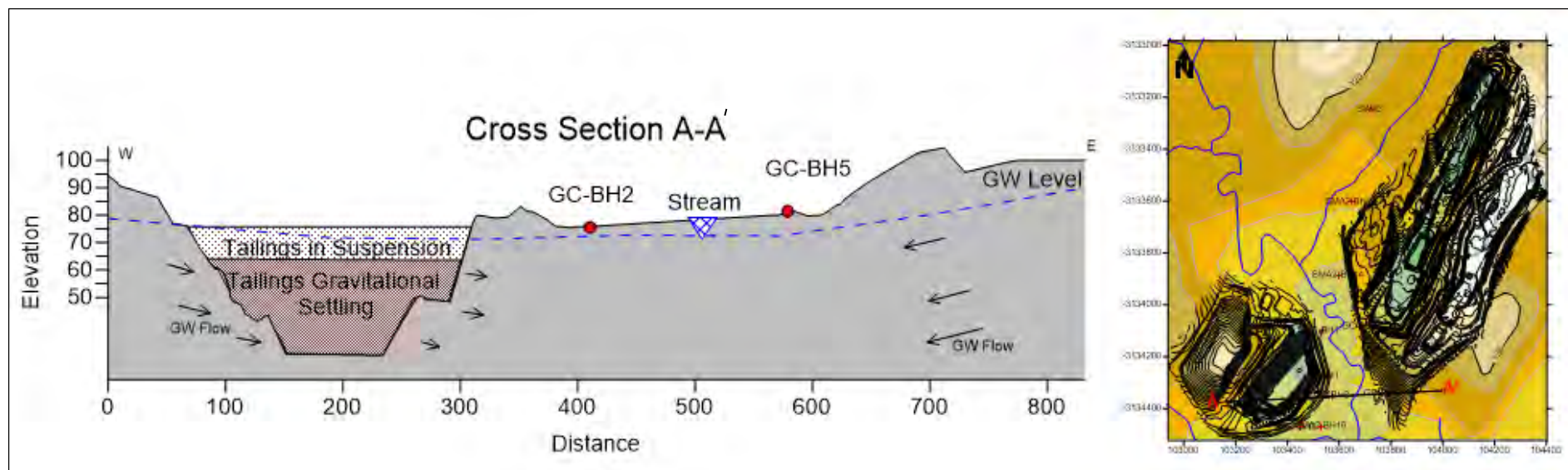


Figure 6-2: Conceptual model cross section A-A'

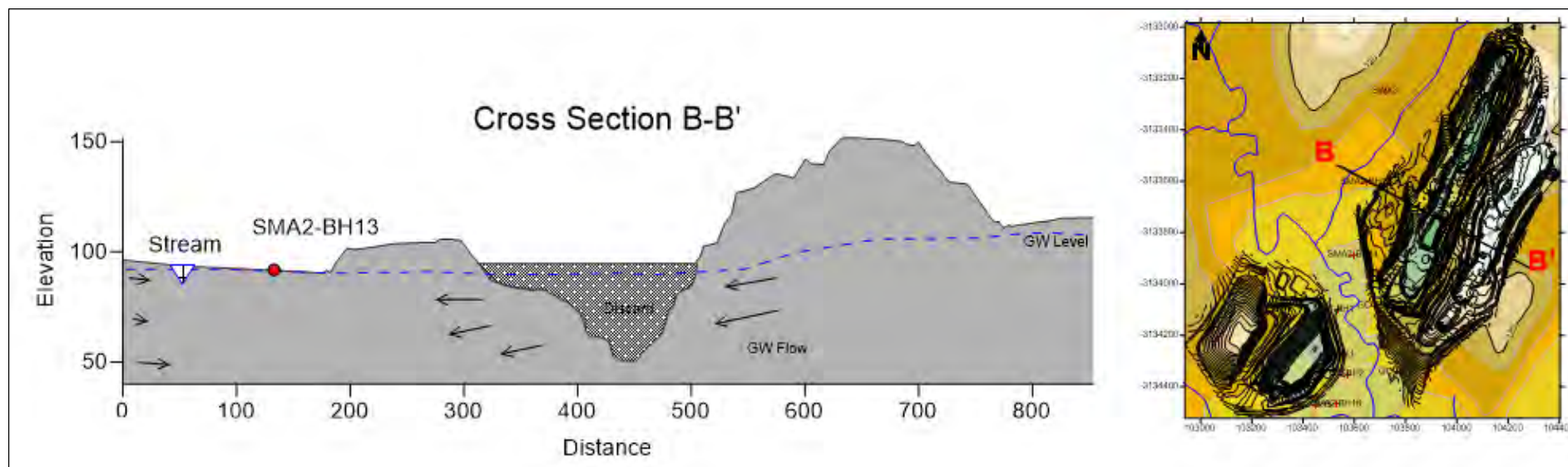


Figure 6-3: Conceptual model cross section B-B'

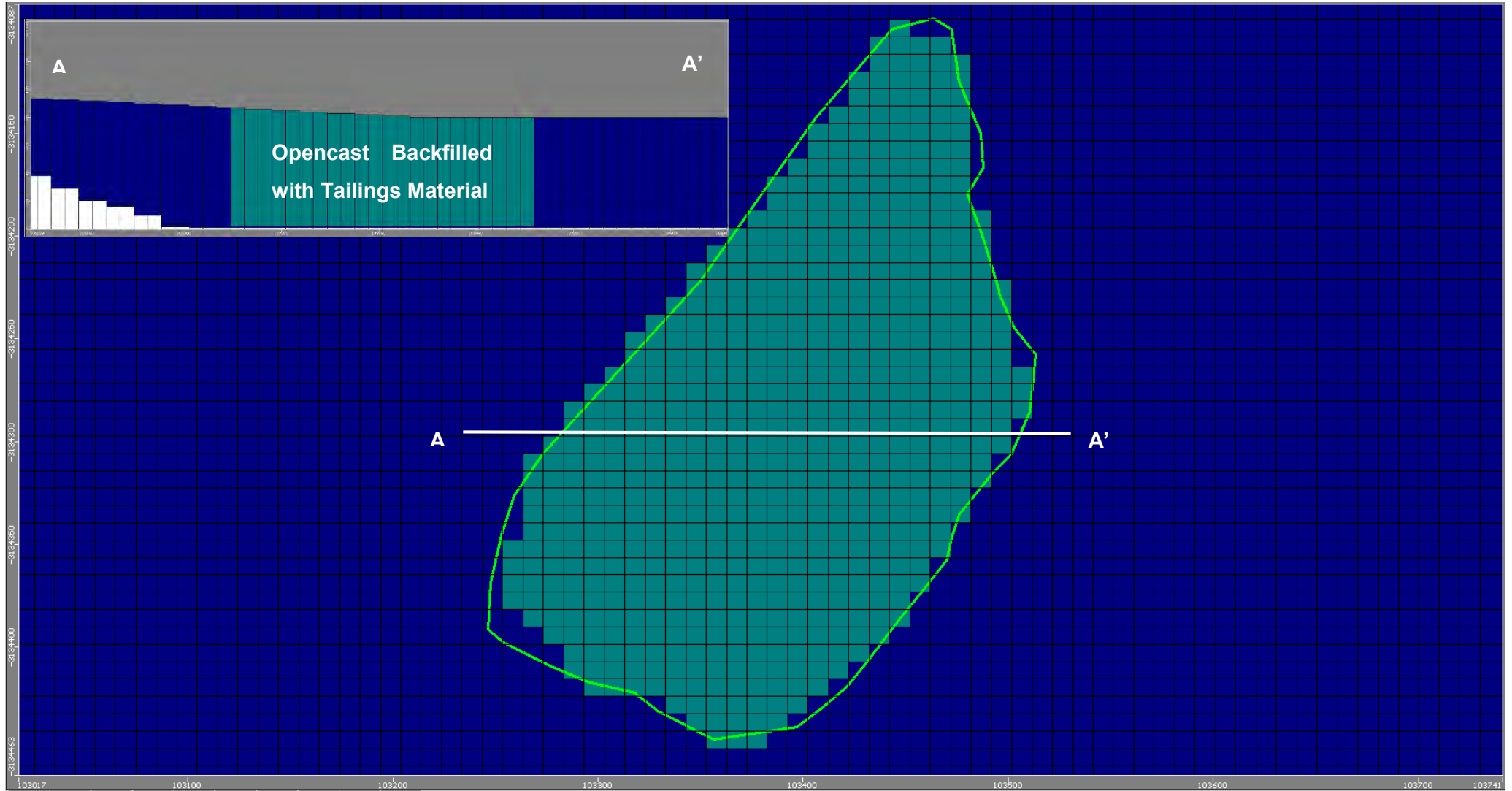


Figure 6-5: Opencast pit backfilled with tailings

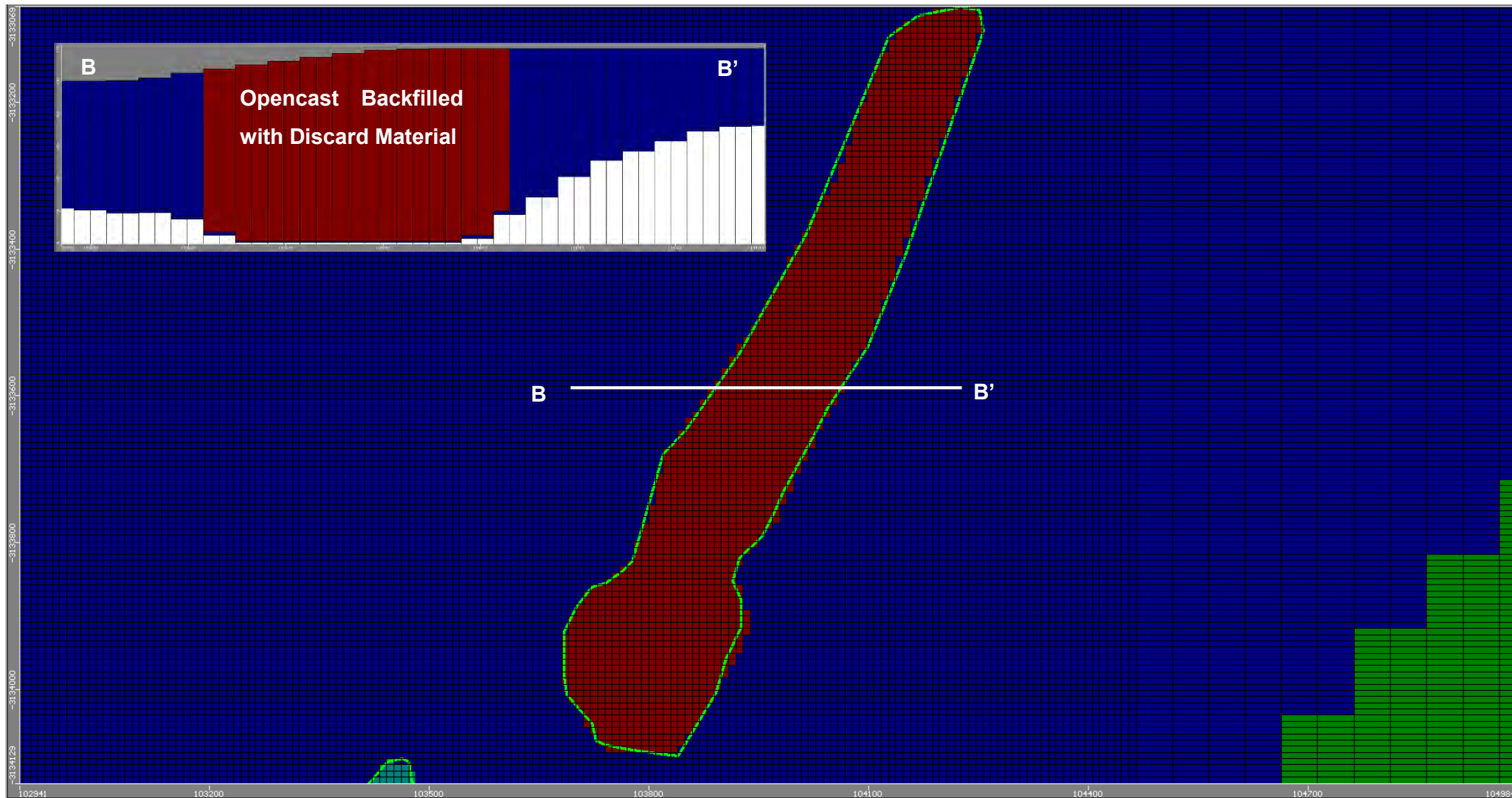


Figure 6-6: Opencast pit backfilled with discard

6.2 FLOW MODEL AND CALIBRATION

The model was initially calibrated for groundwater levels and flow using trial and error methods. Small variations to the parameters were made within the realistic ranges determined during the study. The groundwater levels calculated were compared to historical and present data. A combination of 2008 to 2015 data was applied for observation purposes and model calibration. It was assumed that pre-mining water levels are mainly topographically controlled, as discovered during the literature review.

The flow model constructed is a steady state model, therefore the following applies:

- The recharge and evaporation is constant for the entire model simulation period;
- Constant head boundaries were applied to topographical heights for the entire model simulation period; and
- River/stream boundary outflows are constant during the entire model simulation period.

The correlation between the calculated and observed groundwater levels for all the steps (2008 to 2015) in the steady state model is illustrated by Figure 6-7 and the simulated predominant flow directions and groundwater flow velocities are represented in Figure 6-8. Groundwater flow is predominantly towards the centrally located stream situated between the opencast voids. This is expected for there is a good relationship between the groundwater elevation and topographic elevation.

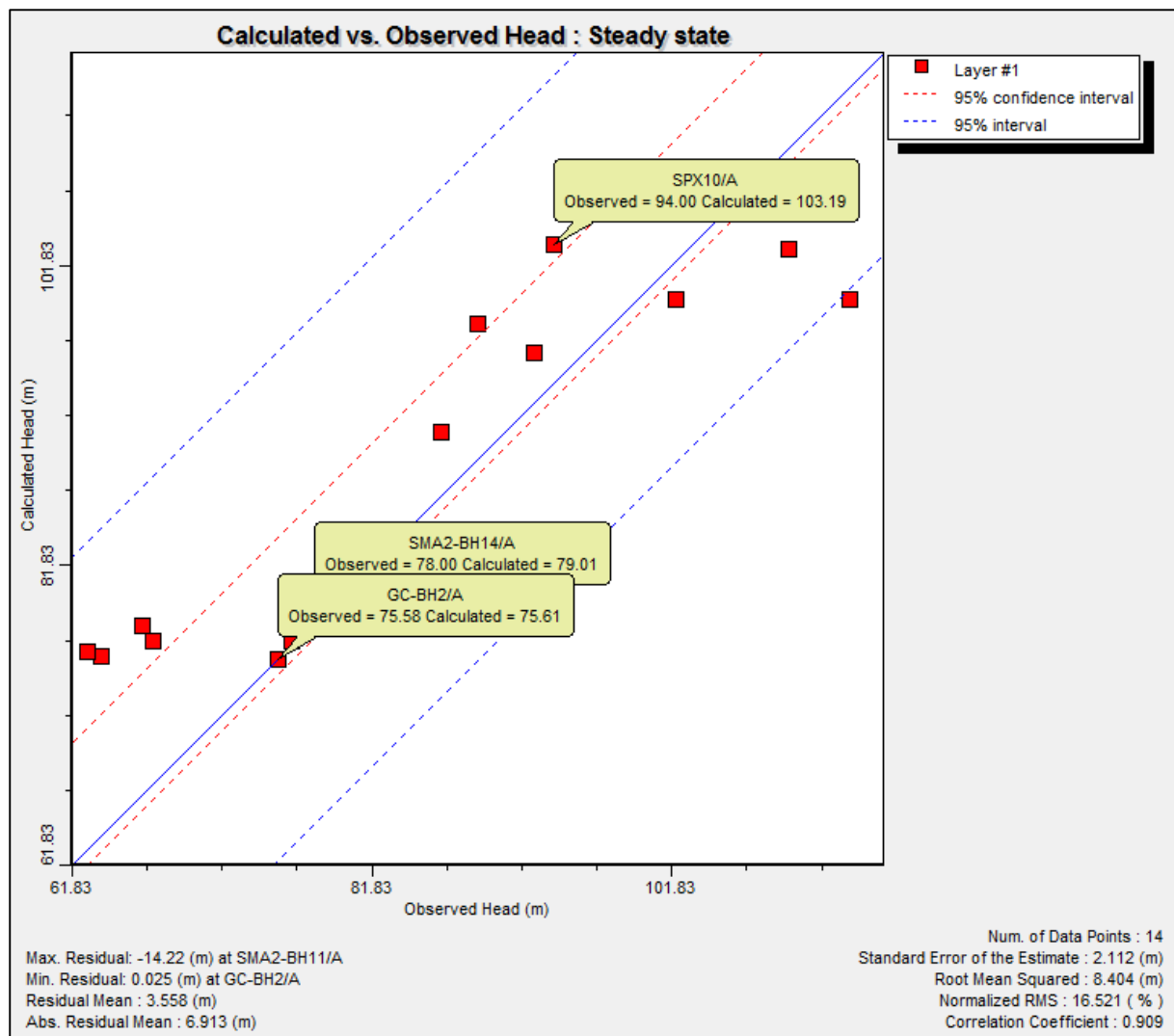


Figure 6-7: Calculated vs observed heads calibrated (steady state)

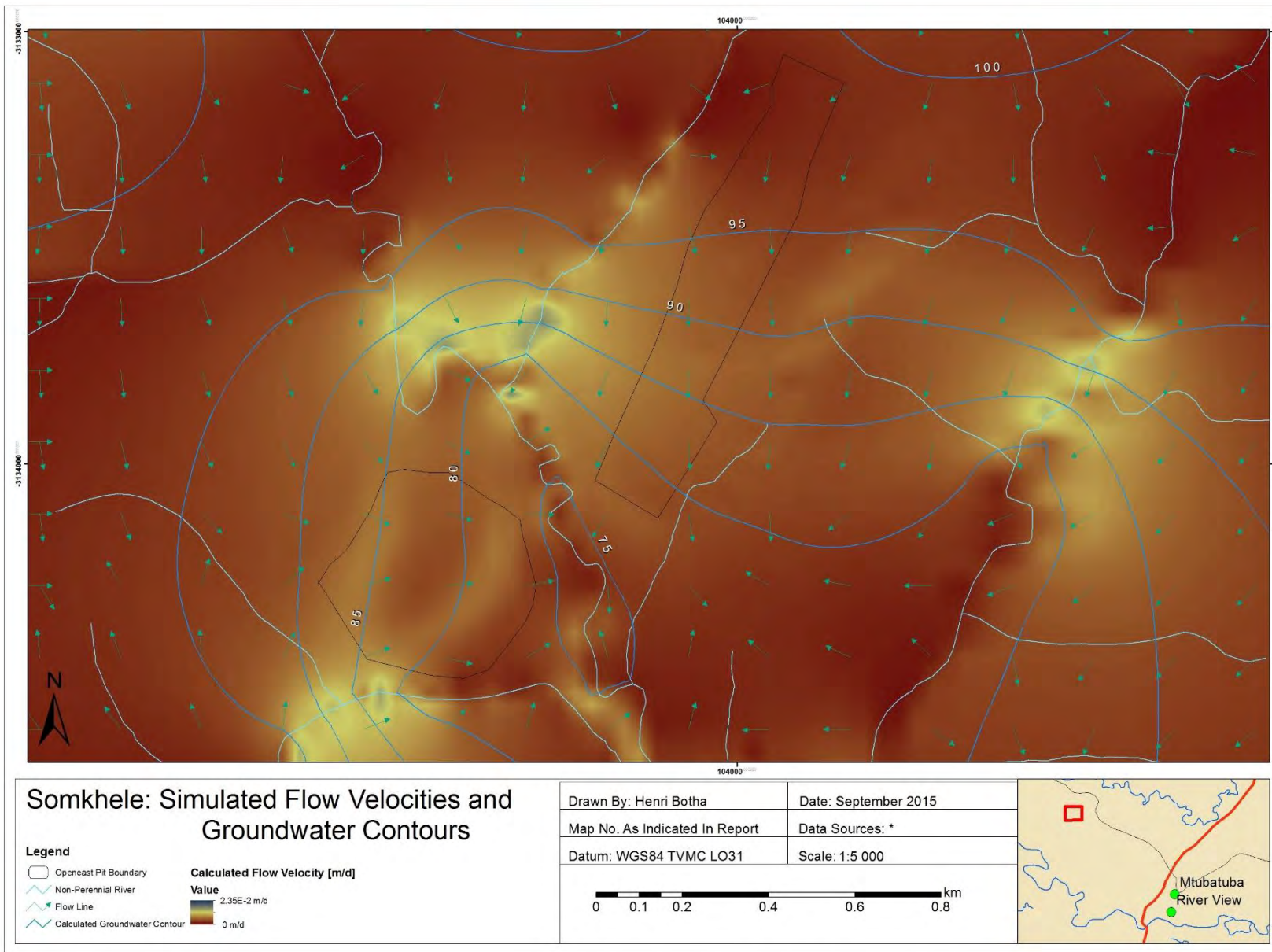


Figure 6-8: Groundwater flow directions and flow velocity map

6.3 SENSITIVE ANALYSES

A sensitivity analysis was carried out on the calibrated steady state model using zones to assess the influence on groundwater level and flow dimensions by running the model in the PEST (Parameter Estimation Simulation) and sensitivity mode. The results for the PEST analysis is discussed in this section. It was discovered that horizontal hydraulic conductivity (kx) is the most sensitive to changes, especially for layer 3. The final parameters used in the numerical model are listed in Table 6-2.

Figure 6-9 indicates the Jacobian (neutral) variations. Kx and Ky are the horizontal conductivities with respect to the cells on the X and Y plane. Kz is the vertical hydraulic conductivity of the cell on the elevation plane. The bar charts illustrates the sensitivity of the model to the minor hydraulic changes applied by PEST. It can be seen that vertical hydraulic conductivities for all layers are very sensitive to changes. The legend indicates the observation index for the amount of observations that were made during the PEST run after the adjustment of the parameters.

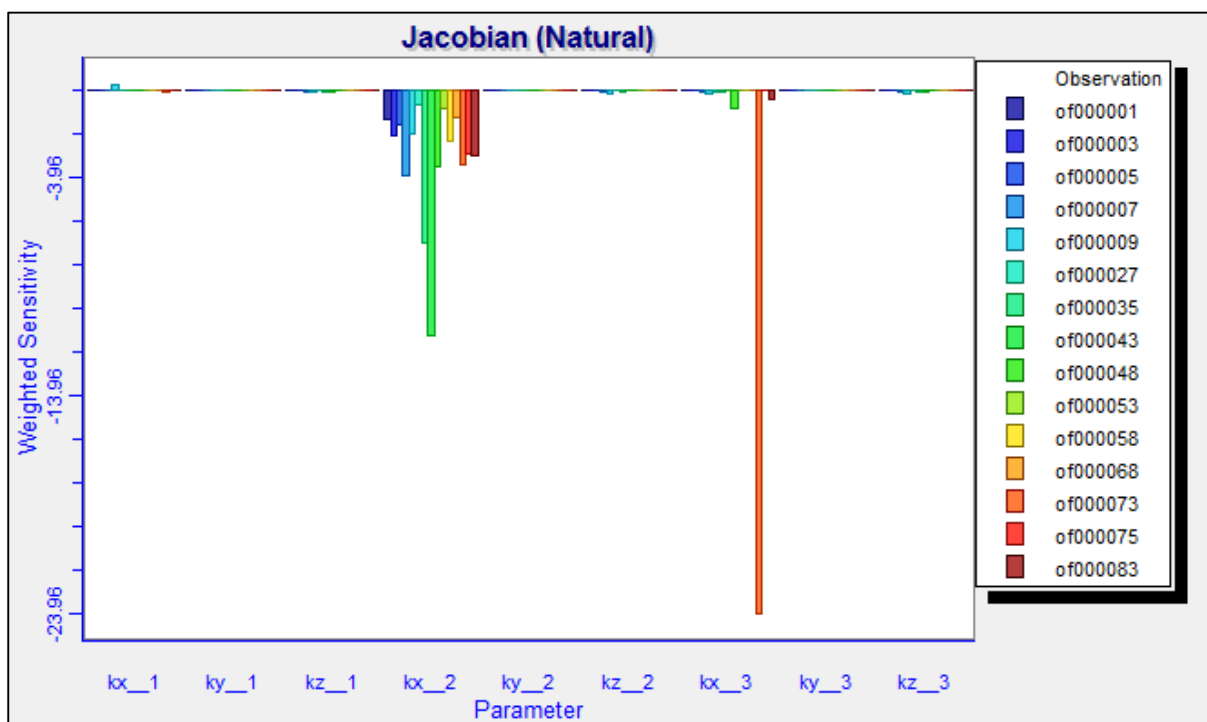


Figure 6-9: Sensitive Analysis: Jacobian (neutral) variations

Figure 6-11 indicated the calibrated residuals histogram for the PEST runs. The graph illustrates the normal distribution of the hydraulic parameters (vertical and horizontal conductivities) after changes. It can be seen that the flow model's response to the slight changes made by PEST on average are still well distributed. The normalised residuals on average is in the order of -4.66 and falls skew to the left.

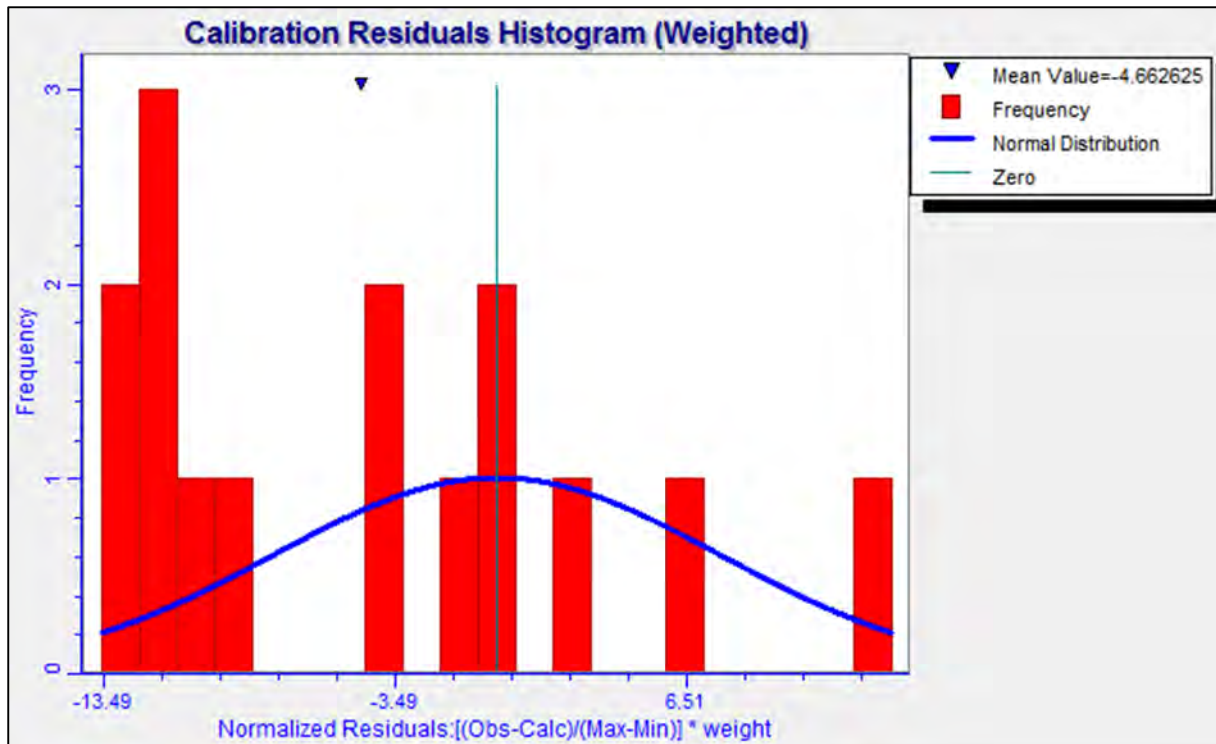


Figure 6-10: Sensitive Analysis: Calibrated residuals histogram

Figure 6-11 indicates the hydraulic conductivity sensitivity recorded during the PEST run. The legend lists the horizontal (kx and ky) as well as the vertical (kz) hydraulic conductivities. From the figure it can be seen that only the horizontal hydraulic conductivity (kx for layer 2 and layer 3) is sensitive to changes. Therefore, horizontal conductivity (kx) is very sensitive to changes.

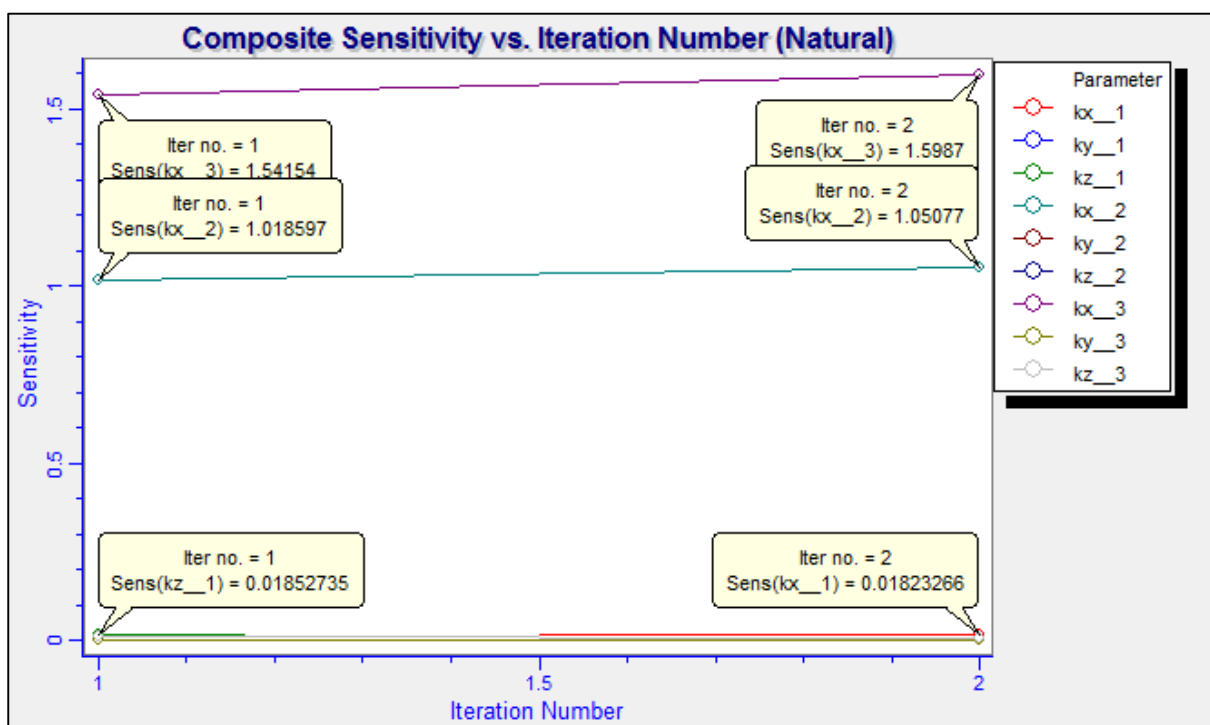


Figure 6-11: Sensitive Analysis: Hydraulic conductivity sensitivity

Figure 6-12 illustrates the calculated versus the observed weight for observations used during the PEST run. The legend indicates the weighted water levels of the heads within the chosen proximity boreholes used to calibrate the model. The observed heads formed the objective function which PEST used to make small changes to K_x , K_y and K_z in order to approximate calculated parameters to actual observed conditions.

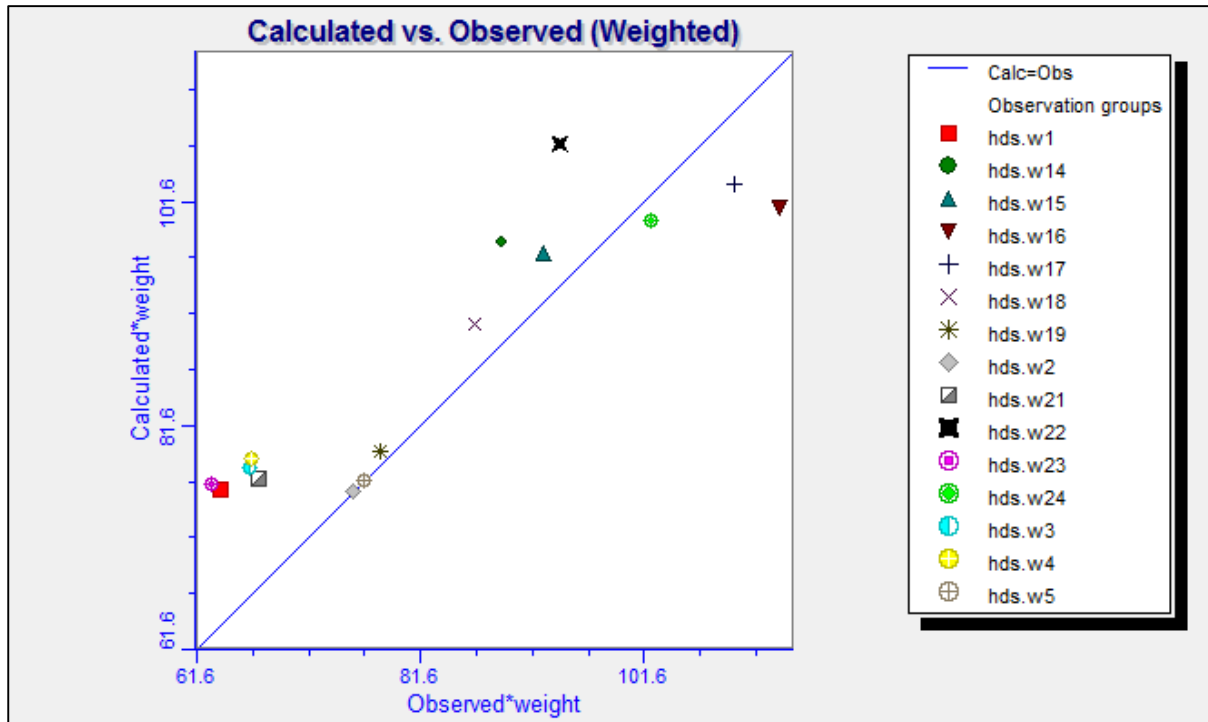


Figure 6-12: Sensitive Analysis: Calculated versus the observed heads

Figure 6-13 indicates the uncertainties of the parameters changed as a standard deviation. It can be seen that K_y layer 2, K_z layer 2 and K_y layer 3 had some uncertainties during the PEST run. The standard deviations provide only an indication of parameter uncertainty. They rely on a linearity assumption which may not extend as far in parameter space as the standard deviations themselves.

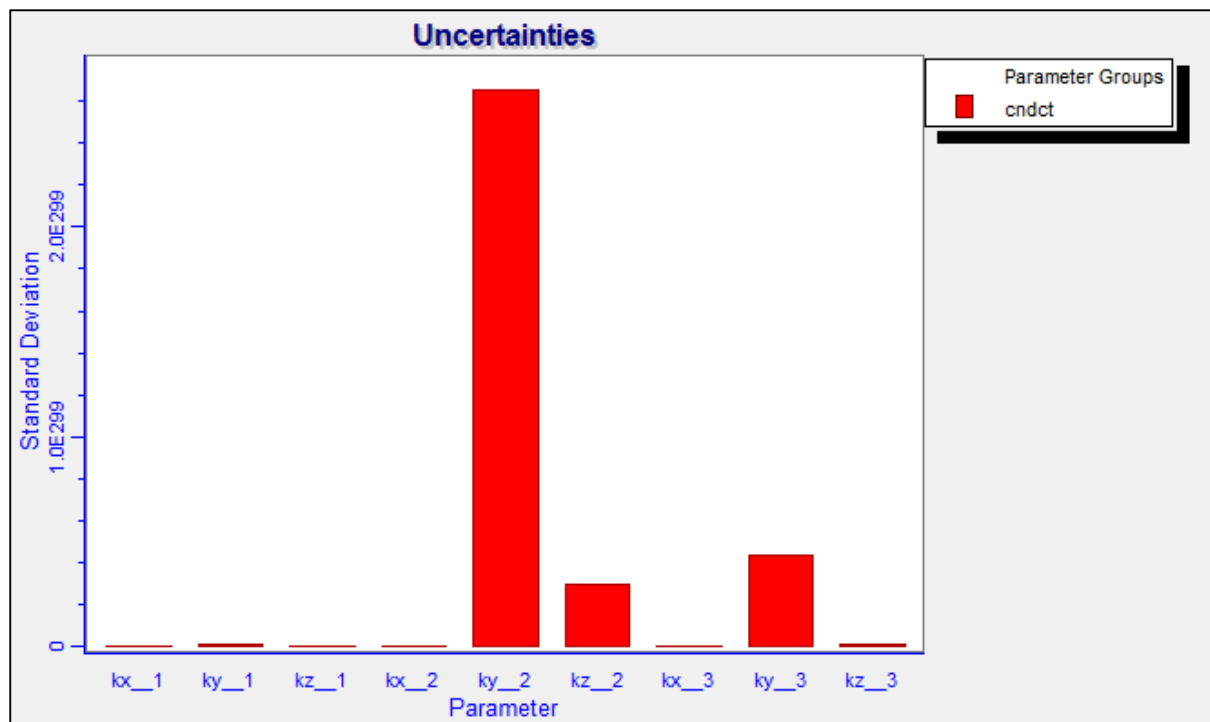


Figure 6-13: Sensitive Analysis: Uncertainties of the parameters

Table 6-2: Final parameters for the flow model (after calibration)

| Parameter | Values used (determined by PEST) |
|-----------------------------------|---|
| Horizontal hydraulic conductivity | |
| (Kx layer 1): | 1.01 x10 ⁻⁴ m/d |
| (Ky layer 1): | 9.61 x10 ⁻⁴ m/d |
| (Kx layer 2): | 3.01 x10 ⁻² m/d |
| (Ky layer 2): | 1.047 m/d |
| (Kx layer 3): | 4.07 x10 ⁻² m/d |
| (Ky layer 3): | 0.43 m/d |
| Vertical hydraulic conductivity | |
| (Kz layer 1): | 2.33 x10 ⁻⁴ m/d |
| (Kz layer 2): | 3.00 x10 ⁻² m/d |
| (Kz layer 3): | 1.4 x10 ⁻³ m/d |
| Storage coefficient | 6.4 x 10 ⁻³ (Cooper-Jacob Analysis and DWAF, 2006) |
| Specific yield | 0.25 (Morris and Johnson, 1967) |
| Recharge | 40 mm/y |
| Evaporation | 10 mm/y |
| Porosity | 0.25 - 0.35 (Davis, 1969) |
| Top elevation | Corresponds to pre-mining surface topography |
| Bottom elevation of 1st layer | Corresponds to opencast pit depth. |
| Bottom elevation of 2nd layer | Wedged between layer 1 and 2 at a fix width of 1.5m |
| Bottom of 3rd layer | Fixed at an elevation of 0 mamsl |

6.4 TRANSPORT MODELLING OF DISPOSAL OPTIONS

Following the calibration of the flow model, a contaminant transport model was constructed for the two waste disposal scenarios. MT3DS is a transport model for simulating advection, dispersion, and chemical reactions of contaminants in groundwater flow systems. It solves the transport equation after the flow solution has been obtained from groundwater flow model (SWS, 2014). In order to illustrate the potential long term effect of the disposal practices on the groundwater quality, the post-operational migration of contamination was simulated. Sulphate (SO₄²⁻) was chosen as the parameter to be modelled. Sulphate is one of the end-products of pyrite oxidation which is associated with saline rock drainage, as was observed during the geochemical testing.

The transport modelling approach consisted out of two scenarios:

1. **Conventional disposal** of tailings and discard as currently implemented at the Somkhele anthracite mine was simulated. As discussed in the previous sections the western pit, in the study area, is being backfilled with coal tailings and the eastern pit is being backfilled with discard material.
2. **Co-disposal** of coal waste into both the opencast voids was simulated.

The attributes and chemistry data observed during the geochemical testing were applied to the backfilling void areas (as per the tested material) and the groundwater sulphate plume from these sources were simulated. Constant concentrations were applied to the relevant pollution source areas (the opencast voids). The input constant concentration values were applied to specific time steps to mimic the salt loads observed during the kinetic leach testing. The time steps of importance as well as the concentrations assigned for each scenario are outlined by Table 6-3 and Table 6-4.

Table 6-3: Time steps and constant concentrations (conventional disposal)

| Time Step | Corresponding Date | Description | Sulphate Concentration |
|-----------|--------------------|---|---|
| 0 | 2008 | Mining Starts at both western and eastern pit | <p>A constant concentration in the order of 3000 mg/l was applied to the eastern pit backfilled with discard at time step 1825. A linear decrease was observed for the kinetic leach test performed on discard. Therefore, every 365th (1 year) time step the concentrations were decreased by approximately 200-300 mg/l.</p> <p>A constant concentration in the order of 2000 mg/l was applied to the western pit backfilled with coal tailings at time step 1095. A exponential decrease was observed for the kinetic leach test performed on tailings. Therefore, every 365th (1 year) time step the concentrations were decreased by approximately 300-800 mg/l.</p> |
| 1095 | 2011 | Backfilling of tailings into western pit | |
| 1825 | 2013 | Backfilling of discard into eastern pit | |
| 4380 | 2020 | Closure | |
| 8030 | 2030 | 15 Years after closure | |
| 15330 | 2050 | 35 Years after closure | |

Table 6-4: Time steps and constant concentrations (co-disposal)

| Time Step | Corresponding Date | Description | Sulphate Concentration |
|-----------|--------------------|---|---|
| 0 | 2008 | Mining Starts at both western and eastern pit | A constant concentration in the order of 1500 mg/l was applied to both opencast pits. An exponential decrease was observed for the kinetic leach test performed on the co-disposed material. Therefore, every 365 th (1 year) time step the concentrations were decreased by approximately 300-800 mg/l. |
| 1095 | 2011 | Co-disposal starts | |
| 1825 | 2013 | Co-disposal finishes | |
| 4380 | 2020 | Closure | |
| 8030 | 2030 | 15 Years after closure | |
| 15330 | 2050 | 35 Years after closure | |

6.4.1 Conventional disposal

Figure 6-14 indicates the simulated groundwater sulphate concentration trends that are generated by the opencast voids as a result of conventional disposal methods (separate disposal). OBS1 Pit A is a downstream groundwater observation point relative to the western pit backfilled with coal tailings material. OBS1 Pit B-E is a downstream groundwater observation point relative to the eastern pit backfilled with discard material (refer to Figure 6-15).

From the simulated plumes it can be seen that the discard waste produces a plume and trend similar to the laboratory observed sulphate leachate trend (refer to Figure 5-13). There is a linear decrease in the sulphate produced by the coal discard as time progresses. The coal tailings produces an exponential decreasing trend similar to the kinetic leach test performed in the laboratory for tailings material (refer to Figure 5-14).

Figure 6-15 indicates the generated sulphate plumes for 5 years, 15 years and 35 years after disposal. It can clearly be seen that the spatial distribution of the discard produced sulphate plume, is much larger than what is observed for the tailings material. Furthermore, the discard plume is more prominent and present for longer at greater concentrations, than what is observed for the coal tailings material.

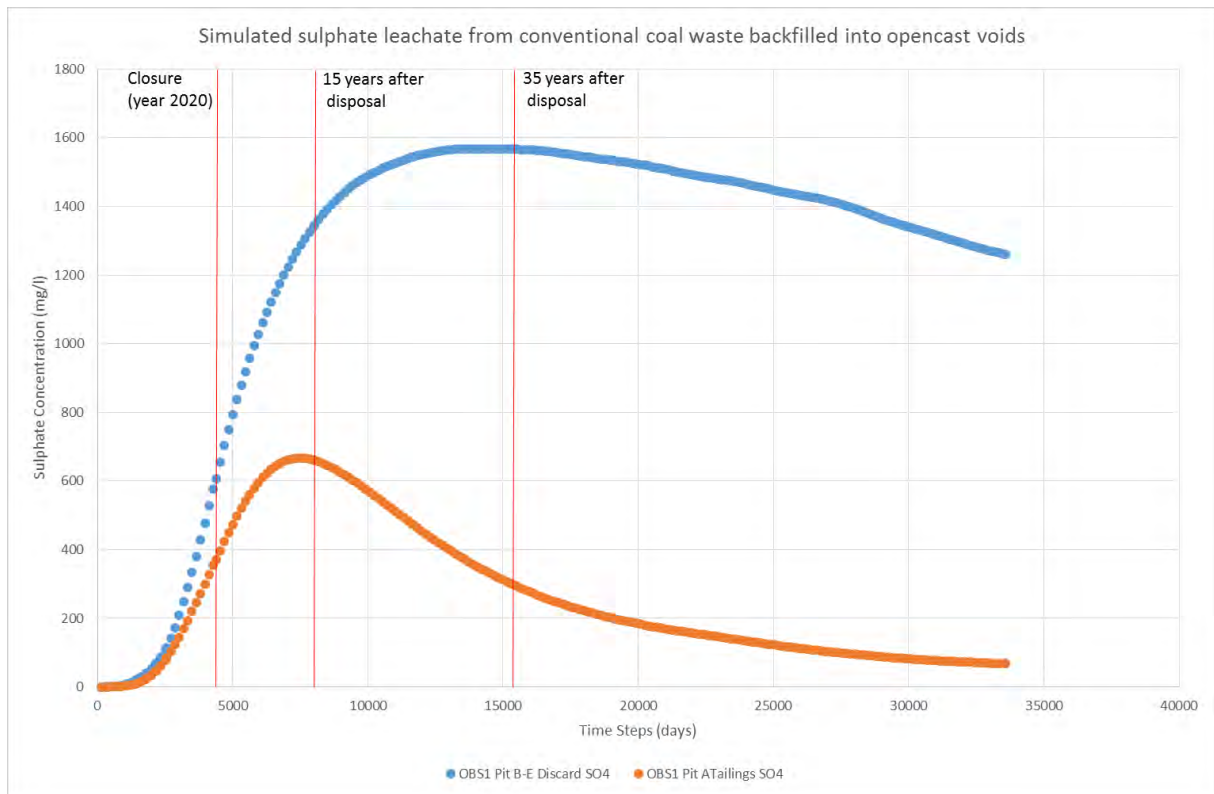


Figure 6-14: Simulated groundwater sulphate concentrations for conventionally disposed coal wastes at selected observation points

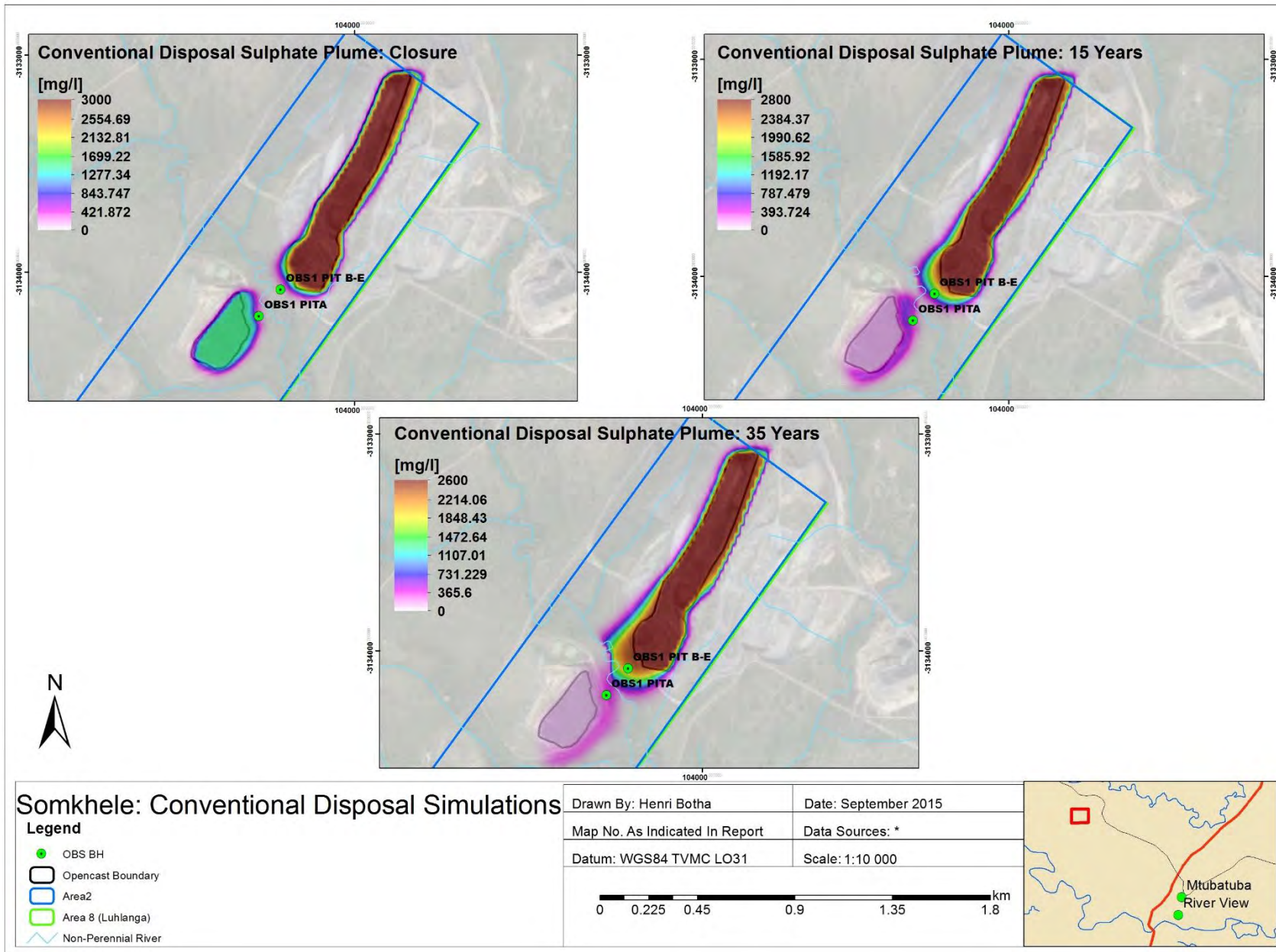


Figure 6-15: Simulated sulphate plumes for conventional disposal of tailings and discard into an opencast void

6.4.2 Co-disposal

The same transport model used to produce the plumes observed for conventional disposal of the coal waste products was used to simulate co-disposal. Constant concentration, porosity and hydraulic conductivity for the pit area (to simulate the hydrogeological characteristics of a theoretical co-disposed medium) were the only model parameter that were changed.

The concentrations observed during the geochemical testing of the co-disposed material was applied to the transport model. The concentrations assigned coincided with the time of mining and the time the backfilling of waste would have taken place. The same downstream observation points were used to assess the theoretical groundwater sulphate plume produced.

Figure 6-16 indicates the simulated groundwater sulphate concentration trends that are generated by the opencast voids as a result of the co-disposed coal waste. It can clearly be seen that the sulphate concentration spectrum is much lower than the conventional disposal sulphate spectrum observed in Figure 6-14 (conventional disposal sulphate trends). Furthermore, the prominent exponential decrease in sulphate leached from the material is observed at the downstream observation points. This coincides with what was observed during the geochemical testing of the co-disposed material (refer to Figure 5-15).

Figure 6-17 indicates the generated sulphate plumes for 5 years, 15 years and 35 years after disposal. From the sulphate plumes produced it can be seen that the spatial distribution is greatly reduced and that after 15 years the plume concentrations are reduced by 75%.

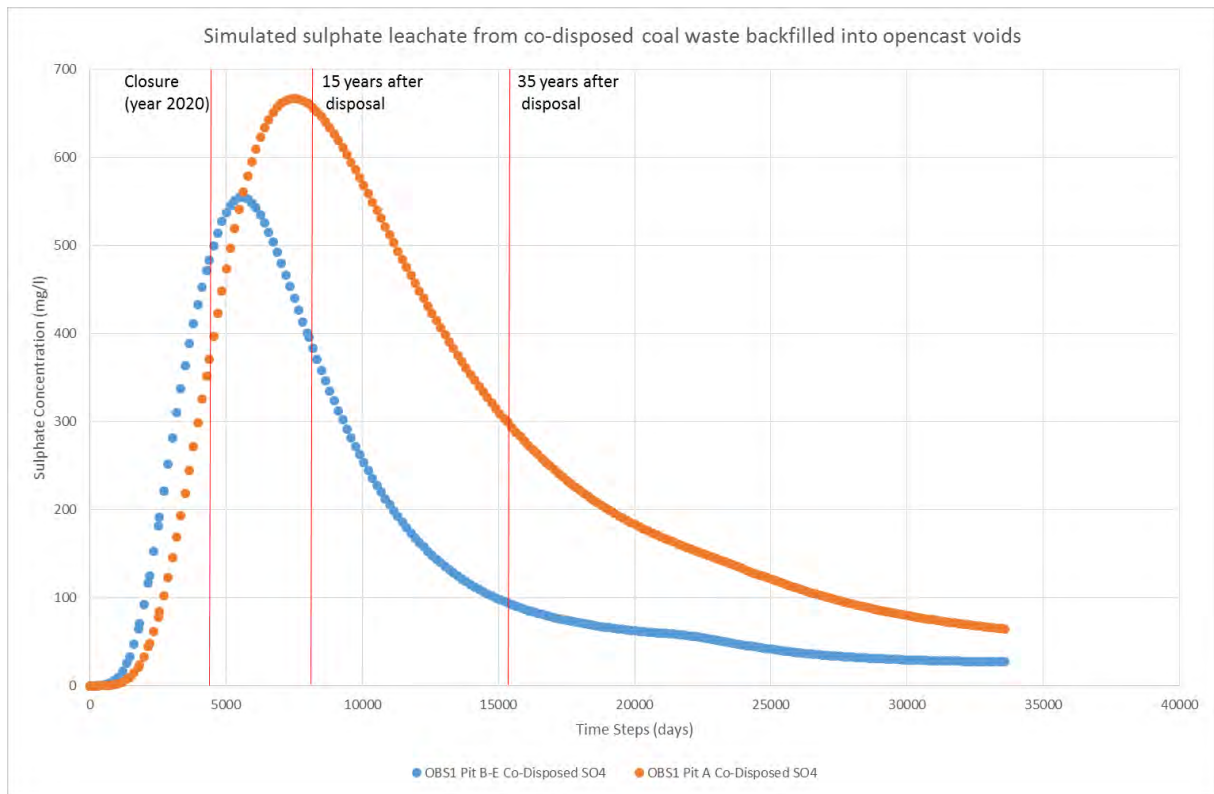


Figure 6-16: Simulated groundwater sulphate concentrations for co-disposed coal wastes at selected observation points

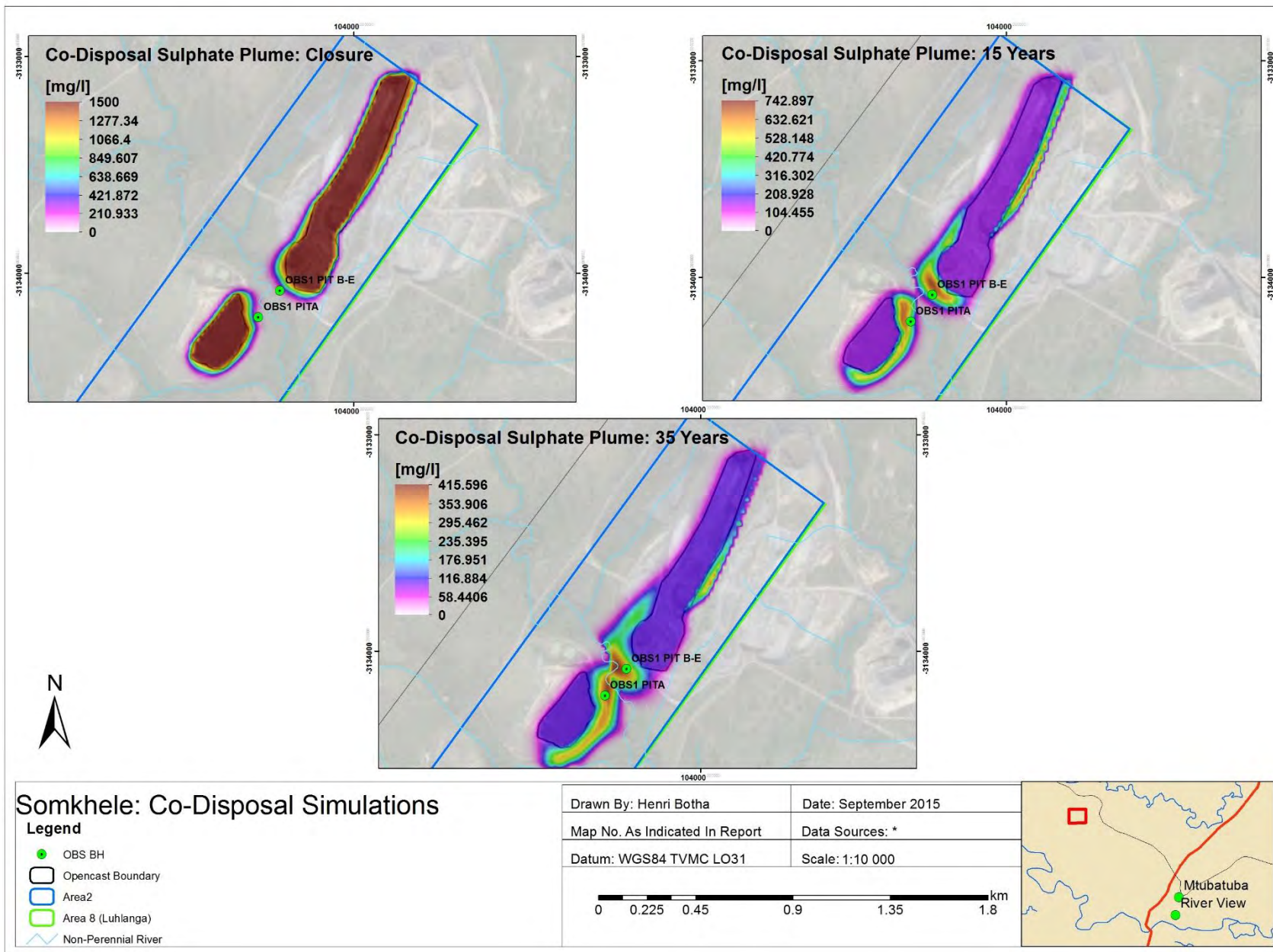


Figure 6-17: Simulated sulphate plumes for co-disposal of tailings and discard into an opencast void

7 CONCLUSION

7.1 CONCLUDING REMARKS ON GEOCHEMICAL TESTING

The static ABA, NAG and peroxide tests performed on the samples indicated that all the coal waste products have the potential to produce acid. However, the kinetic humidity leach tests indicated that the static tests do not accurately describe the acid potential or saline potential of the waste material.

Furthermore, the laboratory data suggested that discard waste disposed on its own has the potential to produce large salt loads when exposed to the atmosphere and water (INAP, 2014). Tailings disposed on its own has the potential to produce a reduced salt load. The reduced total dissolved solids (TDS) in the leachate produced could be due to the washing of the coal tailings, allowing most of the chemical reaction to take place within the processing plant prior to deposition. The tailings backfilled into the pit could therefore, already be leached of most elements subjected to oxidation processes.

When both waste products are co-disposed the bulk physical properties are altered (sorting, particle distribution, degree of saturation and water retention capacity) and this seems to buffer against chemical changes. Aubertin et. al. (2003) compared diffusion coefficient values measured on soils and tailings material and noted that as the degree of saturation increases, the effective diffusion coefficient of oxygen decreases. They found that at a degree of saturation above 85% the oxygen diffusion essentially becomes eliminated. Therefore, in a co-disposed state the decrease in salt load observed can be explained due to this phenomena. The small irregularly shaped tailings particles (with similar clay like platy structures and attributes see. Qiu and Sego, 2001) retain water within the co-disposed material matrix, increasing the degree of saturation of the discard material and reduces the oxygen ingress and oxygen diffusion rates in the material (Fetter, 1994; Gowan and Williams, 2010). Therefore, it is anticipated that anoxic (reduction environment) conditions are induced limiting oxidation processes within the material (Equation 1).

From the geochemical results obtained it is clear that under co-disposing conditions the bulk physical properties of the material is altered. It is anticipated that, co-disposal acts as a physical buffer against chemical changes and the long term saline drainage potential of the coal material is reduced. The impact on the groundwater aquifer is also reduced in terms of leachate produced and salt that can be released into the aquifer system. Co-disposal into an opencast void will reduce the visual impact the mine has on the environment, as well it will allow the mine to put back some of the material that was removed and produced during mining. Geochemical and geotechnical testing of coal material further explores the potential for effective waste and groundwater management in any coal environment.

7.2 CONCLUDING REMARKS ON NUMERICAL AND TRANSPORT MODEL

From the constructed transport models and simulated sulphate plumes the following conclusions are made:

- Conventional disposal of the coal discard and coal tailings material indicated conditions similar to what was observed during the kinetic leach testing of the material. It was observed that the discard material has a great sulphate leachate production capacity and that the plume concentration from the source will gradually (linearly) decrease over time. The spatial distribution from of the sulphate plume from the source is also much larger.
- The coal tailings material disposed on its own also indicated a trend similar to what was observed during the geochemical kinetic leach tests. Though the material has a high sulphate leaching capacity, the ability for the material to release the leachate is very low. The sulphate plume produced is therefore smaller and shows an exponential decrease in sulphate concentrations with time.
- The sulphate plumes and the sulphate concentration trends produced for the co-disposal scenario indicated that the spatial distribution of the plume produced is limited. The concentrations of the sulphate released into the aquifer is also greatly reduced and lower concentrations to that of the conventional disposal counterpart is observed.
- The co-disposed scenario indicates the potential to reduce the salt load (in terms of SO_4) of leachate produced by the coal waste products, as well as to reduce the rebound period of the sulphate leached.

7.3 CONCLUDING REMARKS REGARDING HYPOTHESIS

As shown by the geochemical results of this study the hypothesis was proven to be true. Co-disposal of waste into a previously mined opencast void, is indeed anticipated to be a better solution to prevent and buffer against chemical changes in the coal material. Though there are still many challenges with implementation of co-disposal techniques, the concept is promising and may provide mines in South Africa with cost effective, long term solutions to acid and saline drainage problems.

7.4 WAY FORWARD AND FURTHER RESEARCH

The research and findings of this dissertation sets the foundation of a sound theory to help prevent and buffer against acid and saline drainage. The way forward is marked by this foundation, and further research will help to build up on the principles learned and help to further define the co-disposal concept in more detail.

The way forward and further research to be conducted will involve more detailed geochemical testing of various co-disposal ratios. Furthermore, detailed geotechnical studies regarding the physical properties (permeabilities, water retention capacities and porosity) of the bulk physical co-disposed mixture needs to be further explored.

The issue relating to a conservative flow and transport model was noted during this project. A dynamic geochemical model needs to be developed. In doing so oxidation and reduction environments can be simulated. Furthermore, a geochemical model will make it possible to simulate the kinetic degradation of pyrite bearing minerals, as well as the degradation of compounds (FeOH and SO_4) contained in the leachate. This will give a much better understanding, as well as a more accurate representation of the actual constituent concentrations associated with saline or acid drainage from a co-disposal source.

8 REFERENCES

- Adams, S., Titus, R., Pietersen, K., Tredoux, G., & Harris, C. 2001. Hydrochemical characteristics of aquifers near Sutherland in the Western Karoo, South Africa. *Journal of Hydrology*, 241(1), 91-103.
- Anderson, M. P., & Woessner, W. W. 1992. Applied groundwater modeling: simulation of flow and advective transport (Vol. 4). Gulf Professional Publishing, Chicago.
- Anon. 2013. Geonics Limited: EM34-3/EM34-3XL. Access Site: <http://www.geonics.com/html/em34-3.html>. Date of access: 10/10/2015.
- Anon. 2014. Open-pit mining a general overview. Retrieved from: <http://protectecuador.org/portfolio/open-pit-mining-general-overview-2/>. Date of access 20/03/2014.
- Anon. 2015. Geotron Model G5 Proton Memory Magnetometer. Site Accessed: <http://www.geotron.co.za/new%20site/magnetometer.htm>. Date of access: 31 Oct. 15.
- Apello, C.A.J. and Postma, D. 2007. Geochemistry, groundwater and pollution. 2nd Edition. A.A. Balkema Publishers. ISBN 0415364280.
- Aubertin, M., Mbonimpa, M., Bussière, B., & Chapuis, R. P. 2003. A model to predict the water retention curve from basic geotechnical properties. *Canadian Geotechnical Journal*, 40(6), 1104-1122.
- Bastian, O., Krönert, R., & Lipský, Z. 2006. Landscape diagnosis on different space and time scales—a challenge for landscape planning. *Landscape Ecology*, 21(3), 359-374.
- Boggs, S. 2011. Principles of sedimentology and stratigraphy. 5th edition. 195-198. Pearson Prentice Hall. ISBN 978-0321643186.
- Botha, G.A., Singh, R. 2012. Geological, geohydrological and development potential zonation influences; Environmental management framework for Umkhanyakude district, Kwazulu-Natal. Council of Geoscience.
- Davis, S.N., Porosity and permeability of natural materials. Flow through porous media, ed. R.J.M. De Wiest, Academic Press, New York, 54-89, 1969.
- Dennis, R. 2013a. Geophysics: EM. Lecture by Dr. Rainier Dennis from the North-West University, Potchefstroom Campus. Supplied by lecturer in 2013. [PowerPoint presentation]

Dennis, R. 2013b. Geophysics: Magnetometer. Lecture by Dr. Rainier Dennis from the North-West University, Potchefstroom Campus. Supplied by lecturer in 2013. [PowerPoint presentation]

DME. 2005. 27½32 St Lucia. 1:250 000 Geological Series Map. Pretoria: Council for Geoscience.

Dondurur, D., Pamukcy O.A. 2002. Interpretation of magnetic anomalies from dipping dike model using inverse solution, power spectrum and Hilbert transform method. Journal of the Balkan Geophysical Society, Vol.6, No. 2, May 2003, 127-136.

DWA. 2008. Best Practice Guidelines G4: Impact Prediction. Directorate: Resource Protection and Waste. ISBN: 978-0-9802679-9-0.

DWA. 2013. The groundwater Dictionary. 2nd Edition. A Comprehensive Reference of Groundwater Related Terminology. Access Site: <https://www.dwaf.gov.za/Groundwater/GroundwaterDictionary.aspx>. Access date: 1/10/2015.

DWAF. 2006. Groundwater Resource Assessment II (GRA2) - Task 3aE Recharge. Access Site: <https://www.dwaf.gov.za/Geohydrology/gra2/3aEFinalReportA.pdf>. Access Date: 1/10/2015.

DWS. 2015. Department of Water and Sanitation: Hydrological Services. Retrieved from: <https://www.dwa.gov.za/Hydrology/>. Date of access: 14 Nov. 2015.

EPA. 1994. U.S. Technical Document: Acid Mine Drainage Prediction. Environmental Protection Agency. EPA530-R-94-036. Retrieved from: <http://water.epa.gov/polwaste/nps/upload/amd.pdf>.

Fetter, C. W. 1994. Applied Hydrogeology, 3rd edition. Upper Saddle River, NJ: Prentice Hall, Inc. ISBN: 0-13-088239-9.

Fourie, J. 2014. Graphical representation of ABA and NAG screening results [telephonic correspondence]. 11 September 2014.

Fujii, N., Kiyonaga, Y., Watanabe, S., & Yamamura, M. 1984. U.S. Patent No. 4,470,828. Washington, DC: U.S. Patent and Trademark Office.

GCS. 2014. Somkhele Anthracite Mine: 1st Quarter Water Monitoring Report. Private report prepared for Tendele (Pty) Ltd.

Gowan, M., Lee, M., & Williams, D. J. 2010. Co-disposal techniques that may mitigate risks associated with storage and management of potentially acid generating wastes. In *The First International Seminar on the Reduction of Risk in the Management of Tailings and Mine Waste (MINE WASTE 2010)* (pp. 389-404). Australian Centre for Geomechanics.

Grantham, D.G., Ellefsen, K., Haeni, F.P. 1987. Forward-modeling computer program for the inductive electromagnetic ground-conductivity method: EM34. U.S. Geological Survey. Open-File Report 87-213-A. Retrieved from: <http://pubs.usgs.gov/of/1987/0213a/report.pdf>.

Haigh, J.E., Smith, M.J. 1975. Standard curves for interpretation of magnetic anomalies due to thin dykes of finite depth extent. Department of Minerals and Energy. Bureau of Mineral Resources, Geology and Geophysics. Australian Government Publishing Service. Canberra, 1975.

Hammack, R. N. 1990. The effect of oxygen on pyrite oxidation. Retrieved from: <http://www.asmr.us/Publications/Conference%20Proceedings/1990%20Meetings%20Vol%201/Hammack%20257-264.pdf>.

Harbaugh, A. W., Banta, E. R., Hill, M. C., & McDonald, M. G. 2000. MODFLOW-2000, the US Geological Survey modular ground-water model: User guide to modularization concepts and the ground-water flow process (p. 121). Reston, VA, USA: US Geological Survey. Retrieved from: https://water.usgs.gov/nrp/gwsoftware/modflow2000/MNW_text.pdf.

Holmes, P. R., & Crundwell, F. K. 2000. The kinetics of the oxidation of pyrite by ferric ions and dissolved oxygen: an electrochemical study. *Geochimica et Cosmochimica Acta*, 64(2), 263-274.

IIT. 2015. Indian Institute of Technology. E-Content on Slope Engineering. Chapter 11: Mine Water Dump. Retrieved from: <http://www.iitbhu.ac.in/faculty/min/rajesh-rai/NMEICT-Slope/> Date of Access: 1/10/2015.

INAP. 2014. The International Network for Acid Prevention: Global Acid Rock Drainage. Access Site: http://www.gardguide.com/index.php?title=Main_Page.

James, A.R. 1997. The prediction of contamination loads from coarse sulphide-containing waste materials. Water Research Commission Report No: 559/1/97, Pretoria.

James, W.M., Charles, R.F. 1980. Ground-Water Modeling: An Overview. *Ground Water Journal*. Vol. 18, No 2. March-April 1980.

Johnson, M. R., Van Vuuren, C. J., Hegenberger, W. F., Key, R., & Show, U. 1996. Stratigraphy of the Karoo Supergroup in southern Africa: an overview. *Journal of African Earth Sciences*, 23(1), 3-15.

Kalbus, E., Reinstorf, F., & Schirmer, M. 2006. Measuring methods for groundwater-surface water interactions: a review. *Hydrology and Earth System Sciences Discussions*, 10(6), 873-887.

KET. 2014. Coal: ancient gift serving modern man. American Coal Foundation. Retrieved from: <http://www.ket.org/Trips/coal/agsmm/agsmmhow.html>. Date of access: 2014-03-24

Klein, C., Dutrow, B. 2007. *Mineral Science*. 23rd Edition. John Wiley & Sons, Inc. ISBN: 978-0-471-72157-4.

Kresic, N. 2006. *Hydrogeology and Groundwater Modeling*. 2nd Edition. CRC Press. ISBN-13: 9780849333484.

Kruseman, G.P. de Ridder, N.A. 2000. *Analysis and Evaluation of Pumping Test Data*. 2nd Edition. Pp, 61-70. International Institute for Land Reclamation and Improvement. ISBN: 90-70754-207.

Lapakko, K., Lawrence, R. W. 1993. Modification of the net acid production (NAP) test. *Proceedings of the 17th Annual British Columbia Mine Reclamation Symposium in Port Hardy, BC, 1993*. The Technical and Research Committee on Reclamation.

Levine, D. G., Schlosberg, R. H., & Silbernagel, B. G. 1982. Understanding the chemistry and physics of coal structure (A Review). *Proceedings of the National Academy of Sciences*, 79(10), 3365-3370.

Lloyd, P. J. 2000. The potential of coal wastes in South Africa. *Journal South African institute of mining and metallurgy*, 100(1), 69-72.

Meyerhoff, A. A., & Teichert, C. 1971. Continental drift, III: Late Paleozoic glacial centers, and Devonian-Eocene coal distribution. *The Journal of Geology*, 285-321.

Miller, S., Robertson, A. and Donahue, T. 1997. Advances in Acid Drainage Prediction using the Net Acid Generation (NAG) Test. *Proc. 4th International Conference on Acid Rock Drainage*, Vancouver, BC, 0533-549.

Modflow. 2014. Visual Modflow Help. Schlumberger Water Services. Site Accessed: http://novamatrixgm.com/help/vmod/index.html?vm_ch4_input4.htm. Date of access: 8/11/2015.

Morris, P. H., & Williams, D. J. 1997a. Results of field trials of co-disposal of coarse and fine coal wastes. *Transactions of the Institution of Mining and Metallurgy, Section A-Mining Industry*, 106, A38-A41.

Morris, P. H., Williams, D. J. 1997b. Hydraulic sorting of co-disposed coarse and fine coal wastes. Transactions of the Institution of Mining and Metallurgy, Section C-Mineral Processing, 106, C21-C26.

Morris, P. H., Williams, D. J. 1997c. Co-disposal of washery wastes at Jeebropilly colliery, Queensland, Australia. Transactions of the Institution of Mining and Metallurgy, Section A-Mining Industry, 106, A25-A29.

Morris, P. H., Williams, D. J. 2000. The porosity of co-disposed coalmine wastes. International Journal of Surface Mining, Reclamation and Environment, 14(1), 63-73.

NGA. 2015. National Groundwater Archive. Site: <https://www3.dwa.gov.za/NGANet/Security/WebLoginForm.aspx>. Access Date: 5/05/2015.

Parsons, R. 1995. A South African Aquifer System Management Classification. Water Research Commission Report No. KV 77/95.

Petmin. 2013. Integrated Report. Retrieved from: <http://www.petmin.co.za/somkhele-mining-exploration.php>. Date of access: 2014-03-17.

Price, W.A. 1997. Guidelines and Recommended Methods for the prediction of metal leaching and Acid Rock Drainage at Minesites in British Columbia. British Columbia Ministry of Employment and Investment, Energy and Minerals Division, Smithers, BC, p.143.

Pullum, L. 2007. Pipelining tailings, pastes, and backfill. In Proceedings of the 10th International Seminar on Paste and Thickened Tailings, Perth, Australia (pp. 13-15).

Qiu, Y., & Sego, D. C. (2001). Laboratory properties of mine tailings. Canadian Geotechnical Journal, 38(1), 183-190.

Rapantova, N., Grmela, A., Vojtek, D., Halir, J., & Michalek, B. (2007). Ground water flow modelling applications in mining hydrogeology. Mine Water and the Environment, 26(4), 264-270.

SANS. 2011. South African National Standards. Drinking Water. Part 1: Microbial, physical, aesthetic and chemical determinants. South African Bureau of Standards. ISBN: ISBN 978-0-626-26115-3.

Schluter, T. 2008. Geological Atlas of Africa. Springer-Verlag Berlin. ISBN 978354076373-4.

Schüring, J., Kölling, M., & Schulz, H. D. 1997. The potential formation of acid mine drainage in pyrite-bearing hard-coal tailings under water-saturated conditions: an experimental approach. Environmental Geology, 31(1-2), 59-65.

Soregaroli, B. A., Lawrence, R. W. 1998. Update on waste characterization studies. In Mine Design, Operations and Closure Conference. Polson, Montana.

Spitz, K., & Moreno, J. 1996. A practical guide to groundwater and solute transport modeling. John Wiley and Sons.

SWS. 2011. Schlumberger Water Services - Visual MODFLOW Help. Retrieved from: http://novamatrixgm.com/help/vmod/index.html?vm_ch3_global9.htm Date of Access: 4/10/2015

SWS. 2014. Schlumberger Limited. Retrieved from: <http://www.swstechnology.com/groundwater-software/pumping-test-analysis/aquifertest-pro>. Date of access: 2015/03/17.

Tiwary, R. K. 2001. Environmental impact of coal mining on water regime and its management. Water, Air, and Soil Contamination, 132(1-2), 185-199.

Tiwary, R. K., Dhakate, R., Rao, V. A., & Singh, V. S. 2005. Assessment and prediction of contaminant migration in ground water from chromite waste dump. Environmental geology, 48(4-5), 420-429.

Van Hook, R. I. 1979. Potential health and environmental effects of trace elements and radionuclides from increased coal utilization. Environmental health perspectives, 33, 227.

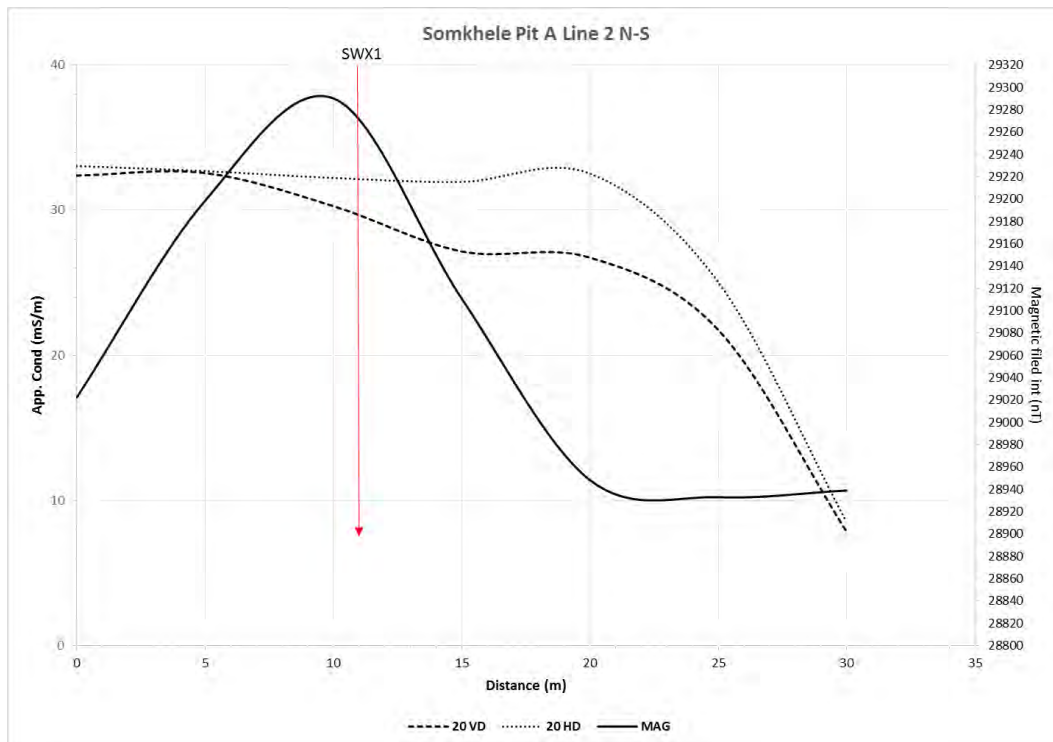
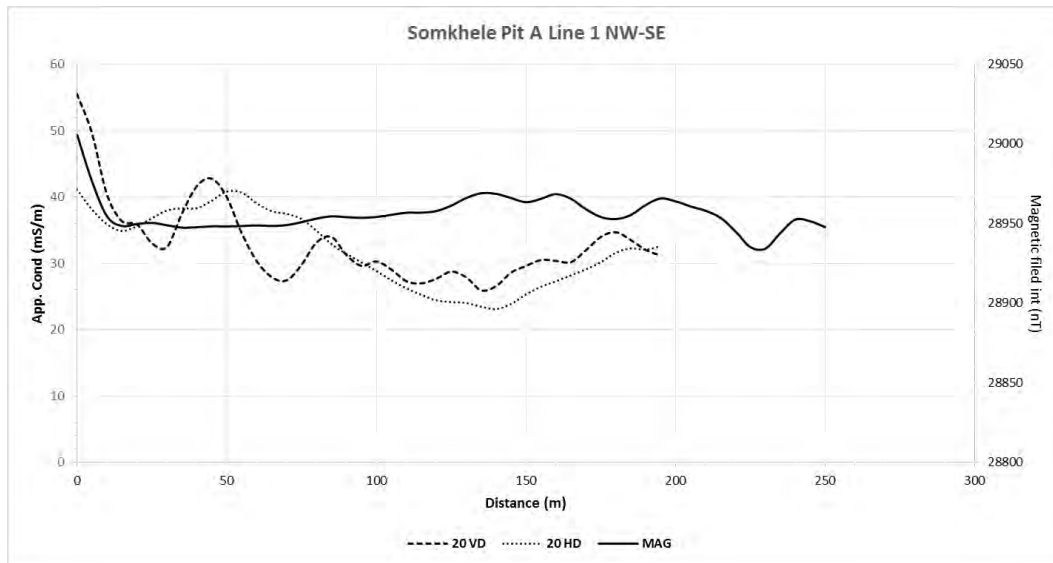
Wang, F.W., Anderson, M.P. 1995. Introduction to Groundwater Modeling. Finite Difference and Finite Element Methods. Academic Press Inc. ISB 0-12-734585-X

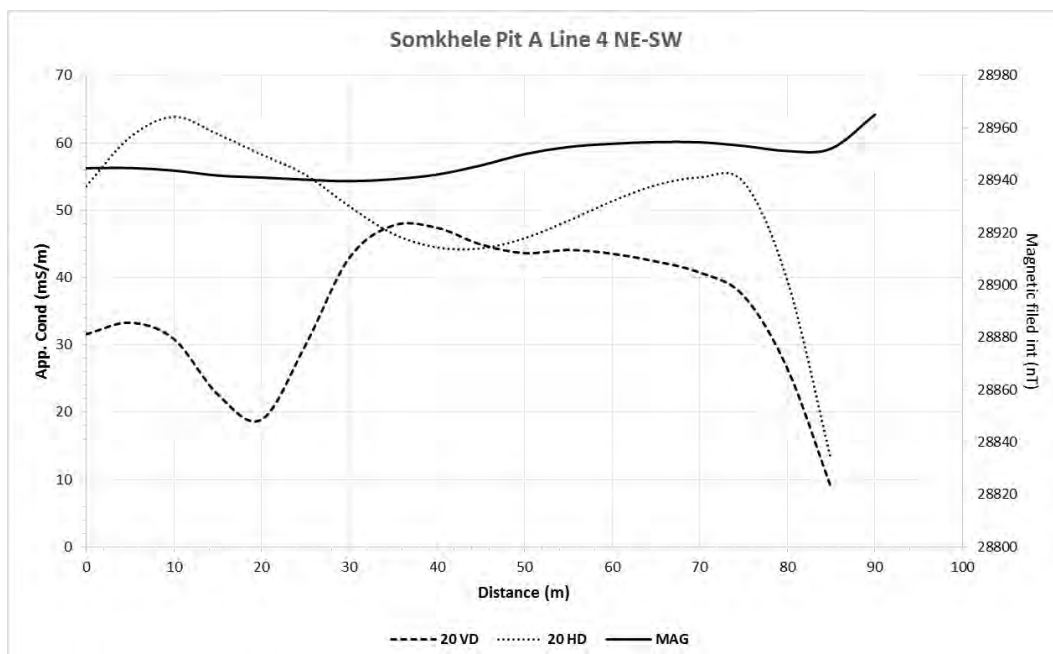
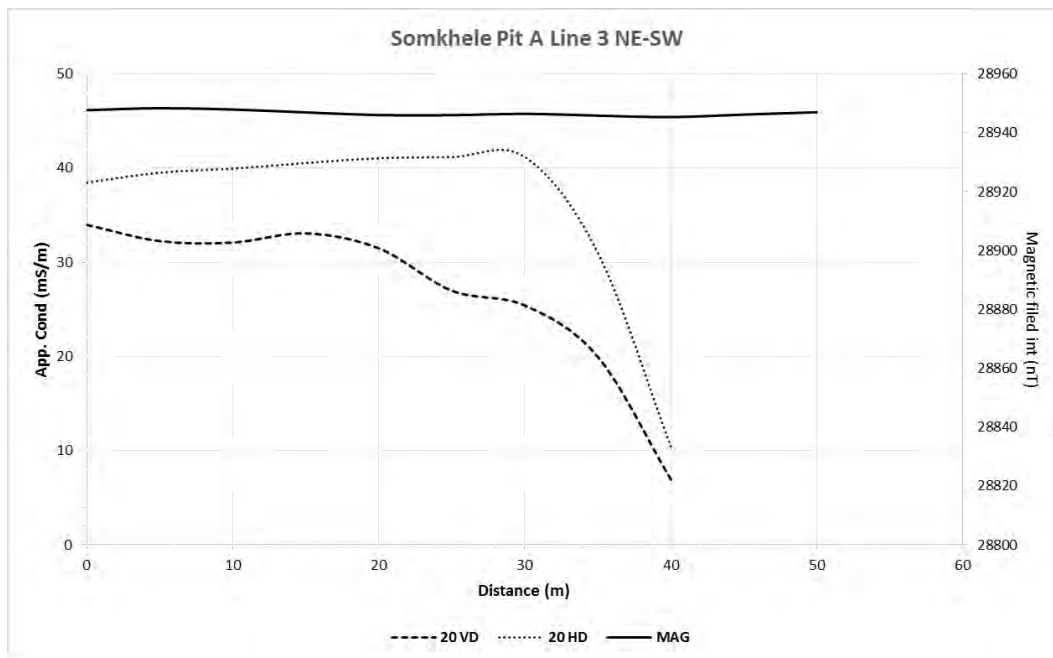
WR2005. 2005. Water Resources of South Africa WR2005 Information System. Version 0.1 - August 18th 2008.

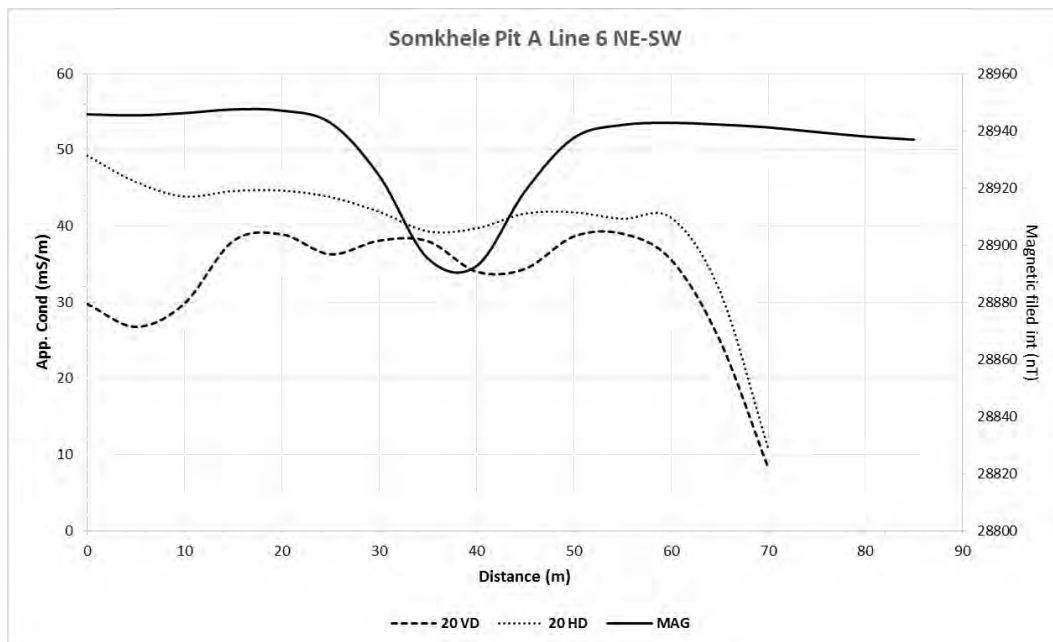
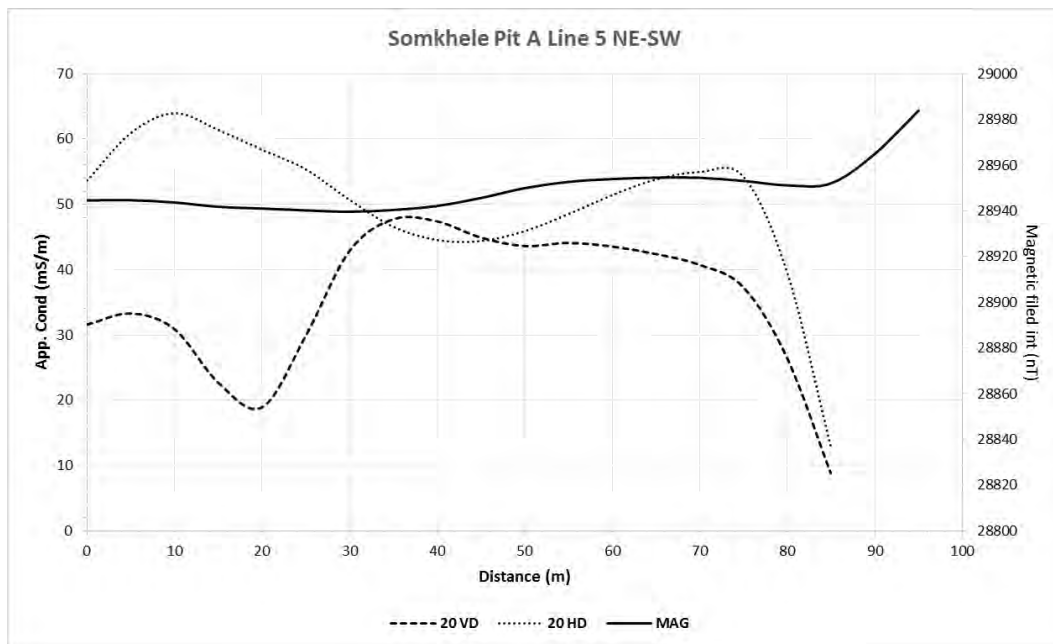
Xia, J. Weis, T.V. Miller, R.D. 2001. Findings from Electromagnetic Surveys Surrounding a Hog Confinement Facility in Western Kansas Over a Two Year Period. KGS Open File Report 2001-7. Site accessed: <http://www.kgs.ku.edu/Geophysics/OFR/2001/07/>. Date of access: 31-10-2015.

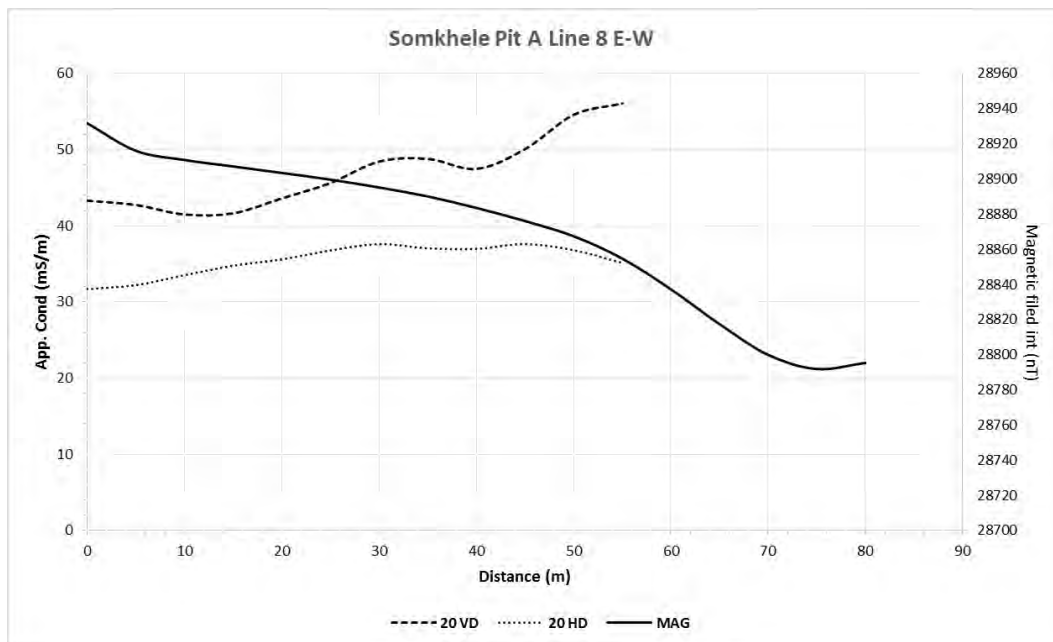
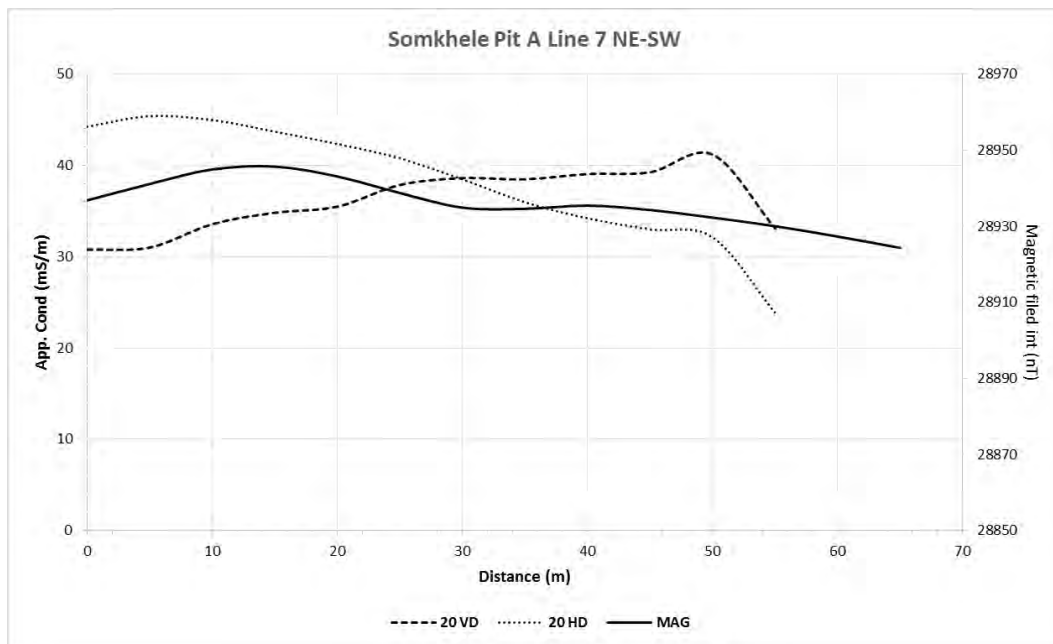
Yilmaz, E. 2011. Advances in reducing large volumes of environmentally harmful mine waste rocks and tailings. Gospodarka Surowcami Mineralnymi, 27, 89-112.

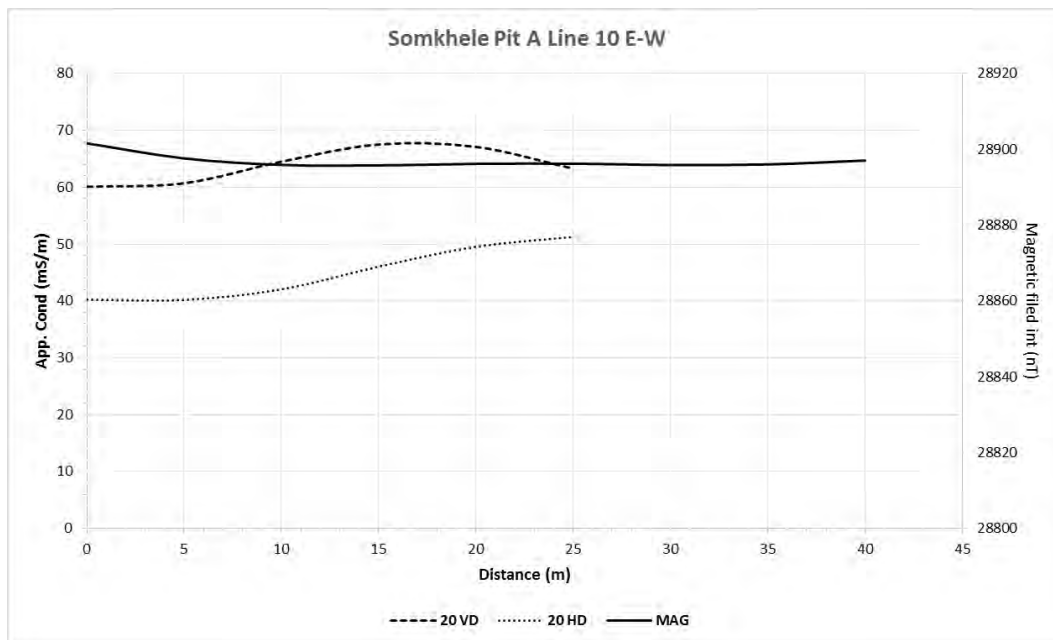
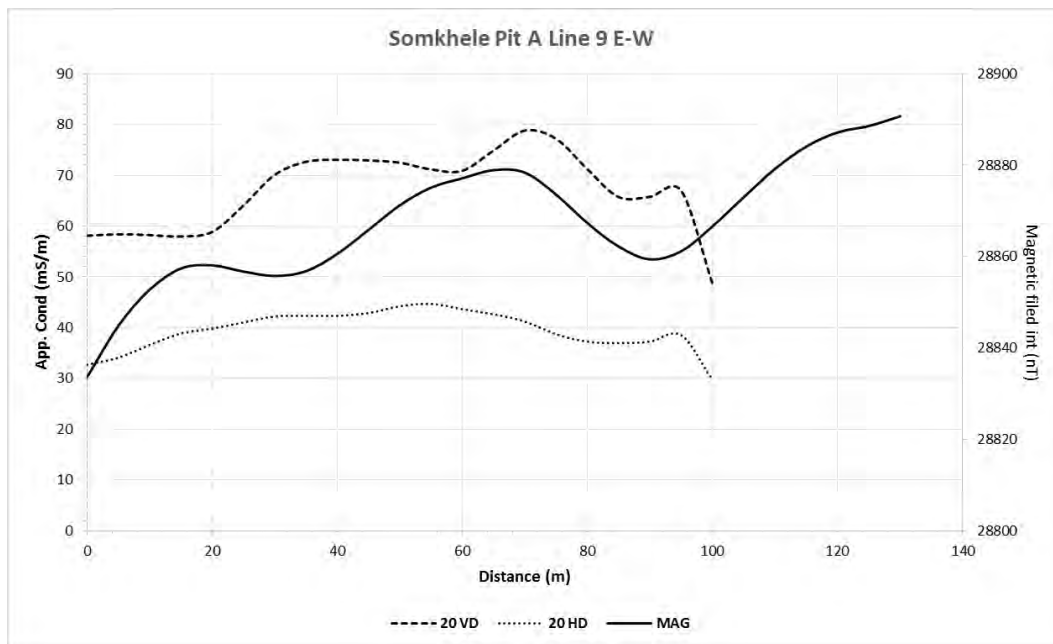
Appendix A: Geophysical data

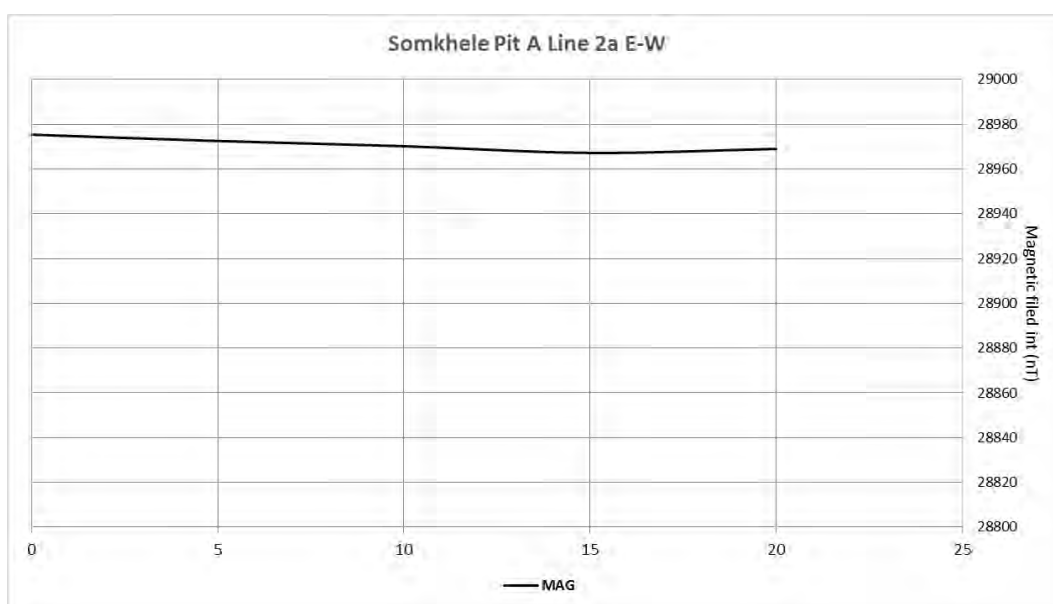
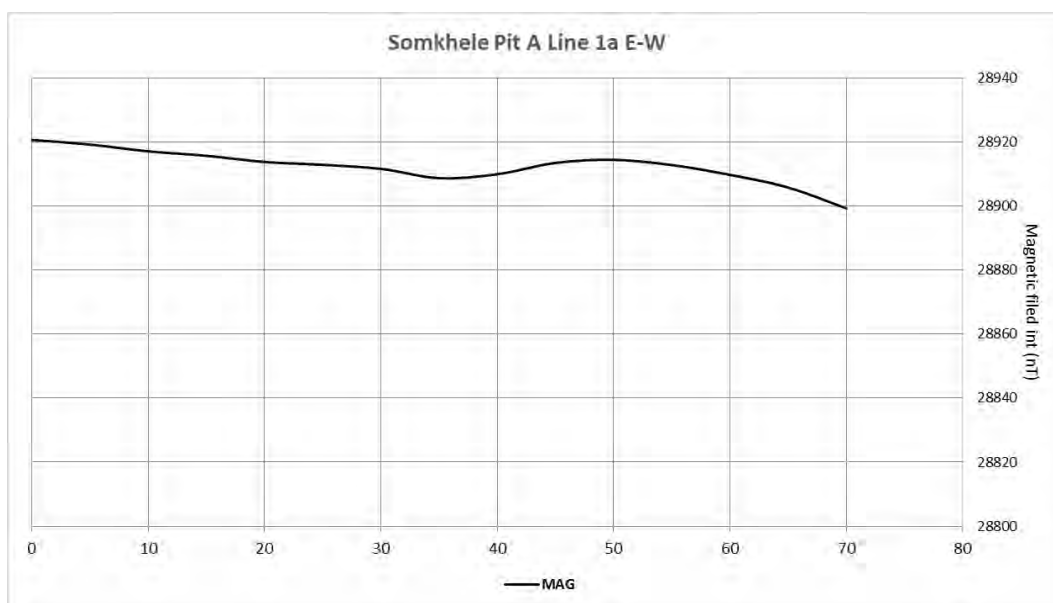
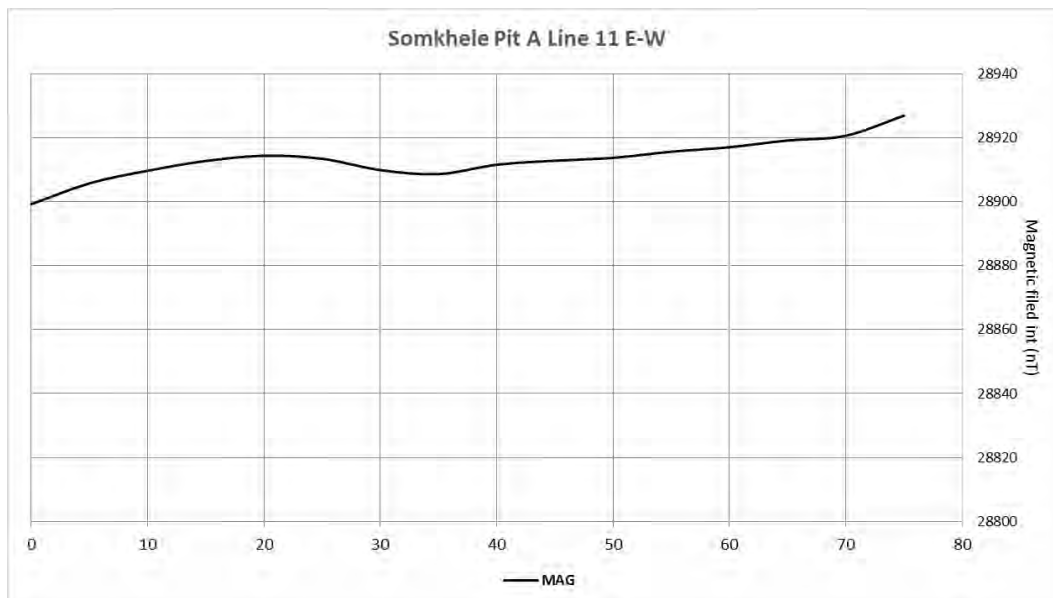


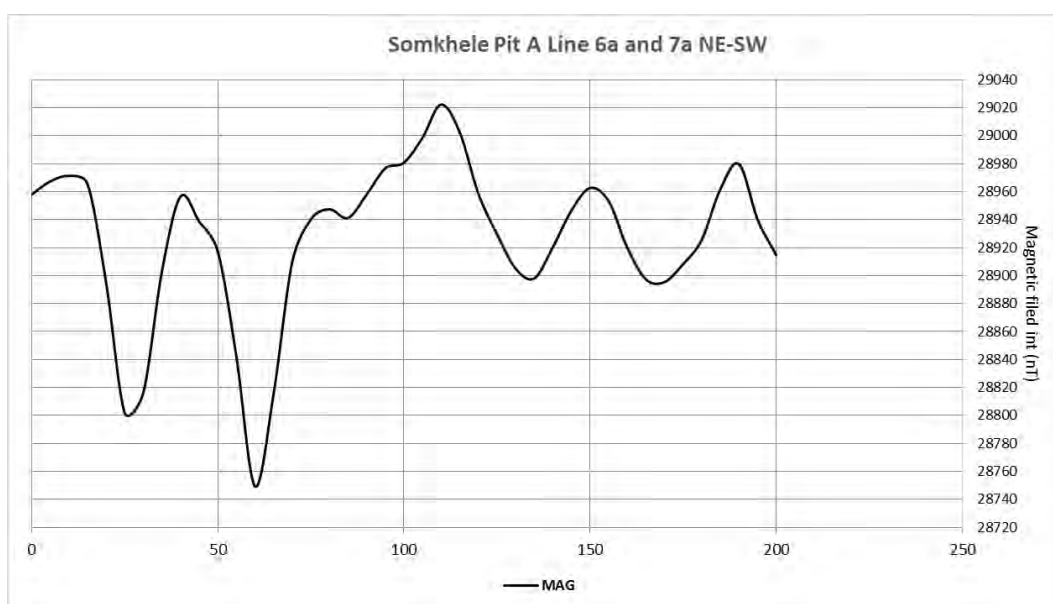
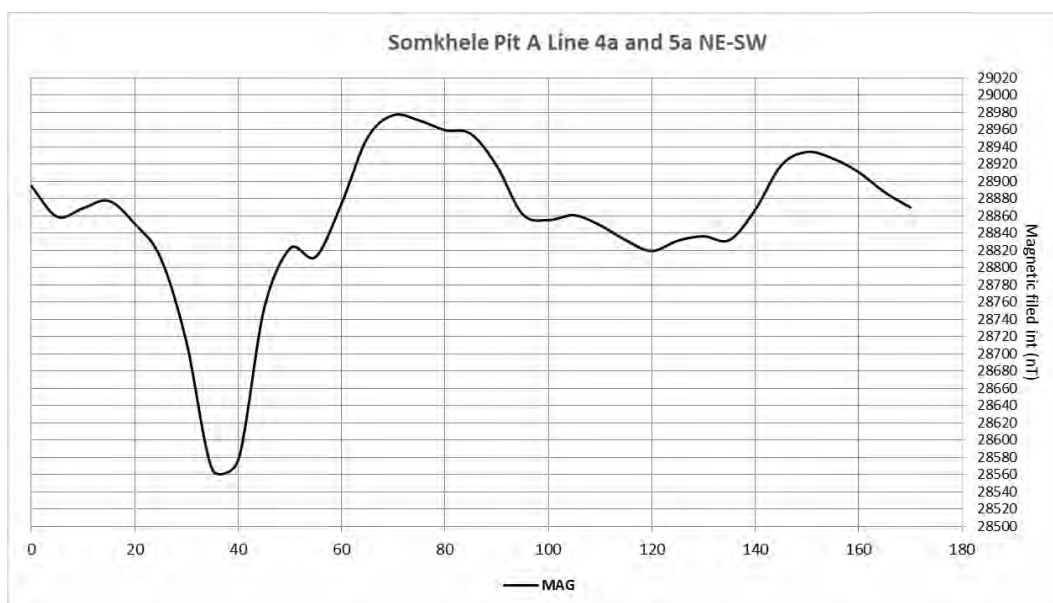
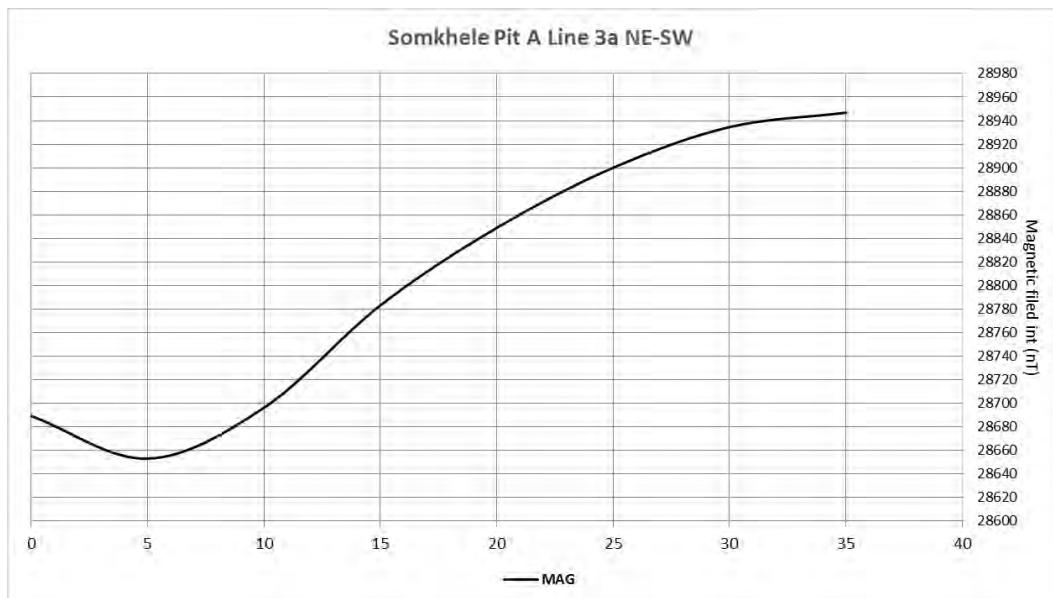


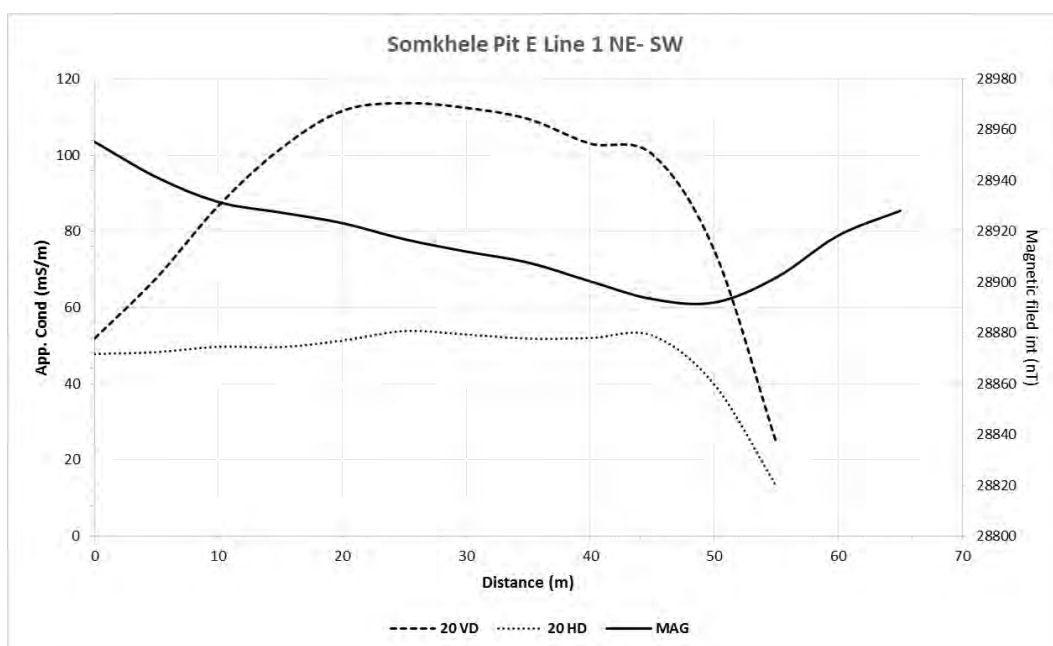
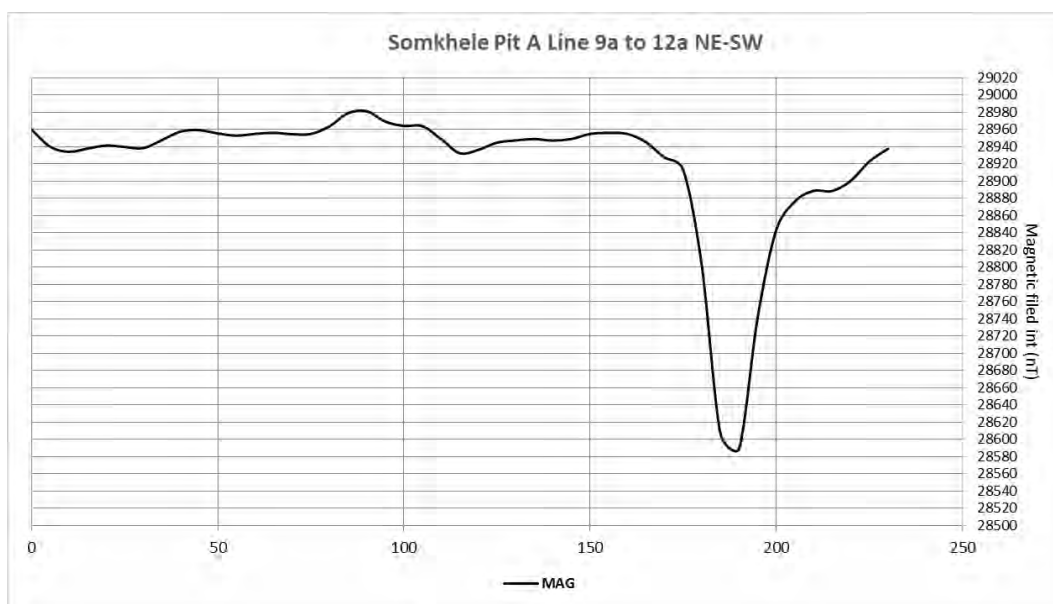
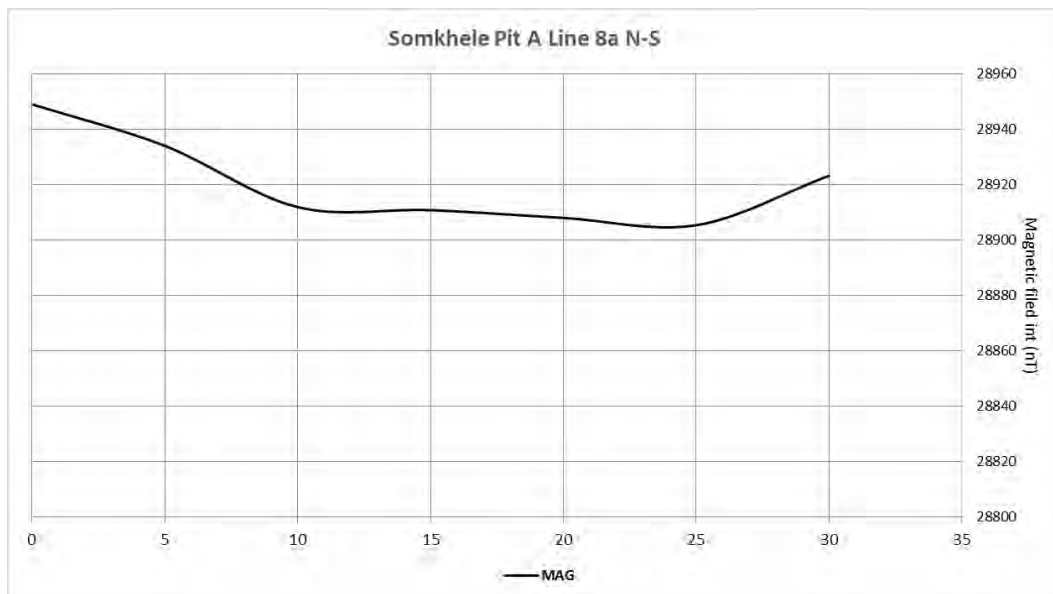


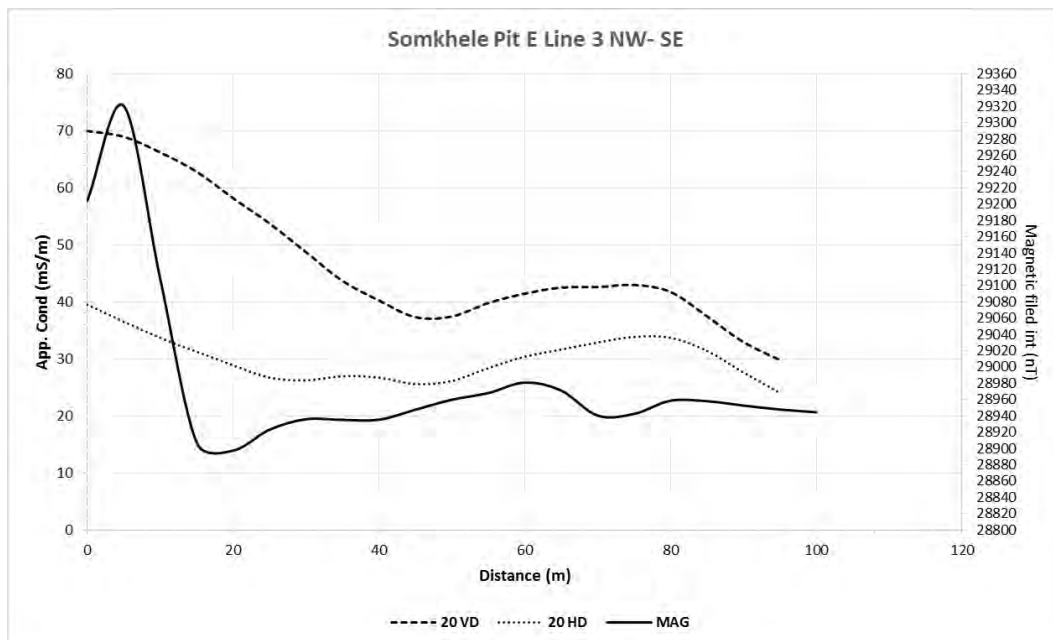
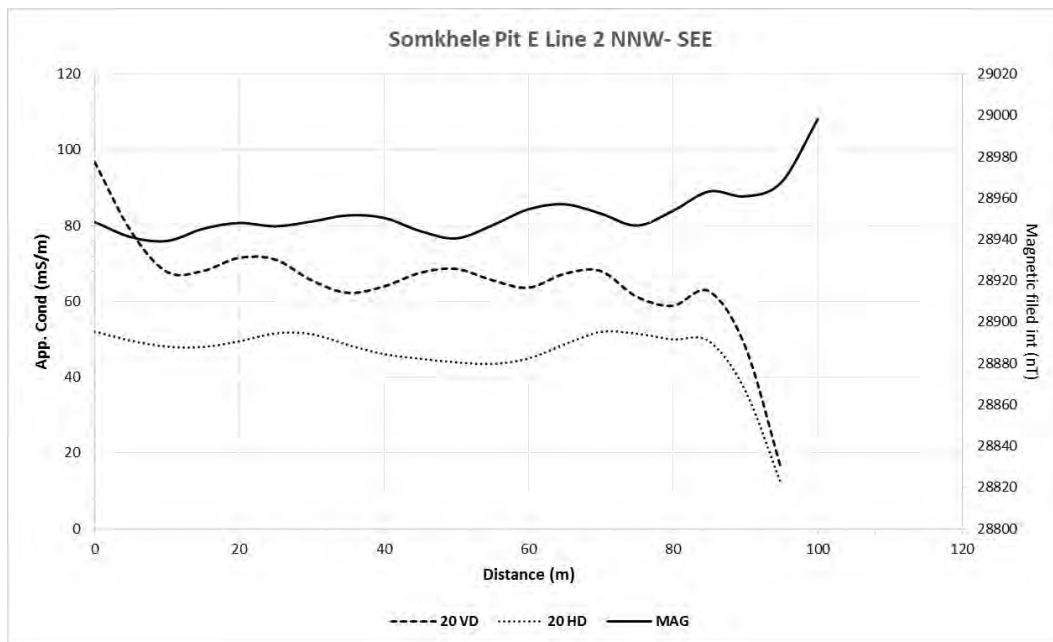


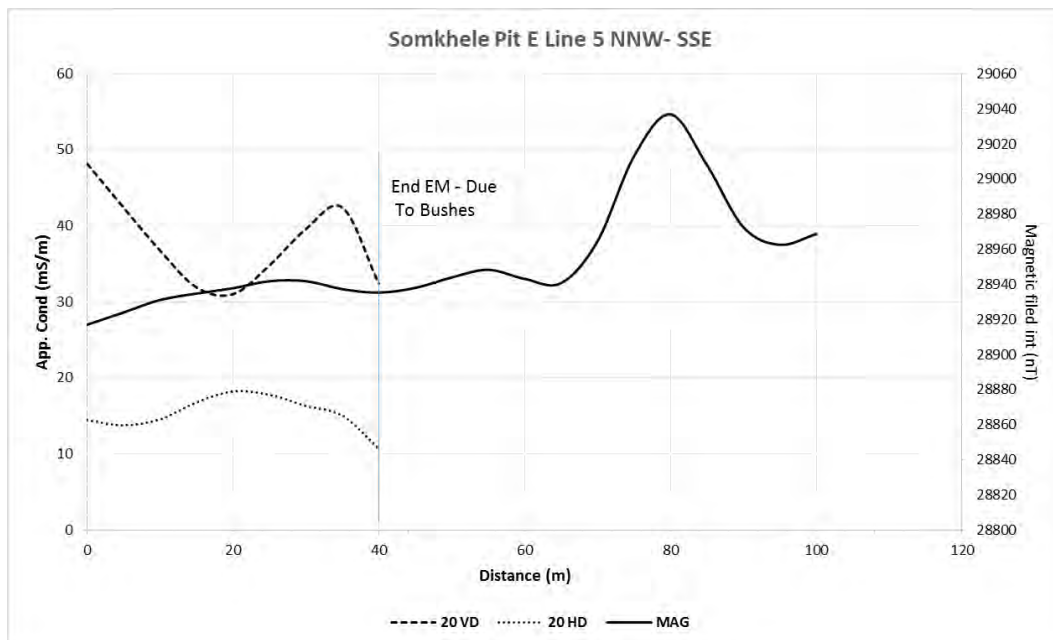
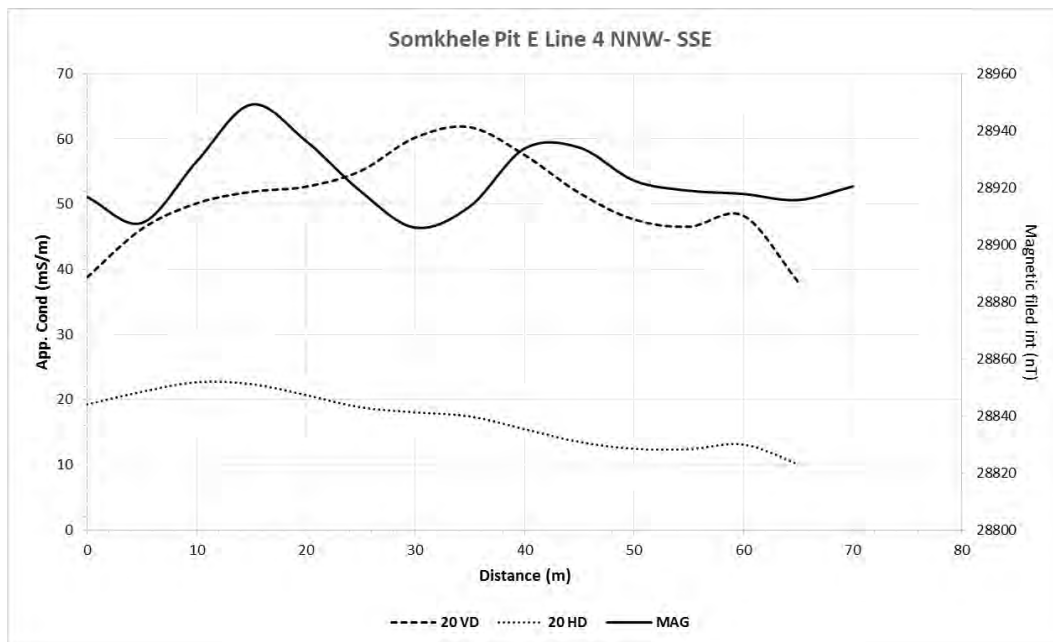


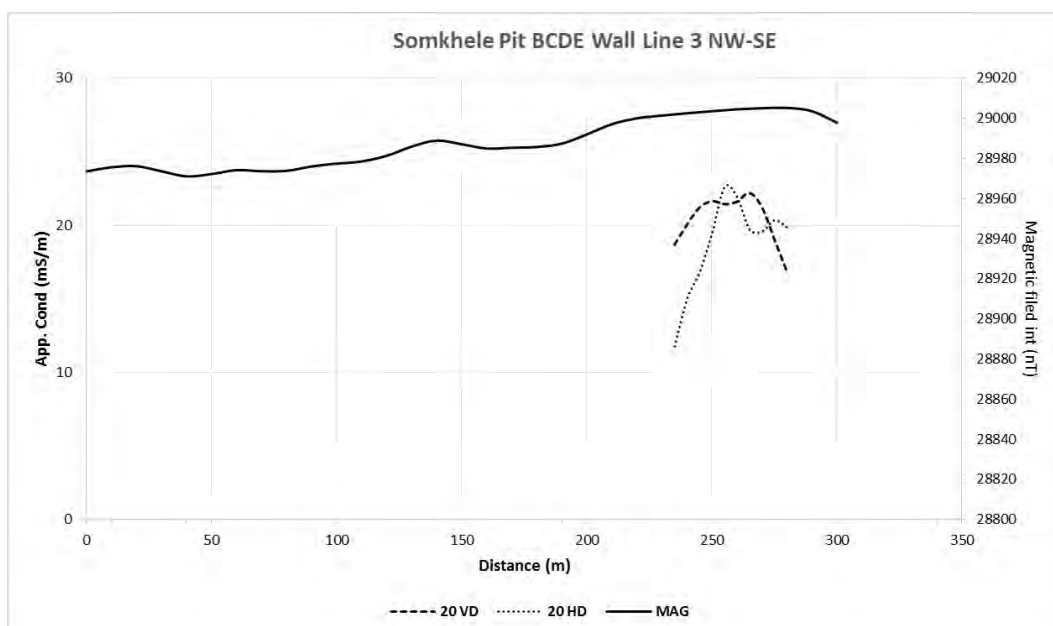
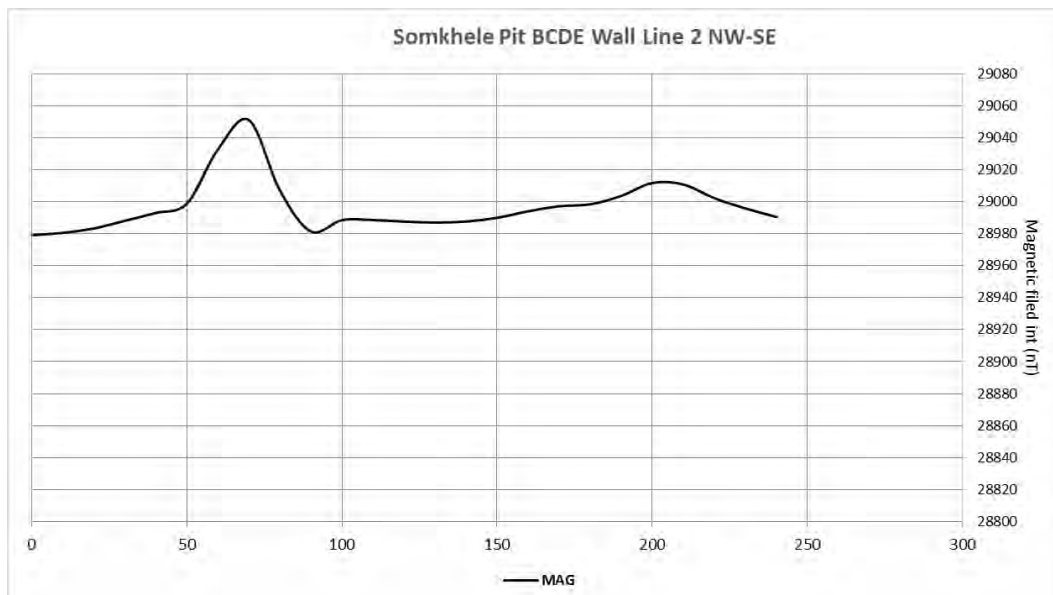
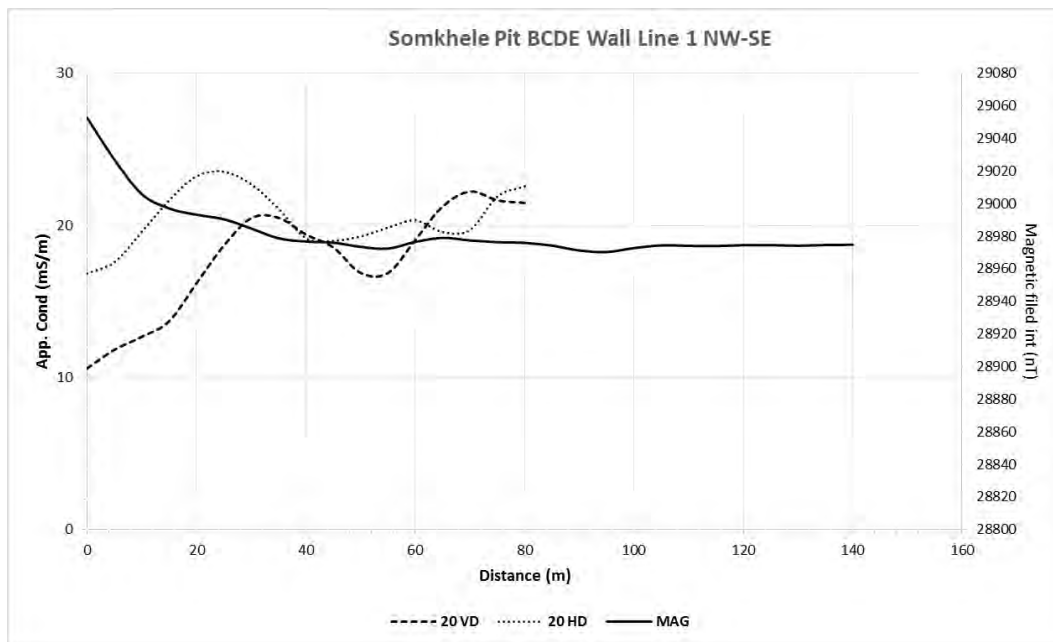


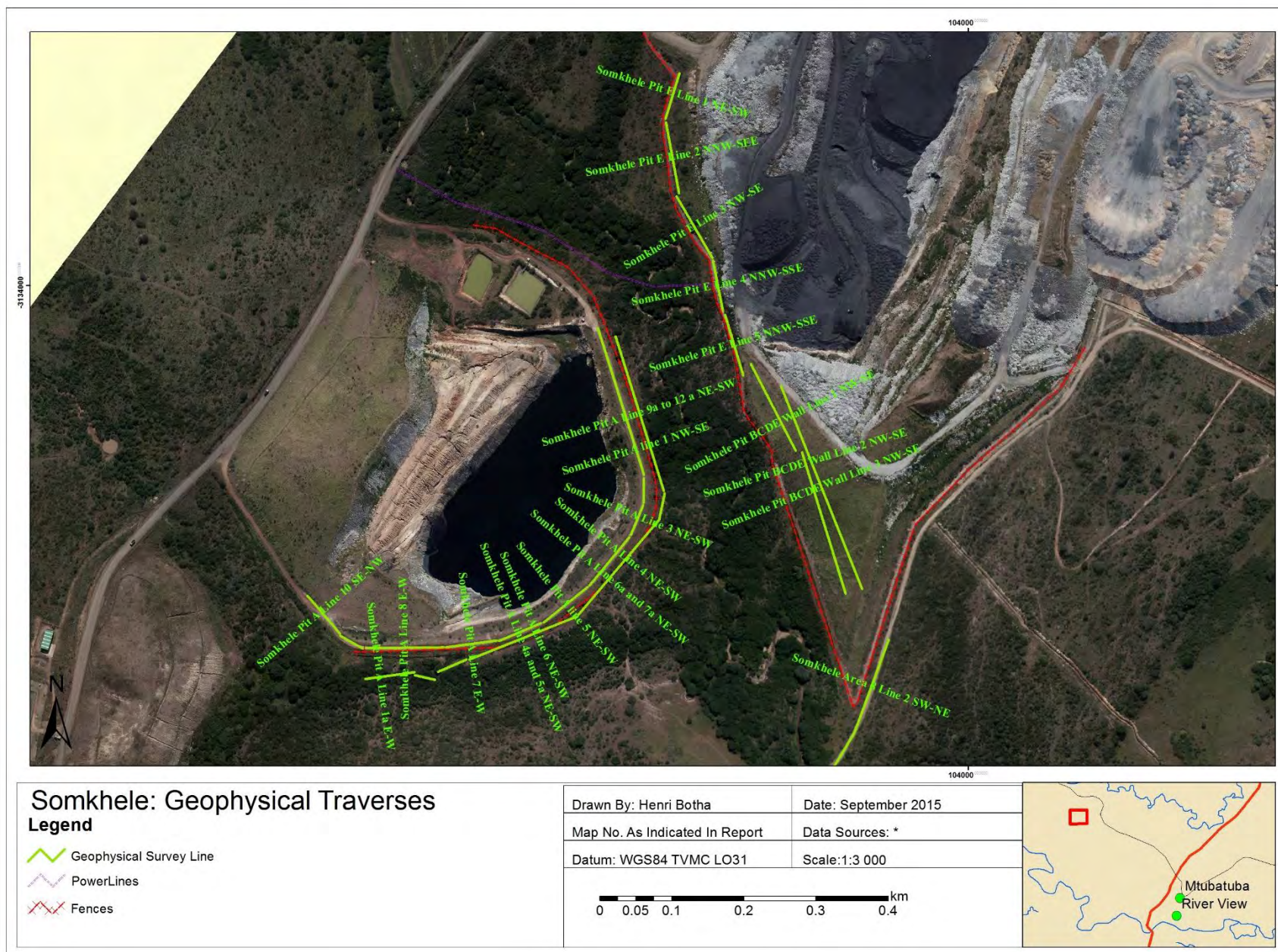




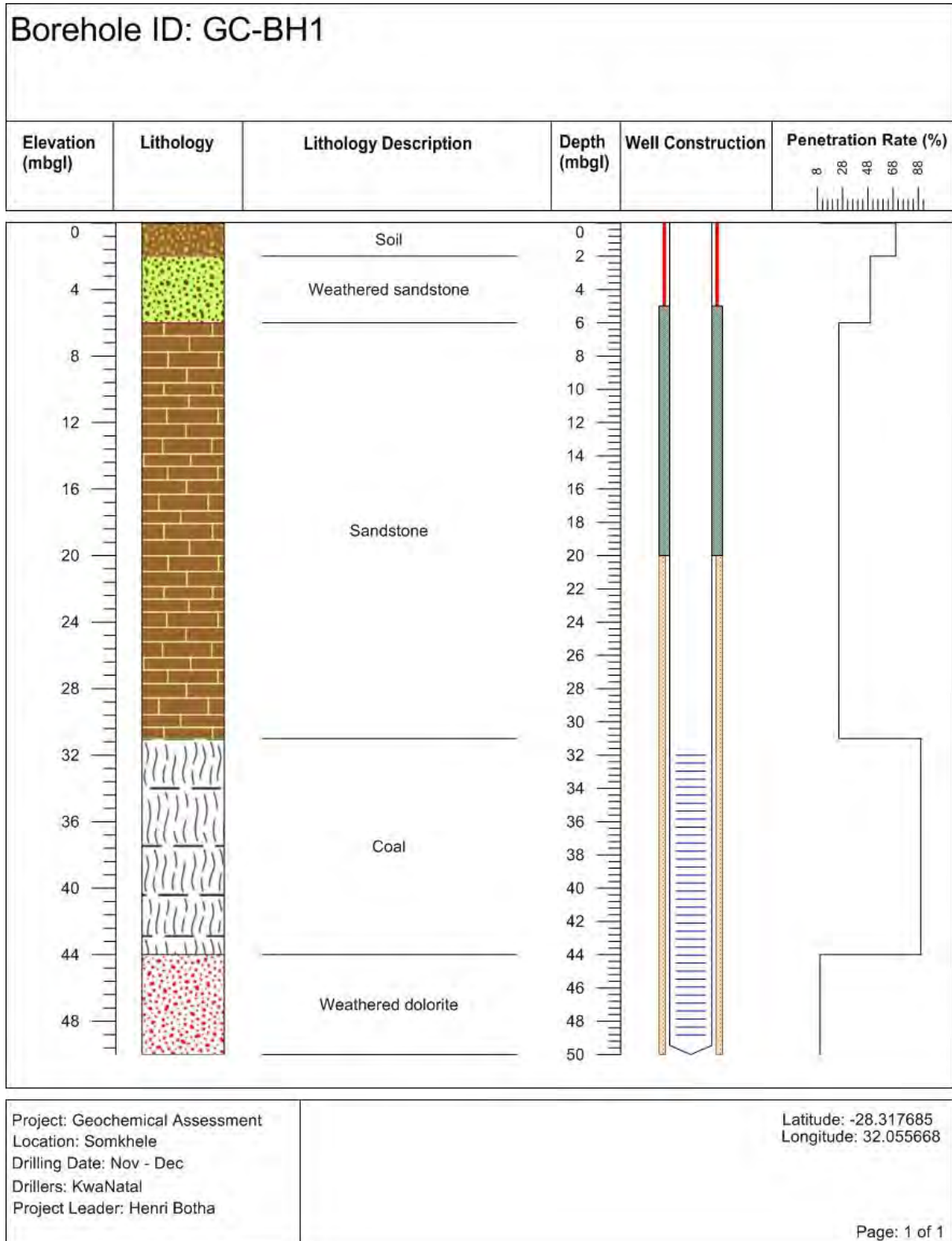






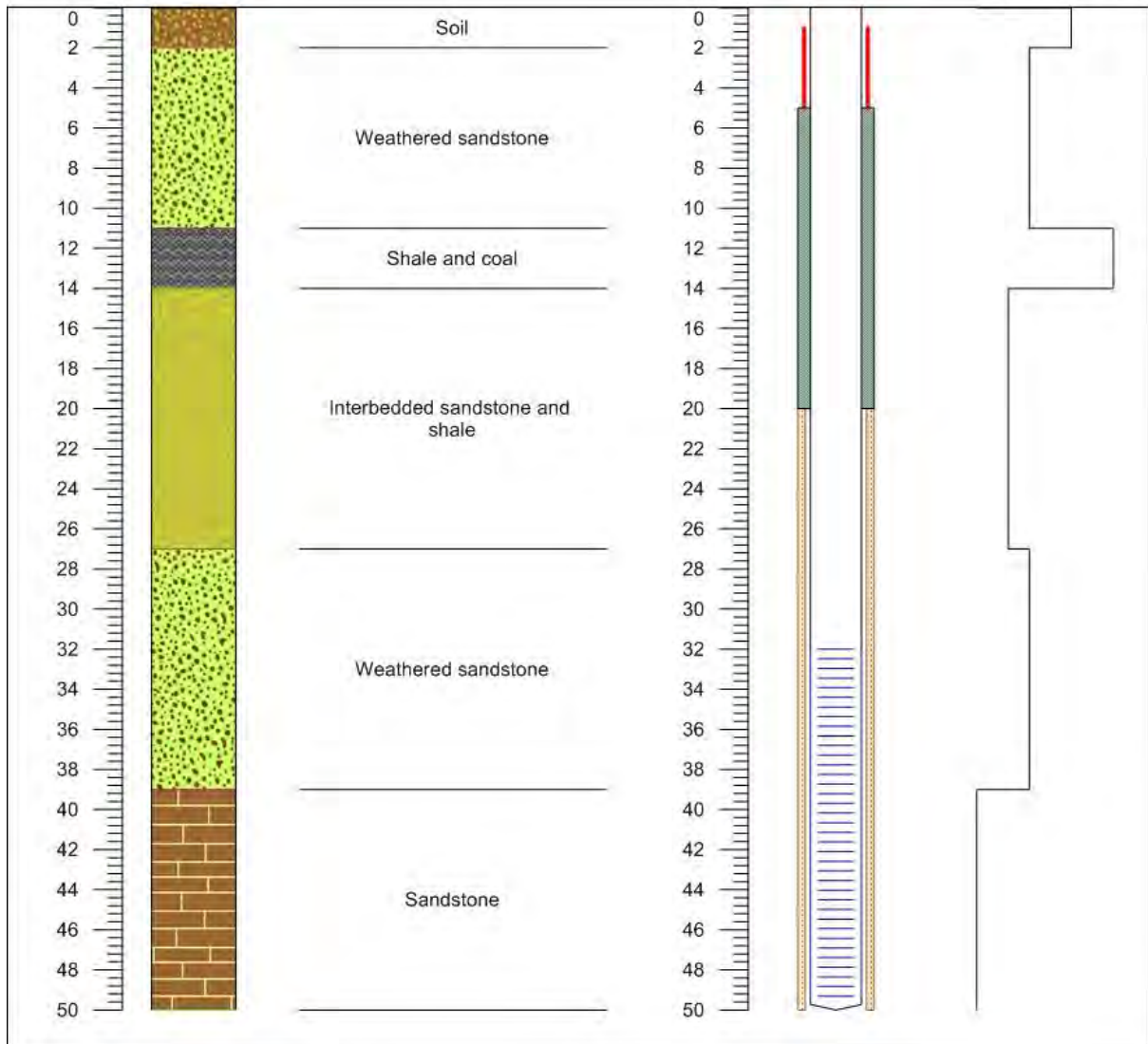


Appendix B: Borehole Logs



Borehole ID: GC-BH2

| Elevation (mbgl) | Lithology | Lithology Description | Depth (mbgl) | Well Construction | Penetration Rate (%) |
|------------------|-----------|-----------------------|--------------|-------------------|----------------------|
| | | | | | 24 44 64 84 |

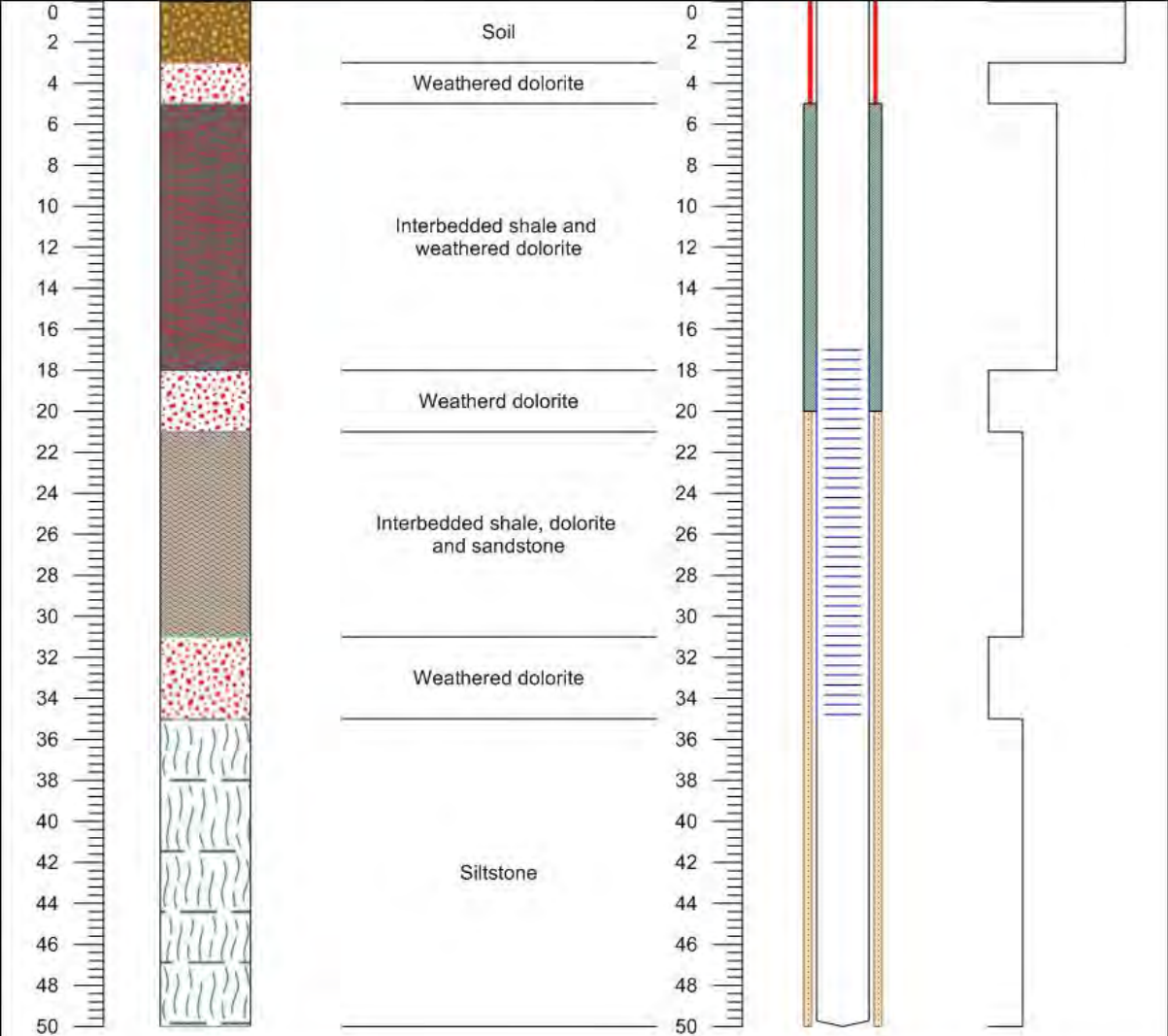


Project: Geochemical Assessment
 Location: Somkhele
 Drilling Date: Nov - Dec
 Drillers: KwaNatal
 Project Leader: Henri Botha

Latitude: -28.319946
 Longitude: 32.05608

Borehole ID: GC-BH3

| Elevation (mbgl) | Lithology | Lithology Description | Depth (mbgl) | Well Construction | Penetration Rate (%) |
|---------------------|-----------|-----------------------|-----------------|-------------------|----------------------|
| | | | | | 8 28 48 68 |

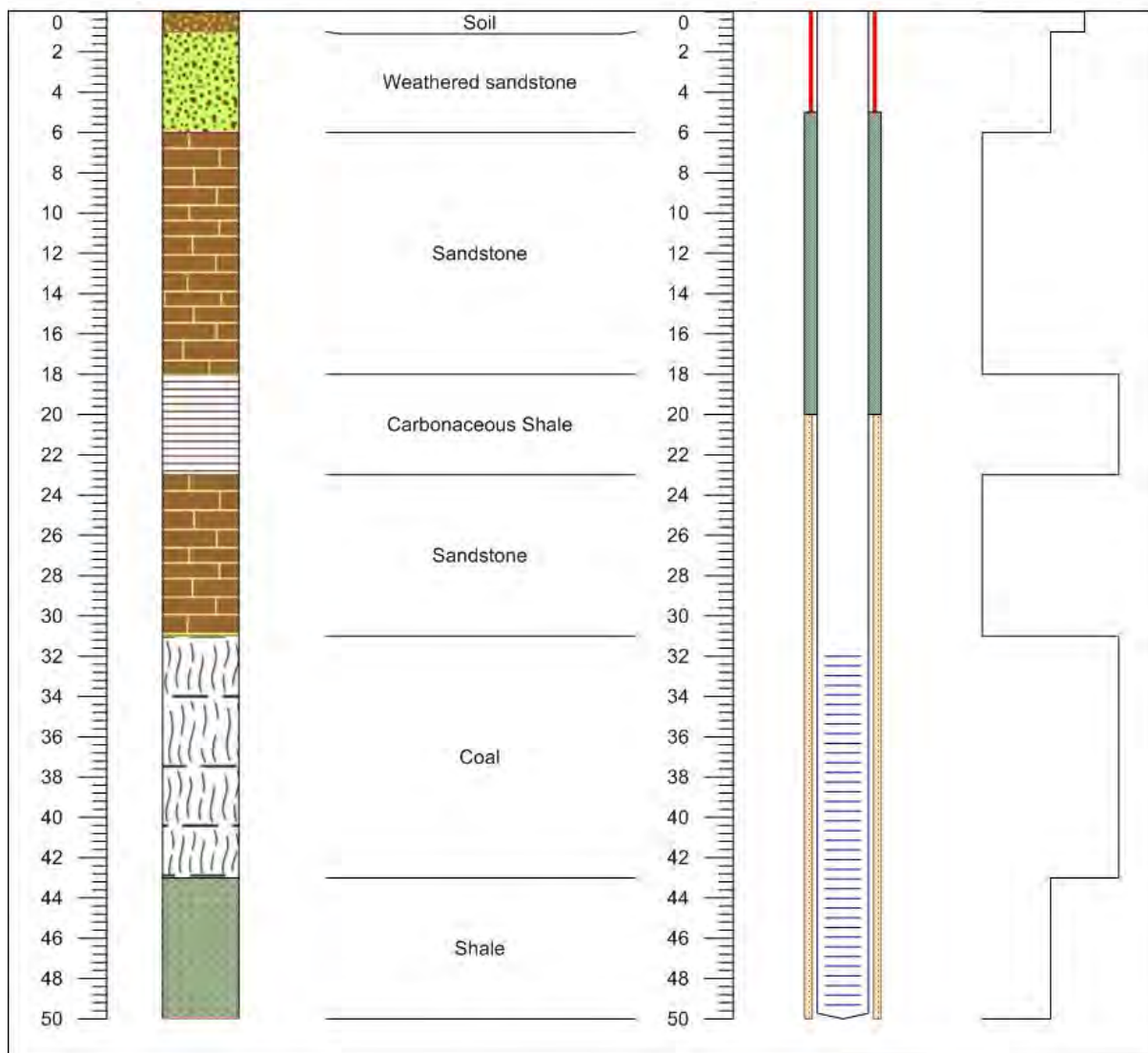


Project: Geochemical Assessment
Location: Somkhele
Drilling Date: Nov - Dec
Drillers: KwaNatal
Project Leader: Henri Botha

Latitude: -28.321049
Longitude: 32.054812

Borehole ID: GC-BH4

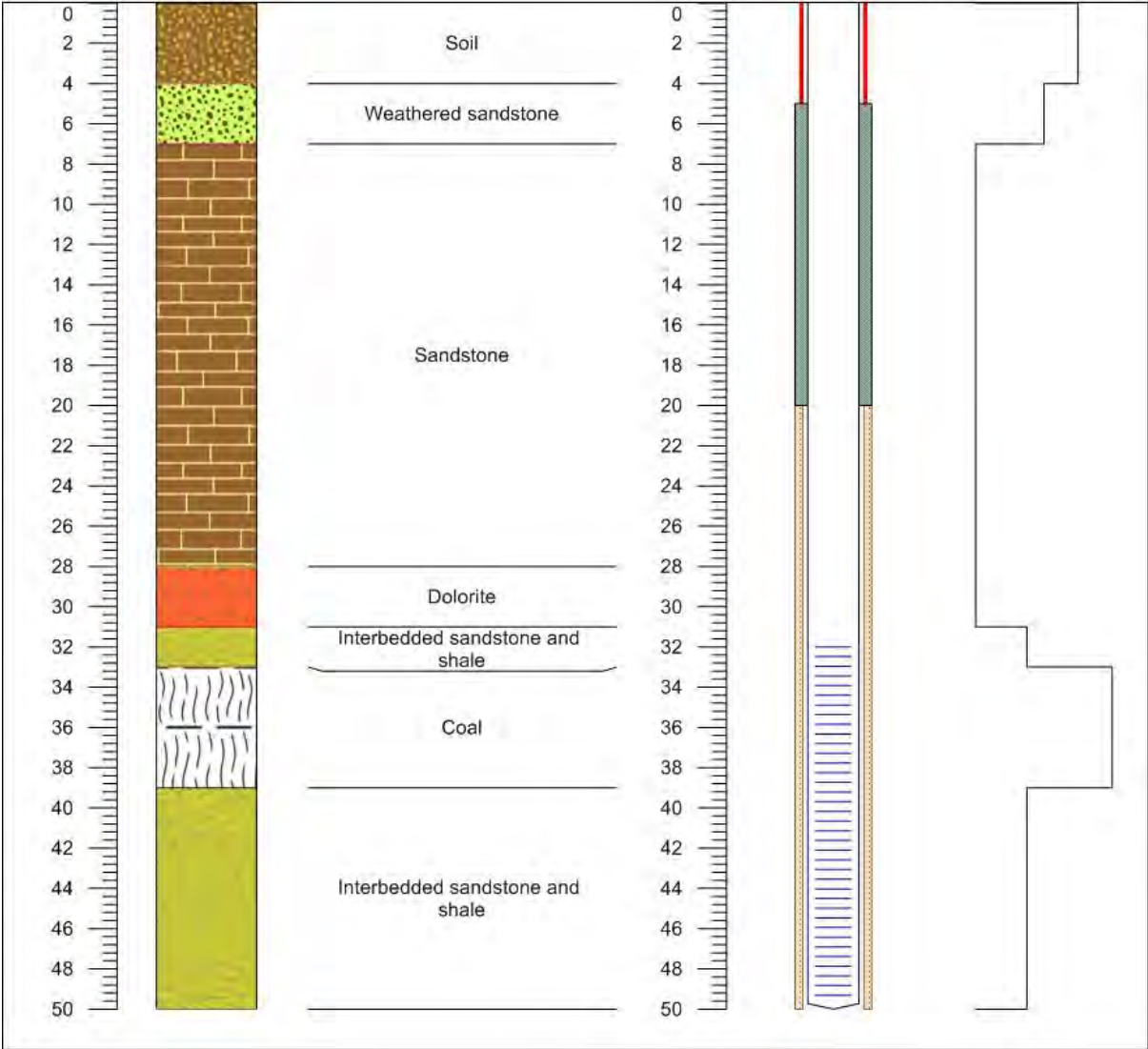
| Elevation (mbgl) | Lithology | Lithology Description | Depth (mbgl) | Well Construction | Penetration Rate (%) |
|------------------|-----------|-----------------------|--------------|-------------------|---|
| | | | | | <div> <div>8</div> <div>28</div> <div>48</div> <div>68</div> <div>88</div> </div> |



Project: Geochemical Assessment
 Location: Somkhele
 Drilling Date: Nov - Dec
 Drillers: KwaNatal
 Project Leader: Henri Botha

Latitude: -28.317542
 Longitude: 32.057146

| Borehole ID: GC-BH5 | | | | | |
|---------------------|-----------|-----------------------|--------------|-------------------|---|
| Elevation (mbgl) | Lithology | Lithology Description | Depth (mbgl) | Well Construction | Penetration Rate (%) |
| | | | | | <div> <div>8</div> <div>28</div> <div>48</div> <div>68</div> <div>88</div> </div> |

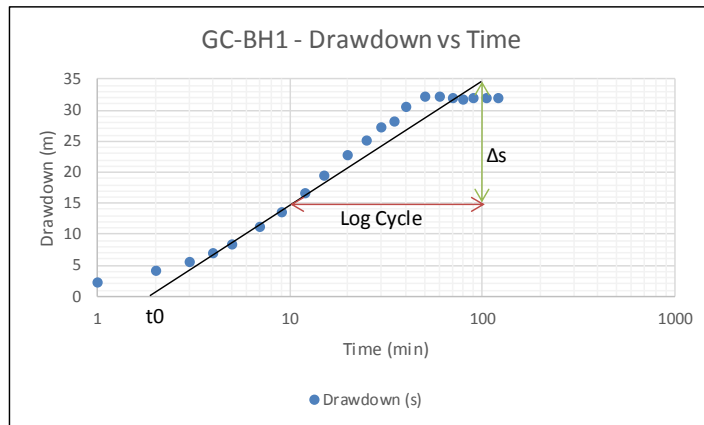


| | |
|--|--|
| Project: Geochemical Assessment Location: Somkhele Drilling Date: Nov - Dec Drillers: KwaNatal Project Leader: Henri Botha | Latitude: -28.319855 Longitude: 32.058042 Page: 1 of 1 |
|--|--|

Appendix C: Pump Test Analysis Results

| Time (min) | Drawdown (s) |
|------------|--------------|
| 2 | 0 |
| 1 | 2.315 |
| 2 | 4.165 |
| 3 | 5.525 |
| 4 | 7.145 |
| 5 | 8.525 |
| 7 | 11.265 |
| 9 | 13.655 |
| 12 | 16.745 |
| 15 | 19.565 |
| 20 | 22.715 |
| 25 | 25.235 |
| 30 | 27.405 |
| 35 | 28.31 |
| 40 | 30.717 |
| 50 | 32.325 |
| 60 | 32.211 |
| 70 | 31.986 |
| 80 | 31.875 |
| 90 | 31.939 |
| 105 | 32.015 |
| 120 | 31.987 |

Excel Calculation using Cooper Jacob Method

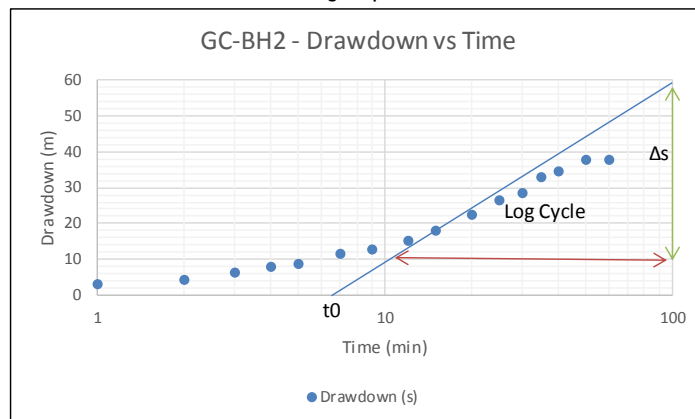


| | | | | |
|------|-----------|------|-----------|----------------------|
| Δs | 20 | m | 0.222222 | slope |
| t0 | 2 | min | 0.0013889 | day(s) |
| Q | 0.25 | l/s | 21.6 | m³/d |
| Δt | 90 | min | | |
| r | 0.165 | m | | (radius of borehole) |
| D | 50 | m | | |
| KD=T | 0.1976704 | m²/d | | |
| S | 0.0226894 | | | |
| K | 0.0039534 | m/d | | |

$$s = \frac{2.30Q}{4\pi KD} \log \frac{2.25KDt}{r^2S}$$

| Time (min) | Drawdown (s) |
|------------|--------------|
| 0 | 0 |
| 1 | 3.117 |
| 2 | 4.469 |
| 3 | 6.579 |
| 4 | 7.929 |
| 5 | 8.769 |
| 7 | 11.804 |
| 9 | 12.819 |
| 12 | 15.169 |
| 15 | 18.193 |
| 20 | 22.435 |
| 25 | 26.639 |
| 30 | 28.529 |
| 35 | 33.043 |
| 40 | 34.844 |
| 50 | 37.864 |
| 60 | 37.953 |
| 70 | 33.631 |
| 80 | 36.944 |

Excel Calculation using Cooper Jacob Method

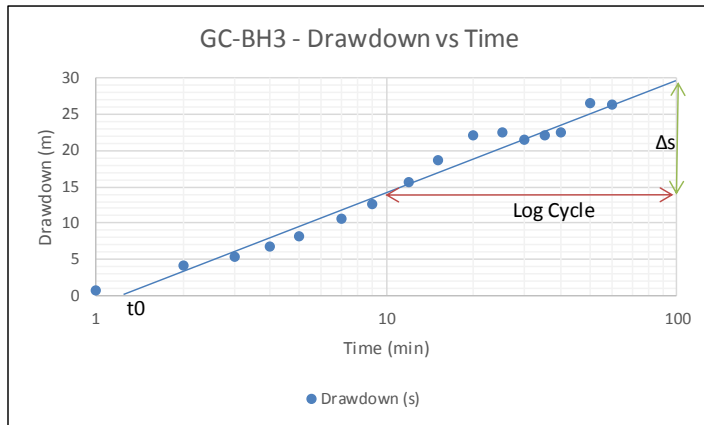


| | | | | |
|------|-----------|------|-----------|----------------------|
| Δs | 50 | m | 0.555556 | slope |
| t0 | 6.8 | min | 0.0047222 | day(s) |
| Q | 0.25 | l/s | 21.6 | m³/d |
| Δt | 90 | min | | |
| r | 0.165 | m | | (radius of borehole) |
| D | 50 | m | | |
| KD=T | 0.0790682 | m²/d | | |
| S | 0.0308576 | | | |
| K | 0.0015814 | m/d | | |

$$s = \frac{2.30Q}{4\pi KD} \log \frac{2.25KDt}{r^2S}$$

| Time (min) | Drawdown (s) |
|------------|--------------|
| 0 | 0 |
| 1 | 0.737 |
| 2 | 4.277 |
| 3 | 5.429 |
| 4 | 6.863 |
| 5 | 8.311 |
| 7 | 10.717 |
| 9 | 12.645 |
| 12 | 15.692 |
| 15 | 18.707 |
| 20 | 22.137 |
| 25 | 22.652 |
| 30 | 21.597 |
| 35 | 22.141 |
| 40 | 22.577 |
| 50 | 26.647 |
| 60 | 26.502 |
| | |
| | |

Excel Calculation using Cooper Jacob Method



| | | | | |
|------|-----------|------|-----------|----------------------|
| Δs | 15 | m | 0.1666667 | slope |
| t0 | 1.3 | min | 0.0009028 | day(s) |
| Q | 0.25 | l/s | 21.6 | m³/d |
| Δt | 90 | min | | |
| r | 0.165 | m | | (radius of borehole) |
| D | 50 | m | | |
| KD=T | 0.2635606 | m²/d | | |
| S | 0.0196642 | | | |
| K | 0.0052712 | m/d | | |

$$s = \frac{2.30Q}{4\pi KD} \log \frac{2.25KDt}{r^2S}$$

Appendix D: Hydrochemistry data

| Station ID | Sampling Date | Water Type | pH (lab) | El. Cond. | TDS | Ca | Mg | Na | K | Cl | Alk | HCO ₃ | CO ₃ | SO ₄ | NO ₂ | NO ₃ | Al | Fe |
|------------|---------------|---------------------------|----------|-----------|-------|----------|----------|----------|----------|------|-----|------------------|-----------------|-----------------|-----------------|-----------------|------------|------------|
| GC-BH1 | 01/09/2015 | Na-Ca-Cl | 6.5 | 4840 | 3180 | 326 | 109 | 835 | 7.77 | 1645 | 390 | 390 | <1 | 1.11 | | 2.68 | <0.003 | 0.023 |
| GC-BH1 | 01/06/2015 | Na-Cl-HCO ₃ | 6.82 | 4360 | 2742 | 121.7584 | 96.16318 | 695.7328 | 6.328031 | 1201 | 490 | 0 | 0 | 86.2 | | 0 | 0 | 0.025807 |
| GC-BH2 | 01/09/2015 | Na-Cl | 7.1 | 7130 | 4700 | 129 | 197 | 1367 | 10.1 | 1853 | 880 | 880 | <1 | 773 | | 2.68 | <0.003 | 0.017 |
| GC-BH2 | 01/06/2015 | Na-Mg-Cl-SO ₄ | 6.96 | 6310 | 4708 | 124.914 | 190.3927 | 1204.442 | 9.175517 | 1467 | 840 | 840 | 0 | 897 | | 0 | 0 | 0 |
| GC-BH3 | 01/09/2015 | Na-Cl | 6.9 | 5130 | 3380 | 138 | 81.2 | 939 | 8.21 | 1578 | 570 | 310 | 260 | 8.12 | | 2.68 | <0.003 | 0.007 |
| GC-BH3 | 01/06/2015 | Na-Cl | 7.12 | 4640 | 2984 | 133.1528 | 72.42915 | 837.5051 | 6.057123 | 1459 | 575 | 575 | 0 | 4.78 | | 0 | 0 | 0 |
| GC-BH4 | 01/09/2015 | Na-Mg-Cl | 7.3 | 6610 | 4350 | 230 | 205 | 1155 | 15.8 | 1738 | 590 | 450 | 140 | 582 | | 2.68 | <0.003 | 0.05 |
| GC-BH4 | 01/06/2015 | Na-Cl-SO ₄ | 7.07 | 6560 | 4730 | 205.0117 | 171.9223 | 1173.805 | 16.52419 | 1509 | 665 | 665 | 0 | 1334 | | 0.24708 | 0 | 0.010339 |
| GC-BH5 | 01/09/2015 | Na-Cl | 8.2 | 3570 | 2400 | 50.8 | 50.6 | 740 | 20.2 | 846 | 570 | 350 | 220 | 75.3 | | 2.68 | <0.003 | 0.022 |
| GC-BH5 | 01/06/2015 | Na-Cl-HCO ₃ | 7.48 | 3780 | 2036 | 63.98444 | 53.05518 | 646.1435 | 12.45513 | 803 | 610 | 570 | 40 | 48.3 | | 0 | 0 | 0 |
| KQP113 | 14/08/2014 | Na-Mg-Cl | 7.1 | 11660 | 8353 | 314.8 | 283.3 | 1535 | 31.2 | 3985 | 570 | 570 | | <0.05 | | <0.05 | 0.3 | 0.15 |
| KQP21 | 01/06/2015 | Na-Cl-HCO ₃ | 7.33 | 2029 | 1220 | 46.24727 | 37.52505 | 337.1817 | 3.04462 | 324 | 460 | 460 | 0 | 31.4 | | 0.8236 | 0 | 0 |
| KQP21 | 01/06/2015 | Na-Cl-HCO ₃ | 7.33 | 2029 | 1220 | 46.24727 | 37.52505 | 337.1817 | 3.04462 | 324 | 460 | 460 | | 31.4 | | 0.8236 | 0 | 0 |
| KQP21 | 12/12/2014 | Na-Mg-Cl-HCO ₃ | 8.1 | 1970 | 1250 | 65.77914 | 78.70724 | 525.7098 | 4.762773 | 380 | 550 | 550 | | 39 | | 8.6057 | 0.06440205 | 0.00194231 |
| KQP21 | 21/05/2014 | Na-HCO ₃ -Cl | 7.3 | 1570 | 984 | 44 | 28 | 316 | 3.4 | 307 | 519 | 633 | | 52 | | | 0.15 | 0.06 |
| KQP21 | 27/01/2014 | Na-Cl-HCO ₃ | 7.7 | 2215 | 1180 | 49 | 36 | 366 | 2.9 | 399 | 446 | 544 | | 58 | | | <0.003 | 0.02 |
| KQP74 | 14/08/2014 | Na-Mg-Cl | 6.9 | 11320 | 7637 | 234.2 | 263.5 | 1541 | 22.4 | 3755 | 600 | 600 | | 2.1 | | <0.05 | 0.13 | 0.53 |
| KQP86 | 12/12/2014 | Na-Mg-Cl | 6.9 | 10790 | 3768 | 274.2794 | 276.0346 | 1590 | 15.09973 | 3685 | 555 | 555 | | <0.05 | | <0.05 | 0.09314099 | 0.1374108 |
| KQP86 | 14/08/2014 | Na-Mg-Cl | 7 | 10980 | 6782 | 257.5 | 257.3 | 1515 | 27.2 | 3567 | 555 | 555 | | <0.05 | | <0.05 | 0.11 | 0.32 |
| SBH2 | 01/06/2015 | Na-Mg-Cl | 6.87 | 19230 | 15168 | 434.6713 | 726.6168 | 2771.06 | 17.03806 | 6529 | 660 | 660 | 0 | 1163 | | 27.05526 | 0 | 0 |

| Station ID | Sampling Date | Water Type | pH (lab) | El. Cond. | TDS | Ca | Mg | Na | K | Cl | Alk | HCO ₃ | CO ₃ | SO ₄ | NO ₂ | NO ₃ | Al | Fe |
|------------|---------------|------------------------|----------|-----------|-------|----------|----------|----------|----------|------|------|------------------|-----------------|-----------------|-----------------|-----------------|------------|-----------|
| SBH2 | 12/12/2014 | Na-Mg-Cl | 7.6 | 14520 | 9133 | 371.859 | 450.9042 | 1945.762 | 12.77385 | 4613 | 850 | 850 | | 620 | | 3.612269 | 0.1259222 | 0.1666897 |
| SBH2 | 14/08/2014 | Na-Mg-Cl | 7.1 | 17330 | 13904 | 380.1 | 587.3 | 2350 | 45.6 | 6092 | 755 | 755 | | 861 | | 16.8 | 0.17 | 0.03 |
| SBH2 | 21/05/2014 | Na-Mg-Cl | 6.8 | 18490 | 14524 | 692 | 1173 | 2931 | 29 | 6972 | 783 | 955 | | 968 | | | 0.09 | 0.007 |
| SBH2 | 27/01/2014 | Na-Cl | 6.9 | 19180 | | 439 | 412 | 2703 | 12.5 | 6121 | 491 | 599 | | 391 | | | <0.003 | 0.01 |
| SBH3 | 01/06/2015 | Na-Cl | 7.08 | 7160 | 4546 | 142.9726 | 157.4184 | 1165.742 | 8.774184 | 2010 | 840 | 840 | 0 | 175 | | 0 | 0 | 0 |
| SBH3 | 12/12/2014 | Na-Cl-HCO ₃ | 8.3 | 7080 | 4074 | 124.4754 | 141.6184 | 1262.504 | 7.966829 | 1967 | 1020 | 1020 | | 143 | | 7.043039 | 0.07637303 | 0.1170985 |
| SBH3 | 14/08/2014 | Na-Cl-HCO ₃ | 7.3 | 5520 | 3318 | 101 | 106.7 | 917 | 21.6 | 1440 | 985 | 985 | | 179 | | <0.05 | 0.22 | 0.67 |
| SBH3 | 21/05/2014 | Na-Cl-HCO ₃ | 7.1 | 5680 | 3672 | 137 | 129 | 1370 | 10.7 | 1665 | 1142 | 1392 | | 132 | | | 0.009 | 0.02 |
| SBH3 | 27/01/2014 | Na-Cl-HCO ₃ | 7.3 | 0 | | 106 | 97 | 945 | 5.2 | 1306 | 825 | 1006 | | 159 | | | <0.003 | <0.001 |
| SBH4 | 14/08/2014 | Na-Cl | 7.3 | 9570 | 6333 | 217.8 | 212.1 | 1429 | 33.1 | 3044 | 625 | 625 | | 140 | | <0.05 | 1.44 | 0.64 |
| SBH4 | 21/05/2014 | Na-Cl | 6.9 | 3090 | 1916 | 72 | 61 | 754 | 8.9 | 1007 | 289 | 352 | | 58 | | | 0.5 | 8.9 |
| SBH4 | 27/01/2014 | Na-Cl | 7.1 | 11000 | | 240 | 207 | 1538 | 12.8 | 2705 | 436 | 532 | | 143 | | | <0.003 | 0.05 |
| SBH6 | 01/06/2015 | Na-Cl | 7.09 | 5520 | 3962 | 193.7444 | 97.33366 | 946.6786 | 14.24036 | 1774 | 510 | 510 | 0 | 70.2 | | 0 | 0 | 0.1415675 |
| SBH6 | 12/12/2014 | Na-Cl | 8 | 6080 | 4148 | 198.2335 | 109.7479 | 880.4846 | 12.76946 | 1981 | 620 | 620 | | 67.3 | | <0.05 | 0.0724301 | 0.1069623 |
| SBH6 | 14/08/2014 | Na-Cl | 7.3 | 6120 | 3958 | 185.4 | 88.2 | 896 | 25.4 | 2004 | 605 | 605 | | 62 | | <0.05 | 0.09 | 0.41 |
| SBH6 | 21/05/2014 | Na-Cl-HCO ₃ | 7.2 | 5440 | 3556 | 229 | 85 | 952 | 12.7 | 1770 | 712 | 868 | | 68 | | | 0.04 | 0.04 |
| SBH6 | 27/01/2014 | Na-Cl | 7.1 | 6250 | | 205 | 80 | 893 | 9.6 | 1623 | 507 | 618 | | 89 | | | <0.003 | 0.008 |
| SBH7 | 01/06/2015 | Na-Cl-HCO ₃ | 7.33 | 4230 | 2938 | 73.79835 | 66.60754 | 983.2454 | 6.341935 | 922 | 910 | 910 | 0 | 474 | | 41.18 | 0 | 0.0140726 |
| SBH7 | 12/12/2014 | Na-Cl-HCO ₃ | 8.8 | 5040 | 2981 | 69.39558 | 61.98757 | 948.6552 | 6.582839 | 910 | 1012 | 1012 | | 315 | | 60.47009 | 0.1473534 | 0.1177943 |
| SBH7 | 14/08/2014 | Na-Cl-HCO ₃ | 7.7 | 4510 | 3042 | 48.6 | 34.6 | 899 | 17.5 | 907 | 920 | 920 | | 395 | | 139 | 0.42 | 0.15 |
| SBH7 | 21/05/2014 | Na-Cl-HCO ₃ | 7.2 | 5230 | 3600 | 83 | 62 | 1218 | 8.1 | 1234 | 1301 | 1586 | | 330 | | | 0.07 | 0.06 |
| SBH7 | 27/01/2014 | Na-Cl-HCO ₃ | 7.2 | 7120 | | 109 | 87 | 1019 | 5.2 | 1607 | 832 | 1014 | | 188 | | | <0.003 | 0.001 |

| Station ID | Sampling Date | Water Type | pH (lab) | El. Cond. | TDS | Ca | Mg | Na | K | Cl | Alk | HCO ₃ | CO ₃ | SO ₄ | NO ₂ | NO ₃ | Al | Fe |
|------------|---------------|---------------------------|----------|-----------|------|----------|----------|----------|----------|------|-----|------------------|-----------------|-----------------|-----------------|-----------------|------------|------------|
| SBH8 | 01/06/2015 | Na-Cl | 7.32 | 4200 | 3332 | 102.8841 | 91.9 | 1031 | 10.74404 | 1911 | 380 | 380 | 0 | 114 | | 0 | 0 | 0.3163871 |
| SBH8 | 12/12/2014 | Na-Cl | 8.1 | 6230 | 3593 | 105.9094 | 89.34388 | 958.6277 | 9.551021 | 1978 | 430 | 430 | | 120 | | <0.05 | 0.05739626 | 0.1112753 |
| SBH8 | 14/08/2014 | Na-Cl | 7.6 | 5900 | 3499 | 93.8 | 76.8 | 981 | 21.5 | 1910 | 430 | 430 | | 169 | | 9.2 | 0.07 | 0.35 |
| SBH8 | 21/05/2014 | Na-Cl-HCO ₃ | 7.3 | 5730 | 3644 | 143 | 105 | 1184 | 11.3 | 1880 | 718 | 875 | | 112 | | | 0.02 | 0.09 |
| SBH8 | 27/01/2014 | Na-Cl | 7.1 | 5800 | | 80 | 60 | 980 | 7.5 | 1585 | 270 | 329 | | 139 | | | <0.003 | 0.02 |
| SBH9 | 01/06/2015 | Na-Cl | 7.19 | 7660 | 6622 | 122.1944 | 115.9611 | 1998 | 10.79265 | 3278 | 440 | 440 | 0 | 191 | | 0 | 0 | 0.2213592 |
| SBH9 | 12/12/2014 | Na-Cl | 7.1 | 11180 | 743 | 207.8858 | 213.1777 | 1736.063 | 12.2399 | 3589 | 495 | 495 | | 183 | | <0.05 | 0.08877959 | 0.111348 |
| SBH9 | 14/08/2014 | Na-Cl | 7.6 | 11390 | 8101 | 182.6 | 190.1 | 1802 | 34.3 | 4054 | 400 | 400 | | 220 | | <0.05 | 0.09 | 0.27 |
| SBH9 | 21/05/2014 | Na-Cl | 7.6 | 10260 | 7120 | 202 | 180 | 2152 | 14.5 | 3806 | 628 | 766 | | 289 | | | 0.04 | 0.02 |
| SBH9 | 27/01/2014 | Na-Cl | 7.4 | 11560 | | 168 | 175 | 1846 | 9.3 | 3546 | 239 | 291 | | 183 | | | <0.003 | 0.003 |
| SM6 | 01/06/2015 | Na-Cl-HCO ₃ | 7.45 | 2606 | 1904 | 62.61455 | 69.42613 | 574.1498 | 3.129656 | 598 | 750 | 750 | 0 | 45.8 | | 0 | 0 | 0 |
| SM6 | 12/12/2014 | Na-Cl-HCO ₃ | 8.6 | 3230 | 1994 | 65.87984 | 77.74542 | 567.2767 | 4.533217 | 622 | 923 | 923 | | 45.1 | | 2.846432 | 0.2384118 | 0.04066013 |
| SM6 | 14/08/2014 | Na-Cl-HCO ₃ | 8.5 | 3260 | 1951 | 59.9 | 65.1 | 560 | 15.7 | 718 | 730 | 730 | | 50.2 | | 0.2 | 0.08 | 0.02 |
| SM6 | 21/05/2014 | Na-HCO ₃ -Cl | 7.3 | 2900 | 1854 | 61 | 57 | 598 | 3.5 | 679 | 972 | 1185 | | 50 | | | 0.03 | 0.03 |
| SM6 | 27/01/2014 | Na-Cl-HCO ₃ | 7.4 | 3280 | 1784 | 59 | 56 | 533 | 2.2 | 580 | 698 | 851 | | 57 | | | <0.003 | 0.01 |
| SM7 | 01/06/2015 | Na-Mg-Cl-HCO ₃ | 7.39 | 3000 | 1736 | 86.25137 | 95.89793 | 469.757 | 3.948523 | 638 | 680 | 680 | 0 | 122 | | 0 | 0 | 0 |
| SM7 | 12/12/2014 | Na-Mg-Cl-HCO ₃ | 8.4 | 3130 | 1781 | 91.95921 | 112.6368 | 479.5979 | 4.745389 | 727 | 735 | 735 | | 91.1 | | <0.05 | 0.08235954 | 0.124975 |
| SM7 | 14/08/2014 | Na-Mg-Cl-HCO ₃ | 8.5 | 3130 | 1777 | 75 | 86.5 | 453 | 13.9 | 673 | 660 | 660 | | 115 | | 0.3 | 0.1 | 0.02 |
| SM7 | 21/05/2014 | Na-Cl-HCO ₃ | 7.4 | 2690 | 1700 | 81 | 79 | 500 | 4 | 619 | 855 | 1042 | | 97 | | | 0.02 | 0.02 |
| SM7 | 27/01/2014 | Na-Mg-Cl-HCO ₃ | 7.4 | 3120 | 1660 | 79 | 77 | 423 | 2.5 | 569 | 602 | 734 | | 91 | | | <0.003 | 0.03 |

| Station ID | Sampling Date | Water Type | pH (lab) | El. Cond. | TDS | Ca | Mg | Na | K | Cl | Alk | HCO ₃ | CO ₃ | SO ₄ | NO ₂ | NO ₃ | Al | Fe |
|------------|---------------|---|----------|-----------|------|----------|----------|----------|----------|-----|------|------------------|-----------------|-----------------|-----------------|-----------------|------------|------------|
| SMA2-BH11 | 01/06/2015 | Na-Cl-HCO ₃ | 7.5 | 2921 | 1900 | 62.19804 | 75.68279 | 552.1076 | 2.392064 | 580 | 705 | 705 | 0 | 208 | | 0 | 0.06152377 | 0.0859975 |
| SMA2-BH11 | 12/12/2014 | Na-Mg-Cl-HCO ₃ | 8.7 | 3040 | 1890 | 68.51907 | 92.26632 | 522.7291 | 3.386494 | 517 | 657 | 657 | | 287 | | <0.05 | 0.07055265 | 0.01691477 |
| SMA2-BH11 | 14/08/2014 | Na-Cl-HCO ₃ | 8.6 | 3010 | 1734 | 53.3 | 62.8 | 497 | 11.2 | 568 | 740 | 740 | | 90 | | <0.05 | 0.06 | 0.15 |
| SMA2-BH11 | 21/05/2014 | Na-HCO ₃ -Cl-SO ₄ | 7.7 | 2570 | 1788 | 79 | 83 | 653 | 3.5 | 430 | 741 | 903 | | 384 | | | 0.02 | 0.02 |
| SMA2-BH11 | 27/01/2014 | Na-Mg-SO ₄ -HCO ₃ -Cl | 7.8 | 3060 | 1996 | 91 | 104 | 431 | 2.1 | 262 | 378 | 461 | | 761 | | | <0.003 | 0.008 |
| SMA2-BH12 | 01/06/2015 | Na-SO ₄ | 7.83 | 4260 | 3678 | 40.64936 | 150 | 1200 | 2.307828 | 310 | 435 | 375 | 60 | 2468 | | 0 | 0 | 0.04452981 |
| SMA2-BH12 | 12/12/2014 | Na-SO ₄ -Cl | 8.9 | 4180 | 2688 | 15.68816 | 75.7606 | 810.1511 | 3.150758 | 431 | 689 | 469 | | 827 | | 15.34329 | 0.05667981 | 0.2025681 |
| SMA2-BH12 | 14/08/2014 | Na-Cl-HCO ₃ | 8.8 | 3390 | 1873 | 1.87 | 18.7 | 670 | 11.8 | 667 | 730 | 730 | | 142 | | 11.9 | 0.01 | 0.06 |
| SMA2-BH12 | 21/05/2014 | Na-HCO ₃ -Cl | 8.8 | 2920 | 1888 | 5.1 | 32 | 938 | 4.3 | 581 | 1001 | 1123 | | 191 | | | <0.003 | 0.09 |
| SMA2-BH12 | 27/01/2014 | Na-Cl-HCO ₃ | 8.7 | 3460 | 1828 | 5.3 | 30 | 714 | 1.6 | 561 | 816 | 958 | | 169 | | | 0.01 | 0.006 |
| SMA2-BH13 | 01/09/2015 | Na-Mg-CO ₃ -Cl | 8.1 | 2520 | 1660 | 79.5 | 87.8 | 483 | 3.51 | 322 | 720 | 300 | 420 | 263 | | <0.05 | <0.003 | 0.039 |
| SMA2-BH13 | 01/06/2015 | Na-Mg-SO ₄ -HCO ₃ -Cl | 7.43 | 2493 | 1550 | 67.27798 | 72.9201 | 465.72 | 1.43767 | 296 | 620 | 620 | 0 | 497 | | 0 | 0 | 0.00887155 |
| SMA2-BH13 | 12/12/2014 | Na-Mg-HCO ₃ -Cl-SO ₄ | 8.8 | 2740 | 1711 | 67.80515 | 81.70744 | 470.7548 | 2.486501 | 294 | 757 | 757 | | 338 | | <0.05 | 0.05403543 | 0.06968715 |
| SMA2-BH13 | 14/08/2014 | Na-HCO ₃ -Cl-SO ₄ | 8.6 | 2620 | 1666 | 49.7 | 64.8 | 445 | 10 | 318 | 725 | 725 | | 402 | | 0.2 | 0.04 | 0.31 |
| SMA2-BH13 | 21/05/2014 | Na-HCO ₃ -Cl | 7.4 | 2330 | 1588 | 74 | 69 | 620 | 2.7 | 310 | 862 | 1051 | | 319 | | | <0.003 | 0.03 |
| SMA2-BH13 | 27/01/2014 | Na-HCO ₃ -Cl | 7.5 | 2675 | 1564 | 60 | 57 | 432 | 1.3 | 285 | 701 | 855 | | 237 | | | <0.003 | 0.02 |
| SMA2-BH14 | 01/06/2015 | Na-Mg-Cl-SO ₄ -HCO ₃ | 7.32 | 3640 | 2556 | 99.26708 | 108.4723 | 706.9329 | 4.486909 | 598 | 675 | 675 | 0 | 625 | | 0 | 0 | 0.06790469 |

| Station ID | Sampling Date | Water Type | pH (lab) | El. Cond. | TDS | Ca | Mg | Na | K | Cl | Alk | HCO ₃ | CO ₃ | SO ₄ | NO ₂ | NO ₃ | Al | Fe |
|------------|---------------|--|----------|-----------|------|----------|----------|----------|----------|------|-----|------------------|-----------------|-----------------|-----------------|-----------------|------------|------------|
| SMA2-BH14 | 12/12/2014 | Na-Mg-Cl-HCO ₃ -SO ₄ | 8.5 | 4110 | 2500 | 87.42675 | 109.6382 | 686.6383 | 4.716616 | 650 | 856 | 856 | | 507 | | 5.002284 | 0.1507963 | 0.9847507 |
| SMA2-BH14 | 27/01/2014 | Na-Cl-HCO ₃ | 7.7 | 3840 | 2202 | 60 | 73 | 644 | 2.8 | 643 | 73 | 927 | | 252 | | | <0.003 | 0.002 |
| SMA2-BH15 | 27/01/2014 | Na-Cl-HCO ₃ | 7.7 | 6300 | 3446 | 87 | 104 | 1032 | 9.3 | 1595 | 728 | 888 | | 137 | | | <0.003 | <0.001 |
| SMA2-BH15 | 27/01/2014 | Na-Cl-HCO ₃ | 7.7 | 6300 | 3446 | 87 | 104 | 1032 | 9.3 | 1595 | 728 | 888 | | 137 | | | <0.003 | <0.001 |
| SMA2-BH16 | 01/09/2015 | Na-Cl | 7.9 | 4230 | 2790 | 108 | 52.9 | 1124 | 10.1 | 1604 | 570 | 410 | 160 | 7.57 | | 8.11 | <0.003 | 0.028 |
| SMA2-BH16 | 01/06/2015 | Na-Cl | 7.44 | 3320 | 2726 | 84.06343 | 42.37715 | 878.7678 | 10.04907 | 1309 | 515 | 515 | 0 | 12.1 | | 0 | 0 | 0 |
| SMA2-BH16 | 14/08/2014 | Na-Cl | 8.5 | 5430 | 2893 | 82.7 | 57.3 | 927 | 16.5 | 1608 | 625 | 625 | | 12.1 | | 0.2 | 0.06 | 0.09 |
| SMA2-BH16 | 21/05/2014 | Na-Cl-HCO ₃ | 7.3 | 4620 | 2812 | 82 | 59 | 1241 | 6.3 | 1481 | 763 | 930 | | 10.9 | | | 0.01 | 0.05 |
| SMA2-BH16 | 27/01/2014 | Na-Cl-HCO ₃ | 7.5 | 5795 | 3082 | 85 | 77 | 948 | 3 | 1440 | 716 | 873 | | 29 | | | <0.003 | 0.02 |
| SPX10 | 01/06/2015 | Na-Cl | 7.04 | 8170 | 6096 | 244.2749 | 218.4605 | 1534.986 | 14.74464 | 2803 | 740 | 740 | 0 | 218 | | 0 | 0 | 0 |
| SPX10 | 01/06/2015 | Na-Cl | 7.04 | 8170 | 6096 | 244.2749 | 218.4605 | 1534.986 | 14.74464 | 2803 | 740 | 740 | | 218 | | 0 | 0 | 0 |
| SPX10 | 12/12/2014 | Na-Mg-Cl | 7.3 | 9470 | 6225 | 246.3263 | 226.0953 | 1331.372 | 12.24596 | 2742 | 880 | 880 | | 182 | | 7.122721 | 0.09528449 | 0.03268542 |
| SPX10 | 14/08/2014 | Na-Cl | 7.3 | 9670 | 6291 | 244.3 | 214.7 | 1502 | 32.4 | 3092 | 765 | 765 | | 203 | | <0.05 | 0.17 | 0.05 |
| SPX10 | 21/05/2014 | Na-Cl | 7.1 | 8750 | 6064 | 275 | 199 | 1490 | 10.4 | 2983 | 872 | 1063 | | 186 | | | 0.05 | 0.04 |
| SPX10 | 27/01/2014 | Na-Cl | 7 | 8750 | 6064 | 275 | 199 | 1490 | 10.4 | 2983 | 872 | 1063 | | 175 | | | 0.05 | 0.04 |
| SWX1 | 01/09/2015 | Na-Mg-Cl-SO ₄ -HCO ₃ | 8.1 | 3420 | 2250 | 110 | 145 | 655 | 20.3 | 587 | 850 | 610 | 240 | 520 | | 32.94 | <0.003 | 0.091 |
| SWX1 | 01/06/2015 | Na-Mg-Cl-HCO ₃ -SO ₄ | 7.34 | 2626 | 2550 | 95.65238 | 120.9659 | 650.8455 | 21.89597 | 540 | 810 | 810 | 0 | 542 | | 0 | 0 | 0.188985 |
| SWX1 | 12/12/2014 | Na-Mg-Cl-SO ₄ -HCO ₃ | 8.6 | 4140 | 2361 | 99.30974 | 143.2284 | 653.4533 | 12.92325 | 601 | 734 | 734 | | 731 | | <0.05 | 0.1666897 | 0.08662444 |
| SWX1 | 14/08/2014 | Na-Mg-SO ₄ -Cl-HCO ₃ | 7.8 | 4340 | 3322 | 89.1 | 147.1 | 734 | 17.3 | 673 | 660 | 660 | | 928 | | 0.06 | 0.05 | 0.04 |

| Station ID | Sampling Date | Water Type | pH (lab) | El. Cond. | TDS | Ca | Mg | Na | K | Cl | Alk | HCO ₃ | CO ₃ | SO ₄ | NO ₂ | NO ₃ | Al | Fe |
|------------|---------------|--|----------|-----------|------|----------|----------|----------|----------|-----|-----|------------------|-----------------|-----------------|-----------------|-----------------|------------|-----------|
| SWX1 | 21/05/2014 | Na-Mg-Cl-HCO ₃ -SO ₄ | 7.2 | 3630 | 2668 | 90 | 134 | 700 | 4.7 | 615 | 815 | 994 | | 776 | | | 0.05 | 0.08 |
| SWX1 | 27/01/2014 | Na-Mg-Cl-SO ₄ -HCO ₃ | 7.3 | 4040 | 2472 | 70 | 106 | 616 | 2.4 | 521 | 573 | 699 | | 622 | | | <0.003 | 0.007 |
| SWX3 | 01/09/2015 | Mg-Na-Ca-SO ₄ | 8.1 | 3610 | 2380 | 289 | 434 | 381 | 3.58 | 374 | 460 | 280 | 180 | 1987 | | 6.38 | <0.003 | 0.217 |
| SWX3 | 01/06/2015 | Mg-Na-Ca-SO ₄ | 7.29 | 3830 | 3356 | 282.0157 | 296.785 | 367 | 1.737239 | 336 | 310 | 310 | 0 | 2169 | | 0 | 0 | 0.4851762 |
| SWX3 | 12/12/2014 | Mg-Na-Ca-SO ₄ -Cl | 8.5 | 3740 | 3108 | 236.349 | 269.6326 | 325.4462 | 2.735686 | 346 | 567 | 567 | | 1252 | | <0.05 | 0.09074135 | 4.474068 |
| SWX3 | 14/08/2014 | Mg-Na-Ca-SO ₄ -Cl | 8.2 | 3400 | 3384 | 219.6 | 246.1 | 281 | 11.2 | 330 | 365 | 365 | | 1477 | | 3.2 | 0.08 | 1.09 |
| SWX3 | 21/05/2014 | Mg-Na-Ca-SO ₄ -Cl | 7.4 | 2800 | 2548 | 236 | 245 | 300 | 2.7 | 336 | 343 | 418 | | 1202 | | | 0.03 | 0.18 |
| SWX3 | 27/01/2014 | Mg-Na-Ca-SO ₄ -Cl | 7.5 | 2849 | 1636 | 144 | 139 | 229 | 1.1 | 275 | 256 | 312 | | 778 | | | <0.003 | 0.01 |

Appendix E: ICP-OES Results

Table 8-1: ICP-OES results of the peroxide leach testing

| Parameters (mg/l) | Peroxide Leach (1:100) | | | | SANS 241:2011 | | |
|----------------------|------------------------|-----------|------------|------------|-------------------|----------------------|-------------|
| | Discard 1 | Discard 2 | Tailings 1 | Tailings 2 | 0-50% of limit | 50%-100% of limit | Above limit |
| | AIS871 | AIS872 | AIS876 | AIS877 | | | |
| Al | 2.240 | 1.418 | <0.1 | 1.393 | <0.15 | 0.15-0.3 | >0.3 |
| As | <0.02 | <0.02 | <0.02 | <0.02 | <0.005 | 0.005-0.01 | >0.01 |
| Ba | 0.051 | 0.048 | <0.02 | 0.059 | - | - | - |
| Be | <0.02 | <0.02 | <0.02 | <0.02 | - | - | - |
| Ca | 104 | 115 | 61.9 | 105 | - | - | - |
| Cd | <0.02 | <0.02 | <0.02 | <0.02 | <0.0015 | 0.0015-0.003 | >0.003 |
| Co | 0.043 | 0.032 | <0.02 | 0.041 | <0.25 | 0.25-0.5 | >0.5 |
| Cr | <0.02 | <0.02 | <0.02 | <0.02 | <0.025 | 0.025-0.05 | >0.05 |
| Cu | 0.114 | 0.101 | <0.02 | 0.151 | <1 | 1-2 | >2 |
| Fe | 50.1 | 20.7 | 0.214 | 47.89 | <1 | 1-2 | >2 |
| K | 1.18 | 1.01 | <1 | 1.39 | - | - | - |
| Mg | 3.92 | 5.36 | 2.49 | 5.42 | - | - | - |
| Mn | 1.40 | 1.57 | 0.202 | 1.96 | <0.25 | 0.25-0.5 | >0.5 |
| Na | 3.31 | 3.74 | 4.61 | 5.06 | - | - | - |
| Ni | 0.071 | 0.058 | <0.02 | 0.066 | <0.035 | 0.035-0.07 | >0.07 |
| Pb | <0.02 | <0.02 | <0.02 | <0.02 | <0.005 | 0.005-0.01 | >0.01 |
| Se | <0.02 | <0.02 | <0.02 | <0.02 | | | |
| Sr | 0.207 | 0.295 | 0.116 | 0.288 | - | - | - |
| V | <0.02 | <0.02 | <0.02 | <0.02 | <0.1 | 0.1-0.2 | >0.2 |
| Zn | 0.363 | 0.294 | 0.049 | 0.442 | <2.5 | 2.5-5.0 | >5 |

Table 8-2: ICP-OES results (Sample AIS 871, Discard)

| Parameters (mg/l) | AIS871 | | | | | | | | | SANS 241:2011 | | |
|-------------------|--------|-------|-------|-------|-------|-------|-------|-------|-------|----------------|-------------------|-------------|
| | | | | | | | | | | 0-50% of limit | 50%-100% of limit | Above limit |
| Leach | 0 | 1 | 2 | 3 | 6 | 10 | 15 | 20 | 25 | | | |
| Al | 4.14 | 0.026 | 0.028 | 0.023 | <0.02 | <0.02 | <0.02 | <0.02 | <0.02 | <0.15 | 0.15-0.3 | >0.3 |
| As | 0.023 | <0.02 | <0.02 | <0.02 | <0.02 | <0.02 | <0.02 | <0.02 | <0.02 | - | - | - |
| Ba | 0.028 | <0.02 | <0.02 | <0.02 | <0.02 | <0.02 | <0.02 | <0.02 | <0.02 | - | - | - |
| Be | <0.02 | <0.02 | <0.02 | <0.02 | <0.02 | <0.02 | <0.02 | <0.02 | <0.02 | - | - | - |
| Ca | 292 | 331 | 355 | 286 | 330 | 257 | 319 | 89.8 | 76.8 | - | - | - |
| Cd | <0.02 | <0.02 | <0.02 | <0.02 | <0.02 | <0.02 | <0.02 | <0.02 | <0.02 | <0.0015 | 0.0015-0.003 | >0.003 |
| Co | 0.458 | 0.136 | 0.055 | 0.034 | <0.02 | <0.02 | <0.02 | <0.02 | <0.02 | <0.25 | 0.25-0.5 | >0.5 |
| Cr | <0.02 | <0.02 | <0.02 | <0.02 | <0.02 | <0.02 | <0.02 | <0.02 | <0.02 | <0.025 | 0.025-0.05 | >0.05 |
| Cu | 0.141 | <0.02 | <0.02 | <0.02 | <0.02 | <0.02 | <0.02 | <0.02 | <0.02 | <1 | 1-2 | >2 |
| Fe | 30.6 | 0.241 | <0.02 | <0.02 | <0.02 | 0.184 | <0.02 | <0.02 | <0.02 | <1 | 1-2 | >2 |
| K | 7.50 | 6.24 | 5.98 | 4.20 | 4.01 | 3.09 | 3.10 | <1 | <1 | - | - | - |
| Mg | 115 | 99.5 | 85.5 | 64.0 | 41.8 | 14.2 | 10.3 | 1.74 | 1.6 | - | - | - |
| Mn | 7.99 | 5.42 | 3.73 | 2.61 | 1.07 | 0.086 | <0.02 | <0.02 | <0.02 | <0.25 | 0.25-0.5 | >0.5 |
| Na | 152 | 111 | 81.8 | 41.0 | 12.0 | 1.56 | 1.34 | <1 | <1 | - | - | - |
| Ni | 1.06 | 0.357 | 0.221 | 0.093 | 0.092 | 0.041 | 0.116 | 0.035 | <0.02 | <0.035 | 0.035-0.07 | >0.07 |
| Pb | 0.503 | <0.02 | <0.02 | <0.02 | <0.02 | <0.02 | <0.02 | <0.02 | <0.02 | <0.005 | 0.005-0.01 | >0.01 |
| Sr | 1.14 | 1.16 | 1.03 | 0.846 | 0.648 | 0.456 | 0.513 | 0.202 | 0.151 | - | - | - |
| V | <0.02 | <0.02 | <0.02 | <0.02 | <0.02 | <0.02 | <0.02 | <0.02 | <0.02 | <0.1 | 0.1-0.2 | >0.2 |
| Zn | 1.90 | 0.604 | 0.627 | 0.281 | 0.563 | 0.238 | 0.734 | 0.271 | 0.109 | <2.5 | 2.5-5.0 | >5 |

Table 8-3: ICP-OES results (Sample AIS 878, Tailings Opencast Pit)

| Parameters (mg/l) | AIS878 | | | | | | | | | SANS 241:2011 | | |
|-------------------|--------|-------|-------|-------|-------|-------|-------|-------|-------|----------------|-------------------|-------------|
| | | | | | | | | | | 0-50% of limit | 50%-100% of limit | Above limit |
| Leach | 0 | 1 | 2 | 3 | 6 | 10 | 15 | 20 | 25 | | | |
| Al | | 0.037 | <0.02 | <0.02 | <0.02 | <0.02 | <0.02 | <0.02 | <0.02 | <0.15 | 0.15-0.3 | >0.3 |
| As | | <0.02 | <0.02 | <0.02 | <0.02 | <0.02 | <0.02 | <0.02 | <0.02 | - | - | - |
| Ba | | 0.044 | <0.02 | 0.021 | 0.022 | 0.023 | <0.02 | 0.021 | <0.02 | - | - | - |
| Be | | <0.02 | <0.02 | <0.02 | <0.02 | <0.02 | <0.02 | <0.02 | <0.02 | - | - | - |
| Ca | | 381 | 152 | 34.0 | 43.2 | 38.2 | 26.5 | 30.4 | 25.2 | - | - | - |
| Cd | | <0.02 | <0.02 | <0.02 | <0.02 | <0.02 | <0.02 | <0.02 | <0.02 | <0.0015 | 0.0015-0.003 | >0.003 |
| Co | | <0.02 | <0.02 | <0.02 | <0.02 | <0.02 | <0.02 | <0.02 | <0.02 | <0.25 | 0.25-0.5 | >0.5 |
| Cr | | <0.02 | <0.02 | <0.02 | <0.02 | <0.02 | <0.02 | <0.02 | <0.02 | <0.025 | 0.025-0.05 | >0.05 |
| Cu | | 0.022 | <0.02 | <0.02 | <0.02 | <0.02 | <0.02 | <0.02 | <0.02 | <1 | 1-2 | >2 |
| Fe | | 0.069 | 0.031 | 0.073 | <0.02 | <0.02 | 0.022 | <0.02 | <0.02 | <1 | 1-2 | >2 |
| K | | 18.5 | 8.39 | 3.51 | 4.53 | 2.79 | 1.00 | <1 | 1.38 | - | - | - |
| Mg | | 175 | 52.8 | 12.7 | 17.1 | 11.1 | 5.72 | 4.29 | 3.56 | - | - | - |
| Mn | | 0.118 | 0.071 | 0.026 | 0.043 | 0.049 | <0.02 | <0.02 | <0.02 | <0.25 | 0.25-0.5 | >0.5 |
| Na | | 941 | 330 | 45.6 | 4.86 | <1 | <1 | <1 | <1 | - | - | - |
| Ni | | 0.063 | 0.198 | 0.112 | <0.02 | <0.02 | <0.02 | <0.02 | <0.02 | <0.035 | 0.035-0.07 | >0.07 |
| Pb | | <0.02 | <0.02 | <0.02 | <0.02 | <0.02 | <0.02 | <0.02 | <0.02 | <0.005 | 0.005-0.01 | >0.01 |
| Sr | | 2.41 | 0.949 | 0.216 | 0.230 | 0.179 | 0.104 | 0.135 | 0.119 | - | - | - |
| V | | <0.02 | <0.02 | <0.02 | <0.02 | <0.02 | <0.02 | <0.02 | <0.02 | <0.1 | 0.1-0.2 | >0.2 |
| Zn | | 0.998 | 0.578 | 0.318 | 0.325 | 0.297 | 0.229 | 0.238 | 0.077 | <2.5 | 2.5-5.0 | >5 |

Table 8-4: ICP-OES (Sample AIS 878 and AIS 871 in 1:1 ratio)

| Parameters (mg/l) | AIS871-878 | | | | | | | | | SANS 241:2011 | | |
|----------------------|------------|-------|-------|-------|-------|-------|-------|-------|-------|-------------------|----------------------|----------------|
| | | | | | | | | | | 0-50% of limit | 50%-100% of limit | Above limit |
| Leach | 0 | 1 | 2 | 3 | 6 | 10 | 15 | 20 | 25 | | | |
| Al | 0.021 | 0.073 | <0.02 | <0.02 | <0.02 | <0.02 | <0.02 | <0.02 | <0.02 | <0.15 | 0.15-0.3 | >0.3 |
| As | <0.02 | <0.02 | <0.02 | <0.02 | <0.02 | <0.02 | <0.02 | <0.02 | <0.02 | - | - | - |
| Ba | 0.045 | <0.02 | 0.026 | 0.029 | 0.048 | 0.037 | 0.033 | 0.028 | 0.055 | - | - | - |
| Be | <0.02 | <0.02 | <0.02 | <0.02 | <0.02 | <0.02 | <0.02 | <0.02 | <0.02 | - | - | - |
| Ca | 348 | 164 | 73.5 | 86.3 | 80.3 | 72.6 | 43.3 | 38.5 | 46.2 | - | - | - |
| Cd | <0.02 | <0.02 | <0.02 | <0.02 | <0.02 | <0.02 | <0.02 | <0.02 | <0.02 | <0.0015 | 0.0015-0.003 | >0.003 |
| Co | <0.02 | <0.02 | <0.02 | <0.02 | <0.02 | <0.02 | <0.02 | <0.02 | <0.02 | <0.25 | 0.25-0.5 | >0.5 |
| Cr | <0.02 | <0.02 | <0.02 | <0.02 | <0.02 | <0.02 | <0.02 | <0.02 | <0.02 | <0.025 | 0.025-0.05 | >0.05 |
| Cu | <0.02 | <0.02 | <0.02 | <0.02 | <0.02 | <0.02 | <0.02 | <0.02 | <0.02 | <1 | 1-2 | >2 |
| Fe | <0.02 | 0.226 | <0.02 | <0.02 | <0.02 | <0.02 | <0.02 | <0.02 | <0.02 | <1 | 1-2 | >2 |
| K | 17.4 | 8.21 | 5.40 | 5.02 | 4.23 | 2.71 | <1 | <1 | 1.68 | - | - | - |
| Mg | 190 | 47.9 | 23.9 | 26.3 | 16.9 | 12.8 | 7.43 | 5.09 | 7.65 | - | - | - |
| Mn | 0.355 | 0.136 | 0.080 | 0.147 | 0.460 | 0.256 | 0.182 | 0.046 | 0.026 | <0.25 | 0.25-0.5 | >0.5 |
| Na | 816 | 130 | 57.5 | 38.7 | 19.4 | 6.39 | 1.48 | <1 | 1.16 | - | - | - |
| Ni | <0.02 | <0.02 | <0.02 | <0.02 | <0.02 | <0.02 | <0.02 | <0.02 | <0.02 | <0.035 | 0.035-0.07 | >0.07 |
| Pb | <0.02 | <0.02 | <0.02 | <0.02 | <0.02 | <0.02 | <0.02 | <0.02 | <0.02 | <0.005 | 0.005-0.01 | >0.01 |
| Sr | 3.17 | 1.00 | 0.383 | 0.385 | 0.239 | 0.180 | 0.095 | 0.106 | 0.123 | - | - | - |
| V | <0.02 | <0.02 | <0.02 | <0.02 | <0.02 | | <0.02 | <0.02 | <0.02 | <0.1 | 0.1-0.2 | >0.2 |
| Zn | 0.206 | 0.111 | 0.130 | 0.180 | 0.170 | 0.106 | 0.100 | 0.050 | 0.103 | <2.5 | 2.5-5.0 | >5 |